THE STRUCTURAL IN-PLANE SEISMIC PERFORMANCE OF TALL WOOD-FRAME WALLS

by

ANTHONY PETERSON

B.Eng., McGill University, 2004

A THESIS SUBMITTED IN PARTIAL FULFILMENT OF
THE REQUIREMENTS FOR THE DEGREE OF

MASTER OF APPLIED SCIENCE

in

THE FACULTY OF GRADUATE STUDIES

(Civil Engineering)

THE UNIVERSITY OF BRITISH COLUMBIA

August 2006

ABSTRACT

Large commercial and industrial developments such as warehouses and other open-concept designs have long been built utilizing tilt-up concrete, steel-frame and masonry technologies. More recently, tall wood-frame walls have emerged as a promising alternative to the existing structure types. Research is currently being performed to investigate tall wood-frame wall design properties. Tall wood-frame wall responses to gravity, wind and seismic loading scenarios need to be looked into. This thesis focuses on the in-plane performance, specifically seismic performance, of tall wood-based walls. Though small wood-frame residential buildings have shown exceptional seismic response performance in the past, wood tall wall performance is relatively unknown.

Full-scale wood-based tall walls were monotonically and cyclically tested. Stud material and spacing, sheathing type and thickness, and nail style and spacing were investigated, as was the influence of blocking and the influence of vertical loading. In addition, a simplified stud-to-plate hold-down connection was also used in the full-scale walls. These stud-to-plate connections were tested separately as well, with the aim being to more thoroughly understand the behaviour of these inexpensive and more easily constructed connections. Finally, individual sheathing-to-framing connections were tested. These were needed to permit subsequent analytical modelling of the tall walls.

Verification of the full-scale tall wall tests as well as predictive wall responses of untested wall configurations was done utilizing the wood-based structural analysis software, CASHEW. The experimental results and analytical results were analyzed and compared with the significant findings presented. The CASHEW results were difficult to correlate with the experimental results, though an effort was made. Expected tall wall behaviours are presented and discussed. Moreover, wood-based tall wall design limitations and recommendations are given. These findings help provide a seismic design basis for wood-based tall walls.

TABLE OF CONTENTS

LIST OF TABLES

LIST OF FIGURES

ACKNOWLEDGEMENTS

This project would not have been possible without the support, both financial and intellectual, of the Natural Sciences and Engineering Research Council of Canada (NSERC), the Department of Civil Engineering at the University of British Columbia (UBC) and Forintek Canada Corporation and its members; for this I thank them.

I thank Dr. Marjan Popovski of Forintek for his thorough supervision, advice and assistance as well as Dr. Helmut Prion and Dr. Carlos Ventura from UBC. The knowledge and support they provided was much appreciated. I would also like to thank Dr. Erol Karacabeyli of Forintek for his support and interest in this project, Dr. Colin Rogers from McGill University, and Brian Folz for his assistance with the CASHEW software utilized.

In particular, at Forintek, I would like to thank Henley Fraser and Paul Symons for their extensive and immeasurable assistance during the experimentation phase of this project as well as Tony Thomas, Jules Gardy, Bill Deacon, Ciprian Pirvu, Alan Matsalla and Gay Chan.

To my father Ivan, my mother Victoria and my brother Alan, I thank them for their lifetime of support. Finally, Katherine Hikita I thank for her answers to my questions on shearwalls, as well as Blake Goddard, Steve Armistead, Brent Williams, Jason LaBarbera, Natalie Telewiak, Victoria Lake and all my other friends that supported me.

1. INTRODUCTION

1.1 Background

Residential construction within North America has long been done utilizing wooden structural members, especially in the case of low-density dwellings. The methods utilized over the past 200 years have resulted in remarkably resilient structures to most loading scenarios. The advantages of the simple efficient designs of modern wood-frame houses have perpetuated a familiarity and a level of comfort with their continued usage; the wood-frame housings of today account for over ninety percent of new home construction in North America. With this being said, a vast untapped market for wood construction has been overlooked. Though there is a current drive to introduce larger and higher density wood-based residential structures into modern cities and towns, the large markets of commercial and industrial complexes continues to be seemingly set aside for concrete, masonry and steel. To permit the expansion of timber construction into profitable markets such as those mentioned, research needs to be carried out to allay any concerns that may arise regarding a perceived shortcoming in wood structural performance. In addition to general reluctance regarding wood as a viable structural material for designers, there exists an actual void in guidance for wood design. Though wood has been investigated on a large scale to determine species specific properties as well as for design guidelines for small wooden structural systems, it has not been studied in any depth for larger structures. It is true that current design techniques can be conservatively applied to small hotel complexes, apartment developments and other similar buildings; however this is not always the case. Specifically, to facilitate the construction of large commercial and industrial building systems the need for walls of over five metres in height is often encountered; tall walls are needed. Structural wooden wall systems capable of providing ceilings of said height and that allow for the open floor plans needed in supermarkets, arenas, convention halls and industrial warehouse complexes need to be investigated.

The Canadian Wood Council has recognized the need for design guidance for wood-based tall wall structures. The "Design and Costing Workbook" gives design information for single storey buildings with floor areas of under 14400 square metres (CWC, 1999). The "Tall Walls Workbook" (CWC, 2000), gives design guidance for tall walls used in commercial and industrial buildings. These workbooks provide a basis for which designers can base designs

upon, however more intricate designs as well as difficult design scenarios remain an issue. Stud tables for both dimension lumber as well as engineered wood products are found in the latter publication, and these tables will continue to expand as more research is carried out. As noted in the graduate thesis of Daniel Leonard (Leonard, 2004), the prelude document to this thesis, current restrictions in the Canadian Wood Design Code as well as supplemental publications seem overly conservative and fail to take into account beneficial wall properties such as composite action between the sheathing and stud when loading occurs perpendicular to a wall. In addition, stud spacing restrictions of conventionally sized shearwalls, about 610 mm on centre, further hamper practical designs if applied to taller shearwalls. This thesis will delve further into the behaviour of tall walls, similar to that of its predecessor; however the focus will be on in-plane seismic tall wall behaviour. In-plane behaviour of tall walls, of which is essential to understand with regards to seismic loading, will further permit wood to expand into other building markets.

1.2 Research Objectives

As a continuation of a Forintek Canada Corporation research program, certain objectives have already been outlined, but new ones are also present. The main objective of helping facilitate the expansion of the forestry products sector into large commercial and industrial building design, often of box-type shape, remains consistent. This thesis's focus on the in-plane wall response helps addresses this. The subsequent objectives of this thesis are as follows:

- Increase the understanding of wood-based tall wall performance with respect to in-plane load response behaviour.
- Produce design recommendations and restrictions with regard to the use of larger sized studs and sheathing in wood-based tall wall structures.
- Investigate the Canadian Wood Design Code CSA-O86 restrictions on current shearwall design.
- Investigate the advantages of the use of blocking in tall walls.
- Examine commercially available and unconventionally used hold-downs and anchorages for studs with regard to in-plane load response, so as to facilitate efficient wall construction.

- Examine commercially available, shearwall specific software, to determine its appropriateness in design with regard to tall wall response verification and prediction.

1.3 Scope

The scope of this thesis is as follows and is geared toward attaining the previously indicated objectives:

- Perform an in-depth literature review to ascertain current tall wall research and knowledge. A focus toward in-plane loading wall response will be made.
- Perform monotonic and cyclic in-plane full-scale tall wall tests to ascertain true wall behaviour for a multitude of different wall configurations.
- Perform monotonic uplift tests of stud-to-plate connections to ascertain the performance of economical and commercially available connectors that are used unconventionally; they are used as the main structural hold-down/anchorage components.
- Perform monotonic and cyclic sheathing-to-framing connection tests of multiple configurations so as to provide a better understanding of the connection response and to permit software modelling.
- Attempt to use commercially available software to verify the aforementioned in-plane tall wall tests as well as to analytically predict untested wall configurations.
- Make design recommendations based on the experimental and analytical findings of this study to help with the expansion of the wood structural products and design methods into the commercial and industrial building sector.

1.4 Thesis Outline

This thesis is setup to logically proceed through the testing program; presenting results and statements focussed on the objectives of the study. A literature review is provided in Section 2, with results from all experimental aspects of the study given in Sections 3 to 6 including material, full-scale tall wall, stud-to-plate and sheathing-to-framing tests. Software modelling is

covered, with both experimental verification and analytical prediction, in Section 7. Finally, Section 8 gives a project summary statement, significant findings, design recommendations, as well as future research possibilities. References, acknowledgements and appendices are also provided.

2. LITERATURE REVIEW

2.1 Wood-Frame Construction

The wood-frame construction market has dominated the residential building market for many years. Unfortunately, the wood products industry is unable to expand this building materials use into larger structures such as factories, warehouses, big-box stores and alike. With close to 90% of American residences constructed using wood frame shearwalls as the main lateral load resisting system as of 1997 (Portland, 1997), an expansion to these markets should be a goal.

These alternatives (industrial and commercial) are currently saturated in design with tilt-up concrete, steel and masonry building techniques. With North American non-residential construction close to US$300 billion a year (1999 figures indicate the United States market to be US$273.5 billion) there appears plenty of growth potential (USBC, 2000). Non-residential construction, commonly up to 90%, is four stories or lower; this is significant since many building codes that are currently in-use cap wood as a structural material to a certain height. This non-residential market however used less than 11% of the amount of wood products used in residential construction in 1995, with this figure shown to be declining further (McKeever and Adair, 1998). This is troubling since the steel and concrete industries continue to pursue the residential market as a means of expansion; it is therefore paramount that the wood industry expands its usage into traditionally concrete and steel markets. It has been estimated that a small and attainable ingress of timber-based construction into the American non-residential market place of only 2% would add an additional US$5.4 billion a year (USBC, 2000), with non-structural and finishing applications adding more income potential.

To facilitate an expansion of wood-based frame construction into these larger industrial and commercial markets, further knowledge is required on the expected performance of these wood-based designs. Though there exists plenty of knowledge, both experimental and historical, on the performance of conventionally sized wood-frame designs, those being around 2.5 metres in floor-to-floor height, a lack of information exists with regard to wood-based tall walls. Tall walls may be argued to be defined as consisting of heights ranging from 3.6 to 10.7 meters; the majority of non-residential buildings consist of floor-to-floor heights taller than 3.6 meters (Leonard, 2004). It is difficult to ascertain the precise impact that wood-based tall wall design

will have on the non-residential construction market both economically and performance wise, though through experimentation and sound usage of engineering principles the latter concern can be mitigated—with the former concern taken as nothing but a positive.

In addition to the lack of code developments being a hindrance to wood expansion into non-residential construction other issues are present as well. Gaston et al. (2001) discussed these issues. Included into their reasoning of why timber construction faces problems dealing with expansion are issues such as the aforementioned code limitations, as well as total design and installation costs. Wood has been referred to as lacking in cost-competitiveness with regard to other materials, especially steel, though concrete too can have significant cost savings based on its known long-term robustness and resistance to impacts and vandals. In an attempt to allow further insight into tall wall wood-frame potential, perhaps a market based on walls of over five meters should be investigated, since the wood-based structures are considered possibly more cost competitive at these taller heights. In 1995, the categories of "stores" and "industrial buildings" together accounted for 58% of all non-residential floor area built. The potential incremental volume for wood in these categories is 2.0 million cubic metres of lumber and 140 million square metres of panels for stores and 340,000 cubic metres of lumber and 130 million square metres of panels for industrial buildings. The total value of these indicators in 2002 dollars is CAD$1.94 billion (Leonard, 2004). This maximum potential incremental market for wood technology in the commercial and industrial building construction is large and also assumes that other appropriate elements of the building are also constructed of wood along with the tall exterior walls. Most current building code limitations will not permit all of these gains due to hazardous occupancy classifications and combustibility concerns, though potential still exists for schools, office and public buildings as well as health care facilities to take advantage of tall wall design as it becomes a more viable design option for engineers. These more viable designs may also spring from continued research into engineered wood products that can compliment conventional lumber and allow for much larger structures due to their inherent consistent and strong properties. Advances in engineered wood, much like the introduction of Glulam® and oriented strandboard (OSB) into construction, will further enhance wood-based designs.

As alluded to earlier, there is a general confidence in the wood-frame construction industry based on primarily historical building results, as well as more current experimental studies.

Simple loading scenarios as well as wind loading have been shown to provide this confidence, though some dynamic high-wind forces are still concerning, namely hurricane and tornado type loads. Seismic design is not excluded from this basis either, with wood-frame shearwalls most commonly being used as the lateral load resisting element in most residential buildings (Folz and Filiatrault, 2001), and are the reason why they perform well under overload conditions (Leiva-Aravena, 1996). The 1995 Kobe earthquake helped instil some satisfaction into the wood industry with regard to performance for it was found that common single-family dwellings in the presence of large liquefaction proved resilient as opposed to steel high-rises. Unfortunately, larger wood-frame buildings were not as successful as their smaller counterparts. Floor irregularities as well as wall openings were considered problems of primary concern. In 1994, the Northridge earthquake saw fatalities and financial loss as a result of wood-frame building failures. These two earthquakes and the close scrutiny afterward gave rise to expanded research into wood-frame construction (Durham et al., 2001; Foliente et al., 2000). To improve the wood-frame performance found in today's modern structures the FEMA-funded CUREe-Caltech Woodframe Project was initiated in the United States in 1998, at a cost of US$6.9 million (Durham et al., 2001). Other researchers realized the need for an overall assessment of seismic design provisions, such as the force modification factor R found in the 1995 National Building Code of Canada (NBCC, 1995) and the similar q factor found in the Eurocode 8 (CEN, 1994) (Ceccotti and Karacabeyli, 2002). Wood has been recognized to provide for the high ductile performance necessary for seismic event mitigation (NBCC, 2005) due to its efficient use of steel fasteners, though continued research remains necessary.

2.2 Structural Materials

Since this study is a continuation of existing work there is obvious duplication in the necessary material needed to be presented. For the sake of completeness, within this thesis, the following section outlines the advantages and disadvantages of utilizing wood-based tall walls as well as tilt-up concrete, steel and masonry in a comparative form. Daniel Leonard (Leonard, 2004) compiled most of the following information concisely and efficiently, and as such it will be presented essentially unchanged though slightly summarized with some current additions necessary for the seismic event focus of this thesis.

2.2.1 Tall Wood-Frame Construction

Wood-frame construction is as it sounds; conventional construction consists of stud-based walls utilizing mostly 38 mm x 89 mm dimension lumber studs along with either plywood or OSB sheathing. Gypsum wallboard is also utilized in the design aspect, since it is usually specified due to fire code requirements. These studded walls are conventionally of height 2.4 metres to near 3.6 metres, and are rarely seen higher. The tall wall realm of construction is much more massive, with the need for thicker, deeper and longer studs as well as comparable increases in both fastener and sheathing sizes. These structures, as previously mentioned, are thought of as walls that are anywhere from 3.6 metres to 10.7 metres in floor-to-floor height. Current code requirements usually specify close stud spacing, no more than 610 mm, and other geometric constrains that do not take into account the enormity of the materials that are used. Building code evolution will need to address these concerns to further allow tall wall wood-frame design concepts to prosper. A listing of the advantages and disadvantages of wood-frame design now follows.

2.2.1.1 Advantages

- Wall fabrication is faster than in concrete tilt-up and masonry construction. The tilt-up concrete construction process includes the fabrication of perimeter forms, installation of reinforcement steel and lifting inserts, blocking of openings and the placing of the concrete. A tall wood-frame wall system can be framed and fabricated on mass one assembly at a time, and then simply lifted into place so long as proper anchorage is accounted for.
- The steel fastener elements of a wooden shearwall provide ductile elements to the wall assembly that aid in seismic energy dissipation.
- Wooden shearwalls are flexible in construction in that they can be altered onsite, including reinforcement and other structural enhancements once installed so as to accommodate openings and other structural changes that are deemed necessary or are desired.
- Wood, as a base material, has a high strength-to-weight ratio and consequently can allow for more simplistic construction techniques.

- Wood-frame construction does not require curing time for the wall panels unlike tilt-up concrete construction which usually require ten days before a panel lift can be made.
- When using wood-frame walls there is no concern about delays due to cold and freezing weather conditions since wood is very accommodating to shifts in weather. Concrete tilt-up construction requires supplemental heating if temperatures are too cold, with placement halted typically if temperatures drop below -5°C.
- Less expensive and lower capacity cranes can be utilized when lifting and placing wood-based tall walls.
- Labour costs for wood-frame construction are lower due to a lower amount of skilled trades necessary to frame the walls. Masonry is a highly skilled profession, and tilt-up concrete requires numerous subcontractors to complete the process. Subcontractors encompassing formwork, reinforcing steel, concrete placement and finishing, welding and sealant application may all need to be used. Steel-frame construction can also utilize costly tradespeople such as welders.
- Tilt-up concrete is further limited in flexibility by limited casting space. It may be difficult, if space is limited, to form more than a handful of walls at a time, whereas wood-frame tall walls can be quickly manufactured and subsequently stacked to avoid worksite space issues.
- The lower masses involved with a wood-based tall wall lessen the need for massive connections between the different elements of the structure. Connections between the roof and walls become cheaper while the foundations become smaller.
- The most important benefit of using lighter tall wood-frame walls will be in the regions with high seismic activity, where large seismic forces are generated in buildings that use concrete or masonry walls. This is significant since the proposed peak ground accelerations and seismic loads, for most cities in Canada and the United States will increase in proposed code revisions.
- Wood-based wall systems generally have a lower cost of interior wall finishing for office applications compared to that of concrete tilt-up or masonry designs, due to its often sited architectural benefit.
- Light industrial and commercial buildings of wood-based construction are often regarded as of a higher aesthetic quality than other modes of construction.

- Wood-based buildings usually do not have the problems with isolation and air-conditioning often associated with buildings in other comparable materials.
- Wood is a renewable material and wood-based solutions for structural systems are sought after from an environmental perspective.
- General contractors may prefer wood-frame solutions because they give them more control over the key components of the building, as opposed to subcontracting out large portions of the work. Construction in wood is also more onsite friendly due to its ease of adjustment and alteration to ever changing on-site realities.
- It is easier to achieve the required insulation values in wood-frame construction than in concrete tilt-up, masonry, or steel construction. Tilt-up concrete is not a good system for extreme climates, while steel is inherently a poor insulator from temperature effects. Added insulation will add to the cost of a structure.

2.2.1.2 Disadvantages

- Lack of engineered solutions for tall walls with various wood-based materials used for the studs and sheathing.
- Lack of known design capacities for such engineered solutions for tall walls with various stud spacing and sheathing thickness', subjected to gravity, wind, and seismic loading.
- In the context of shearwalls, wood-based shearwalls can be found to be flexible to a degree that serviceability issues can become present; this can be mitigated by proper design.
- Modelling the structural performance of wood-frame structures by commercial software is difficult due to the non-isotropic material properties of wood.
- Lack of technical solutions and design values for connections used in tall walls.
- External durability concerns related to water ingress.
- Internal durability concerns related to building damage caused by moving equipment and/or machinery.
- Concerns related to building break-in and vandalism.
- Higher insurance premiums.

- Material concerns ranging from warping, shrinkage, swelling, decay, discolouration, splitting and parasitic attack as well as more.

2.2.2 Concrete Tilt-Up Wall Construction

Tilt-up concrete construction is an economical and fast way to construct concrete walls for warehouses and has become a multi-billion dollar industry today, accounting for over 10,000 buildings annually. It is now used for shopping centres, warehouses, manufacturing plants, office buildings, prisons, schools, churches, or any other type of building less than four stories in height. The Tilt-Up Concrete Association (TCA) estimates that over 60 million square metres of tilt-up concrete-based buildings were constructed in 2001 alone (TCA, 2006). Tilt-up concrete has been introduced throughout North America, though in the United States in particular some regions are reluctant to embrace its use such as the East and Northeast American mainland. Its use is usually recommended only when given site and circumstances warrant its usage. The larger the building the more economically sound this technique is due to crew and crane issues. Panels need also to be of a mass smaller than 60 tonnes and have less than 50% openings. If the necessary requirements are met the advantages given at the end of this section over other building materials may be found (Brooks, 1999).

The term tilt-up was first used in the 1940's to describe a method for constructing concrete walls rapidly and economically without the formwork necessary for poured-in-place walls. It is a two step process: First, slabs of concrete, which will comprise the wall, are cast on the building floor slab or separate casting slab. Once enough curing has occurred (usually seven to ten days) they are lifted by crane and set onto the prepared foundations to form the exterior walls. These large wall segments can weigh up to 40 tonnes and average from 152 mm to 200 mm in depth. Little formwork is necessary, with only perimeter forms usually needed. The erected panels are temporarily braced, connected and caulked, and then the roof structure is built and attached. Total construction time often take less than four weeks (Ruhnke and Schexnayder, 2002).

Since the concept was first developed research investment has occurred into the tilt-up concrete constructions process. Refinements resulting from research have enabled panel sizes of over 12 metres in height, faster erection times—with lifting, setting, and bracing of 20 to 30 panels a day, and a wide variety of finishes that are required for architectural accents. To ensure the

availability of qualified field personal, a certification program is being developed jointly by the TCA and the American Concrete Institute. Following is a listing of advantages and disadvantages of tilt-up concrete construction.

2.2.2.1 Advantages

- In areas where tilt-up concrete design and construction expertise are available, particularly a trained crane and rigging crew, tilt-up concrete construction can be more economical than competing construction methods for similar buildings types.
- The growth of concrete tilt-up construction can be attributed in large part to the desire of building owners to shorten the construction process. From the time the floor slab is placed, the typical elapsed time from starting to form the panels until the building shell is completed is four to five weeks (TCA, 2006). This allows for the minimization of construction financing costs.
- Tilt-up concrete buildings usually show less visible signs of aging, although architectural styling is an issue in some older structures.
- Concrete offers high fire protection.
- Concrete, as a material, is relatively inexpensive when compared to materials such as steel.
- Maintenance costs are kept low do to upkeep; often consisting of simple painting every six to eight years.
- The high fire resistance of tilt-up concrete walls results in low insurance premiums.
- Architects have relative freedom to arrange and assemble the panels and a wide choice of surface finishes.
- Expansion can be planned and designed for allowing future wall panel attachment or relocation.
- Unlike steel and wood-based walls, concrete is inherently difficult to break through in an attempted break in. Doors and window openings are the only logical means of forcible entry.
- Low insurance costs, coupled with inherent building durability and security, give rise to a desirable investment for the owner.
- Concrete provides often better sound insulation than that of wood construction.

2.2.2.2 Disadvantages

- The seismic performance of concrete tilt-up buildings is one of the biggest concerns among the engineering community. Since tilt-up walls are held vertically in place by an often precarious connection to the roof, structures built in the tilt-up style are among the most dangerous to occupants in a seismic event. The 1964 8.4 magnitude Alaskan earthquake first presented these seismic design deficiencies found in tilt-up structures, with three of the five bays of the Elmendorf Air Force Base warehouse collapsed. The 1994 Northridge earthquake also saw to the partial collapse or full collapse of more than 400 tilt-up buildings in the San Fernando Valley out of around 1200 existing in the area (Davis, 1999).
- Aside from the aforementioned possible structural seismic performance concerns, serviceability concerns can also be present, with extensive cracks and deflections often manifesting post seismic event.
- Skilled labour is required in the reinforcement placement stage of concrete pouring as well as during the lifting procedure of the tilt-up concrete walls.
- Connections in tilt-up structures have to be designed to sustain large loads, sometimes in excess of 250 kN—often very expensive.
- Costs associated with heating and cooling in tilt-up concrete structures is usually higher than those in other types of structures.
- Large cranes are necessary due to the excessive masses of the concrete walls—not economical for smaller structures.

2.2.3 Masonry Wall Construction

Masonry is one of the oldest forms of building; however, current practices are not the same as those done a few hundred years ago. Currently, the United States utilizes a conventional brick size of 64 mm x 95 mm x 203 mm. Concrete masonry block development has also stemmed from red brick construction. Brick construction can be highly sought after architecturally, with modern concrete based products giving a variety of colours and textures; residential and office buildings, warehouses, municipal buildings, religious institutions, factories, prisons, schools and health-care facilities have all utilized modern masonry. Concrete masonry is a long lasting form

of construction that has actually 15 times the market size as that of concrete tilt-up; it is valued at close to US$40 billion (NCMA, 2003). Masonry is very popular in the Northeast United States. A short itemized listing of the advantages and disadvantages of masonry construction is presented in the following subsections.

2.2.3.1 Advantages

- Masonry construction competes favourably with concrete tilt-up and wood-frame construction for smaller buildings of around 600 square metres or less or where inexpensive masonry materials and labour are available.
- Concrete masonry has a proven record of durability and resistance for building types subject to "abuse" such as industrial structures or prisons.
- Ease of maintenance played a major role in the use of concrete masonry tall slender walls over tilt-up concrete walls; they are inexpensive to upkeep. Coloured concrete masonry retains a more consistent appearance in comparison to tilt-up walls that are painted.
- Masonry walls provide for high fire resistance.
- The high fire resistance and historical durability results in lower insurance premiums.
- Insulation and the subsequent energy efficiency of concrete masonry can be improved by utilizing hollow-core units.
- In comparison to tilt-up concrete, there is no large floor or working space that is needed prior to construction.
- Masonry is efficient with regard to sound insulation.
- Masonry structures often have high initial costs however their overall lifecycle costs are usually lower.
- Architecturally, masonry can have many attractive options, from classic red brick to new texture concrete masonry block types.

2.2.3.2 Disadvantages

- The initial cost of masonry buildings can be prohibitive and unattractive in comparison to tilt-up concrete or steel construction types.
- The need for highly trained and experienced masons to ensure a proper masonry wall further adds to its costs.
- Seismic event susceptibility of masonry structures is a paramount concern. Unreinforced masonry construction has the lowest resistance to earthquake loads of any type of construction. Inherent high stiffness, large mass and the materials' low ductility makes this structure vulnerable to even moderate earthquakes. Steel reinforcing can be added during construction at added cost, or retrofitting can be attempted at an even greater expense. This susceptibility is mirrored on the west coast of the United States with masonry construction often shunned, while the more seismic stable eastern United States utilizes much masonry construction.
- Masonry blocks are water absorbent and as such must be weather-proofed.
- Due to the common concrete masonry block sizes (203 mm x 203 mm x 406 mm) or conventional brick sizes (64 mm x 95 mm x 203 mm) certain wall sizes are designed for, especially for the larger concrete masonry blocks. This modular basis for design can make smooth curved walls, odd dimensions and thickness transitions difficult.
- Conventional solid masonry bricks and concrete blocks have poor insulation properties on their own.
- Masonry construction usually requires the longest period of construction of all competitive construction materials.

2.2.4 Steel-Frame Construction

Steel is key to almost all non-residential construction projects in North America. Whether it is a steel-based building or just steel reinforcing in concrete, it is widely used. It comprises the largest share of the non-residential building market (AISI, 2006) with conservative estimates valuing its share at US$90 billion a year. Though this includes high-rise structures, of which wood-based tall walls could never compete with, it still indicates a significant market player. It

is estimated that steel construction currently has over a 50% share in the market that buildings based around tall wood-frame construction can compete.

Conventional and pre-engineered steel structures are the two main categories that steel buildings fall under. Conventional steel structures are built with hot rolled structural steel elements and engineered by professionals on a building by building basis. Many design calculations are needed as are connection details. Alternatively, pre-engineered buildings usually utilize cold-formed steel elements. These buildings are constructed mainly using standard structural sections and connections. These elements are shipped to construction sites for building assembly. The following listings give steel construction advantages and disadvantages.

2.2.4.1 Advantages

- Steel has the highest strength-to-weight ratio of all common structural materials (clear wood matches this, but it is seldom used for structural building applications).
- Steel structures, due to their comparably light weight to concrete-based structures, attract lower lateral seismically induced loads.
- Smaller foundations are required due to the lower weights with regard to tilt-up concrete.
- Pre-engineered steel buildings can be an additional 30% lighter than conventional steel buildings, with even greater material efficiency.
- Construction design, shop details and erection drawings for prefabricated designs are usually supplied free of charge from the manufacturer.
- Material and erection costs are accurately known based on extensive experience with many other similar buildings.
- Prefabricated structures can be delivered in short amounts of time; often as little as six to eight weeks.
- Steel structures are very exact in their dimensions, thus allowing for efficient erection and minimal lost construction time for improper fitting members. This reduces the need for skilled labour.
- Steel is considered a non-combustible building material.

- Steel being a ductile material with widely known inherent properties can be effectively utilized as the main lateral load resisting element of a structure. Steel cross-bracing, steel-frame designs and steel shearwalls can all be utilized for many types of construction geometries.
- Prefabricated buildings can often be easily expanded since the completed projects are usually kept in electronic format. This allows for designs to be quickly and relatively simplistically altered.
- Steel is easily recyclable, meaning a lessened environmental impact.
- Steel is very resilient with regard to parasitic attack.

2.2.4.2 Disadvantages

- Although considered an advantage, the non-combustibility of steel does not implicitly indicate non-susceptibility to fire damage. Steel can lose its strength when excessively heated. Fire insulation is required to ensure a steel structures integrity stays intact. The fire rating is actually lower than that of concrete or masonry construction types.
- Steel is expensive in comparison to concrete, wood or masonry.
- Though recyclable, the energy requirements needed to make steel is enormous, thus adding to the environmental footprint of the building.
- Steel is a poor insulating material.
- Skilled steel erectors can be difficult to find in some locations.
- Steel is very susceptible to marine climates and precipitation in general.
- After a seismic event certain steel members can be damaged extensively; thus requiring costly full replacement.

2.3 Research Reviews on the Performance of Shearwalls

There have been many studies in the past that have focused on wood-based shearwalls. The concept is not new; however, the expansion of wood-based shearwalls into the building sector of larger structures, both open warehouse designs as well as more intricate designs, is new. As

previously mentioned, the goal of this study is to provide insight into the behaviour of tall wall wood-based shearwalls with regard to in-plane loading.

To give background on the types of research programs that have been undertaken, a review of some pertinent research projects, papers and publications has been compiled. These reviews include discussions on the performance of conventionally sized wood shearwalls, the behaviour of certain types of tall wall shearwalls and the impact of sheathing type, fastener usage, and geometry actualities. This small selection of research papers all present issues that will be investigated over the course of this thesis. Concepts that are learned and information garnered will be used to interpret the results of this particular research program.

2.3.1 Test Results on the Lateral Resistance of Nailed Shear Walls (Karacabeyli and Ceccotti, 1996)

Forintek Canada Corporation, under the direction of Karacabeyli and Ceccotti (1996) undertook a research project to determine the lateral resistance of conventionally sized (2.4 m x 4.9 m) shear walls. This project was meant as a compliment to previous works by Dolan and Madsen (1992), Yasumura (1992) and Dean et al. (1987). Though these walls are not of the same geometric height as that of the tall walls of concern for this study, the results are applicable to understanding what can be expected in the behaviour of wood-based shearwalls. The researchers understood that most design values for shearwalls come from static tests. This, however, is not generally how seismic action presents itself and as such a more representative baseline for design is needed. In addition, the lateral resistance of certain combinations of plywood, oriented strandboard (OSB) and gypsum wallboard (GWB) was desired. The test program consisted of 2.4 m x 4.9 m sized shearwalls, utilizing 38 mm x 89 mm SPF No. 2 or better studs. OSB and CSP of 9.5 mm thickness were used as was 12.5 mm GWB. Continuous blocking was also provided. Ramp testing as well as cyclic testing was performed on different wall configurations leading to the following main findings.

The hysteretic behaviour of the cyclically tested walls was found to be, in general, symmetric, with the ramp and first cycle peaks corresponding very closely up to 40 mm of displacement for CSP or OSB only walls. This close correlation in ramp and cyclic testing was not found to the same degree with the GWB-only walls corresponding up to only 5 mm, or the OSB and GWB

combination walls corresponding up to only 20 mm. After these levels of displacement, the cyclic tested walls showed strength degradation at a gradual level. Initial elastic behaviour was also observed to around 50% of the nominal displacement level, with inelastic behaviour following. The elastic behaviour can be described by the simplistic ramping tests, whereas the larger displacement levels, where elastic behaviour is no longer held true, the cyclic tests indicate significant degradation in peak strength for the second and third cycle sets. This suggests that design factors should take into account this degradation if based on ramp testing. The third peak load envelope gave the "stabilized lateral resistance".

Superposition was also investigated with regard to predicting the performance of combination walls consisting of GWB and OSB. What was found was that utilizing the "stabilized" envelope curves of both the GWB-only walls and OSB-only walls and combining them gave rise to an indicated behaviour similar to the tested GWB and OSB combination shearwalls. This held true only up to a certain displacement level. Heavy damage to the GWB-only wall post the certain displacement level is what negates the data correlation for the entire wall behaviour. The GWB and OSB walls were found to have the expected increase in peak load compared to the individually sheathed walls; however, ductility did suffer somewhat in comparison to the OSB-only walls. The GWB component of the wall necessitated the ultimate load occurring at a lower displacement level.

2.3.2 Seismic Resistance of Wood Shear Walls with Large OSB Panels (Durham et al., 2001)

The research topic of concern for this particular paper focussed on the impact of utilizing larger than standard (2.4 m x 2.4 m) OSB panels and standard OSB panel sizes (1.2 m x 2.4 m) in wood-frame shearwalls. The walls that were tested were of a conventional size, that being 2.4 m x 2.4 m, with 38 mm x 89 mm SPF lumber studs at a spacing of 400 mm. The interest in the use of large panels stems from perceived possible cost savings and structural performance improvements. With sheets of OSB often produced at 3.3 m x 7.3 m sizes, altering conventional building practices is not inconceivable. Applications for the larger panels include combinations of longer and taller walls that withstand larger loads. Previous studies indicated larger OSB panel sizes achieved strength and stiffness increases of over 100% compared to standard OSB sheathing sizes (Lam et al., 1997). This improvement in performance, however, came at a price

with peak loads occurring at reduced displacements and prompting ductility concerns in seismic events.

The cyclic and dynamic testing performed in this study presented the following trends. The anticipated increases in strength and stiffness for the oversized panel constructed walls over the standard sized panels were observed. Unexpectedly, results indicated that the two types of walls resulted in similar ductility's. The reduced displacements observed in the aforementioned previous study did not manifest in this round of experimentation. The cyclic testing protocol developed by He et al. (1998) utilized in testing, resulted in failure modes that were consistent with the dynamic testing. The failure modes were nail pull-outs from framing or pull-through from sheathing; these are contrary to previous studies using longer cyclic testing protocols that most often resulted in nail fatigue failures.

The larger panel based walls were subjected to larger accelerations and lower drifts during the dynamic testing phase compared to the more flexible conventional walls. These larger accelerations did not result in the wall suffering from added damage. The single large panel walls experienced significantly less damage from the earthquake records chosen than those of a standard wall configuration. The larger OSB panels appear effective in acting as the lateral load resisting element of wood-frame walls.

2.3.3 Lateral Load Capacities of Horizontally Sheathed Unblocked Shear Walls (Ni et al., 2000)

Blocking has been shown through experimentation and history to be a valuable aspect of shearwall performance in wood frame construction. The focus of Ni et al. (2000) is to further investigate the effects of horizontally sheathed shearwalls with blocking. Current building codes provide design values for shearwalls sheathed with wood-based panels oriented vertically or horizontally so long as blocking is present. It is also common to see unblocked horizontally sheathed shearwalls used in practice even though in the United States explicit codes for unblocked shearwalls are not presently available. Forintek Canada Corporation conducted testing for this project, and APA research data from Tissell (1990) also contributed to the findings. The walls of the project were all of conventional height (2.4 m) and of 38 mm x 89 mm lumber stud sizes, with stud spacing ranging from 305 mm to 610 mm.

Analysis and interpretation of the testing results of this study provided some key findings and recommendations. Namely, that unblocked shearwalls can be implemented into codes so long as prudent design parameter factoring is done. The monotonic and cyclic testing revealed that a lack of blocking, depending on the nail spacing configuration and stud spacing, can result in walls close to 40% capacity of similar blocked specimens. Strength adjustment factors for the unblocked wall situations were proposed by means of a J_{ub} factor. This factor relates blocked specimen performance with unblocked performance, taking into account nailing density and stud spacing. These tables were adopted into the CSA-O86 wood design manual (CSA, 2001). Similar tables and factoring will be needed for wood-frame tall walls in the future, so this procedure and methodology is useful. The most relevant finding is the well known dependence of wall performance on density of nailing. The lessoning of stud spacing further allows nailing density to increase as does blocking when it is introduced.

2.3.4 Stiffness and energy degradation of wood frame shear walls (Shenton et al., 1998)

Wood-frame shearwall designs are subject to large dynamic forces when exposed to seismic events. In earthquake prone regions or even high wind locals, repeated cyclic forces can have an impact on both the stiffness and correspondingly the energy dissipation behaviour of a wood-frame wall system. These are the main focuses of this particular research.

It has been found in past research that modelling of wood-based wall degradation is difficult (Foliente, 1995); this is due to the hysteretic behaviour of the joints. This study sheds light on some of the nuances of these detrimental behaviours for design applications as well as future modelling applications. The walls tested were of conventional height (2.4m) and of dimension lumber studs (38 mm x 89 mm) with either plywood or OSB sheathing. Cyclic testing determined that the effective stiffness of the wooden shearwalls of this study decreases linearly when cycled at a particular amplitude and does not stabilize; it also decreases at changes of displacement step levels. Energy dissipation capacity is also affected by cyclic loading, with a dramatic drop in energy dissipation capacity from the first to the second cycles. These drops, however, do not result in poor energy dissipation behaviour for the wall. Energy dissipation capacity was found to increase at a linear level as displacement cycles increased, with the first displacement amplitude incursion proving the most influential to overall performance. The plywood and OSB sheathing based walls that were tested were not found to behave differently

to an appreciable degree; though after peak load was attained, OSB based walls were found to exhibit a greater reduction of energy dissipation capacity. Wall behaviours were more closely related to the choice of fasteners and framing.

2.3.5 Racking Performance of Tall Unblocked Shear Walls (Mi et al., 2006)

The focus of this thesis, of which the Mi et al. (2006) paper is discussed, deals with tall wood-based blocked shearwalls. This topic is relatively new to the wood design field, and as such, extensive literature is lacking; this particular paper deals with the performance of tall unblocked shearwalls and is found to show some interesting and important trends. The walls that were tested were 4.9 m x 4.9 m and consisted of 38 mm x 140 mm SPF studs spaced at 406 mm or 610 mm. Sheathing patterns varied, with horizontally stacked and staggered sheathing present in the testing matrix.

The most glaring observation made from this study is that sheathing orientation is important with regards to response under cyclic loading. A correlation between shearwall strength and the total length of the horizontal unblocked joints was found; with the smallest joint lengths corresponding to the highest strength capacity. This information may possibly be applied to blocked wood-based tall walls in some fashion. Nail spacing and stud spacing were also shown to be very influential to wall behaviour, with increased densities of both resulting in greater load, stiffness and energy dissipation capacities. Design guidelines and factors similar to what has been done in the past by Ni et al. (2000) can possibly be applied for tall walls. In fact, the current adjustment factors used for 2.4 m wooden unblocked walls in CSA-O86 (CSA, 2001) can be conservatively applied to tall walls of the construction type found in this particular study. In order to fully integrate tall wood-frame designs into common design practice, this research should be studied in further detail and in conjunction with other initiatives that investigate wooden tall wall behaviour.

2.3.6 Experimental Investigation of the Effect of Vertical Load on the Capacity of Wood Shear Walls (Dean and Shenton, 2005)

Vertical loading occurs in every wood-frame construction type, whether its snow loading or even just self-weight. Wind in particular is an important loading scenario, since overturning

forces can jeopardize the structure; the same can be said for seismic induced loads. The purpose of this particular paper by Dean and Shenton (2005) aims to further the knowledge base of the impact of vertical loading on the structural performance of wood-based shearwalls. Only limited research has been done to systematically evaluate the effect of vertical loading on static performance; hold-down anchorage concerns in such situations also need to be studied. Conventional wood stud shearwalls (2.44 m in height) were investigated in the presence of a uniform vertical load and subjected to an ASTM monotonic loading protocol. Two different vertical loading quantities were evaluated, as were comparative non-vertically loaded walls.

United States model building codes currently do not consider the effect of vertical loading, though Canada's CSA O86-01 (CSA, 2001) does take into account, implicitly, the effect of vertical loading in shearwall design. Results from this study indicate that the designs that result from current code requirements give rise to overly conservative designs. Vertical loading was found to contribute significantly to lateral load resisting behaviour of applicable walls, with increases in performance ranging from 21% to 28% for peak load increases if hold-downs are present, to increases of nearly 75% for peak load capacity when no hold-downs are present. Wall stiffness was also significantly increased as vertical load was applied to the wood-frame walls. These results indicate, as previously mentioned, that current codes are conservative when vertical loading is present.

3. PROPERTIES OF THE MATERIALS USED IN TESTING PROGRAM

3.1 Introduction

To permit a better understanding of subsequent tall wall behaviour, it was thought necessary to perform numerous material property tests. These tests included simple mass determinations as well as actual member structural properties. The resultant properties determined can be beneficial for modelling techniques as well as allow for accurate design calculations.

3.2 Specimens and Test Setup

All studs, plates, sheathing, wallboard, and frame elements were weighed to determine their mass. The sheathing and type X gypsum wallboard were weighed in full sheet size (1220 mm x 2440 mm) or half sheet size (1220 mm x 1220 mm). The top and bottom plates were also weighed in their installation form. The masses were all determined using a conventional commercial/industrial scale, except for the steel spreader bar of which the top of the tall walls were bolted to; it was weighed via use of a calibrated load cell.

The studs were measured for weak axis stiffness and consequently modulus of elasticity as well as mass by use of an appropriate testing apparatus. Forintek data acquisition software was utilized. This software used the vibration frequency of the stud as well as the stud geometry to calculate and output the modulus of elasticity. The apparatus conformed to the ASTM D6874 standard (ASTM, 2003) for the vibration based flexural determination of wood-based studs. The SPF studs were of average dimensions (38 mm x 234 mm), whilst the 1.5E and 1.7E LSL studs were of average dimensions (44 mm x 242 mm). All studs were tested with an unsupported length of 4755 mm.

3.3 Results and Discussion

The main results from the aforementioned testing are provided in Table 3.1, giving the masses and where applicable, the modulus of elasticity's of the main structural components. In Table 3.1 Mass is the mean mass; σ is the standard deviation of the respective property; and MOE is

the average modulus of elasticity for the material. The MOE was calculated in the weak axis stud orientation.

Table 3.1: Average material properties

Material	Dimensions [mm X mm]	Number of Specimens	Mass [kg]	σ_{mass}	MOE [GPa]	σ_{MOE}
9.5 mm OSB	1220 X 2440	16	18.6	0.80	-	-
15.1 mm OSB	1220 X 2440	56	27.8	0.99	-	-
25.4 mm DFP	1220 X 2440	32	38.6	1.33	-	-
15.9 mm Wallboard	1220 X 2440	8	31.7	0.24	-	-
Steel Spreader Bar	-	1	219.5	-	-	-
No. 2 or better SPF Stud	38 X 234	54	18.4	1.35	8.5	0.88
1.5E LSL Stud	44 X 242	20	37.6	1.30	12.3	0.38
1.7E LSL Stud	44 X 242	20	38.4	0.43	13.5	0.24

As can be observed from Table 3.1, the properties of the structural components used for the tall walls were quite consistent. As expected the engineered wood products such as the LSL studs were, in general, more uniform in behaviour than the inherently more variable natural SPF product. The LSL studs were stiffer and more massive with the SPF studs being significantly more variable in modulus of elasticity. A more in-depth analysis of the material properties was not carried out since it is not needed for the focus of this thesis; although a more thorough analysis of the types of materials used is provided in Leonard (2004).

3.4 Summary

The basic properties of the materials were tested for completeness of this thesis. The information garnered, though necessary, is not particularly insightful. The engineered wood product LSL is stiff and massive in comparison to the dimensional SPF lumber. It also had greater consistency in average properties. The sheathing and type X gypsum wallboard tested showed relatively close average mass. The vibration testing methodology that was used to determine the stud stiffness properties was found to be quick and efficient.

4. FULL-SCALE TALL WALL TESTS

4.1 Introduction

The primary focus of this study and thesis is that of the response and subsequent design of wood-based tall wall shearwalls for dynamic in-plane loading, in such a manner that the walls may be shown as a viable structural option similar to concrete tilt-up walls. With the ever expanding repertoire of wooden products provided by industry and the expanding design guidelines, this is feasible. The knowledge gained through the experimentation of the following outlined walls and analytical modelling thereafter will be used to determine design guidelines in the context of in-plane loading response. As alluded to, the objective of the experimentation of the full-scale tall walls is to observe the response of the structures to cyclic loading that represent, primarily, seismic loading. The responses will be analysed for many aspects, looking into general qualitative behaviour and practicality, as well as quantitative results. These quantitative results are to be used as a basis for which commercial software modelling can be verified against. The model was then to be used to understand the responses of tall wall structures, on an analytical level, that have not been experimentally built and tested. This analytical modelling also relies on subsequently performed connection tests.

4.2 Specimens and Test Setup

Tall shearwalls of 4.88 m x 4.88 m (16' x 16') centre-to-centre stud spacing in size were constructed and investigated. Two distinctive tall wall series were evaluated. The first, referred to as the 600 series, consisted of five walls with spruce-pine-fir (SPF) No. 2 or better studs, while the 700 series included eight walls with Timberstrand® laminated strand lumber (LSL) studs.

4.2.1 600 Series

The 600 series walls utilized eight 1220 mm x 2440 mm (4' x 8') OSB sheathing panels with thickness of 9.5 mm (3/8") or 15.1 mm (19/32") in staggered formation A (Figure 4.1a), and conventional 38 mm x 234 mm (2" x 10") No. 2 or better SPF studs. The studs were vertically oriented and spaced at 610 mm (2') on centre. The top and bottom plates consisted of single 44

mm x 242 mm 1.7E LSL, chosen for their stiffness and strength. The stud-to-plate connections consisted of two main components, Simpson® Strong Tie LU28L joist hangers placed at every stud, and different configurations of Simpson H6 hurricane ties. These were the primary connector for resisting uplift/lateral forces.

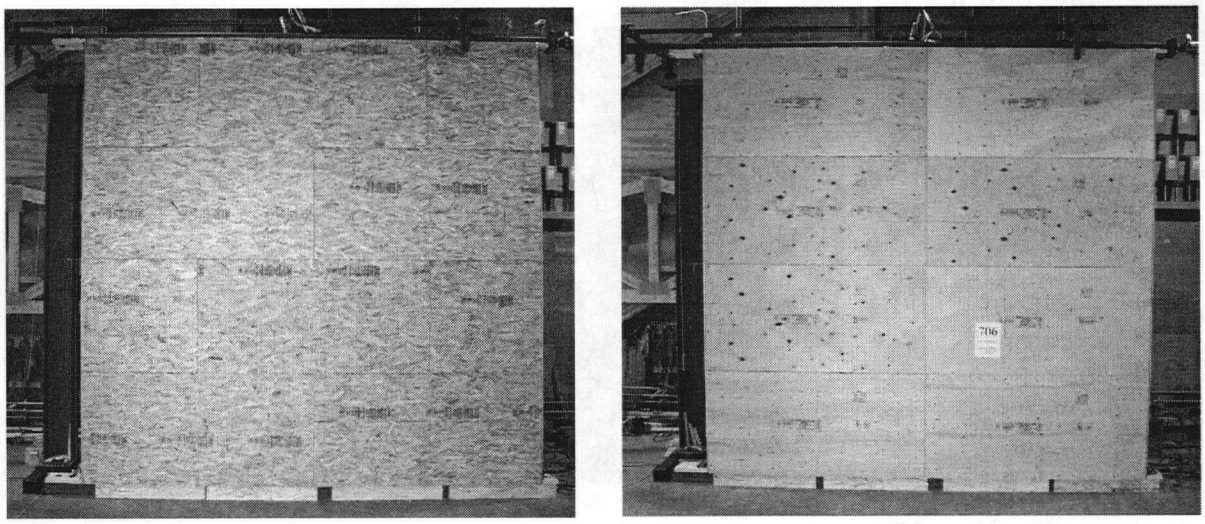

a) b)

Figure 4.1: a) Sheathing formation A; b) Sheathing formation B

For wall 601, the H6 ties were placed on the stud side opposite that of the sheathing at both the top and bottom of all studs (Figure 4.2a). Wall 602 used the same arrangement of ties on all studs except the last two studs on either end of the wall; these studs had H6 ties on both, the sheathing and the opposite side (Figure 4.2b). Walls 603 to 605 utilized the dual H6 tie formation on the end two studs on either side of the specimens as well as on the middle stud, whilst the remaining studs were connected without any H6 ties, as a perceived cost savings was assumed. The hangers and the ties were connected in the full nailing pattern to the studs and plates by conventional 3.75 mm diameter, 38 mm long (10d 1.5") common nails. The H6 ties overlapped under the top and bottom plates, necessitating the nailing of three or four nails through the metal of the underlying tie into the LSL plate. Initially this proved difficult, but with the usage of a set of pliers became quite simple. Walls 601 and 602 were sheathed with 9.5 mm (3/8") OSB, while walls 603 to 605 were sheathed with 15.1 mm (19/32") OSB. All 600 series walls used 2.5 mm diameter, 65 mm long (2.5") spiral nails to connect the sheathing to the studs. All SPF based walls were of a blocked configuration. SPF blocking of the same dimensions to that of the studs was used in all walls and were spaced vertically at 1220 mm on

centre. The blocking was attached to the studs by three toenails or three end nailed nails by 3.3 mm diameter, 83 mm long common nails. The blocking presented some construction issues due to the crowning of many of the studs as well as the blocking itself; as a result a completely flush fit between the blocking and the studs was nearly impossible, though a concentrated effort to ensure as close a contact was made. The test matrix for all walls included in the testing program is presented in Table 4.1.

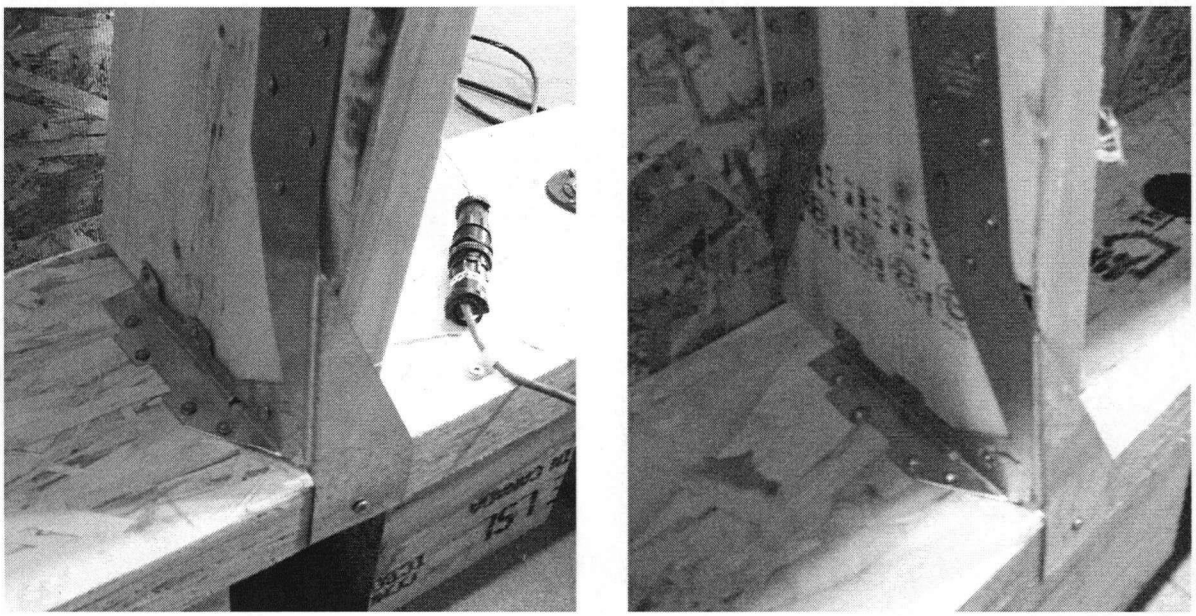

a) b)

Figure 4.2: a) Single H6 tie connection formation; b) Dual H6 tie connection formation

Of note in Table 4.1, is that under the "Load Protocol" column, the arrows represent loading conditions in the following manner: → is monotonic loading; ↔ is cyclic loading; ↔ + ↓ are cyclic and vertical simultaneous loading.

4.2.2 700 Series

Both 1.5E and 1.7E LSL studs and blocking with cross-section of 44 mm x 242 mm were used for the 700 series walls. The two different material designations were used due to a shift in available LSL product and did not appear to impact performance. The top and bottom plates for all 700 series test specimens were single 1.7E LSL. Walls 701 to 703 and wall 708 used 15.1 mm thick OSB connected with 2.5 mm diameter, 65 mm long (2.5") spiral nails, while walls 704 to 707 used 25.4 mm (1") thick Douglas fir plywood (DFP). As a result of the 25.4 mm

thick sheathing, walls 704, 706 and 707 utilized 3.0 mm diameter, 76 mm long spiral nails for sheathing application, while wall 705 used 3.75 mm diameter, 76 mm long common nails. The stud-to-plate connections were consistent for all 700 series walls, with two H6 ties being placed at both the top and bottom stud-to-plate interfaces on all studs, as well as HU9 hangers on all studs (Figure 4.3). The hangers were screwed into the plates using 38 mm long No. 8 (1.5") wood screws and nailed into the studs using 3.75 mm diameter, 38 mm long common nails. The same nails were used for the installation of the H6 ties. The hangers and ties utilized were used in their maximum nailing configuration. As with the 600 series walls, the H6 ties were overlapped under the top and bottom plates, with similar nailing issues encountered.

Table 4.1: Tall wall test matrix

Wall	Stud		Sheathing Thickness [mm] & Type	Nail Spacing and Properties				Load Protocol
	Type	Spacing [mm]		Perimeter [mm]	Interior [mm]	Diameter [mm]	Length [mm]	
601	SPF	610	9.5 OSB	152	305	2.5	65	→
602	SPF	610	9.5 OSB	152	305	2.5	65	↔
603	SPF	610	15.1 OSB	152	305	2.5	65	↔
604	SPF	610	15.1 OSB	152	152	2.5	65	↔ + ↓
605	SPF	610	15.1 OSB	102	152	2.5	65	↔
701	1.5E LSL	1220	15.1 OSB	152	305	2.5	65	→
702	1.5E LSL	1220	15.1 OSB	152	305	2.5	65	↔
703	1.5E LSL	1220	15.1 OSB	152	305	2.5	65	↔ + ↓
704	1.7E LSL	1220	25.4 DFP	152	305	3.0	76	↔
705	1.7E LSL	1220	25.4 DFP	152	305	3.75	76	↔
706[1]	1.7E LSL	2440	25.4 DFP	102	n/a	3.0	76	↔
707[2]	1.7E LSL	1220	25.4 DFP	152	152	3.0	76	↔
708[3]	1.5E LSL	1220	15.1 OSB	152	305	2.5	65	↔

[1]Sheathing placed in sheathing formation B; [2] Unblocked; [3] 15.9 mm thick type X gypsum wallboard added on the non-OSB sheathed side. Screw spacing 203 mm c/c.

Blocking was used for all 700 series walls except wall 707, with the blocking material matching the stud material. Wall 701 used the same type of nailing scheme for the blocking as in the 600 series, that being either three toe- or three end-nails. Walls 702 to 705 and wall 708, however, used four or six nails per blocking connection, while wall 706 used seven or nine nails. All blocking used 3.3 mm diameter, 83 mm long common nails. The change in the blocking nailing scheme was necessitated by the performance of wall 701 and will be explained in the following section. Wall 708 also had 15.9 mm thick type X gypsum wallboard applied to the side opposite

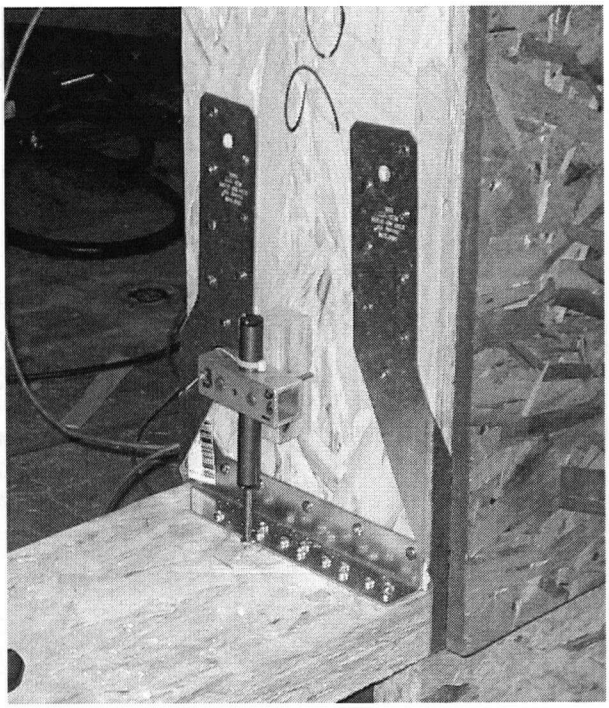

Figure 4.3: LSL stud-to plate dual H6 tie connection formation

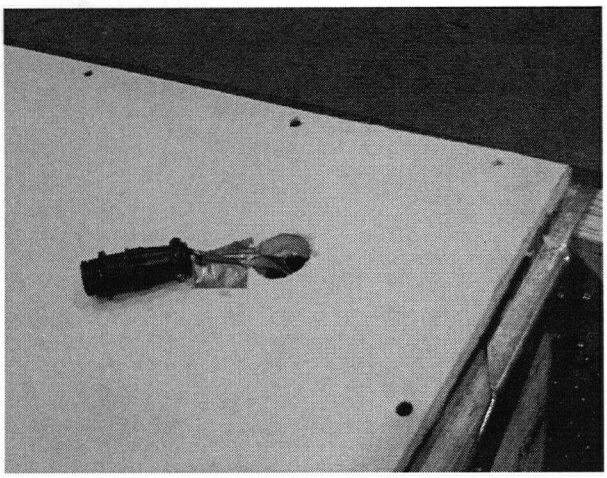

Figure 4.4: Wallboard instrumentation cut-out

the OSB sheathing. It was attached by 41 mm long (1.625") coarse thread drywall screws and then mudded using a conventional commercial compound. The type X gypsum wallboard was placed mostly while the wall was lying on the warehouse floor, with small slots being cut into the wallboard to allow for instrumentation (Figure 4.4). The final row of wallboard was put in place once the wall was raised vertical and anchored into place. The full configuration of the 700 wall series is also given in Table 4.1, including the nail spacing used and other important information. All 700 series walls had the scattered sheathing pattern shown as formation A (Figure 4.1a) except for wall 706; it had the sheathing pattern shown as formation B (Figure 4.1b). The wallboard of wall 708 was configured as in formation A, but upside down.

All the sheathing nails and blocking nails were driven into their respective locations by use of a pneumatic nail gun. The pressure was constantly changed due to the density shifts within all products used.

4.2.3 Test Frame and Anchorage

A reinforced hollow steel beam provided a foundation to which the wall specimens were bolted down, whereas a hollow steel bar bolted to the top plate was used as a load spreader bar (Figure 4.5a). The spreader bar had attachments that allowed for lateral guides to be used to ensure a steady and consistent unidirectional movement of the walls. These roller based lateral guides

were not excessively strong since little significant out-of-plane forces were expected. For most of the walls, the frame (bottom plate) was bolted to the steel beam using 12.7 mm grade five bolts, spaced at 610 mm on centre. Walls 706 to 708 used both 12.7 mm grade 5 and grade 8 bolts. Wall 701, in addition to the aforementioned change in blocking nailing scheme saw to a change in anchorage. As shown in Figure 4.5b and Figure 4.5c, the bolting scheme was different. Figure 4.5b was what was used for all 600 series walls and wall 701. This was due to perceived space limitations for bolting on the east side of the wall. The performance for the 600 series walls was satisfactory; however, the single LSL plate used for wall 701 proved incapable of withstanding the necessary load and consequently failed in bending caused by uplifting. Walls 702-708 all used an anchor bolt 102 mm on centre from the outside end stud on that particular side (the east side). The anchorage on the west side was changed to the 102 mm on-centre spacing following the testing of wall 704. The grade 8 bolts were placed at the anchorage locations outside the outermost studs, due to possible yielding in the grade 5 bolts used in the testing of Wall 705. In all cases, bolts were located on the centre line of the LSL plates. A further explanation of these design changes is given in the following section.

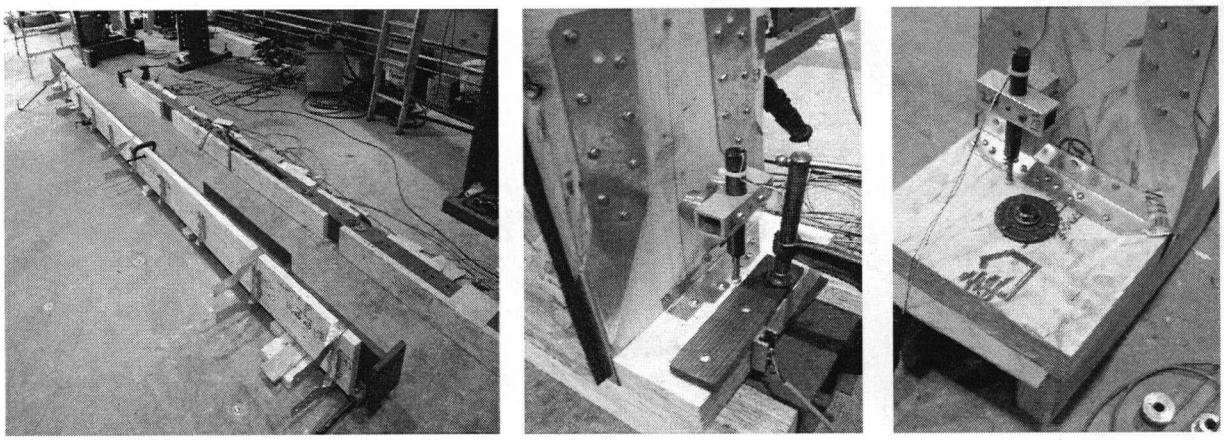

a) b) c)

Figure 4.5: a) Test frame top spreader bar and bottom foundation; b) East end-stud anchor bolt location for 600 series and 701; c) East end-stud anchor bolt location for 702-708

String displacement transducers were placed at the top and at the mid-height of the wall to measure lateral deflection (Figure 4.6). Six other displacement transducers were used at the both end studs and the middle-stud to measure plate-to-stud uplift. In addition, two displacement transducers were used to measure for bottom plate slip and its uplift from the foundation. The transducer locations are shown in Figure 4.6. A modified form of the ISO

16670 cyclic testing standard was used during the testing (ISO, 2003). Such modifications are permitted under section A.2d of the standard. The loading protocol used during the testing is shown in Figure 4.7 and Appendix A.1. Walls 601 and 701 were subjected to a monotonic load pattern with a testing rate of 15.2 mm/min and were used to obtain the necessary parameters such as yield and ultimate displacements. These properties were needed to define the cyclic protocols of their respective series. The cycle pattern used was as follows: One cycle at 1.25%, 2.5%, 5%, 7.5%, and 10% of the ultimate displacement from either wall 601 or 701, and then a series of three cycles at 20%, 40%, 60%, 80%, 100%, and 120% of the ultimate displacements. After each set of three cycles, one cycle at the previous displacement level was applied. The cyclic loading rate was 20 mm/sec.

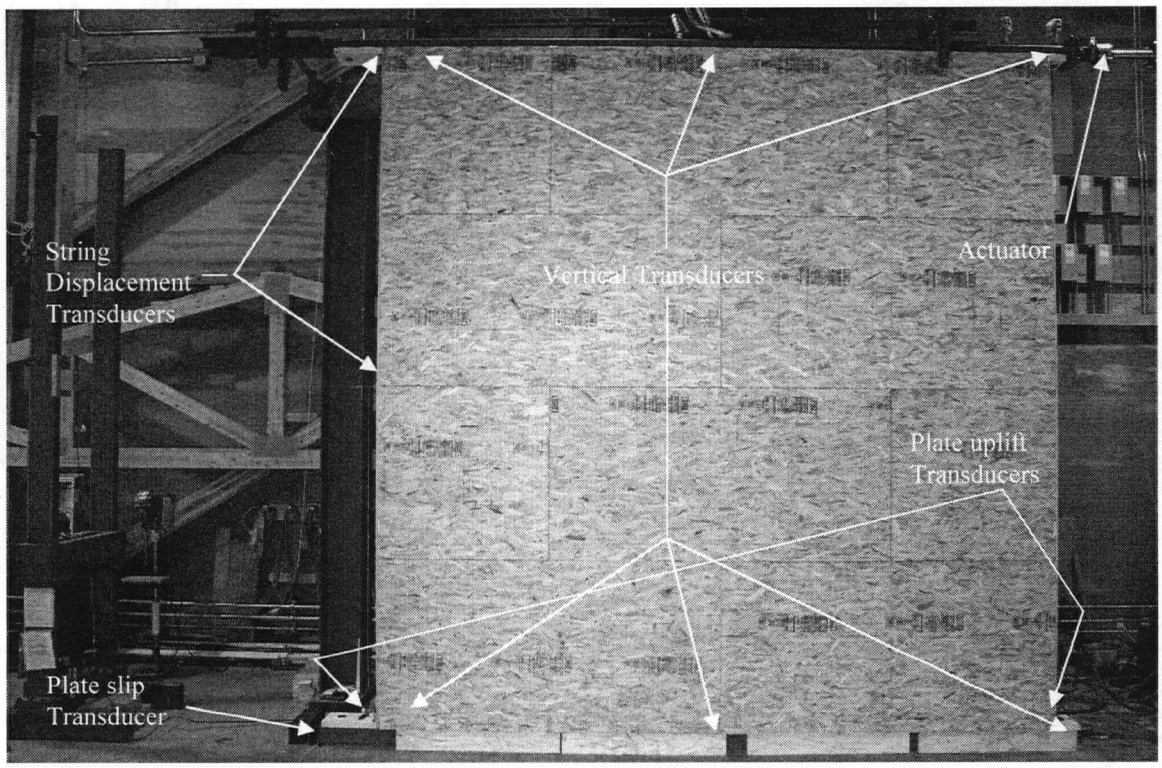

Figure 4.6: Tall wall test instrumentation locations

The loading prescription was provided through an MTS control system with a 110 kN hydraulic actuator providing the force for all tall walls (Figure 4.6). Walls 604 and 705 in addition were connected with a series of 13.3 kN hydraulic actuators oriented vertically between the wall studs. These actuators were to simulate a constant 20 kN/m vertical load. They were placed over the anchor bolt locations, thus becoming part of the anchorage system itself whilst

providing vertical load. The actuators were located every 610 mm on centre within the wall frame (Figure 4.8).

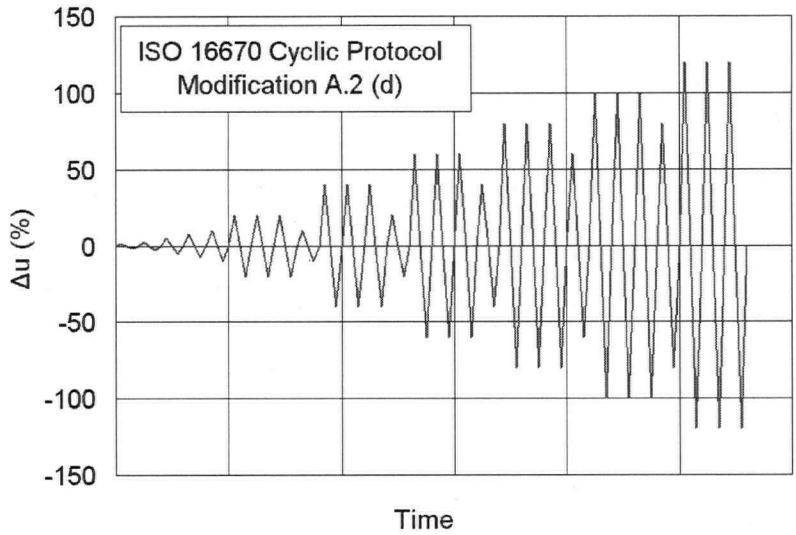

Figure 4.7: ISO 16670 standard with A.2 (d) modification

Figure 4.8: Vertical actuator assembly

4.3 Results and Discussion

4.3.1 600 Series

Some of the most important parameters obtained from the experimental testing are presented in Table 4.2 and Appendix A.2. The symbols used in the table are the following: P_{max} is the maximum load attained by the specimen; V_{LSD} is the tall wall specimen specified shear strength calculated as per the Canadian wood council 2001 Wood Design Manual (CWC, 2001); Δ_{max} is the wall displacement at maximum load as measured at the top of the wall; Δ_{ult} is the top displacement at 80% of the maximum load after maximum load has been attained; P_y is the load at yield; Δ_y is the wall yield displacement; μ is the ductility of the specimen ($\mu = \Delta_u/\Delta_y$); K_{in} is the walls initial stiffness and E is the hysteretic energy dissipated by the wall. The parameters P_y, Δ_y, μ and K_{in} were determined according to the European CEN standard (CEN, 1995) using the first and third envelope curves of the walls cyclic response. Under the specimen heading, the wall and envelope under consideration is described with E1 representing the first envelope and E3 representing the third envelope. The cycle heading indicates the difference between the first push stroke and the first pull stroke; + indicates the first stoke for a particular displacement, with – indicating the subsequent stroke in the other direction.

During the first test (monotonic test of wall 601), torsional failure of some of the studs was observed. The failure was attributed to the eccentricity that occurred between the plane of the sheathing and that of the single ties placed on the studs on the side opposite to the sheathing. Although this is not a problem in conventional shearwalls using relatively narrow 38 mm x 89 mm (2" x 4") studs, it should be taken into account when designing walls with increased stud depth. To mitigate this type of stud failure, certain studs on the remaining walls were connected with dual H6 ties, one on the back and one at the front of the stud. Even though there were issues with the design of wall 601 with regard to response, the monotonic data was still utilized to determine the cyclic loading protocol utilized for walls 602 to 605. This loading protocol was created via the aforementioned ISO 16670 standard (ISO, 2003). Wall 602 did not utilize dual ties on the middle stud of the wall, and as a result, it also experienced a torsional stud failure. No torsional stud failures were observed in the rest of the walls tested since the dual H6 tie formation was subsequently provided to the middle stud. Longitudinal cracking in some non-

tied studs in wall 605 was observed but only after the wall had failed and extensive displacements were imparted.

Table 4.2: Tall wall test results

Wall	Cycle	P_{max} [kN]	V_{LSD} [kN/m]	Δ_{max} [mm]	Δ_{ult} [mm]	P_y [kN]	Δ_y [mm]	K_{in} [kN/mm]	μ Δ_{ult}/Δ_y	E [kJ]
602 E1	+	38.2	4.86	94.4	97.3	27.5	27.8	0.987	3.50	25.0
602 E1	-	36.9	4.69	93.7	102.9	22.1	15.5	1.426	6.63	
602 E3	+	26.3	3.34	61.6	100.5	13.9	8.4	1.642	11.92	
602 E3	-	27.3	3.48	61.3	97.0	15.6	8.3	1.881	11.72	
603 E1	+	39.6	5.04	92.5	135.8	28.8	28.4	1.013	4.78	32.3
603 E1	-	36.6	4.66	93.9	121.7	21.9	16.8	1.300	7.24	
603 E3	+	30.3	3.86	93.0	106.0	14.9	9.7	1.544	10.99	
603 E3	-	28.9	3.68	93.3	104.6	15.3	9.2	1.673	11.40	
604 E1	+	42.1	5.35	93.1	131.7	30.6	26.3	1.163	5.01	34.9
604 E1	-	35.3	4.49	93.9	127.7	21.0	15.4	1.361	8.27	
604 E3	+	31.4	3.99	94.0	109.8	17.4	10.9	1.599	10.11	
604 E3	-	26.5	3.37	61.2	111.9	14.6	7.3	1.985	15.24	
605 E1	+	62.6	7.97	124.8	131.7	47.4	33.6	1.410	3.92	51.6
605 E1	-	52.5	6.68	93.5	136.5	32.8	19.0	1.727	7.18	
605 E3	+	49.6	6.31	92.4	118.9	29.1	15.0	1.937	7.90	
605 E3	-	44.1	5.61	93.5	116.8	24.8	12.5	1.991	9.38	
702 E1	+	53.4	6.79	89.8	98.7	35.2	18.4	1.919	5.38	29.6
702 E1	-	39.4	5.02	92.9	102.3	22.5	11.8	1.906	8.67	
702 E3	+	39.9	5.08	58.7	88.2	20.3	6.2	3.273	14.23	
702 E3	-	30.1	3.82	60.8	77.0	19.2	9.0	2.130	8.55	
703 E1	+	48.1	6.12	90.1	98.9	30.0	14.6	2.058	6.79	29.0
703 E1	-	48.0	6.10	91.9	100.4	32.6	15.8	2.069	6.38	
703 E3	+	35.2	4.48	59.2	67.7	17.9	4.5	3.970	15.00	
703 E3	-	39.6	5.04	61.6	70.0	24.5	10.0	2.439	6.98	
704 E1	+	64.6	8.22	91.1	100.3	44.3	23.7	1.869	4.23	45.8
704 E1	-	56.5	7.18	92.8	102.2	34.3	14.9	2.307	6.87	
704 E3	+	47.2	6.00	92.0	101.6	30.6	12.2	2.503	8.31	
704 E3	-	43.0	5.48	60.7	98.3	27.5	9.7	2.832	10.13	
705 E1	+	77.8	9.90	90.5	105.0	55.6	26.5	2.095	3.96	58.4
705 E1	-	70.8	9.01	89.7	94.5	43.0	14.8	2.907	6.39	
705 E3	+	64.8	8.25	91.6	100.4	41.8	17.3	2.422	5.82	
705 E3	-	61.0	7.76	91.4	100.2	36.6	11.3	3.228	8.84	
706 E1	+	83.2	10.59	91.3	100.5	58.0	22.6	2.562	4.44	51.6
706 E1	-	70.7	9.00	89.4	95.1	44.6	14.6	3.065	6.54	
706 E3	+	65.4	8.33	91.6	99.9	45.4	16.5	2.753	6.05	
706 E3	-	56.4	7.18	90.2	98.6	37.4	11.8	3.163	8.34	
707 E1	+	26.2	3.34	91.7	120.9	19.0	21.5	0.884	5.63	23.0
707 E1	-	22.4	2.85	61.9	104.7	15.3	16.4	0.932	6.37	
707 E3	+	19.3	2.46	60.6	89.2	10.9	8.3	1.315	10.75	
707 E3	-	18.2	2.32	61.7	83.2	12.3	11.5	1.067	7.24	
708 E1*	+	64.1	7.05	59.3	93.8	46.5	17.6	2.650	5.35	32.5
708 E1*	-	53.4	5.87	59.0	76.7	37.0	10.0	3.699	7.66	
708 E3*	+	45.0	4.95	61.3	70.9	33.6	11.3	2.983	6.30	
708 E3*	-	39.9	4.39	58.9	69.0	30.5	7.2	4.240	9.59	

* 15.9 mm type X gypsum wallboard placed on non-OSB sheathed side.

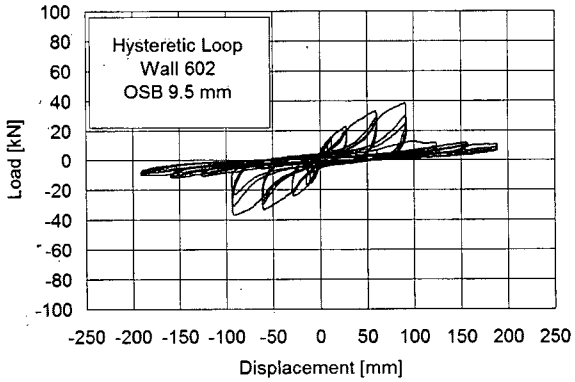

a) Wall 602

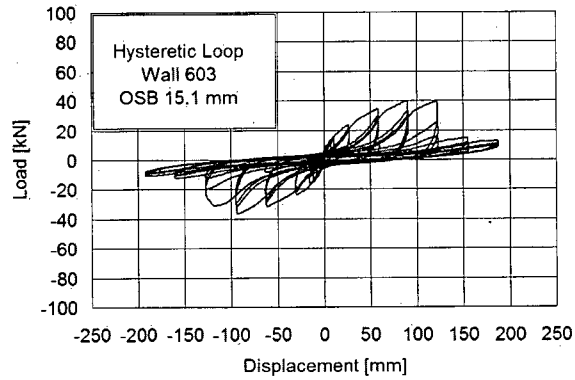

b) Wall 603

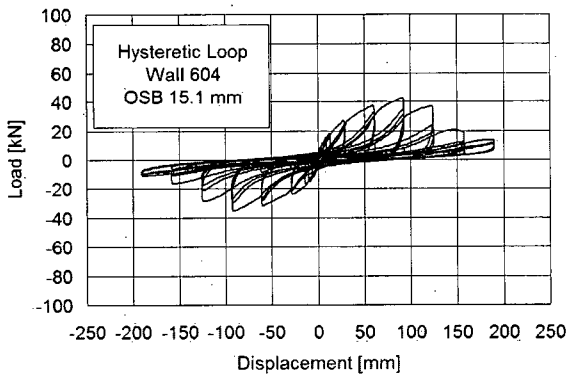

c) Wall 604

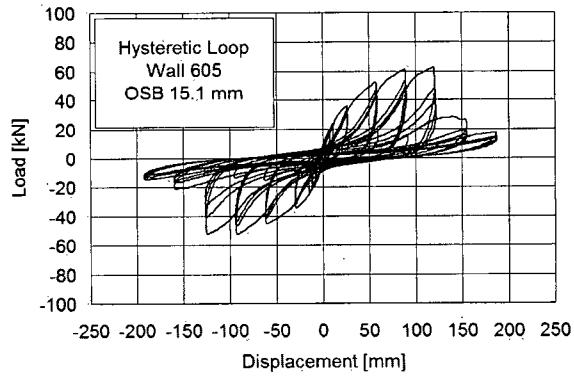

d) Wall 605

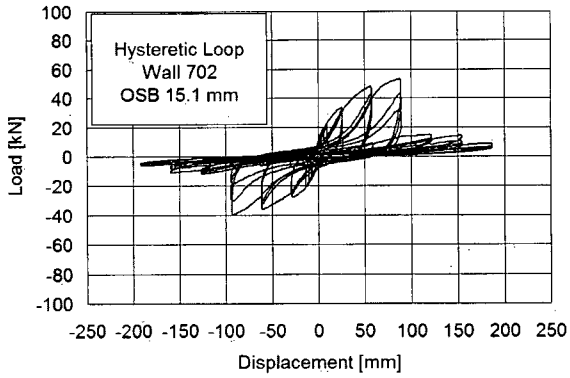

e) Wall 702

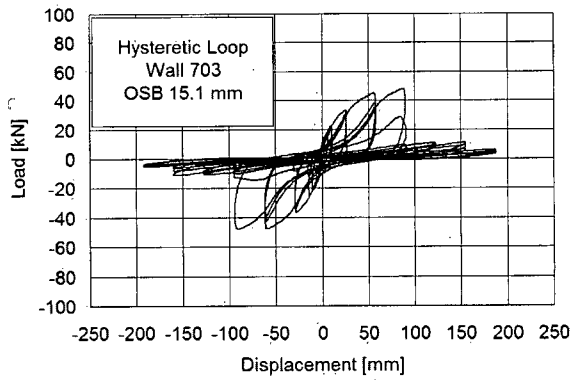

f) Wall 703

Figure 4.9: Load vs. displacement behaviour of tall walls 602-605, 702 and 703;

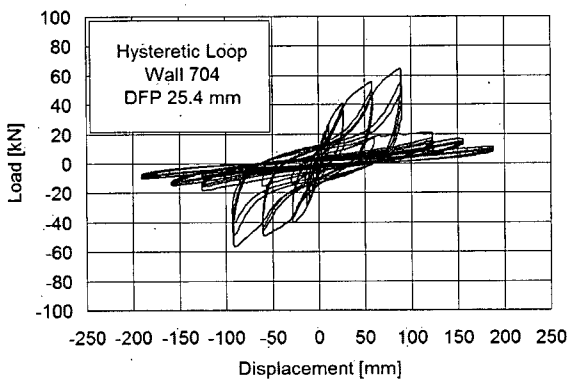

a) Wall 704

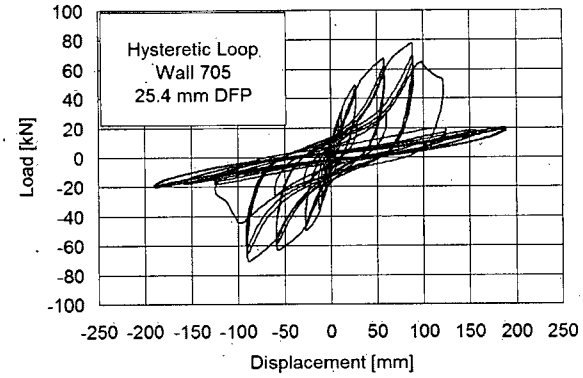

b) Wall 705

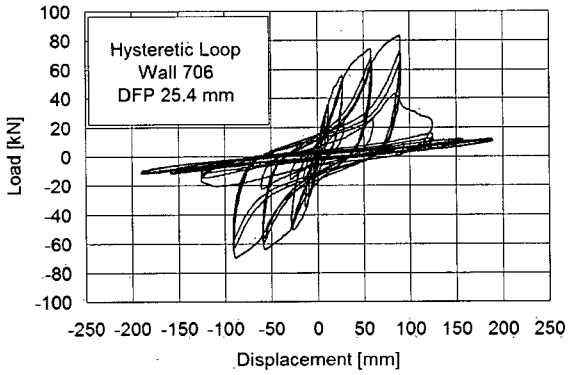

c) Wall 706

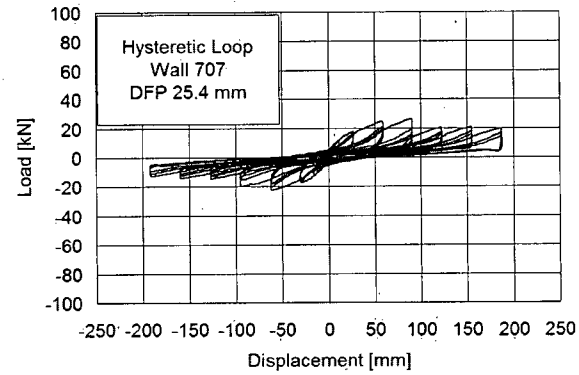

d) Wall 707

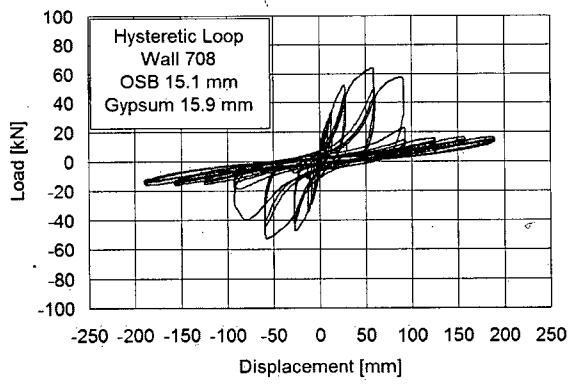

e) Wall 708

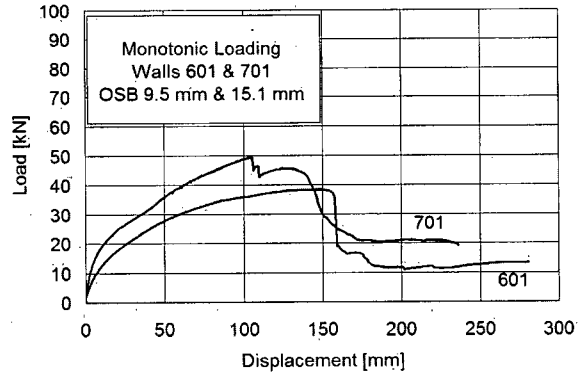

e) Walls 601 and 701

Figure 4.10: Load vs. displacement behaviour of tall walls 704-708, 601 and 701;

When comparing the 9.5 mm OSB sheathed wall 602 with wall 603, the main difference being the sheathing thickness, a couple general observations can be made. The 15.1 mm OSB sheathed wall 603 had higher energy dissipation (Table 4.2). In fact, when compared based on their load vs. displacement plots (Figure 4.9) walls 602 and 603 can be observed to follow similar loading paths with the main difference being that wall 603 was able to go though one

more complete cyclic loop cycle, indicating greater ductility and a greater drift ability. In the walls with the 15.1 mm thick OSB sheathing, the sheathing connections failed due to shear, fatigue and nail chip-out, after being exposed to a number of alternating cycles. These failures were predominantly observed in the bottom row of sheathing paneling, particularly at the end-stud-to-sheathing interfaces. This failure mode was different than that experienced in case of the walls with 9.5 mm OSB sheathing, where nails typically pulled through the sheathing, again most significantly at the end-stud-to-sheathing interfaces. For all the 600 series walls, with the exception of wall 604, the walls failed in a sheathing stepped pattern—each successive panel from bottom to top was pushed further to one side than the panel below. The deformed shape of the SPF walls in elevation (with the exception of wall 604) showed bending (bowing) of the wall studs in the lower half of the wall (Figure 4.11), reminiscent of an L-Shape. The upper half of the studs remained relatively straight during the testing. Wall 604, the wall with the 20 kN/m downward vertical force being applied, did not fail in the L-shape. The failure mode was comprised of the same types of nail failures as mentioned for the other 600 series walls, however, the location of failures concentrated along the mid-height blocking of the wall and created an S-shaped response appearance. The vertical load was of a value high enough that the lower connections were spared the necessary forces for failure due to beneficial downward force. Instead, the load distribution was as such that the mid-height of the wall was subject to the greatest force. The idea that vertical load can be beneficial is known and is often counted on in design. Further qualitative observations with regard to the 600 series walls saw that the lower sheathing-to-plate connections were the connections that failed. The connection steel hardware (the H6 ties and LU28L hangers) used proved effective with regard to performance, even though the connections are not specifically designed to act as part of the main anchorage systems. Uplift of the connections was kept to a minimum, with the only uplift being observed due to the pivoting of the stud on the plate. The anchorage setup also saw to inconsequential wall slip of the bottom plate and uplift of the plate from the foundation where the end-stud connected to the plate.

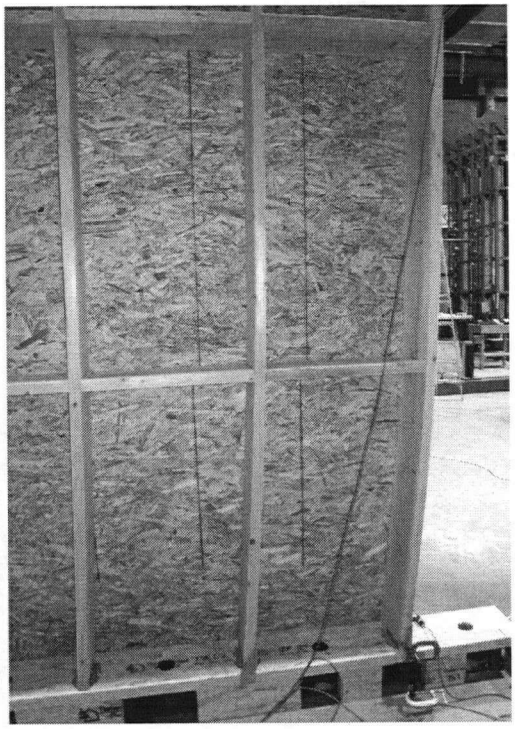

Figure 4.11: Typical bowing (L-shape) wall deflection

More quantitatively, it was found that the strength of a wall is generally linearly related to the nail usage. A percentage increase in the overall nail steel area (i.e. decrease in nail spacing or increase in nail diameter) used, resulted in an almost linear increase in strength. This linear relation seemed to apply to the strength characteristics as well as hysteretic energy dissipation, though the same cannot be said consistently for ductility or stiffness. The increase in nail area for wall 605 was 61.4% with respect to wall 603 and resulted in an increase in maximum load of 57.2% and in hysteretic energy dissipation of 59.7%. Load-deformation relationships for the all cyclically loaded walls, both SPF and LSL based, are shown in Figures 4.9 and 4.10.

Further review of Table 4.2, indicates that wall 605, with the densest nail spacing, had the best performance. It dissipated the most hysteretic energy with 51.6 kJ predominately due, but not limited to, its ability to handle another loading cycle (Figure 4.9), attained the highest load resistance and achieved the greatest drift level when compared to the other 600 series walls. Unfortunately, the increase in the nail usage did impact the ductility of the wall negatively. It showed lower ductility than most of the series' walls, especially when observing the third envelope responses. Wall 605 was also the stiffest wall as indicated by the initial stiffness parameter; however this can be beneficial as well as detrimental depending on resonance issues and desired flexibility. Aside from the aforementioned different failure pattern between walls 603 and 604, all parameters measured and calculated indicate that the addition of the vertical load did little to the general behaviour of the wall with a slight increase in maximum load, an observed increase in energy dissipation, as well as minimal changes in other parameters. In general, blocked tall walls with 38 mm x 234 mm No. 2 or better SPF studs spaced at 610 mm on centre were found to be effective lateral load-resisting systems. They were able to dissipate large amounts of hysteretic energy, especially when the nail spacing was reduced.

4.3.2 700 Series

Though not an issue with the 600 series walls, LSL wall 701 experienced a bottom plate failure due to much higher uplift loads on the tension side of the wall and the non-use of an anchor bolt outside the east end-stud. The forces at the connection resulted in the failure of the plate at the first interior anchor bolt as shown in Figure 4.12a. It was also found that the end-nailing pattern used for the blocking of the wall was not sufficient, as a nail pull-out out of the studs was observed (Figure 4.12b). This blocking failure coupled with the poor anchorage design resulted in a poor wall-frame response. Even so, the monotonic test data was still used as a means of determining the cyclic protocol necessary for the remaining 700 series walls. Other blocking nail patterns were introduced for the rest of the walls. Similarly, changes to the anchor bolt pattern were made for all remaining walls of the 700 series as outlined in the test setup section.

a) b)

Figure 4.12: a) Wall 701 bottom plate failure; b) Wall 701 blocking failure

Wall 702, which had 15.1 mm OSB sheathing, had lower maximum load capacity and energy dissipation compared to wall 704, which had 25.4 mm DFP sheathing (Table 4.2, Figures 4.9, 4.10 and 4.13); however. wall 702 was more ductile. The higher energy dissipation was attributed to the different action and failure mode of the nails, as well as a slight increase in the effective nail percentage due to the increased nail size. It was necessary to use 3.0 mm diameter nails as opposed to 2.5 mm diameter nails since nail lengths necessary for the 25.4 mm DFP sheathing could not be obtained in a 2.5 mm diameter spiral nail. In walls with thinner OSB

sheathing, the nails tended to develop one plastic hinge along the length, but in the case of the walls with 25.4 mm thick DFP, the nails were observed to develop up to four plastic hinges along the shank (Figure 4.14). Both sheathing thicknesses were able to prevent nail pull-through failures, thus allowing the nails to reach loads that resulted in nail failures. The nails that failed in shear/fatigue in the 25.4 mm DFP walls (generally on the end-studs and along the bottom sheathing-to-plate interface) failed not only in single shear, but often in double shear with one shear plane within the DFP and the other at the sheathing-to-framing interface. Wall 705, that utilized large diameter nails, had the highest hysteretic energy dissipation of all walls; however, the common nails used in this wall experienced many withdrawals. This was not the case for other walls where spiral nails were used.

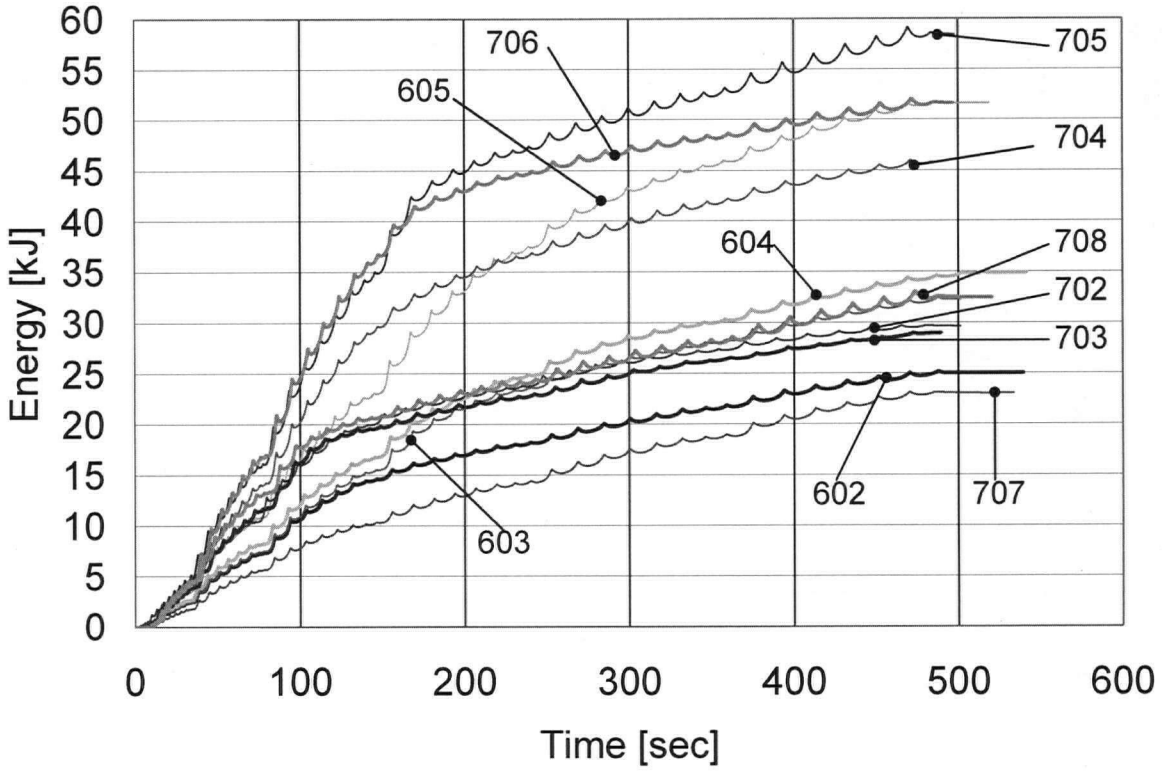

Figure 4.13: Tall wall hysteretic energy dissipations

Wall 706, having the largest centre-to-centre stud spacing of all walls (2440 mm instead of 1220 mm), was also able to carry the highest load of all walls. This is attributed to the combination of 25.4 mm DFP sheathing, larger diameter nails and smaller nail spacing. The use of large stud spacing did not seem to have any significant negative consequences on the wall's cyclic loading performance. The comparison of wall 704 with wall 706, based on the numerical values found

in Table 4.2, show higher maximum loads, stiffer response and higher hysteretic energy dissipation, though marginally, for wall 706. When using tall walls with large (2440 mm) stud spacing, it should be noted that some issues related to load transfer from the roof have to be addressed. Due to the larger span of the top plate, the use of two top plates is recommended. The only unblocked wall tested, wall 707, experienced the lowest maximum load and hysteretic energy dissipation of all other walls (Table 4.2, Figures 4.9, 4.10 and 4.13). Its behaviour was in correlation with previous findings from tests on 2.44 m unblocked shearwalls (Ni et al., 2000). The use of an engineered wood product such as LSL should be carefully thought out in the case of unblocked tall walls. The effect of using a higher strength (and relatively more expensive) product is offset by the lower wall strength and overall performance due to lack of blocking.

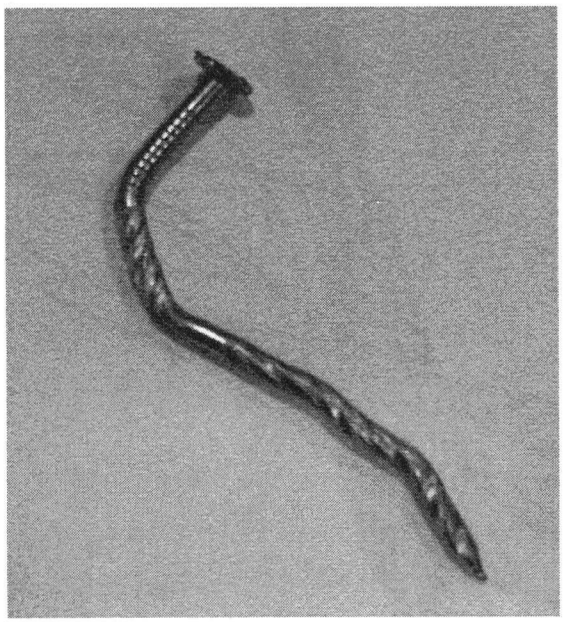

Figure 4.14: Typical plastic hinges for nails in 25.4 mm DFP

Similar to the 600 series walls, the 700 series walls performed adequately, with small design changes being necessitated by observed wall response. The dual H6 tie and HU9 stud-to-plate connections proved, once again, to be very efficient and cost effective as a means of mitigating the vertical uplift forces. As improvements were made the anchorage pattern also proved effective. The east end-stud anchorage pattern walls 705 to 708 utilized was an unbolted span of 254 mm and consequently experienced no further uplifting issues. The studs for the 700 series walls in general did not experience uplift from the bottom plate, but acted similar to the 600 series walls. Wall 706, however, proved to be inadequate with regards to the stud-to-plate connections. The dual H6 ties, the main vertical/lateral force resisting element, yielded and allowed a significant uplift to be experienced. In addition to the observed yielding, the nails withdrew from the H6 ties, thus leading to eventual failure. The observed yielding is beneficial since it is an indication of ductile performance.

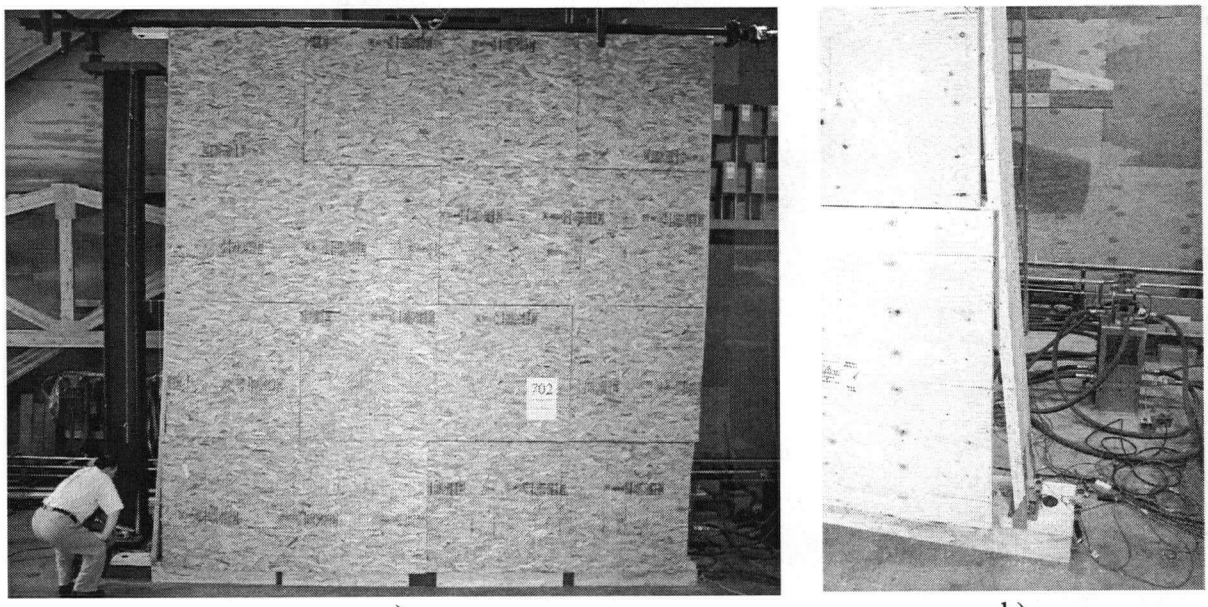

a) b)

Figure 4.15: a) Typical tall wall deformed pushover state; b) Sheathing-to-framing failure from end-stud

When 15.9 mm type X gypsum wallboard was applied to the opposite side of wall 708, an increase in initial stiffness was observed in contrast to the equivalent non-wallboard reinforced wall 702. An increase in maximum load and hysteretic energy dissipation (Table 4.2) was also found; though, ductility did suffer marginally. The maximum load occurred at a lower displacement when compared to the non-gypsum equivalent wall 702, 59 mm as opposed to around 90 mm. The type X gypsum wallboard failure mode was screw tear-out at lower displacement levels than those of the OSB sheathing. After the gypsum wallboard failure, the OSB sheathing was able to withstand another load cycle. The observed force levels were similar to wall 702, with the peak load levels at around 90 mm being for the compressive and tension cycles, 53.4 kN and 39.4 kN for wall 702 and 57.1 kN and 39.8 kN for wall 708 (Figures 4.9 and 4.10). While the wallboard gives a stiffer wall and an approximately 20% increase in maximum load for the first cycle direction, its overall behaviour, once the wallboard has been damaged/loosened, reverts back to the expected behaviour of a non-wallboarded wall. The NBCC-2005 gives the option of disregarding the type X wallboard in design analysis. The seismic force reduction factor, R_d, can being taken as 3 rather than 2. This option should be chosen with care, since it was shown that true wall behaviour has been altered by the addition of the wallboard.

Figure 4.16: Adapted washer design at end-stud locations

The stud spacing of 1220 mm used throughout the 700 series walls did not appear to cause any detrimental wall behaviour under cyclic loading. Similar ductility values were found for each type of sheathed walls, with the OSB sheathed walls performing, generally, in a slightly more ductile fashion than walls with DFP. Ductility was apparently related to the material of the sheathing used, the material of the studs, wall stud geometry and the type of fasteners used. Wall 706, with a stud spacing of 2440 mm, was found to have a ductility level similar to that of other walls in this test program. It also carried the highest level of lateral load and dissipated a high 51.6 kJ of hysteretic energy, with only wall 705 dissipating more. Wall 705 did have a significant percentage more nail area. It used larger diameter nails and as a result had the greatest overall cross-sectional area of nail steel present in the respective walls. The deformed shape of the LSL walls in elevation was similar to that of the SPF walls and included bending of the studs in the lower half of the wall (Figure 4.15a). The upper half of the wall remained relatively straight during the testing. The wall failure mode included connection failures of sheathing-to-plate fasteners along the bottom of the wall and up the sides (Figure 4.15b). Unlike the SPF walls, where the wall failure mode and failure location were affected by the addition of the 20 kN/m vertical load, the same load level did not have any significant effect on the 700 wall series. Larger vertical loads, that unfortunately exceeded the capacity of the test frame setup, would have been necessary for the LSL studded walls to receive any positive effect from the vertical load.

As implied earlier, the capacity and overall performance of the inexpensive off-the-shelf connectors used in the testing program were satisfactory. The dual H6 tie configuration wrapped under the bottom plate along with the joist hangers and the dense nailing pattern used, provided for an effective connection detail. With the exception of wall 706, no significant uplift of the studs occurred in any of the tests when such anchorage was provided. High uplift loads did

cause minor transverse bowing of the bottom plate in some instances. Wider washers for the anchor bolts were used to mitigate this issue (Figure 4.16).

4.3.3 600 and 700 Series Comparison

Both the SPF-based blocked walls and the LSL-based blocked walls performed well when subjected to lateral loading. When nail spacing was decreased, such as in SPF wall 605, SPF walls withstood force levels and dissipated hysteretic energy comparable to that of the LSL walls that used a less dense nailing pattern. An hysteretic energy comparison and load vs. displacement comparison between walls 605 and 702 effectively illustrates this point (Table 4.2, Figures 4.9, 4.10 and 4.13). A simple material cost analysis shows that wall 702 is approximately 57% more expensive in material than wall 605. A costing of the walls is given in Table 4.3 and it effectively illustrates the SPF and LSL-based wall cost differences. As shown in Table 4.3, the cost of the LSL walls can be more than double that of SPF walls, even before construction time and labour factors are included. This is significant to mention since cost issues related wall materials are often a bigger concern than the labour related to driving more nails into a wall. This cost and weight advantage of SPF-based walls can be utilized in applications where the larger vertical and lateral load-carrying capacity of the LSL-based walls is not required. Wall 702 when compared to the similar, aside from the difference in stud material and stud spacing, wall 603, displays a definite increase in maximum load capacity in the first loading cycle direction, 53.4 kN to 39.6 kN; but on the subsequent cycle, this advantage is markedly smaller. Hysteretic energy dissipation is in fact larger in wall 603, at 32.3 kJ, as opposed to 29.6 kJ for wall 702. As for ductility, the walls are comparatively close as well; with initial wall stiffness perhaps being the greatest difference between the two walls. Wall 702, the LSL-based wall, is much stiffer than wall 603. This, by no means, shows that SPF walls are to be taken as superior to that of LSL-based walls; it merely shows that SPF stud-based walls can be utilized effectively. LSL stud-based walls, if nailed in a denser pattern, would be expected to perform better than a wall based around SPF studs with all other parameters held constant.

Table 4.3: Tall wall material costing in Canadian dollars at time of construction*

Wall	Hardware [$]	Sheathing [$]	Framing [$]	Total [$]
601	118	137	367	621
602	160	137	367	663
603	129	201	367	696
604	129	201	367	696
605	131	201	367	698
701	214	201	683	1098
702	214	201	683	1098
703	214	201	683	1098
704	216	419	683	1319
705	219	419	683	1322
706	134	419	547	1100
707	128	419	478	1026
708	217	342	683	1242

* Time of construction was March 2005 to September 2005

When walls utilizing the larger 25.4 mm DFP are compared to the smaller SPF studded walls comparative similarities breakdown. The SPF walls would not be well suited to accommodate the larger sheathing due to the tendency to split the studs when utilizing the necessary larger diameter nails. As a result, the larger sheathed LSL walls are capable of attaining significant increases in hysteretic energy dissipation, maximum loads, yield loads and stiffness. Even ductility needs to be carefully examined. Although the ductility of the LSL-based walls is generally lower than that of the SPF-based walls, the maximum loads and displacements permitted through the use of the larger members and sheathing for the LSL walls can counter ductility concerns. The specified shear strengths per unit length, V_{LSD} (Table 4.2), is usually an important quantity to investigate. To derive V_{LSD}, Equation 1 was utilized where L_w is the length of the shearwall element.

$$V_{LSD} = 1.863\left(\frac{P_{\max}}{3L_w}\right) \tag{1}$$

Specified shear strengths determined through use of the Wood Design Manual, 2001 (CWC, 2001) is difficult and does not serve a design interest in the case of the tall walls of this study. The tabulated design values and the corresponding guidelines do not provide for walls of this scale and for the materials used.

It must be noted that the ductility results that have been commented on are based on numeric definitions resulting in often large differences between loading directions. The large discrepancies are due to the significant differences found between the first and third quadrant responses with regard to load and displacement. Responses based on the first quadrant, and that correspondingly have larger peak loads, usually have lower initial stiffness, that in turn result in larger yield displacements and smaller ductility's. The drastic differences in ductility's, when observing the load vs. displacement plots (Figures 4.9 and 4.10), are not intuitive, but depend upon the definition on numerical definitions provided by the European CEN standard (CEN, 1995). Though differences in wall responses due to loading direction are often encountered, the degree of differences found in some of the walls in this study, such as wall 706, give pause to the assigning ductility of a wall based on purely numerical methods. As a comparative tool, however, it is still effective so long as the quadrants are compared as a couple.

Splitting and warping of the SPF studs due to material irregularities and on-site construction technique can lead to poor fitting, delays in construction, and consequently, potential loss of strength. All the walls constructed in the manner tested can be prefabricated within a factory setting to mitigate some of these issues, then transported and tilted up on the construction site. This option allows these wall systems to further compete directly with conventional tilt-up concrete walls and steel braced frames.

4.4 Summary

Tall walls constructed for the purpose of mitigating in-plane dynamic forces appear to be viable. Dimension lumber, SPF 38 mm x 234 mm No. 2 or better studs and engineered LSL 44 mm x 242 mm studs performed well when used in conjunction with the sheathing and nailing configurations of this testing program. SPF studs spaced accordingly, at no more than 610 mm on centre, allow walls to dissipate large quantities of energy and withstand large lateral loads. LSL studs also reacted well to the prescribed loading patterns, at stud spacing ranging from 1220 mm on centre to 2440 mm. SPF-based walls utilizing sheathing thicknesses larger than 9.5 mm were found to be competitive with LSL-based walls when anticipated lateral loads and vertical loads are relatively low, due to the significant cost increase when utilizing LSL studs. However, the LSL studs and subsequent larger sheathing and nails are promising for structural

situations requiring large vertical load capacity and large lateral load capacity—essential for large structures in seismically active regions. These walls appear to act in manners appropriate for use in markets utilizing tilt-up concrete walls. The 2001 Wood Design Manual (CWC, 2001) is found to be limited in its use with regard to predicting tall wall behaviour due to a lack of reference material.

The use of the relatively simple connection and anchorage system employed through this testing program was shown to be a convenient and efficient setup when designed accordingly. The setup provides for the mass production of walls similar to conventional interior wall construction and consequently reduces costs. It also provides for a ductile element that could possibly be designed for; that being the H6 ties.

5. STUD-TO-PLATE CONNECTION TESTS

5.1 Introduction

The tall walls that are tested in this project utilize stud connections of unconventional design. The stud-to-plate connections shown in Figure 5.1 are generally not thought of as a means of structurally connecting studs to plates, primarily at the ends of walls, where specialized anchorage connections are usually found. The system of construction used to build the tall walls of this project lends itself to modular construction techniques with the stud-to-plate connections being an important element to this. By not using conventional anchorage connections at the ends of the walls the mass-production of these particular tall walls can be done within the efficient confines of manufacturing plants or on-site. The purpose of this testing program element was to determine the properties of the particular connection setups utilized in the full-scale tall-wall testing phase. The knowledge obtained may be used to adjust future software model parameters with regard to connections and system stiffness. It also provides an opportunity to investigate an alternative function of a readily available commercial product. The results may lead to less expensive wall erection and subsequent foundation connection.

5.2 Specimens and Test Setup

A relatively small testing sample size was utilized for this testing phase. Five SPF stud-to-1.7E LSL plate specimens (Figure 5.1a) and four 1.7E LSL stud-to-1.7E LSL plate specimens (Figure 5.1b) were created for the purpose of destructive monotonic testing. All specimens were 900 mm in total height and of conventional width; 234 mm for the SPF studs and 242 mm for the LSL studs, with the bottom LSL plate being 600 mm in length with a width of 242 mm. The metal hardware utilized included two H6 hurricane ties and either one LU28L (SPF-to-LSL connection) or HU9 (LSL-to-LSL) Simpson joist hanger. The hangers that are used provide very limited uplift resistance but provide for a standardized and uniform connection matrix. In addition, they act against out-of-plane forces. It should be noted that for two tested tall walls (walls 601 and 602), the connection form of one H6 tie and one LU28L was utilized. This connection setup was not tested since it was observed to perform less than adequately during the tall wall tests and as such is not considered a viable connection option.

Table 5.1: Stud-to-plate connection test matrix

Specimen Group	Number of Specimens	Stud Material	Ties	Hangers
Uplift 3 - 6	4	44 mm x 242 mm 1.7E LSL	2 x H6	1 x LU28L
Uplift 7 - 11	5	38 mm x 234 mm No.2 SPF	2 x H6	1 x HU9

The H6 ties when installed were each nailed by a full arrangement of sixteen 38 mm common nails into the stud and plate. Three or four nails on the underside of the plate needed to penetrate both the plate as well the other H6 tie due to overlap. The LU28L hanger when installed was nailed by fourteen 38 mm common nails into the stud and plate. The HU9 hanger when installed had ten 38 mm common nails into the stud and twenty-four No. 8 coarse thread wood screws into the plate. A complete listing of the specimens and significant sample descriptors is provided in Table 5.1.

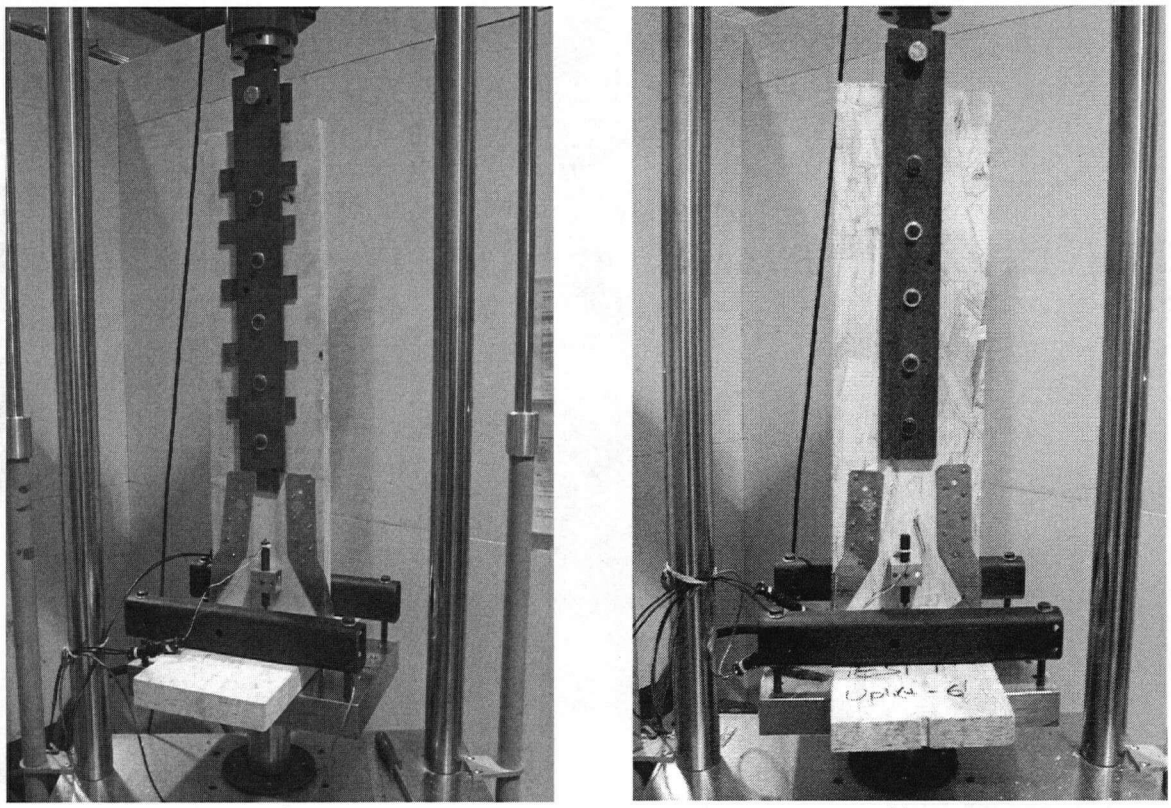

a) b)

Figure 5.1: a) SPF stud-to-LSL plate connection; b) LSL stud-to-LSL plate connection

The testing was carried out in a setup utilizing an 89 kN actuator. The actuator was connected to the specimens by two steel plates with five 12.7 mm grade 5 bolts. The studs of the samples had five corresponding bolt holes drilled to accommodate the connection setup and the bolts

were hand tightened. The plate was restrained by two hollow steel sections that were bolted into the steel base plate of the actuator setup by hand. This bolting action and securing of the specimen was done with care so not to implement unwanted tensile or compressive forces in the samples prior to testing; constant actuator adjustment was necessary. The test setup with specimens ready for testing is shown in Figures 5.1a and 5.1b.

The monotonic testing was performed on the two sets of test specimens. The ramping speed of the tests was 12.7 mm/min and allowed for a good representation of the connection behaviour. Data acquisition was done via Forintek software. Five parameters were recorded, including the stroke of the actuator head, the load applied as well as three displacement transducer measurements—one on either side of the stud measuring stud-to-plate uplift and one transducer measuring plate uplift from the steel base plate of the test setup. In Table 5.2, the displacement values given are based on the actuator movement due to observed non-symmetric uplift response of the stud with regard to the two transducers measuring stud uplift.

5.3 Results and Discussion

The SPF stud-to-1.7E LSL plate connections and the 1.7E LSL stud-to-plate connections tests indicate that both types of connections are relatively consistent in loading response, with the LSL-to-LSL connections being more so. The SPF stud connections gave average maximum load capacity values of 29.5 kN at an average displacement of 16.0 mm, whereas the LSL stud connections gave 51.3 kN capacities at average displacement values of 17.8 mm. This information is provided in Figure 5.2, Table 5.2 and Appendix A.3. As can be seen, the LSL-based connections are far stronger, by an average of 74%. Table 5.2 displays force and displacement results: P_{max} is the mean maximum sustained force; Δ_{max} is the mean displacement at the maximum force; Δ_{ult} is the mean displacement at 80% the maximum load after the peak load has been attained; P_y is the mean yield displacement; Δ_y is the mean yield displacement; K_{in} is the mean initial stiffness of the connection; and μ is the mean ductility. P_y, Δ_y, K_{in}, and μ are all calculated via the European CEN standard (CEN, 1995).

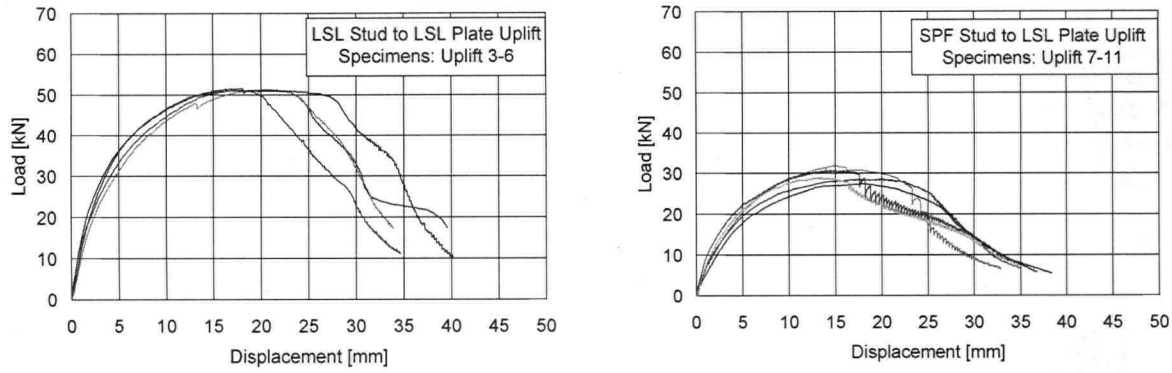

a) b)

Figure 5.2: a) LSL stud load vs. displacement test results; b) SPF stud load vs. displacement test results

Table 5.2: Average stud-to-plate connection test results

Specimen Group	P_{max} [kN]	Δ_{max} [mm]	Δ_{ult} [mm]	P_y [kN]	Δ_y [mm]	K_{in} [kN/mm]	μ
Uplift 3-6	51.3	17.8	27.0	35.9	3.8	9.3	7.4
Uplift 7-11	29.5	16.0	23.6	22.2	4.2	5.5	5.2

On a quantitative level the SPF-studded connections and the LSL studded connections did not perform similarly with major differences found in the capacity limits. In addition, the LSL-based connections were found to be stiffer and more ductile than that of their SPF based counterparts. Qualitatively, failure for both connection types first occurred in a manner where the nails in the H6 tie furthest from the sheathing side slowly withdrew from the stud. Continuation of the testing led to the eventual withdrawal of the nails from the sheathing side H6 tie. This failure tended to occur in a slow, controlled manner and can be observed in the graphical representations of Figures 5.2a and 5.2b. The plateau in load responses represents this slow progression of nail withdrawal. In addition, in both test scenarios the hangers did not provide significant uplift resistance. The nails tore out the bottom of the SPF studs, whereas in the LSL studs the hanger's nails withdrew (Figures 5.3a and 5.3b). Also observed was a non-symmetrical uplifting behaviour for all specimens. The vertical uplift progression of the tests showed that the studs bowed toward the stud side that did not have the H6 straps. Elongated nail holes were also observed in all studs post-test. This was more pronounced in the SPF studs. This observation is numerically displayed by the lower stiffness response of the SPF-based connections. The SPF studs allowed for wood compression and consequently a less stiff connection.

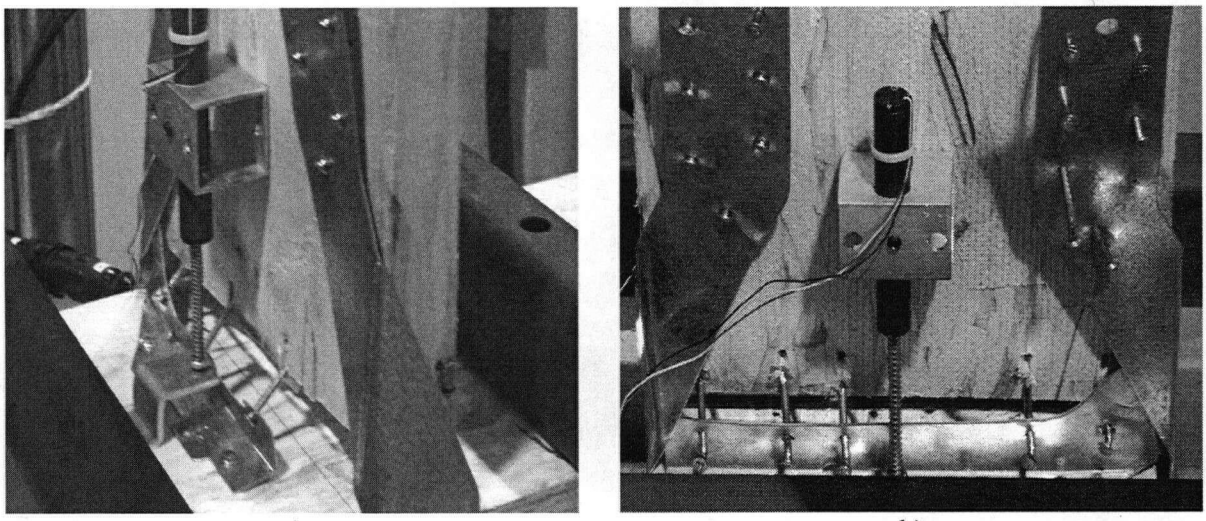

a) b)

Figure 5.3: a) SPF stud based connection nail withdrawal with LU28L hanger; b) LSL stud based connection nail withdrawal with HU9 hanger

Of last note is that since the SPF connections could not attain the same level of force as the LSL-based connections; the compressive force experienced by the LSL plates by the wrapped H6 ties was significantly less. As a result, the SPF based connection's LSL plate was not as compressed by the ties as the LSL based connections. The compressive behaviour can be seen in Figure 5.4.

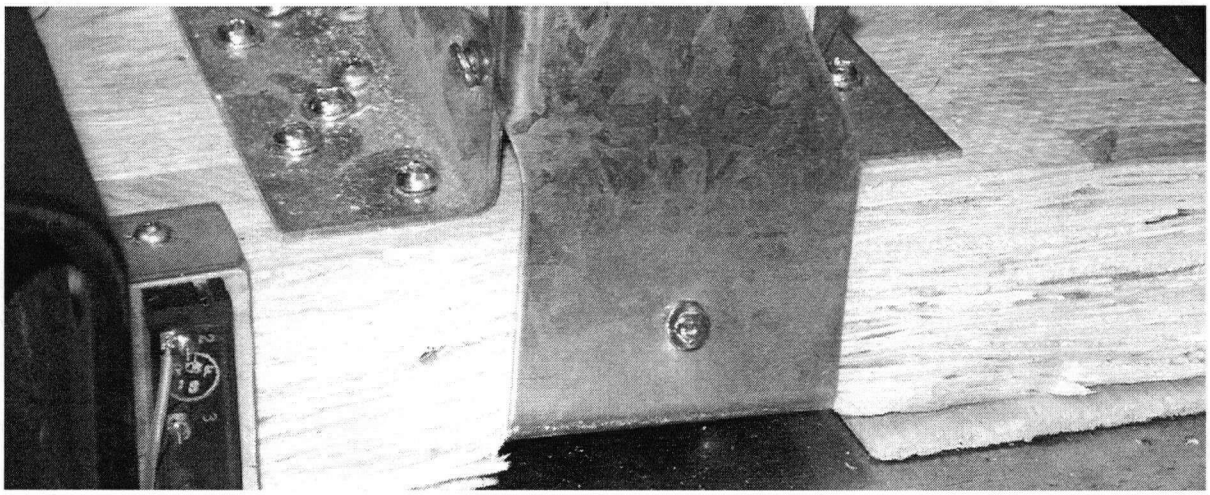

Figure 5.4: H6 tie compressive interaction with LSL plate

5.4 Summary

The results found in Table 5.2 show that these types of connections are able to withstand significant forces and should be investigated further as a means of restraining the vertical/lateral forces of large shearwalls. This connection setup must also rely on a conscientious anchorage choice for the bottom plate to foundation interface. During the full-scale tall wall tests, limited bottom plate bowing was observed in some tests. To mitigate this, closer anchorage (in this case, bolts) should be used to limit the potential bowing development. As alluded to in the full-scale wall test section these connections have the potential to be significantly less expensive than those in structures that use conventional end-stud hold-downs and anchorages. However, also ascertained from the testing is that for structures needing to withstand larger in-plane forces than those tested for would still be required to use conventional anchorage techniques. The development of thicker gauge ties and the coupling of two bottom plates could address this issue and should be further researched.

6. SHEATHING-TO-FRAMING CONNECTION TESTS

6.1 Introduction

Mechanical fasteners such as nails are the most prevalent form of connecting wood structures. This tall wall project is no exception, with the wood-based shearwalls being constructed primarily with nails. To understand the responses expected from the tall wood-based walls both in conceptual design and practice, a better understanding of the basic sheathing-nail-framing connection is required. Since this tall wall project focuses on in-plane cyclic testing to give an indication of seismic performance, the cyclic response of the individual connections used is desirable. Monotonic tests have been performed on some of the connections used in this study in the past (Leonard, 2004), however, the cyclic loadslip response of the connections is needed to be able to model accurately the true response of the walls under cyclic loading. The connections tested are found in the full-scale wall tests of this study, but also include connection designs not found. The purpose of this is to permit the analytical analysis of a greater array of tall walls, utilizing software that requires individual connection response parameters. It is infeasible to test every plausible tall wall setup, so the analytical behaviour of unconstructed walls is important.

6.2 Specimens and Test Setup

In total, 28 monotonic sheathing-to-framing connection tests were conducted and 42 cyclic sheathing-to-framing connection tests were performed. The total number of tests was deemed sufficient to gain the required information for the purpose of modelling and analysis. More tests could be performed so as to increase the library of known connection type responses. Within the number of samples indicated two test specimen configurations were present. A longitudinal specimen type (Figure 6.1a) and a perpendicular specimen type (Figure 6.1b). The difference between these two test setups is that the longitudinal specimens have the stud subjected to loading that is parallel with the stud as opposed to loading perpendicular to the stud as found in the perpendicular specimens. The longitudinal connection test results were primarily used since the tall wall load path predominantly corresponds with this direction, and as such the focus of the results from this testing phase is the longitudinal connection response, more specifically the cyclic response. The full compilation of test specimens, their orientations as well as other

descriptive particulars are given in Table 6.1. The test specimen group names found in Table 6.1 that end in PARA are the longitudinal test specimens, while the PERP specimens are the perpendicular.

Table 6.1: Sheathing-to-framing connection test matrix

Specimen Group	No. of Tests		Stud Type	Sheathing Type	Nail Properties		
	Mono	Cyclic			Diameter [mm]	Length [mm]	Type
APARA	2	3	LSL	25.4mm DFP	3.0	76	Spiral
APERP	2	3	LSL	25.4mm DFP	3.0	76	Spiral
BPARA	2	3	LVL	25.4mm DFP	3.0	76	Spiral
BPERP	2	3	LVL	25.4mm DFP	3.0	76	Spiral
CPARA	2	3	LSL	25.4mm DFP	3.75	76	Common
CPERP	2	3	LSL	25.4mm DFP	3.75	76	Common
EPARA	2	3	LSL	15.1mm OSB	2.5	65	Spiral
EPERP	2	3	LSL	15.1mm OSB	2.5	65	Spiral
FPARA	2	3	LVL	15.1mm OSB	2.5	65	Spiral
FPERP	2	3	LVL	15.1mm OSB	2.5	65	Spiral
HPARA	2	3	SPF	15.1mm OSB	2.5	65	Spiral
HPERP	2	3	SPF	15.1mm OSB	2.5	65	Spiral
IPARA	2	3	SPF	9.5mm OSB	2.5	65	Spiral
IPERP	2	3	SPF	9.5mm OSB	2.5	65	Spiral

The specimens were constructed and tested over the course of six weeks. Preparation of the samples included the LSL and laminated veneer lumber (LVL) stud representatives being trimmed to dimensions of 76 mm x 280 mm x their respective depths; nominal depths of 44 mm for the LSL studs, and 41 mm for the LVL studs, and 114 mm x 280 mm x 38 mm for the SPF studs. The sheathing samples, 9.5 mm and 15.1 mm OSB as well as 25.4 mm DFP, were also created with the dimensions of 102 mm x 280 mm x their respective thicknesses. These specifications are in close agreement with the dimensions given under standard ASTM D1761 (ASTM, 2002), however are altered slightly to be accommodate the testing apparatus.

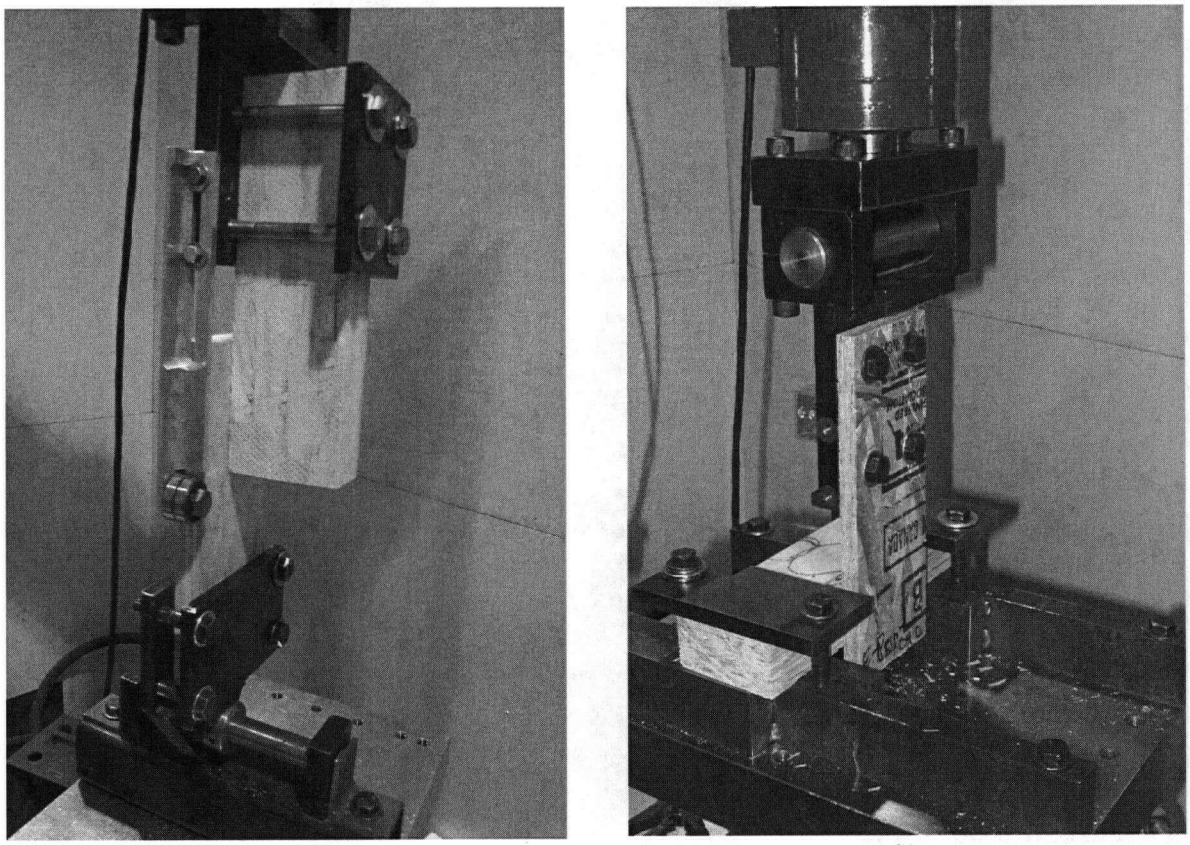

a) b)

Figure 6.1: a) Longitudinal loading test setup; b) Perpendicular loading test setup

The two wooden material constituents, the sheathing and stud materials, were then connected by one nail. The nailing procedure followed the same method as walls were constructed in practice, with the usage of a nail gun. Three nail sizes were utilized in the test specimens. These included the following: 65 mm x 2.5 mm and 76 mm x 3.0 mm spiral nails, and 76 mm x 3.75 mm common nails. The embedment lengths of the nails into the studs were thus kept greater than 50 mm.

The testing apparatus utilized was based around the same 89 kN actuator setup as that of the stud-to-plate connection tests. Bracketing used in previous studies to attach the samples to the actuator was also utilized. Figures 6.1a and 6.1b show the testing setup that resulted from the specimens produced. The total specimen length for the longitudinal specimens was approximately 460 mm, whereas the perpendicular specimens were approximately 280 mm. In the longitudinal test setup, both the stud and the sheathing were restrained by compressive friction force. This was accomplished by hand tightening the respective bolts. The

perpendicular specimen's sheathing was restrained by four bolts hand-tightened through drilled holes in the sheathing, whereas the stud was restrained by two restraining hollow steel sections overlapping the stud, acting as hold-downs. In both test setups, a careful balance of specimen securing and applied actuator force was done. The lateral guides observed in Figure 6.1a were utilized for the cyclic testing phase of the longitudinal tests. Since only one nail was used, care needed to be taken to prevent in-plane buckling of the sample upon compressive actuator action, with the hand-tightening of the respective clamping components also aiding in this.

The measurements obtained from the tests include the stroke of the actuator head, the relative displacement of the sheathing and stud, as well as the load applied. The relative displacement of the sheathing-to-framing could only be carried out on the monotonic tests due to apparatus geometric constraints. The data was collected via Forintek data acquisition software in a form easily manipulated to spreadsheet format. The testing comprised of two distinct phases. The monotonic tests were performed first. The loading rate of 12.7 mm/min was applied. It was consistent for all tests and was within the limits set out by standard ASTM D1761. The data obtained from the monotonic tests was used to create the loading protocol for the cyclic testing phase. The cyclic testing protocol used was derived using the monotonic test data from the corresponding specimen groups and subjected to the ISO standard 16670 specifications for the determination of the testing protocol. This proved a poor choice when the initial cyclic tests were performed with the APARA specimen grouping. The hysteretic behaviour and data plot that resulted after directly implementing the ISO standard 16670 loading protocol gave an insufficient number of hysteretic loops and created a hysteretic energy plot that proved difficult to utilize. As a result, the ISO standard 16670 protocol was modified with the following change. Rather than the 100% displacement value found from the monotonic tests being used for the basis of the ISO standard 16670, the displacement value used was half the 100% displacement. In essence, the standard loading protocol displacement value was half the displacement found at 80% the maximum load after peak load. This alteration provided well constructed hysteretic loops, thus allowing for easy interpretation of the data for use in subsequent modelling. The loading rate of the cyclic tests was 127 mm/min.

6.3 Results and Discussion

The monotonic tests of the connection types were all completed prior to the cyclic testing program due to the aforementioned parameter needed for the ISO standard 16670. The connection tests' main numerical results are given in Tables 6.2 and 6.3. These results are for the cyclically loaded longitudinal specimens. P_{max} is the mean maximum load; σ is the standard deviation for the maximum load; Δ_{max} is the mean displacement at maximum load; K_{in} is the mean initial stiffness of the connection and E is the mean hysteretic energy dissipation of the connection. The initial stiffness is calculated as per the European CEN standard (CEN, 1995) methodology. The two tables (Tables 6.2 and 6.3) present the two quadrant responses of the connection tests, those being the retraction response in quadrant 1 (Table 6.2), and the extension response in quadrant 3 (Table 6.3). Figure 6.2 shows all of the monotonic and cyclic longitudinal hysteretic responses for the tested specimens. Appendix A.4 gives the hysteretic and monotonic responses of the both the longitudinal and perpendicular specimens.

Table 6.2: Quadrant 1 longitudinal sheathing-to-framing connection test results

Specimens (Cyclic)	P_{max} [kN]	σ	Δ_{max} [mm]	K_{in} [kN/mm]	E [J]
APARA	1.70	0.27	7.6	1.18	97
BPARA	2.11	0.28	10.9	0.73	110
CPARA	2.10	0.18	11.0	1.51	203
EPARA	1.07	0.13	8.3	0.66	65
FPARA	1.58	0.06	10.5	0.59	83
HPARA	1.01	0.05	9.8	0.54	97
IPARA	1.00	0.05	14.0	0.31	71

Table 6.3: Quadrant 3 longitudinal sheathing-to-framing connection test results

Specimens (Cyclic)	P_{max} [kN]	σ	Δ_{max} [mm]	K_{in} [kN/mm]	E [J]
APARA	1.86	0.13	7.6	1.31	97
BPARA	1.92	0.31	10.9	1.27	110
CPARA	2.18	0.11	8.6	2.77	203
EPARA	1.21	0.20	8.3	0.89	65
FPARA	0.90	0.15	7.8	1.20	83
HPARA	0.89	0.20	9.7	0.75	97
IPARA	0.95	0.00	11.2	0.55	71

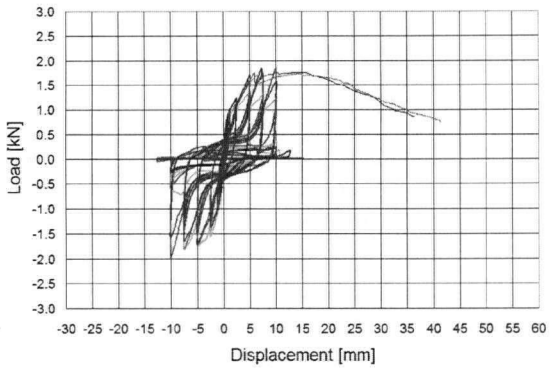

a) Connection group APARA

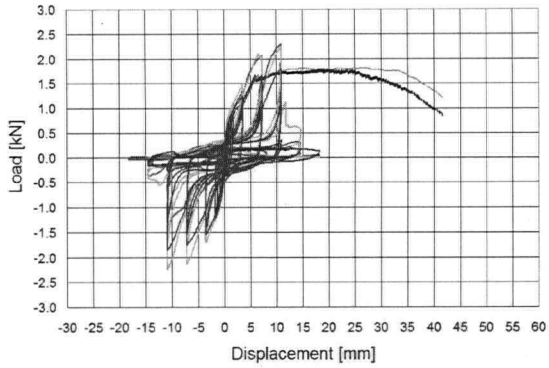

b) Connection group BPARA

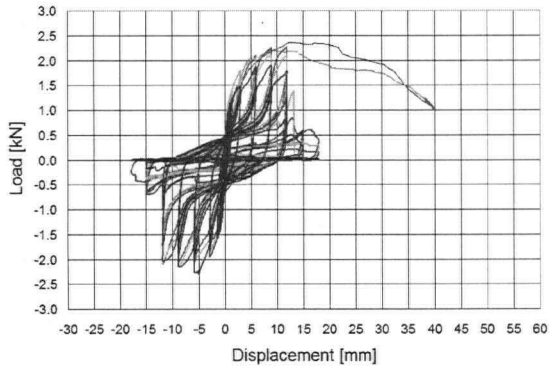

c) Connection group CPARA

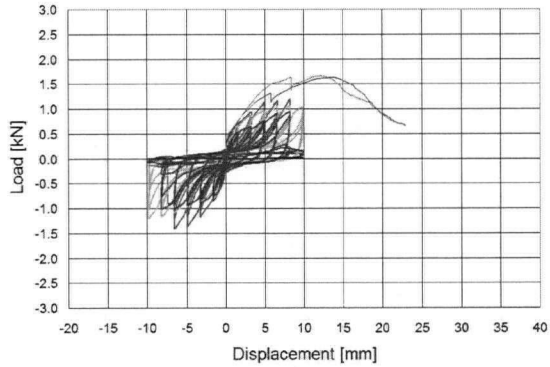

d) Connection group EPARA

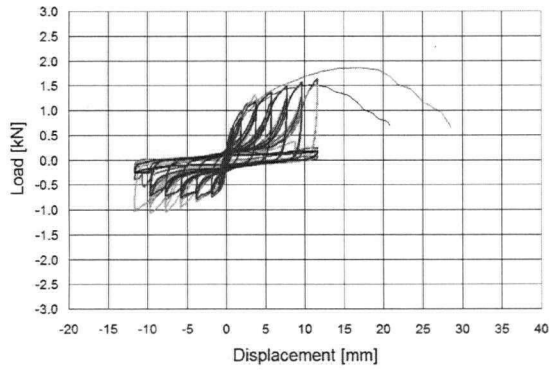

e) Connection group FPARA

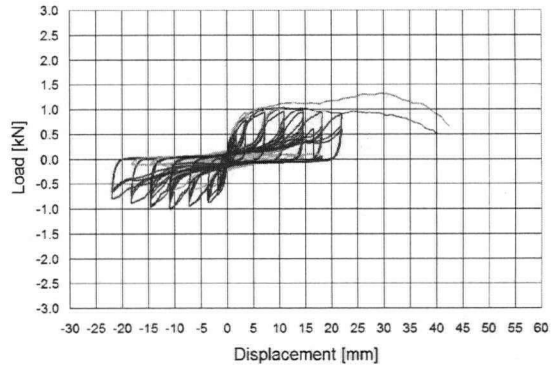

f) Connection group HPARA

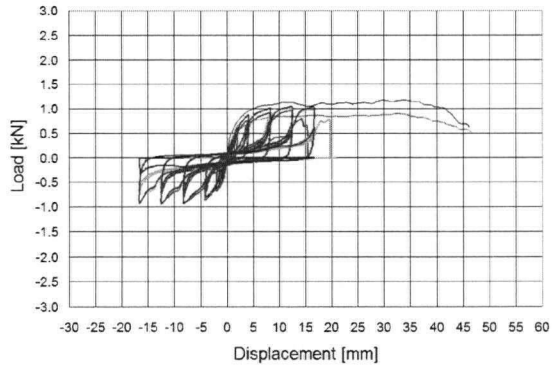

g) Connection group IPARA

Figure 6.2: Monotonic and cyclic sheathing-to-framing connection responses for the longitudinal specimens;

When quantitatively comparing different connection types amongst each other a few general observations can be made. As expected, the thicker sheathed connections were able to attain higher maximum loads, dissipate more hysteretic energy, and provide for a stiffer connection response. The CPARA grouping showed a consistent strength performance when comparing the two quadrant responses, as well as the stiffest response. The larger nails that were used resulted in the largest hysteretic energy dissipation by almost 85% compared to the next highest dissipater of energy, the BPARA grouping. Further comparison of Tables 6.2 and 6.3, show that the LVL studded connections performed more than equally to that of the LSL connections. The SPF connections provided for the least strong and stiff connections, however their hysteretic energy dissipation was still comparable to that of the LVL and LSL studded connections due to the larger displacements that the connections were able to sustain. When observing the monotonic and hysteretic responses of the connection specimens in Figure 6.2, it is important to note the variability present in most of the connections with regard to the displacement at failure. This factor is more prominent for the cyclic specimens, especially for the specimens with the thinner sheathing. The ability of the nail to adjust in such a manner that nail fatigue is lessened may be the reason for this. The relatively stiff properties that the thicker sheathed specimens show do not allow this adjustment.

When the monotonic specimens were examined, the 25.4 mm DFP-based connections (LSL or LVL) all had eventual failure of the connection through nail withdrawal from the stud, for both the longitudinal and perpendicular specimens. There was also nail penetration into the sheathing face in these cases, but this ceased after one or two plywood plies. This was not the case for the 15.1 mm OSB connections with LSL and LVL as nail pull-through's were predominant. As the nail pulled through the sheathing, significant nail bending occurred. When the 9.5 mm and 15.1mm OSB test specimens made with SPF studs were tested, the anticipated nail pull-through did not occur. This was due to the flexibility of the sheathing itself (9.5 mm OSB) as well as the studs ability to compress and permit greater nail mobility. These two factors led to the SPF specimens permitting less acute nail bending and consequently more direct nail pulling force being applied. The nails were observed to withdrawal from the stud material (SPF) rather than pull-through the sheathing. Nail slots were created in the SPF studs, but no significant slotting occurred in the LSL or LVL studs.

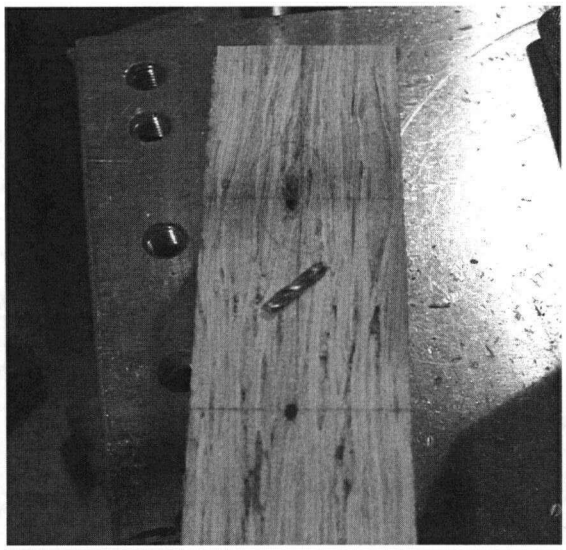

Figure 6.3: Dual fatigue nail failure

Comparing cyclic test observations, the 25.4 mm DFP based connections experienced dual shear fatigue failure (Figure 6.3). This trend was observed for both the perpendicular and longitudinal specimens as well as for both the LSL and LVL studs. The nails eventually failed in fatigue, as was the case in the full scale tall wall tests. The 15.1 mm OSB based specimens with LSL and LVL studs did not generally experience dual nail shear, although it did occur in a few specimens. The LVL-based connections appear slightly stronger that that of the equivalently constructed LSL-based connections (Tables 6.2 and 6.3) though a larger sample size would allow for a more definitive statement. There was significant stud slotting by the nail with regards to the LSL and LVL based specimens. This is to be expected since any concentrated prying action would be expected to cause compressive behaviour on the studs. In addition to the mentioned actions, the LSL and LVL-based specimens also experienced significant nail embedment into the sheathing face. The SPF-based specimens reacted differently to cyclic loading than that of the LSL and LVL-based specimens. As observed in the full scale tall wall tests, the SPF is less inclined to prevent nail withdrawal, as such the 15.1 mm and 9.5 mm OSB samples both longitudinal and perpendicular saw the sheathing pry away from the stud. In addition, only single nail shear failures were observed in the SPF based tests. Elongated nail holes in the studs and nail embedding into the sheathing were also observed.

6.4 Summary

The sheathing-to-framing connection tests were effective in capturing the general behaviour of the types of connections that are found in the full-scale tall wall tests. The anticipated strength differentiations were also apparent, with larger nails and larger sheathing resulting in higher capacities with regard to strength as well as stiffer connections. The connection tests involving 25.4 mm DFP resulted in the dual shear fatigue failure of nails that were also apparent in the tall wall tests. Care must be taken when utilizing the connection results as fully representing the

true connection behaviour as found in the full-scale testing however, since the test setup is of a much more rigid construction than that found in actual structures. The rigid setup and consequent inability of the connection to fully adjust to the loading scenario may have resulted in connection results that overestimate true in-wall connection behaviour. This belief was further strengthened when modelling of the tall walls was attempted. This is further discussed in the following section.

7. MODELLING

7.1 Introduction

To aid in the implementation of wood-based tall wall designs in practice, the ability to accurately model and concurrently predict, to a high degree of confidence, wall behaviour is important. It is to this end that the following verification and prediction modelling of in-plane full-scale wood-based tall wall behaviour is performed. Initially the tall walls that were tested were to be used as a baseline for which modelling software results can be compared against for accuracy and appropriateness. The second phase of this modelling is an analytical investigation to predict untested wall configurations with regard to in-plane loading response. The software chosen to attempt these two goals is CASHEW: Cyclic Analysis of wood SHEar Walls, a computer program for cyclic analysis of wood shearwalls. This software was developed as part of the CUREe-Caltech Woodframe Project "Earthquake Hazard Mitigation of Woodframe Construction", (Folz and Filiatrault 2000). This software was thought to be a prudent choice due to its wood design basis, simplicity of use, and large institutional testing program that was used as the models performance verification.

7.1.1 CASHEW Methodology

To help facilitate the evolution of building codes with respect to seismic design the testing program of which CASHEW resulted from was undertaken. Spearheaded by Folz and Filiatrault (2000), the development of CASHEW spawned from the aforementioned CUREe-Caltech Woodframe project. A focus of cyclic racking wooden shearwall response was made, since prevalent in current seismic design theory is unrealistic monotonic loading response. Full-scale testing of conventionally sized shearwalls (heights of around 2.4 meters) is common; however, consistency in testing protocols and methodology remains elusive. Many cyclic loading protocols exist, including the ISO standard 16670 protocol used for the experimental testing of this particular project. Some studies have focused on the aforementioned loading protocols as a means of developing an accurate way of predicting wall performance (He et al., 1998; Rose, 1994; Skaggs and Rose, 1996) while others have focused on wall response degradation (Shenton et al., 1998), panel size influences (Lam et al., 1997), openings (He et al., 1999), fastener types as well as gypsum wallboard contributions (Karacabeyli and Ceccotti,

1996) and hold-down and anchorage influences (Commins and Gregg, 1994). The studies, though varied, have provided insight into wall behaviour, though the simple and accurate modelling of wooden shearwalls remains an issue. CASHEW was developed through an extensive testing program to speed up the study of these walls. An extensive numerical study of wooden shearwalls in conjunction with experimental studies was done, and resulted in the development of CASHEW; a model that aims to accurately predict shearwall behaviour that is also simple to use and computationally efficient.

Though not as sophisticated as existing finite element modelling techniques (Dolan and Foschi, 1991; White and Dolan, 1995), CASHEW has been found to perform accurately for the walls of the CUREe-Caltech Woodframe Project and the loading protocols applied therein. Simplistic models that attribute wall behaviour to the non-linear load deformations of the sheathing-to-framing connectors (Gupta and Kuo, 1985, 1987; Filiatrault, 1990) were examined, as were finite element counterparts. Simple non-linear dynamic analysis models were also investigated (Stewart, 1987; Foliente, 1995) during CASHEW's development. What was found was that though many models exist, none seemed to combine the practicality and efficiency of the simple models with the more accurate yet computationally taxing complex models. The ability to model shearwalls simply and accurately was a main development goal of the CASHEW model.

CASHEW uses a user-friendly input methodology. To analyse a shearwall attention is paid to four main structural components: Framing members, sheathing panels, sheathing-to-framing connectors and hold-down anchorage. An example of the input file format is provided in Appendix B.3. There are many assumptions ingrained into CASHEW. They are as follows:

- The program uses an incremental-iterative displacement control strategy of load application and analysis.
- Under loading, the orthogonal grid of the wall distorts into a parallelogram with the top and bottom plates remaining essentially horizontal.
- The bottom plate remains fully anchored to the foundation so uplift is effectively eliminated.
- Framing members do not bend; they remain rigid with pin-ended connections.
- Sheathing panels develop uniform in-plane shear deformations.

- Individual deformations of framing members and sheathing panels are negligible.
- Sheathing-to-framing connector response is decomposable to horizontal and vertical components.
- The sheathing-to-framing connectors are described by a set of parameters from a load vs. displacement connection response plot as shown in Figure 7.1. These parameters can be the basis of an accurate wall response representation.

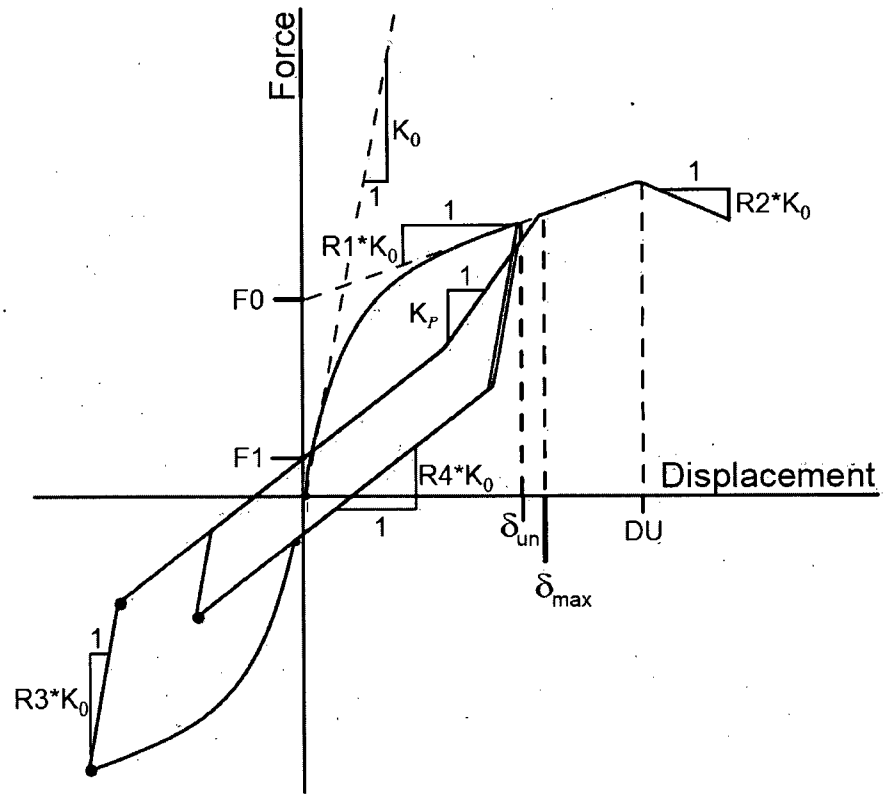

Figure 7.1: CASHEW sheathing-to-framing connection hysteretic response input parameters (Folz and Filiatrault, 2000)

The parameters that describe the sheathing-to-framing response are not the only material parameters that need to be known, but they are the main component. In addition to the connection parameters, the wall geometry must be inputted as well as the sheathing elastic shear modulus. This is potentially beneficial for designers since it permits quick design analysis. All the assumptions made and the required parameter inputs including geometric wall inputs and connection property inputs results in a relatively simplistic calculation procedure for the model. The basis of wall response calculation for CASHEW is stiffness matrix manipulation. Governing the process is the concept of virtual work. The accompanying literature to the

CASHEW computer program that Folz and Filiatrault (2000) provided is detailed with regards to the computational processes it uses.

7.2 Experimental Test Verification

The verification procedure employed within this paper consisted of the testing of sheathing-to-framing connections and then using their behaviours as a means of developing input parameters for CASHEW. The geometry of the walls was also inputted as was the elastic shear modulus of the sheathing. Small geometric deviations as well as assumptions were made with regard to the input values of all aspects of the CASHEW inputs. The inputs are described in the following sub-sections and are more thoroughly explained within the CASHEW software literature. Lastly, the loading protocol that was utilized was based on the true wall tests. The cyclic loading displacement input values were those found for the full-scale tall wall tests cycle displacements.

The program is based on displacement control as a means of the analysis. Both monotonic analysis as well as cyclic analysis is permitted, with the model outputting the significant results. User prescribed displacement based loading protocols are permitted. The main results can include all or some of the following: Initial wall stiffness, ultimate lateral load, displacement at ultimate load, as well as values describing the hysteretic response characteristics and hysteretic energy dissipation. The entire wall response can be plotted, as can the energy dissipation rate. Of note, is that regardless of the modelled responses determined by CASHEW, the behaviour of the walls cannot be truly approximated. Two main reasons for this are that the tested tall walls of this program have the previously noted significant non-symmetric load vs. displacement plots. The first quadrant and third quadrant load vs. displacement envelope curves of the tested walls are significantly different in most cases, whereas the CASHEW model predicts symmetric quadrant responses. The second reason for the inherent non-conformity between the model and the tested responses is that the ISO standard 16670 (ISO, 2003) loading protocol utilized is approximated by the program, CASHEW, since it can only account for two consecutive displacement cycles at the same load level. ISO 16670 has three identical cyclic displacements per displacement level. As a result, the connection input data must approximate the behaviour of the true connection response by underestimating the second cycle response and

overestimating the third. This may not be the dominating reason for non-conformity of the model to reality, though it does add more uncertainty.

7.2.1 Sheathing-to-Framing Parameter Inputs

The majority of the input parameters come from the sheathing-to-framing connection data. In total, ten parameters are included from this data into the CASHEW input file, however an additional three parameters are also found to facilitate the determination of the required input values. All necessary parameters are shown in Figure 7.1. The parameters are all intended to accurately describe the envelope curve of the connection behaviour. This fact presented the first obstacle in using the CASHEW software. The ISO 16670 standard used for the sheathing-to-framing connection tests of this study was similar to the loading input provided to the full-scale tall wall tests. The software requires the input parameters of connection behaviour, however their determination is subject to varying interpretation. To determine the input parameters of the sheathing-to-framing connections of this project, their load vs. displacement plots were examined and parameters manually derived. Though error is possible through this methodology, error and approximation issues will present in any parameter search, whether computational in nature or not. A short spreadsheet was created so as to compile the parameter information, and to allow for the direct exhibition of the parameters needed for input.

The connection parameters are self-explanatory when observing Figure 7.1, though there are necessary comments to be made. The CASHEW software was found to be unable to process efficiently the load degradation behaviour characterized by the R2 parameter. Since the load degradation response of the cyclic sheathing-to-framing connection tests performed in this study give steep load declines with regard to the envelope curves generated after maximum load has been attained and not a slow force drop characterized by monotonic test results, the CASHEW software becomes unstable. It was necessary to give the R2 parameter incorrect values (a more gradual slope characterization) to facilitate the model use. As a result, the resulting CASHEW full-scale wall verification results cannot be taken as accurate after peak load has been attained. This did not appear to be a problem for the software developers and could be a result of the use of a user-defined loading protocol instead of the CUREe-Caltech Woodframe Project (2000) testing protocol that the model has pre-programmed. The remaining parameters were taken as

best could be determined from the load vs. displacement plots. As can be seen, calculation is needed to determine two of the needed input parameters, those being the α and β parameters. The α parameter is a hysteretic model parameter that aids in the stiffness degradation interpretation of the connection data. It is found via use of Equation 2. The β parameter is another hysteretic model parameter determined via Equation 3. In short, both the α and β parameters are determined as a result of fitting the parameter outlining model shown in Figure 7.1 with the connection data. The input parameters and corresponding sheathing-to-framing connection test load vs. displacement plots are provided in Appendix B.1.

$$K_P = K_O \left(\frac{\delta_O}{\delta_{\max}} \right)^{\alpha} \tag{2}$$

$$\beta = \left(\frac{\delta_{\max}}{\delta_{un}} \right) \tag{3}$$

7.2.2 Sheathing Elastic Shear Modulus

The elastic shear modulus of the sheathing panels used is a required input value for the CASHEW modelling. The shear modulus' that are used for the input values of this project were taken from CSA O86-01 (CSA, 2001). They are taken from the design standard as opposed to experimentally determined because the modelling of the walls for design purposes in practise needs to be done with as little added effort as possible or risk facing opposition from designers. The CSA-O86 standard has extensive tabulated sheathing property charts and as such should be utilized. It is understood errors may arise from this action, however, as later modelling results will show, there are more significant sources of error and other issues that impact the reliability of CASHEW with regard to this projects tall wall modelling. The three shear modulus values used in the subsequent modelling are as follows: 9.5 mm OSB has a shear modulus of 1.05 GPa, 15.1 mm OSB has a shear modulus of 0.79 GPa, and 25.4 mm DFP has a shear modulus of 0.51 GPa.

7.2.3 Wall Geometry

The wall geometry that is represented in the input file for each particular wall analysed in CASHEW is simple. As shown in Figure 7.2 and in Appendix B.3, the necessary information for the walls and sheathing is relatively compact. The only main hurdle with the geometry representation is the compatibility of the nail spacing interpretations. The nail spacing, for symmetry, must be evenly divisible into the total sheathing size; what this means is that the wall lengths and heights indicated are not the same for every wall. For example, walls with nail spacing around 152 mm must use a total wall height/length dimension of 4880 mm and a nail spacing of 152.5 mm, whereas a wall with nail spacing around 102 mm, must actually use a total wall height/length of 4881.6 mm and a nail spacing of 101.7 mm. These small differences in total wall size are inconsequential.

Figure 7.2: Screen shot of CASHEW input file for wall 602

7.2.4 Loading Protocol

The displacement based loading protocols that were provided for the CASHEW modelling of the full-scale tests of this project were based on the full-scale test results themselves for obvious reasons. The displacement CASHEW inputs were developed with the 100% displacement cycle values of the tall wall tests exactly corresponding with the matching 100% displacement values of the CASHEW inputs. The CASHEW input values were then expanded upon with the 100% displacement values acting as a basis for the other percent displacements needed for the ISO standard 16670, this included the intermediate cycles present in the modified ISO 16670 standard that was utilized in the full-scale tests. The exact loading protocols of the true tests could not be utilized for the CASHEW modelling due to unforeseen instability of the model with regard to the step sizes that were recorded from the full-scale tests. The full-scale tests were not conducted to such small displacement steps to ensure smooth operation of the CASHEW software. The loading protocols were also difficult to implement due to the limited number of input displacement steps permitted by the available CASHEW version, that being 20,000 data points. The only software alteration that was made for this study was the recompiling of the Fortran based software to accommodate up to 999,999 data points for user-defined displacement loading steps.

7.2.5 Software Usage Procedure

The initial use of the CASHEW software is that of a verification tool for the full-scale wall tests that have been performed for this project. The accompanying literature to the CASHEW software outlines a type of verification procedure that the developers decided was appropriate. The procedure involves the intermixing of spring representations for the individual connections of the wall (whether single or dual non-linear uncoupled springs). In short each sheathing-to-framing connector was represented by two orthogonal uncoupled non-linear springs. The specified connector spacing was then adjusted so that the monotonic load-displacement response agreed, in terms of energy dissipated by the wall up to a prescribed drift level, with the prediction based on using only one non-linear spring per connector with the spacing unchanged. Researchers found that this was a method that was able to lessen the incorrect over predictions of initial wall stiffness and ultimate load capacity (Folz and Filiatrault, 2000).

With this knowledge, a less rigorous verification schedule was used since efficiency and ease-of-use is wanted when utilizing software for analysis. Over-predictions are present in the results that are displayed further in this document, though it must be said that over-predictions are also present in some of the verified and adjusted results of the CASHEW developers. The verification procedure that was utilized for this project is as follows:

1. Choose experimental wall to verify, insuring behaviour of the experimental wall is one that can reasonably be expected and does not contain obvious irregularities not attributable to the reasonable behaviour of the wall.
2. Obtain the envelope curves of the connections that are to be used.
3. Determine the required input parameters for the model based on interpreting the connections envelope properties, as shown in Figure 7.1.
4. Create an input file including the geometry of the wall, connection properties from step 3, and other properties necessary for the analysis such as the shear modulus. A subsequent loading protocol is also included for this project since the cyclic protocol used in the tall wall testing is not that of which is provided for in the internal programming.
5. Run the model, stopping the analysis after the initial monotonic testing has finished.
6. Check the monotonic results with that of the first quadrant of the full-scale tests. If unsatisfactory correlation is presented, the re-examination of the input connection data is performed making justifiable small alterations to the input parameters. Steps 4 to 6 are repeated until justifiable input parameter alteration is no longer possible.
7. The analysis is run, allowing for completion of the analysis including the cyclic user-defined loading protocol.
8. The entire data output is then plotted and checked for correlation with the experimental results. Focus for behaviour correlation is made on the loading up to maximum loading response, since degradation of the modelled wall behaviour will not correlate with the true wall response, though effort is still made to accommodate observed behaviour as best can be done.
9. If correlation is not adequate, steps 7 and 8 are repeated, slightly and justifiably altering the connection input parameters relating to the cyclic input parameters.

Hysteretic energy absorption is also looked at as a means of determining what types of adjustments need to be made.

10. The verification procedure is complete, with values tabulated and presented in an orderly fashion.

Run times for the CASHEW program varied from run to run, though on average the time required to run one analysis approached two hours on a personal computer with a 3.06 GHz Intel® Pentium 4 processor and 512 MB of RAM. The software source code and its Fortran basis is simple though results in long computation time.

7.3 Experimental Wall Verification Results and Discussion

The results presented focus on how the direct usage of experimentally tested connection data manifests themselves in the complete tall wall modelling. The modelling results are shown subsequently and they are provided in Appendix B.2 as well. There are three primary behaviours that are of concern when modelling the behaviour of shearwalls, that being the load response capacity, displacement response as well as the hysteretic energy that the wall can dissipate. As shown in Figures 7.3, 7.4 and 7.5, the load vs. displacement responses generated by CASHEW, appear to display relatively poor correlation with that of the true wall behaviours. This is not entirely true however. The responses of the CASHEW walls do show a degree of correlation with the true wall behaviours when observing the load paths prior and up to true tall wall failure. The model, in general, has difficulty post peak load, due impart to model instability at failure caused by sudden load changes at small displacements and the R2 parameter described earlier. The model also results in wall load capacities being overestimated. The load overestimations were expected. The overestimations may be related to the initial connection input values, since the sheathing-to-framing connection test data used resulted from tests that cannot portray the exact connection response experienced by the full-scale tall walls. The connection tests, though important, overestimate strength and response as mentioned before due to the rigid test setup. The overestimation of wall response given by CASHEW can be minimal, as seen for wall 705 at a CASHEW load overestimation of 3.5%, or very large. This instability in prediction is concerning, though more familiarity with the model may mitigate this issue. Maximum load (P_{max}), the displacement at maximum load (Δ_{max}) and the hysteretic energy

dissipation (E) are given in Table 7.1. Of note with regard to Table 7.1, is that the tall-wall values of maximum load and displacement at maximum load presented are from the first quadrant response where applicable, and the hysteretic energy dissipation values for both the tall wall tests and the model are recorded at the displacement step associated with the cycle peak set corresponding with wall failure. All three cycles of that displacement step are taken into account. In addition, the results that are commented on are from the CASHEW cyclic response values, the monotonic results that are given by CASHEW are very close to the cyclic envelope results however were not used since the experimental wall behaviour is cyclic in nature. As can be observed in Table 7.1, for walls 704, 706 and 707, there are two CASHEW response values shown. The (A) set of values is from the initial connection input interpretation whereas the second set of values presented (B) are from an adjusted set of input parameters, more specifically, the F0 parameter. The F0 parameter dictates the load axis intercept associated with the force uptake behaviour of the wall after initial resistance has been over come; this is show in Figure 7.1. This value was arbitrarily decreased 20% and resulted in a better correlation. A more standardized treatment of connection response data such as arbitrary parameter alterations done in a formulaic manner may be worth investigating.

Table 7.1: Tall wall tests and CASHEW modelling results

Wall	Experimental Results			CASHEW Results		
	P_{max} [kN]	Δ_{max} [mm]	E [kJ]	P_{max} [kN]	Δ_{max} [mm]	E [kJ]
602	38.2	94.4	14.2	37.1	94.3	14.9
603	39.6	92.5	23.1	39.3	93.5	21.4
605	62.6	124.8	36.2	70.8	111.1	36.5
702	53.4	89.8	19.4	44.0	78.4	19.0
704A	64.6	91.1	28.3	72.8	88.7	33.4
704B*	64.6	91.1	28.3	63.5	88.9	31.8
705	77.8	90.5	33.1	81.0	105.6	37.2
706A	83.2	91.3	35.0	106.1	90.7	46.1
706B*	83.2	91.3	35.0	93.1	90.5	44.1
707A	26.2	91.7	10.0	31.7	78.0	15.5
707B*	26.2	91.7	10.0	27.6	77.4	14.7

* CASHEW input parameter F0 was decreased by 20%; all other non-calculated parameters remained unchanged from the initial CASHEW input file

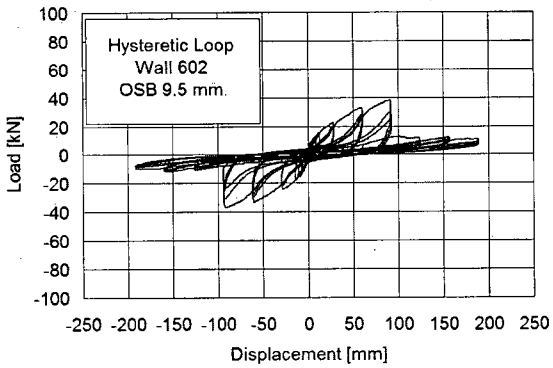

a) Experimental wall 602

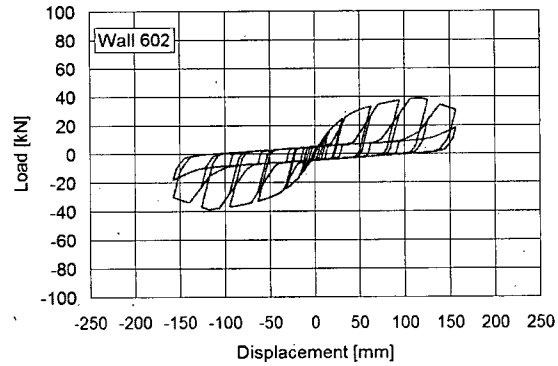

b) CASHEW wall 602

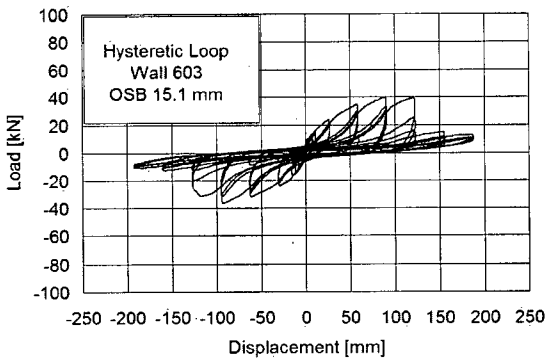

c) Experimental wall 603

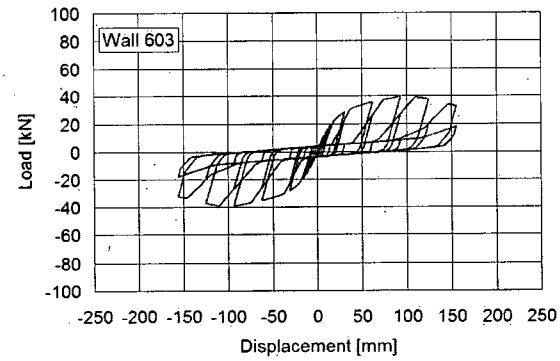

d) CASHEW wall 603

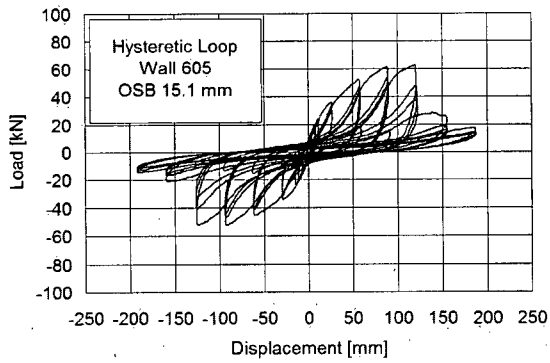

e) Experimental wall 605

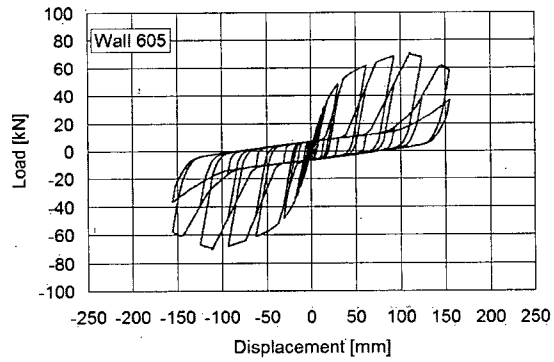

f) CASHEW wall 605

Figure 7.3: Load vs. displacement behaviour of experimental tall walls and corresponding CASHEW modelled tall walls 602, 603, and 605;

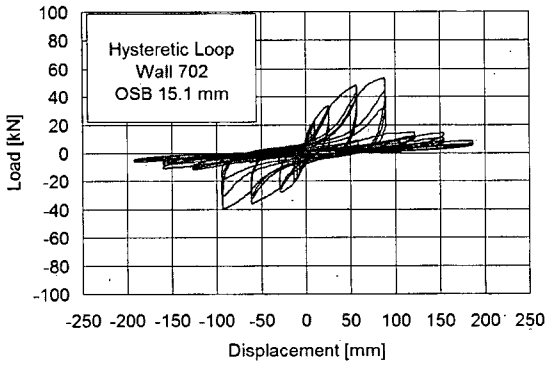

a) Experimental wall 702

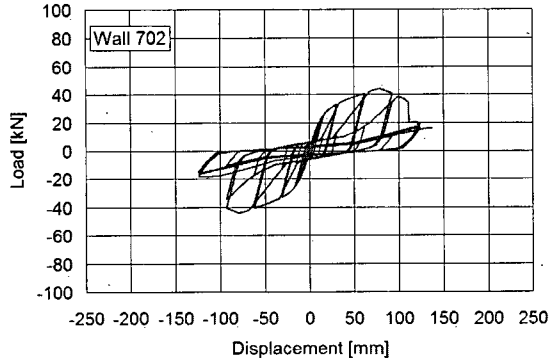

b) CASHEW wall 702

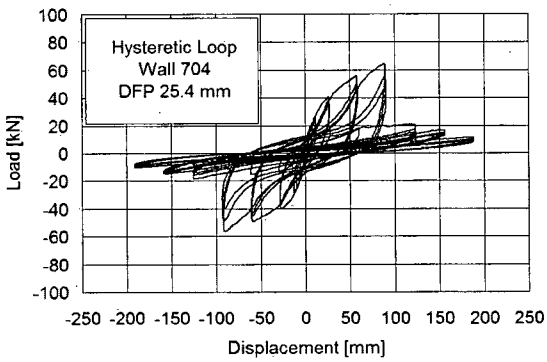

c) Experimental wall 704

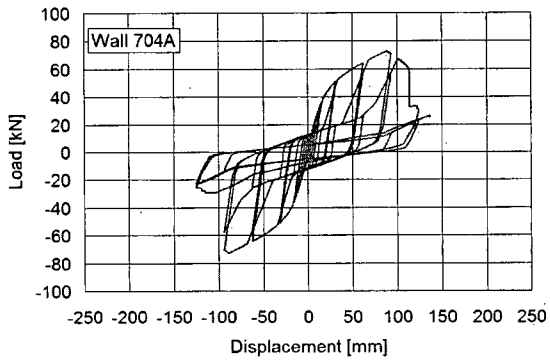

d) CASHEW wall 704A

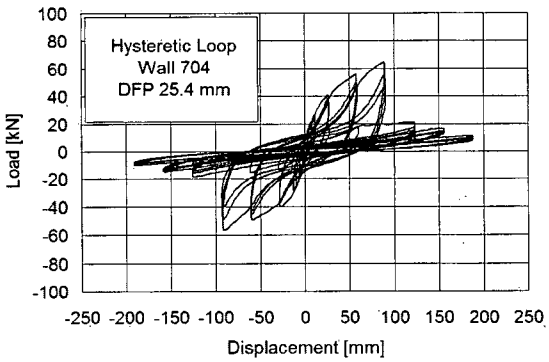

e) Experimental wall 704

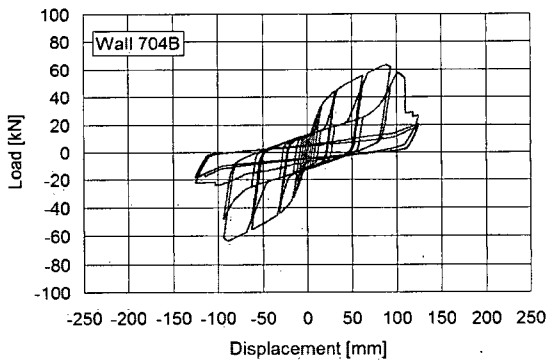

f) CASHEW wall 704B

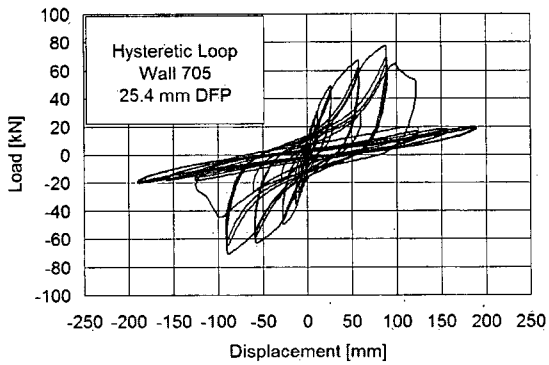

g) Experimental wall 705

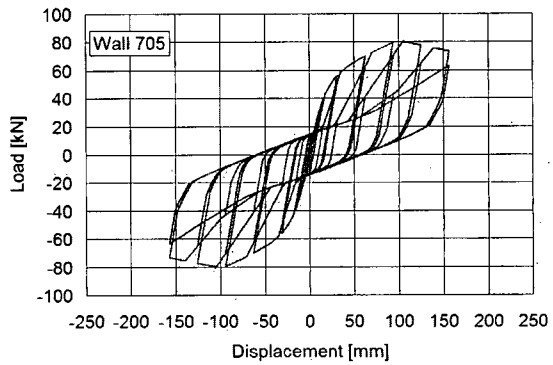

h) CASHEW wall 705

Figure 7.4: Load vs. displacement behaviour of experimental tall walls and corresponding CASHEW modelled tall walls 702, 704 and 705;

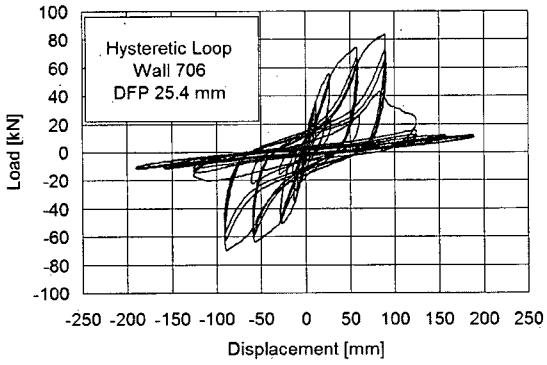

a) Experimental wall 706

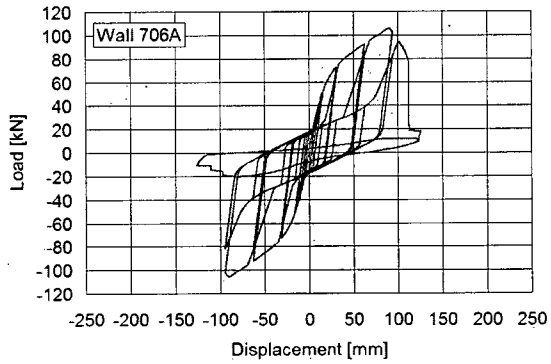

b) CASHEW wall 706A

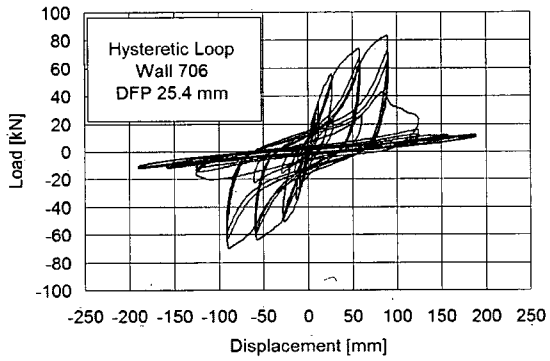

c) Experimental wall 706

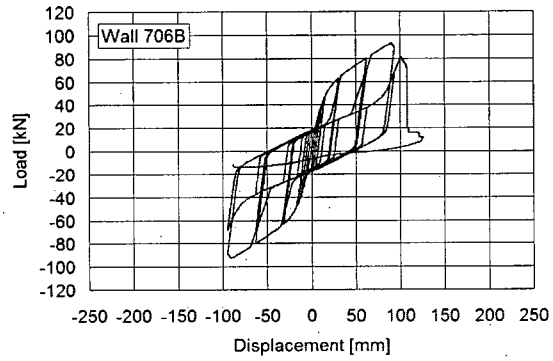

d) CASHEW wall 706B

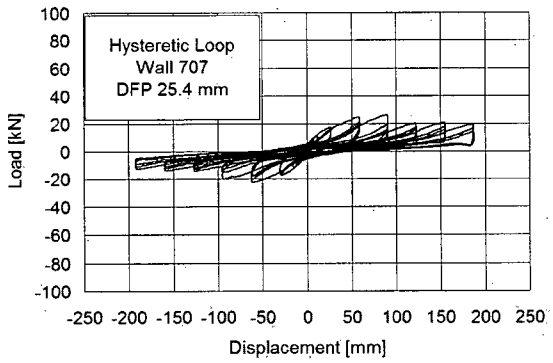

e) Experimental wall 707

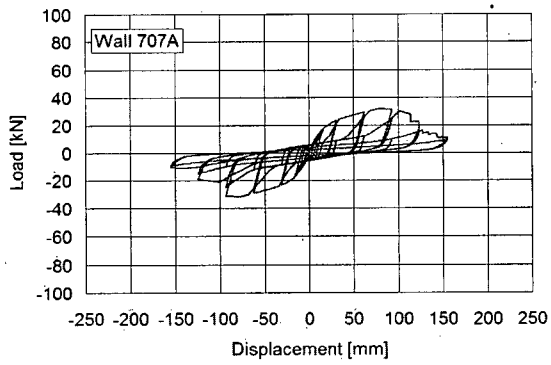

f) CASHEW wall 707A

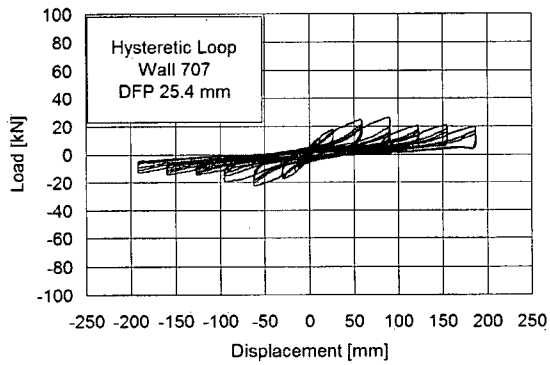

g) Experimental wall 707

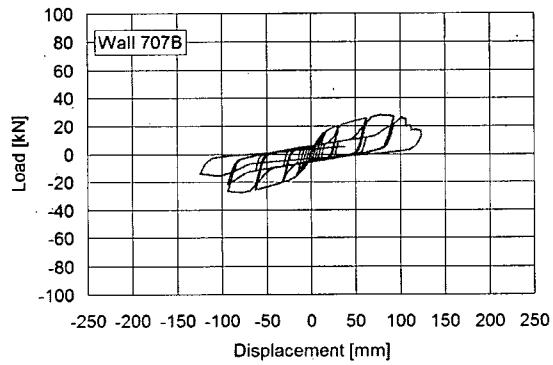

h) CASHEW wall 707B

Figure 7.5: Load vs. displacement behaviour of experimental tall walls and corresponding CASHEW modelled tall walls 706 and 707;

The behaviours predicted by CASHEW as aforementioned are overestimates of performance, though some are more striking than others. The OSB based walls with SPF studs appeared to give better correlation than that of the DFP based walls with LSL based studs. The OSB walls with LSL studs were somewhere in between the two extremes with regard to performance correlation. These assertions are made with observations of both hysteretic energy and load vs. displacement behaviours taken into account. The unblocked wall 707 appeared to correlate most poorly. The CASHEW model was developed in conjunction with conventionally sized shearwalls, those being of 2.4 m in height with 38 mm x 89 mm studs and with blocking at midheight. The tall walls of this study due to their tall stature do not react in the same manner as 2.4 m shearwalls. The manner in which the tall walls in reality displace when loaded, that being flexing at the bottom of the wall and maintaining rigidity at the top as discussed previously, may be dissimilar enough with regards to the smaller, regular sized shearwalls that modelling the behavioural characteristics becomes difficult for CASHEW.

As with the load vs. displacement responses, the hysteretic energy predictions (Table 7.1 and Figures 7.6 and 7.7) are encouraging, though further investigation into the model responses is still needed. Unlike the load vs. displacement responses, the hysteretic energy calculations needed to be scaled to that of the tall wall test data. Since the loading protocol used in the software is displacement based and the data acquisition from the true tall wall tests was time based, obvious data correlation issues were present. To relate the two differing types of data, the CASHEW results were compared to the experimental wall behaviour by converting the experimental wall time based performance into a displacement based behaviour. As a result, the hysteretic energy dissipation plots shown in Figures 7.6 and 7.7 show energy dissipation per cumulative displacement travelled by the wall.

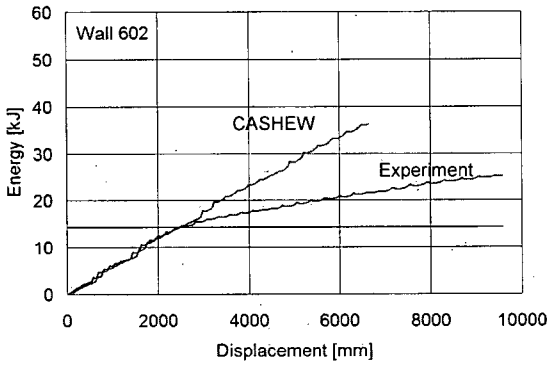

a) Experimental and CASHEW wall 602

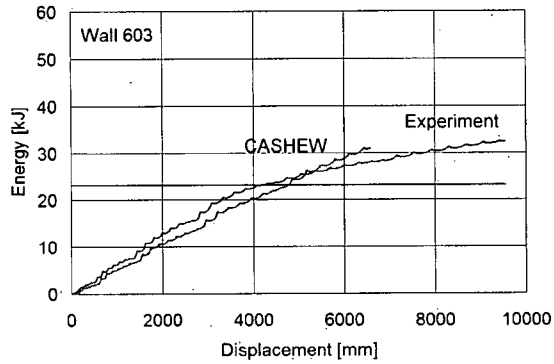

b) Experimental and CASHEW wall 603

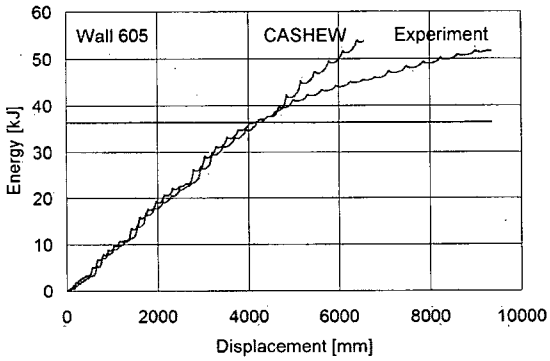

c) Experimental and CASHEW wall 605

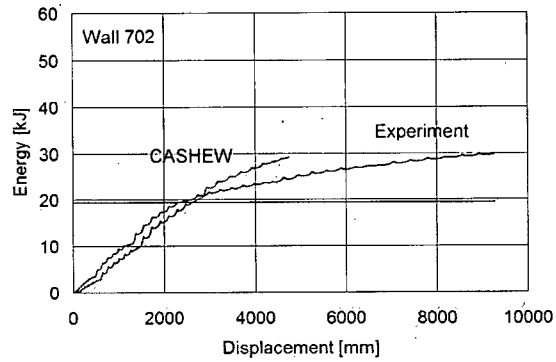

d) Experimental and CASHEW wall 702

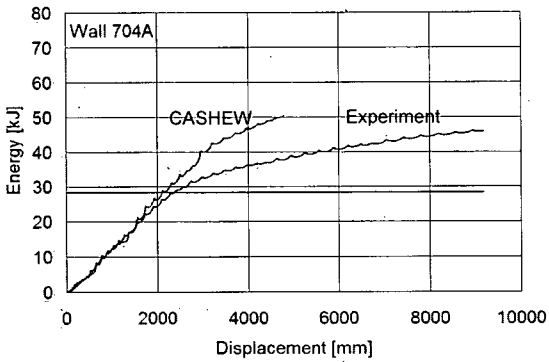

e) Experimental and CASHEW wall 704A

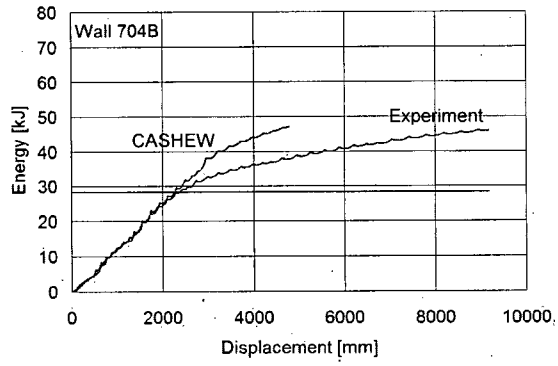

f) Experimental and CASHEW wall 704B

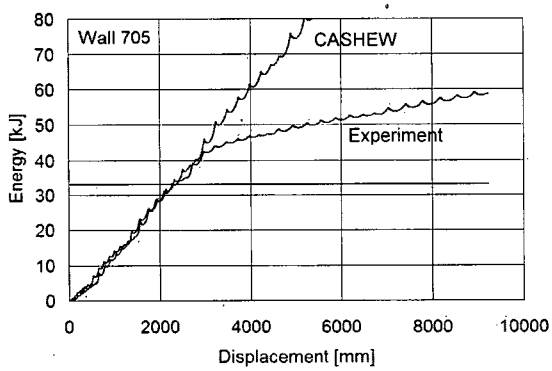

g) Experimental and CASHEW wall 705

Figure 7.6: Hysteretic energy dissipations for walls 602-605, 702,704 and 705; experimental (blue), CASHEW (red), total energy dissipated after peak load cycle set (black);

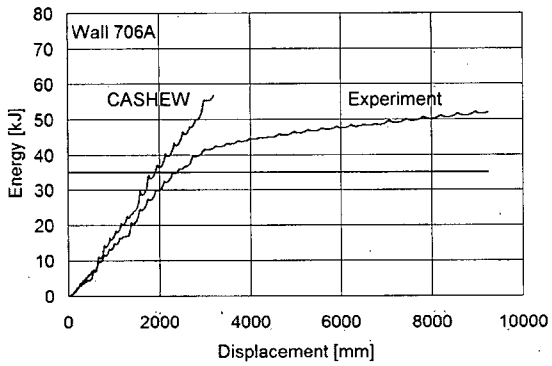

a) Experimental and CASHEW wall 706A

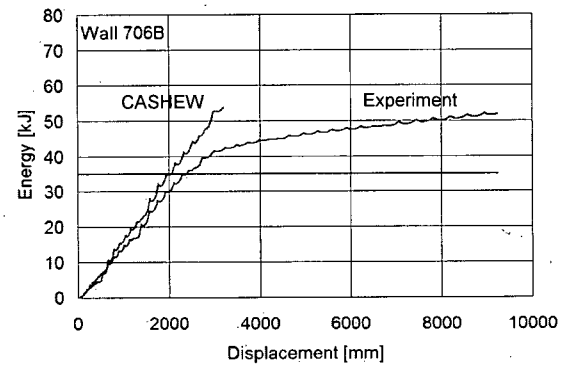

b) Experimental and CASHEW wall 706B

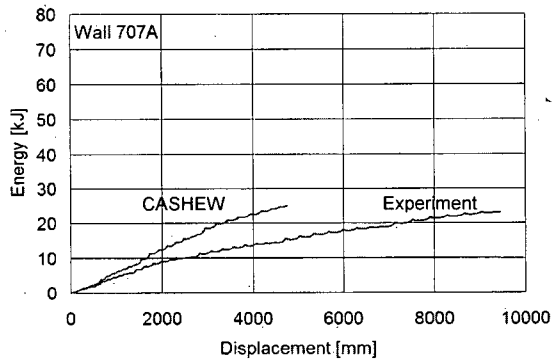

c) Experimental and CASHEW wall 707A

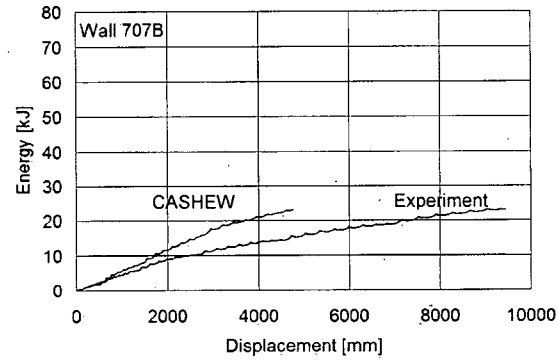

d) Experimental and CASHEW wall 707B

Figure 7.7: Hysteretic energy dissipations for walls 706 and 707; experimental (blue), CASHEW (red), total energy dissipated after peak load cycle set (black);

The SPF walls when modelled react in a very similar manner to that of the true walls with regard to energy response (Figure 7.6) this is not a large surprise, since the cyclic load vs. displacement predictions appear close prior to failure (Figure 7.3). The divergence of the modelled energy response corresponds to that of the divergence of the displacement response of the model from that of the true wall response after wall failure. The maximum load locations of the true wall behaviours are shown in Figures 7.6 and 7.7. This demonstrates further the assertion that wall behaviour is not predicted well at a point in time past the maximum load response. The analytical response however does show that up to the maximum load as well as for a time past it, the energy dissipation of a wall can be predicted accurately in most cases. The LSL based walls utilizing 25.4 mm DFP appear to be more difficult to predict with regard to hysteretic energy response than that of the SPF based walls. The overestimations of peak load response found in the majority of the LSL based walls (Figures 7.4 and 7.5) translate to overestimations of hysteretic energy dissipation. It can be surmised that if the load vs.

displacement response of the overestimated walls is more in tune with that of the true response, the hysteretic energy dissipation predicted would also better correlate and visa versa.

7.4 Predictive CASHEW Modelling Results and Discussion

A key goal of this project was to develop a method of utilizing a piece of software, in this studies case CASHEW, to predict the behaviour of wood based tall walls. As noted in the previous section, verification proved difficult utilizing CASHEW software; however it does appear to have merit in some instances. The SPF based tall walls with 9.5 mm and 15.1 mm OSB showed decent model correlation up to wall failure, and as such some predictive behaviour of experimentally untested walls of these materials can be shown. Some predictive modelling of 15.1 mm OSB and 25.4 mm DFP walls with LSL studs of untested configurations was also to be undertaken. Finally, LVL studded wall configurations were tested purely analytically by CASHEW software. A fluidly working method of utilizing CASHEW software with regards to tall walls would result in the LVL based wall predictions shown later, as well as the SPF and LSL based wall predictions to be held with an acceptable degree of confidence. Unfortunately, due to the issues already discussed in the previous section, the modelled predictive results shown are provided only for comparison and completeness purposes within this study. Though, given that the CASHEW results are generally poor to the same degree for most walls, inter-relating of the results can show general trends.

Table 7.2: CASHEW wall prediction test matrix

Wall	Stud		Sheathing Thickness [mm] & Type	Nail Spacing and Properties				Load Protocol*
	Type	Spacing [mm]		Perimeter [mm]	Interior [mm]	Diameter [mm]	Length [mm]	
606	SPF	1220	15.1 OSB	152	305	2.5	65	↔
608	SPF	1220	15.1 OSB	102	152	2.5	65	↔
709	LSL	610	15.1 OSB	152	305	2.5	65	↔
710	LSL	610	25.4 DFP	152	305	3.0	76	↔
711	LSL	1220	25.4 DFP	102	152	3.0	76	↔
801	LVL	1220	15.1 OSB	152	305	2.5	65	↔
802	LVL	1220	15.1 OSB	102	152	2.5	65	↔
804	LVL	1220	25.4 DFP	152	305	3.0	76	↔
805	LVL	1220	25.4 DFP	102	152	3.0	76	↔

* ↔ is cyclic loading

Table 7.3: CASHEW hysteretic response results of all modelled walls

Modelled Wall	P_{max} [kN]	Δ_{max} [mm]
602	37.1	94.3
603	39.3	93.5
605	70.8	111.1
606	39.0	114.7
608	67.6	114.5
702	44.0	78.4
704A	72.8	88.7
704B	63.5	88.9
705	81.0	105.6
706A	106.1	90.7
706B	93.1	90.5
707A	31.7	78.0
707B	27.6	77.4
709	45.7	77.5
710B	65.8	87.4
711B	109.8	92.0
801	55.2	94.7
802	96.6	106.2
804	80.3	119.1
805	138.0	123.6

The sheathing-to-framing connection parameter inputs are the same for this predictive study as that of the previous verification portion and as such will not be discussed. Walls utilizing the (B) input parameters (710B and 711B) were analyzed as such since the verified walls utilizing the (B) connection type showed better correlation. Table 7.2 shows the modelling matrix for this predictive portion of this study. The results of the modelling that are shown in Table 7.3 include those modelled responses of the verified walls as well. Table 7.3 shows maximum load (P_{max}) and displacement at maximum load (Δ_{max}). This allows for a relative comparison between all types of walls that were modelled. The loading protocol applied to the predictive tall walls is based on the 100% displacement value discussed in the previous section; the 100% displacement value for all predicted walls (606, 608, 709, 710B, 711B. 801, 802, 804 and 805) was 160 mm.

As can be seen from the results indicated in Table 7.3, the walls with closely spaced nails show greater load responses. This is expected, with the results of wall 608 indicating a high lateral load response of 67.6 kN, even with its 1220 mm stud spacing. A result that is significant even with its known overestimation. Similarly, the LSL and LVL walls show decent performance with regard to their modelled configurations. Again, the closely nailed walls demonstrate the highest load responses with both walls 711B and 805 showing capacities of 109.8 KN and 138

kN respectively. It appears, in general, that the predicted LVL walls, with their connection interpretations, give rise to stronger walls than that of the predicted LSL walls. More testing, including full scale tests, should be carried out prior to the assertion being made though. The 1220 mm stud spacing that has been investigated in both the experimental phase and that of the modelling phase shows design promise. Figures 7.8 and 7.9 show the hysteretic motion responses as predicted by the CASHEW software, whereas Figures 7.10 and 7.11 show the anticipated hysteretic energy dissipations.

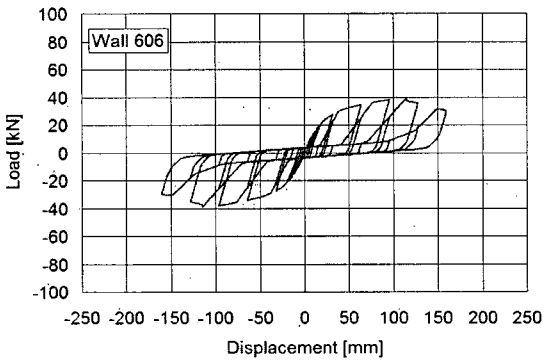

a) CASHEW wall 606

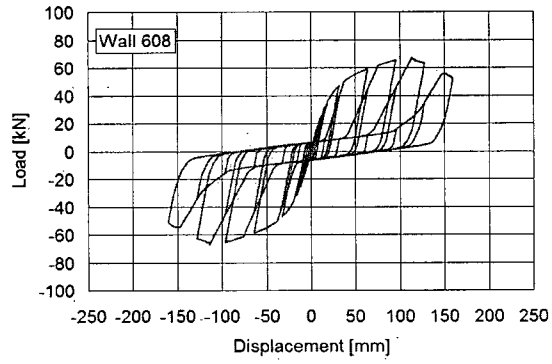

b) CASHEW wall 608

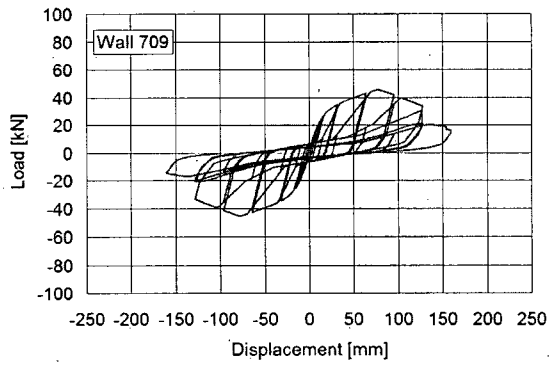

c) CASHEW wall 709

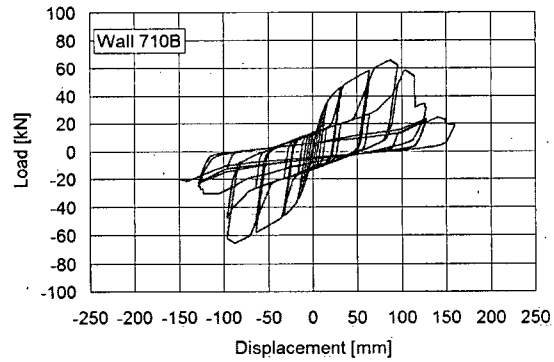

d) CASHEW wall 710B

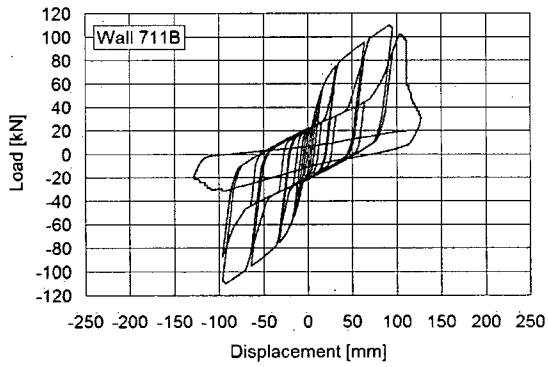

e) CASHEW wall 711B

Figure 7.8: Predictive CASHEW load vs. displacement responses for walls 606, 608, 709, 710B and 711B;

The energy dissipations have been provided only in graphical form, since it is not possible to know with any certainty where the energy response deviates from the probable true response, and that of the CASHEW correlation anticipated post peak load. One could use the peak load of the CASHEW wall responses, but as shown earlier, the true wall responses dictated where correlation ended, with CASHEW responses often carrying on past that of the true behaviour. Any energy values attained in this manner would have large uncertainty.

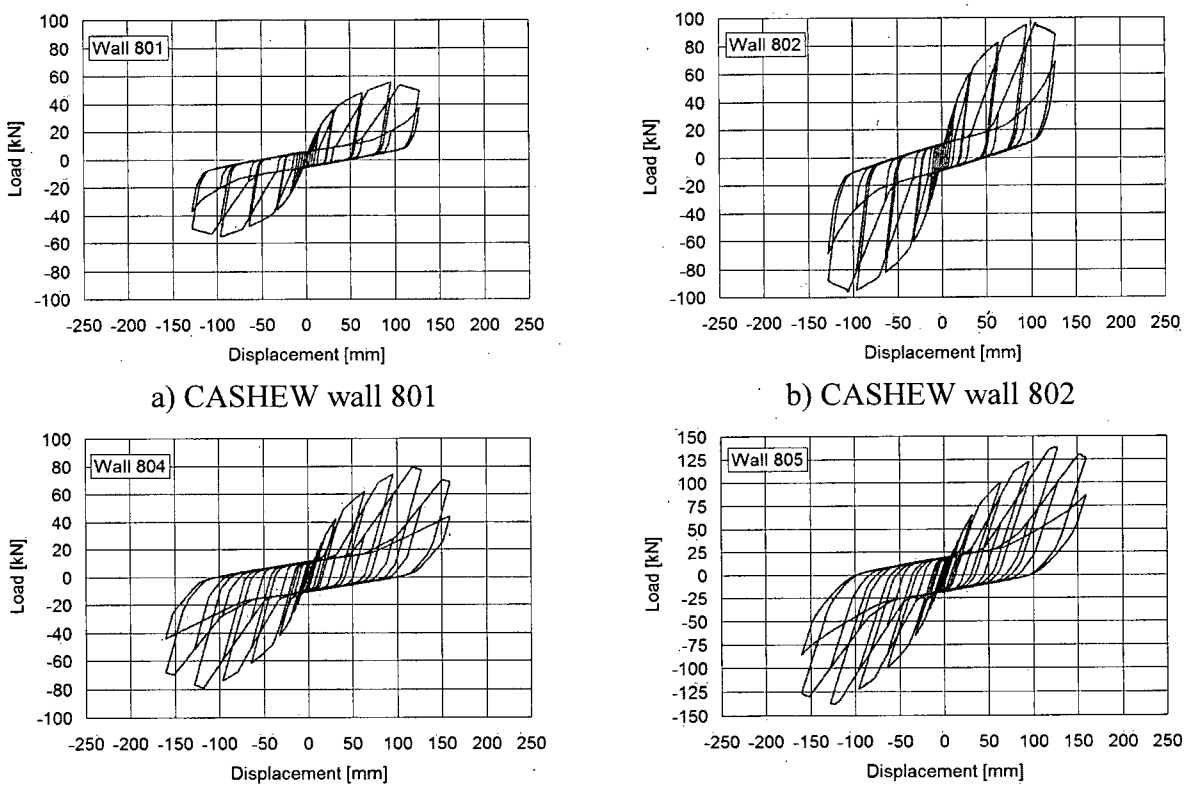

a) CASHEW wall 801

b) CASHEW wall 802

c) CASHEW wall 804

d) CASHEW wall 805

Figure 7.9: Predictive CASHEW load vs. displacement responses for walls 801, 802, 804 and 805;

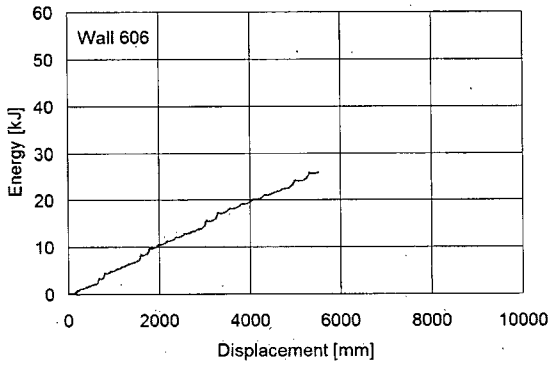

a) CASHEW wall 606

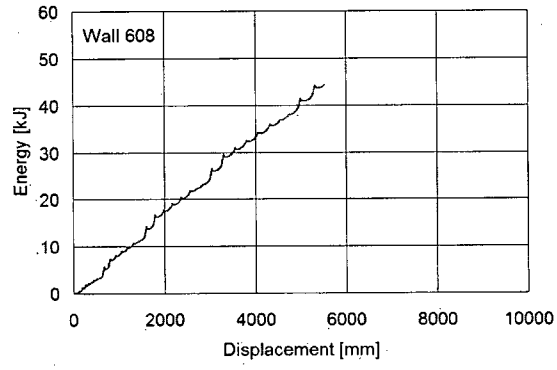

b) CASHEW wall 608

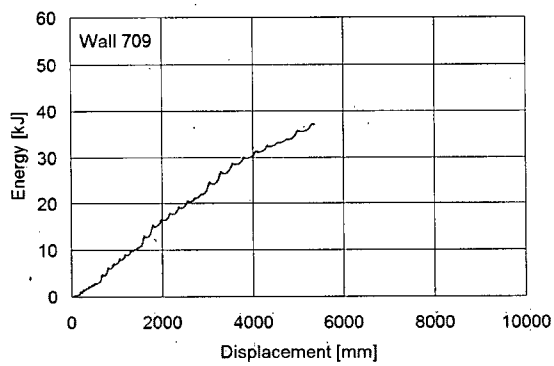

c) CASHEW wall 709

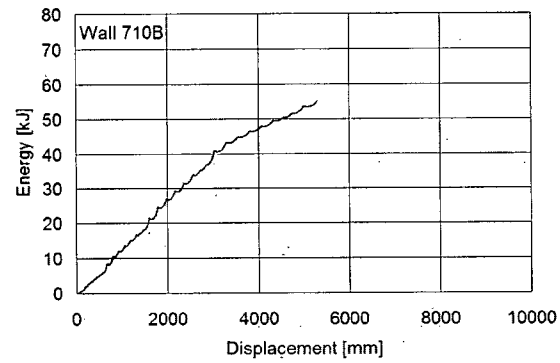

d) CASHEW wall 710B

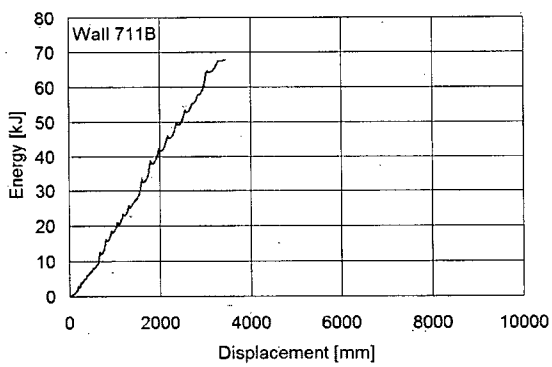

e) CASHEW wall 711B

Figure 7.10: Predictive CASHEW hysteretic energy dissipations for walls 606, 608, 709, 710B and 711B;

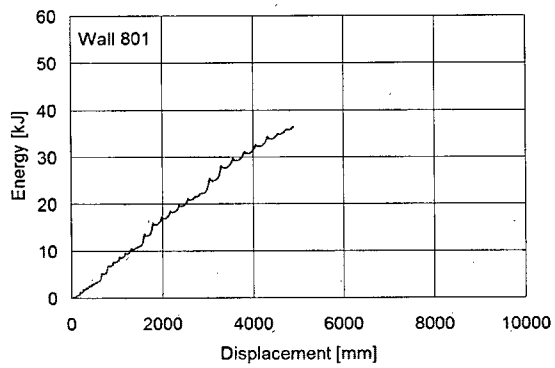

a) CASHEW wall 801

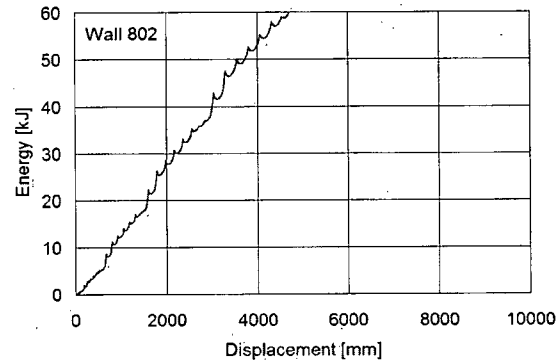

b) CASHEW wall 802

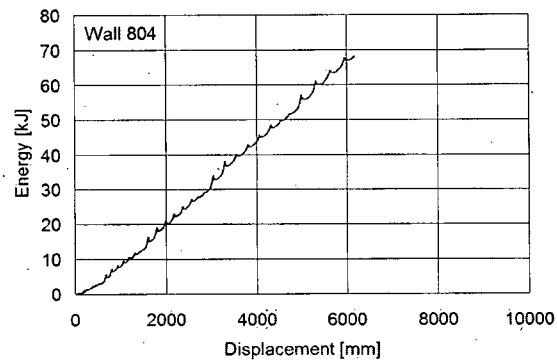

c) CASHEW wall 804

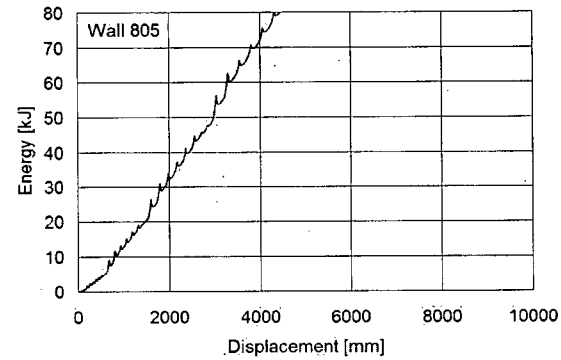

d) CASHEW wall 805

Figure 7.11: Predictive CASHEW hysteretic energy dissipations for walls 801, 802, 804 and 805;

7.5 Summary

Though the CASHEW software was found to be difficult to utilize for the tall walls studied, verified and predicted some general observations, trends, and suggestions can made based on the information attained. The tall walls that were verified by the CASHEW software showed some correlation between the modelled and experimental results especially up to maximum load, with correlation ceasing beyond this point. The SPF studded walls with 9.5 mm and 15.1 mm OSB sheathing showed decent agreement between the modelled and true wall behaviours, with hysteretic energy dissipation showing the greatest degree of correspondence. With a more finely tuned CASHEW analysis procedure it is foreseeable that CASHEW can be effectively utilized. The 15.1 mm OSB and LSL studded walls also showed some behaviour correlation though an expanded study into the models usage is definitely needed. Since the CASHEW software was developed based on conventional lumber studs in addition to conventionally sized wall heights, it is expected that some issues arise for tall wall modelling. A more thorough

investigation of the poorly corresponding 25.4 mm DFP and LSL studded walls needs also to be carried out. The poor correspondence may be due to a few different issues including the sheathing-to-framing connection tests themselves; being of a testing configuration that gives unrealistic behaviour, or the CASHEW software being unable to model the different tall wall behaviour in comparison to the conventionally sized walls. A further expansion and continuation of tall wall verification should be undertaken to further examine CASHEW's ability to accurately analyse tall wall behaviour.

The analytical prediction portion of this section must be viewed in context. The behaviours illustrated give some indication of performance such as general trends that may be expected. Trends such as the high lateral load response behaviour predicted for 1220 mm spaced studded LSL and LVL tall walls give indications that these walls have promise in the tall wall structures market. Further investigation is required to make more use of the prediction results and CASHEW itself, though as previously mentioned it is foreseeable that CASHEW can eventually be effective for the purposes sought out in this study.

8. CONCLUSIONS

8.1 Program Summary

The use of wood-based tall wall structures in current North American developments is low, however with continuing research and innovation this is changing. This particular thesis adds to this research base and provides further insight into the behaviour of tall wood-frame walls. In particular, the in-plane seismic performance of tall wood-frame walls was investigated. Stud type (dimension lumber or engineered wood product) and spacing, nail type and spacing, sheathing type and size, hold-down configuration, the influence of blocking, and the impact of vertical loading were the parameters that were looked at in detail. A review of current research as well as past building practices with regard to wood-based tall walls was performed. This review indicated the aforementioned lack of knowledge in this field, with most design codes and suggested building practices all but ignoring tall wood-based frame design. Upon review, a testing program was decided on in an effort to expand the research in this field. Forintek Canada Corporation in conjunction with the Department of Civil Engineering at the University of British Columbia collaborated on this testing program.

Initially the testing program consisted of full-scale tall wall testing and some material tests, but further expanded to include sheathing-to-framing and stud-to-plate connection tests. In addition, analytical model development and verification of the full-scale tests was done, and subsequently through use of the developed model, analytical predication of untested walls was completed.

The material tests that were performed were basic but necessary. Masses of the different wall constituents were determined as were the weak axis stiffness properties of the studs that were used in the wall designs. The main focus of the testing program came after the material testing. The building of the full-scale specimen walls as well as their testing constituted the majority of the work. The tall walls were erected onto a secure foundation and then subsequently tested either in a monotonic or cyclic fashion. The monotonic tests were used to develop the cyclic loading protocol. In total two monotonic tests were performed, one with dimension lumber (SPF) as the stud material and one with engineered wood product (LSL) as the stud material. The cyclic tests were performed with four and seven tests respectively for the dimension lumber

studded walls and LSL studded walls. OSB, DFP and type X gypsum wallboard were sheathed onto the walls with different types of fasteners. Fastener spacing ranged from 102 mm to 305 mm. Blocking was used in all but one of the walls, and vertical loading was applied to two of the walls. The wall behaviour when these parameters were changed provided a wealth of information regarding the wall performance under in-plane simulated seismic loading.

Once the full-scale tests were completed more specific tests were undertaken. First, stud-to-plate monotonic uplift tests were performed. These connections were tested to understand how the connection assembly behaved. The stud-to-plate connection setup was unique in that it did not utilize a conventional end-stud anchorage device. Instead, two Simpson H6 hurricane ties were used as the main lateral/uplift force resisting element on each stud. The ties were coupled with a joist hanger that provided resistance to out-of-plane forces. This connection setup provided for quick wall construction since the walls could be modularly constructed, then anchored through their bottom plates into the foundation.

Sheathing-to-framing connection tests followed. These tests were done so as to facilitate analytical wall modelling. The modelling software that was utilized was CASHEW and it required sheathing-to-framing connection test data for most of its input parameters. The sheathing-to-framing connection tests involved one nail, with the different specimens consisting of the same materials as those that were found in the full-scale tall wall tests as well as some connection types that were not. In particular, connections utilizing LVL as a stud material were investigated; it being a stud material not found in the full-scale tall wall tests.

Once the testing portions of the program were complete, the analytical portion of the project commenced. As mentioned, CASHEW was utilized as a means of modelling the tall walls that were tested. This software was decided upon due to its wood design basis and its apparent ease of use. The sheathing-to-framing connection data was used to determine the majority of the input parameters for the model. Once run, the outputted data was plotted and verified against the true tall wall experimental responses. This verification was done to the best of ability however the model had some difficulty with fully representing the true wall behaviour. Analytical prediction of untested walls was then carried out utilizing the sheathing-to-framing connection data. These predictions focussed on alternative wall geometries using connections

that were found in the full-scale tall wall tests as well as the connections that were not found in the tall wall tests.

When all the testing and analytical work was completed, the literary documentation was initiated; this thesis being that primary documentation. Significant findings, design recommendations as well as ideas for future research are provided in the following sections.

8.2 Significant Findings

Some of the important project findings are summarized as follows:

- Determining the stiffness and modulus of elasticity of wood-based studs can be done quickly and efficiently if done utilizing a vibration based methodology such as that provided in ASTM D6874.

- Tall wall capacities were found to be strongly influenced by the type and size of both sheathing and fasteners. The 9.5 mm OSB sheathed walls failed primarily in nail pull-through, while the thicker 15.1 mm OSB and 25.4 mm DFP sheathed walls failed primarily due to nail fatigue failure. To benefit from the full energy dissipation properties of the steel fasteners (nails), ensuring the latter failure mode occurs should be a goal. The use of thicker sheathing or the use of smaller diameter nails could accomplish in this.

- The 25.4 mm DFP sheathed walls were observed to have fasteners that developed up to four plastic hinges during testing. In comparison to single plastic hinging behaviour found in the walls with 9.5 mm or 15.1 mm OSB sheathing, this multiple plastic hinging behaviour indicates a greater ability to dissipate energy.

- SPF studded tall walls with 15.1 mm OSB sheathing and 610 mm stud spacing when compared to LSL studded tall walls with 15.1 mm OSB sheathing and 1220 mm stud spacing showed competitive responses. With equivalent nailing patterns the LSL based wall attained a higher maximum lateral load response, 53.4 kN, than the

comparable SPF based wall, 39.6 kN, however the SPF based wall dissipated 11% more hysteretic energy. The aforementioned lateral loads are from the first loading cycle direction response. The subsequent loading cycle direction responses were very similar, at 39.4 kN and 36.6 kN respectively. Their maximum load drifts were also essentially the same at about 1.9%

- Stud spacing is usually limited to 610 mm or less in structural wall elements. This limitation provides for load sharing that occurs between studs in close proximity to each other. The blocked tall walls tested with No. 2 or better 38 mm x 234 mm SPF studs and that had 610 mm stud spacing with perimeter and interior nail spacing of 102 mm and 152 mm respectively attained a maximum lateral load of 62.6 kN at a displacement of 125 mm (drift of 2.6%) and dissipated 51.6 kJ of hysteretic energy. These values are high in comparison to some the LSL studded tall walls that were tested with greater nail spacing. The LSL studded walls were also not tested with 610 mm stud spacing, only 1220 mm or 2440 mm stud spacing was utilized. LSL studded walls at 1220 mm were found to be capable of withstanding lateral loads as high as 77.8 kN or as low as 53.4 kN depending on nail size and spacing as well as sheathing. The LSL studded wall at 2440 mm stud spacing, with 102 mm nail spacing and 25.4 mm DFP reached a maximum load of 83.2 kN and dissipated 51.6 kJ of hysteretic energy. The relatively large stud spacing of 1220 mm did not appear to be detrimental to wall performance, with even 2440 mm stud spacing showing promising behaviour.

- The ductility of the tested walls was found to be dependant on the thickness of the sheathing used and the nail pattern and type. Similarly sheathed walls were found to have similar ductility's. The initial stiffness of the walls was also found to depend on the sheathing used, but more important was the nailing pattern. Densely nailed walls were found to be the stiffest walls in general. Stud spacing did not appear to cause appreciable changes to these two properties.

- Unlike conventional 2440 mm tall shearwalls studded with 38 mm x 89 mm studs stud-to-plate connection geometry was found to be important for the tall walls tested.

The 38 mm x 234 mm SPF studs were susceptible to torsional failure and deformation if the H6 ties used for lateral/uplift load mitigation were exclusively placed on the stud side opposite the sheathing at the stud-to-plate interface. This formation was changed to a dual H6 tie connection setup in addition to a conventional hanger. The use of ties on the sheathed and non-sheathed sides of the connections resulted in the elimination of torsional failures. This dual H6 tie connection was found to be extremely simple and effective in acting as a primary component to the tall wall anchorage and hold-down system. This hold-down assembly was quick to construct and inexpensive to purchase. The H6 ties helped the tall walls attain maximum lateral loads up to 83.2 kN. When failure occurred the ties were found to yield, a beneficial property during a seismic event. Bolting the bottom plates to the foundation was found to be a quick and effective to secure the tall walls. The anchor bolts near the end studs were found to be more effective when bolted closer to the studs at preventing bottom plate lift from the foundation.

- When nail spacing was investigated, it was found that greater nail densities result in corresponding increases in most wall properties. Both SPF and LSL based walls displayed this. Nail density increases resulted in higher resultant maximum loads and hysteretic energy dissipations as well as increases in wall stiffness and maximum drifts. Wall 605 had 61.4% more nails than wall 603, consequently, maximum load and hysteretic energy dissipation both increased approximately 60%. Ductility was found to decrease slightly with an increase in nail density over both wall series as well. When nail density was increased with regard to nail size (larger diameter), increases in maximum loads and hysteretic energy dissipations were also found.

- The blocked walls behaved in a manner that resulted in the failure mode of the walls to be predictable, that being bottom sheathing-to-plate connection failure. Though the type of fastener failure changed with the sheathing thickness, the initial failure location did not change when non-vertically loaded walls were tested. Failure of the walls always occurred at the bottom sheathing-to-plate interface and up the first vertical 1220 mm of the studs connecting to the perimeters of the sheathing. When vertical load was applied, the SPF studded tall wall had a different failure path. It failed at the mid-height at the sheathing-to-blocking interface. This did not happen

in the vertically loaded LSL stud based walls, though it is foreseeable that with a larger vertical load this would occur.

- A direct comparison between unblocked and blocked tall walls revealed that blocked walls perform far better in all comparable aspects with regard to wall behaviour. Of the directly comparable walls (704 and 707) increases of 147% and 99% for maximum load and hysteretic energy dissipation respectively were found for blocked wall 704. The blocked walls, though more expensive, are a justifiable option for construction of large tall wall structures that are expected to incur high lateral loads. Using as engineered wood product such as LSL is an expensive design option for unblocked walls and should be avoided. In addition to the increases in capacities, the blocked tall walls were found to have a definitively different wall response shape. The blocked walls had studs that bent near the bottom half of the walls but remained in a linear shape at the top, whilst the unblocked wall had stud bending in the middle of the wall with more of a linear stud shape at the top and bottom.

- Type X gypsum wallboard was found to increase the initial stiffness of an already 15.1 mm OSB sheathed tall wall as well the maximum lateral load. This maximum lateral load however occurred at a lower displacement level to that of an equivalent non-wallboarded tall wall. This is reflected in the National Building Code of Canada (NBCC, 2005) giving a force modification factor of R_d, as 2. The NBCC-2005 also gives the option of disregarding the wallboard and designing as simply sheathed on one side, with the R_d value as 3. This latter option should be chosen with care, since it was shown that maximum load occurred at a noticeably lower displacement level. The wallboarded wall is also stiffer and consequently the performance of the wall would be miscalculated if the wallboard was disregarded. Once the wallboard failed, the wall response was the same as that of the non-wallboarded wall.

- The LSL stud-to-LSL plate connections were found to be significantly stiffer on average than the SPF stud-to-LSL plate connections when these connections were tested individually.

- SPF based sheathing-to-framing connections are more prone to nail withdrawal from the stud than the relatively more dense LSL and LVL based sheathing-to framing connections. Spiral shank nails were less prone to nail withdrawal than common smooth shank nails

- The sheathing-to-framing connection tests indicated that the perpendicular sheathing-to-framing orientation is stronger with respect to load and dissipates more hysteretic energy in general than that of a longitudinal loading orientation amongst the 25.4 mm DFP and 15.1 mm OSB in combination with LSL or LVL studs. Perpendicular and longitudinal arrangements involving SPF studs displayed similar behaviour or showed that the longitudinal arrangements are stronger. The longitudinal orientation is one in which the loading direction is parallel to that of the stud, while the perpendicular orientation has the loading perpendicular to the stud. LSL based connections appeared to have the greatest differential in properties amongst the differing orientations.

- Sheathing-to-framing connections with thicker sheathing and larger nails withstood larger loads and dissipated more energy. These connections, in general, also had higher initial stiffness compared to thinner sheathed and smaller nailed connections.

- Sheathing-to-framing tests showed that nail failure patterns, in general, corresponded to the types of connection failures observed in the full-scale tall wall tests. The 9.5 mm OSB sheathed specimens experienced nail pull-through while the thicker sheathing had nail fatigue shear failures. The multiple plastic hinges observed in the 25.4 mm DFP tall wall tests were also observed in the individual connection tests, as were limited multiple plastic hinging in some 15.1 mm OSB sheathing-to-framing connection tests.

- The software CASHEW, that was used to verify the tall wall tests of this testing program, resulted in limited analytical correspondence with the true wall behaviour. The thirteen direct and indirect connection input parameters that CASHEW requires are sensitive to their interpretation from the load vs. displacement plots of the

sheathing-to-framing connection tests. This is a potential source of poor accuracy as is the fact that CASHEW was developed using conventionally sized walls (walls around 2.4 m in height). Some correlation between the true tall wall behaviour with that of the modelled did occur. This correlation generally occurred prior to wall failure with load vs. displacement wall response and hysteretic energy dissipation of the SPF based tall walls appearing to have a greater degree of correlation than the LSL based tall walls. The behavioural correlations of all verified walls essentially cease after maximum load is reached by the true tall walls. CASHEW models the walls as continuing to withstand loads after maximum load is reached, while the true walls lack significant load capacity beyond this point. Maximum loads are over-predicted as are the hysteretic energy dissipations for all walls.

- CASHEW model instability at points of sudden load changes over short displacements, as is the case at connection failures, also proved to be problematic. This instability can be mitigated somewhat by reducing the input displacement step however in such cases modelling times increased to a point of inefficiency. Since the load degradation response of the cyclic sheathing-to-framing connection tests performed in this study gave steep load declines after maximum load was attained, the R2 CASHEW input parameter needed to be altered in a manner that displayed the load degradation as more gradual. It is possible to represent the connection failure path including the steep decline in strength degradation at failure, however the added analysis time is counter-productive. Modelling consequently focused on the behaviour of the wall prior to failure. Data output also presented challenges when small step sizes were used; over 350,000 data point pairs were output after each analysis; conventional spreadsheet software could not directly handle this large data input without data being first formatted.

- As indicated previously, CASHEW modelled hysteretic energy correlation could be close prior to wall failure with most discrepancies being overestimations. A source of overestimation is the models inability to present three different cycle envelope curves as required by the ISO 16670 standard protocol used in this testing program.

- Poor correlation prior to maximum load may have resulted due to the software assumption that the wall studs remain rigid. It was observed that this is not the case for the true tall wall behaviour. Over a height of 2.4 metres this rigid stud assumption was deemed satisfactory when CASHEW was developed, but it may not be for taller walls. A more in-depth analysis of this software should be carried out with regard to tall wall modelling.

- The CASHEW software was developed on 2.4 m wood-frame shearwalls. It appears to have limited success in predicting the responses of 4.88 m walls. The simplicity of use and simple connection basis results in the software being tempting to be used, however, some concerns are present including the increased computation time for complicated loading schemes, its limited correlation to true tall wall behaviour up to maximum load and the inability to model tall wall performance after maximum load has been reached.

- As a means of attaining better wall response correlation between true wall behaviour and analytical behaviour a standardized method of treating the sheathing-to-framing connection data could be looked into. When the sheathing-to-framing F0 connection parameter was decreased arbitrarily by 20% for certain walls better wall response correlation resulted. Similar techniques could be investigated as a means of CASHEW being better able to represent true tall wall behaviour.

- To use CASHEW as has been done in this study for accurate wall behaviour prediction, further study including additional tall wall specimen testing should be performed. The model verification showed that significant deviations in analytical and experimental wall behaviours remain. CASHEW should be further investigated with regards to its ability to accurately model tall walls such as those in this project. This is not to say that this software cannot be used in the future, only that with regards to the tall walls of this study its effectiveness is limited.

8.3 Design Recommendations

Based on the significant findings, design considerations from this project are given as follows:

- Do not design tall blocked shearwalls with 9.5 mm OSB sheathing since the nails pull-through the sheathing;

- When designing tall blocked shearwalls with moderately thin sheathing such as 15.1 mm OSB do an in-depth cost analysis of the type of stud base material to be used based on necessary lateral and vertical force requirements, since SPF and LSL studs both present viable options;

- When large lateral and vertical loads are expected, the use of large LSL studs and thick sheathing sizes, such as 25.4 mm DFP, should be considered for use in conjunction with appropriate fastener selection;

- When type X gypsum wallboard is utilized, the NBCC-2005 force modification factor, R_d, as 2, should be used, since the disregarding of the wallboard gives a false sense of wall behaviour;

- Design tall SPF based blocked shearwalls at no more than 610 mm stud spacing, while LSL stud based blocked tall walls should be designed with confidence up to 1220 mm stud spacing, though spacing of up to 2440 mm can be investigated so long as top plate detailing for transfer of vertical load is examined;

- The use of engineered wood product such as LSL should only be used in blocked shearwalls to be cost-effective. The use of the relatively expensive LSL in unblocked situations should be avoided;

- When restraining studs to the bottom plate with significant depth ensure the stud is constrained at both the sheathed and unsheathed side of the wall to prevent torsional deformations of the studs;

- The dual H6 tie and hanger stud-to-plate connection setup along with the foundation anchorage used in this project can be considered as an effective wall hold-down system. It showed large lateral load resistance characteristics along with beneficial yielding behaviour and allows for cost-effective modular construction;

- When utilizing the hold-down assemblage and anchorage of this study care in choosing anchor bolt bolting distance, strength and type of washer is needed;

- When modelling structural performance with the CASHEW structural analysis software for tall walls, conservative usage of predicted maximum loads, maximum displacements and hysteretic energy dissipation is needed, due to a tendency for overestimations of performance;

- The reliance of structural performance data of tall shearwalls based on CASHEW modelling after the point of maximum load should not be done at present if using the methodology shown in this study.

8.4 Future Research Possibilities

This project was large and the findings from it many, however there still exists many avenues of research that can further expand tall wall wood-based frame construction and design. Following is a listing of possible future research endeavours, but not all, since it is impossible to know exactly all of what will be required to ensure wood-based tall wall design is considered as a viable design alternative to that of concrete tilt-up and steel-frame designs.

- Perform more monotonic and cyclic tall wall tests as a means of increasing the available tall wall data researchers can draw upon to make design recommendations. Tests that investigate more types of stud materials, sizes and grades and sheathing materials, sizes and grades should be performed as well as tests that look into different aspects of wall geometry such as blocking, stud spacing, wall openings,

wall heights and connection types. Changes in loading patterns and rates could also be investigated, including the addition of larger vertical loads.

- Perform shake-table tests of full scale tall wall specimens. In-plane seismic tests on a single wall element or six degree of freedom tests on an entire tall wood-frame structure would be beneficial. The correlation of this data and data from racking tests could be done, with structural analysis software used to develop a modelling procedure that correctly verifies tall wall performance. This would give a more accurate understanding of wood-frame tall wall performance in seismic situations.

- Further investigate new ways to anchor and hold-down wood-frame tall walls. The development of new ways to restrain wood-frame walls may help spur on new tall wall designs that can lower construction costs and perhaps result in larger and stronger wood-frame walls.

- Attempt to get CASHEW to better correlate with the experimental tall wall behaviour. This can be done through possible subroutine alterations and additions or by developing a more thorough method of treating the sheathing-to-framing connection test data so as to have CASHEW better portray true wall behaviour.

- Look into software alternatives to CASHEW for tall wall modelling. The investigation of said software may include finite element models as well as other commercially available software.

- Develop sets of seismic force reduction factors as well as other design factors for wood-frame tall walls that can be implemented into Canadian and International building and design codes.

- Create a set of accurate design calculations that can be utilized to give general wood-frame tall wall properties such as expected lateral drift, maximum load, wall stiffness and ductility and possibly expected hysteretic energy dissipation.

9. BIBLIOGRAPHY

AISI (2006). American Iron and Steel Institute website, http://www.steel.org.

ASTM (2002). "Standard Test Methods for Mechanical Fasteners in Wood—D 1761-88 (Reapproved 2000)." *Annual Book of ASTM Standards,* American Society for Testing and Materials, 04(10).

ASTM (2003). "Standard Test Method for Nondestructive Evaluation of Wood-Based Flexural Members Using Transverse Vibration—D 6874-03." *Annual Book of ASTM Standards,* American Society for Testing and Materials, 04(10).

Brooks, H. (1999). *The Tilt-Up Design and Constructional Manual, Fifth Edition.* H.B.A. Publications, Newport Beach, CA.

Ceccotti, A., and Karacabeyli, E. (2002). "Validation of seismic design parameters for wood-frame shearwall systems." *Canadian Journal of Civil Engineering.* Vol. 29: 484-498.

CEN (1994). Design provisions for earthquake resistant structures. Draft ENV 1998-1-1. Eurocode No. 8, Comite Europeen de Normalisation (European Committee for Standardization), Brussels, Belgium.

CEN (1995). Timber structures test methods – cyclic testing of joints with mechanical fasteners, EN TC 124.117, Comite Europeen de Normalisation (European Committee for Standardization), Brussels, Belgium.

Commins, A., and Gregg, R. (1994). "Effect of hold-downs and stud-frame systems on the cyclic behaviour of wood shear walls." *Proceedings of Research Needs Workshop on Analysis, Design and Testing of Timber Structures Under Seismic Loads,* G.C. Foliente, ed., Forest Products Laboratory, University of California, Richmond, CA., 142-146.

CSA (2001). *Engineering Design in Wood (Limit States Design)*, Canadian Standards Association CSA O86-01-2001, Etobicoke, ON.

CWC (1999). *Design and Costing Workbook*, Canadian Wood Council, Ottawa, ON.

CWC (2000). *Tall Walls Workbook*, Canadian Wood Council, Ottawa, ON.

CWC (2001). *Wood Design Manual*, Canadian Wood Council, Ottawa, ON.

Davis, G., (1999, October 14)., "Tilting at Danger.", *Metro Silicon Valley Newspaper.*

Dean, J., Stewart, W., and Carr, A. (1987). "The seismic design of plywood sheathed timber frame shear walls." *Pacific Conference on Earthquake Engineering*, Wairakei, New Zealand. 2: 165-175.

Dean, P., and Shenton, H. (2005). "Experimental Investigation of the Effect of Vertical Load on the Capacity of Wood Shear Walls." *Journal of Structural Engineering*, ASCE, 131(7): 1104-1113.

Dolan, J., and Foschi, R. (1991). "Structural analysis model for static loads on timber shear wall." *Journal of Structural Engineering,* ASCE, 117(3): 851-861.

Dolan, J., and Madsen, B. (1992). "Monotonic and cyclic tests of timber shear walls." *Canadian Journal of Civil Engineering*. Vol. 19: 415-422.

Durham, J., Lam, F., and Prion, H. (2001). "Seismic Resistance of Wood Shear Walls with Large OSB Panels." *Journal of Structural Engineering*, ASCE, 127(12): 1460-1466.

Filiatrault, A. (1990). "Static and dynamic analysis of timber shear walls." *Canadian Journal of Civil Engineering,* 17(4): 643-651.

Foliente, G. (1995). "Hysteresis modeling of wood joints and structural systems." *Journal of Structural Engineering*, ASCE, 121(6): 1013-1022.

Foliente, G., Paevere, P., Saito, T., and Kawai, N. (2000). "Reliability Assessment of Timber Shear Walls Under Earthquake Loads." *Proceedings of 12th World Conference of Earthquake Engineering*, Auckland, New Zealand.

Folz, B., and Filiatrault, A. (2000). "CASHEW - Vesrion 1.0." A Computer Program for Cyclic Analysis of Wood Shear Walls. Division of Structural Engineering, The University of California, San Diego, CA.

Folz, B., and Filiatrault, A. (2001). "Cyclic Analysis of Wood Shear Walls." *Journal of Structural Engineering*, ASCE, 127(4): 433-441.

Gaston, C., Kozak, R., O'Conner, J., and Fell, D. (2001). *Potential for increased wood-use in North Anerican non-residential markets.* Forintek Canada Corporation, Vancouver, BC.

Gupta, A., and Kuo, G. (1985). "Behaviour of wood-framed shear walls." *Journal of Structural Engineering*, ASCE, 111(8): 1722-1733.

Gupta, A., and Kuo, G. (1987). "Wood-framed shear walls with uplifting." *Journal of Structural Engineering*, ASCE, 113(2): 241-259.

He, M., Lam, F., and Prion, H. (1998). "Influence of cyclic test protocols on performance of wood based shear walls." *Canadian Journal on Civil Engineering*, Vol. 25: 539-550.

He, M., Magnusson, H., Lam, F., and Prion, H. (1999). "Cyclic performance of perforated wood shear walls with over sized panels." *Journal of Structural Engineering*, ASCE, 125(1): 10-18.

ISO (2003). "ISO standard 16670, Timber structures—joints made with mechanical fasteners—Quasi-static reversed-cyclic test method." ISO Technical committee on timber structures. Geneva, Switzerland.

Karacabeyli, E., and Ceccotti, A. (1996). "Test Results on the Lateral Resistance of Nailed Shear Walls." *Proceedings of the 1996 International Wood Engineering Conference,* New Orleans, Vol. 2: 179-186.

Lam, F., Prion, H., and He, M. (1997). "Lateral resistance of wood shear walls with large sheathing panels." *Journal of Structural Engineering*, ASCE, 123(12): 1666-1673.

Leiva-Aravena, L. (1996). "Behaviour of Timber Shear Walls Subjected to Reversed Cyclic Lateral Loading." *Proceedings of the 1996 International Wood Engineering Conference*, New Orleans, Vol. 2: 201-206.

Leonard, D. (2004). "The Structural Performance of Tall Wood-Frame Walls Under Axial and Transversal Loads." M.A.Sc. thesis, University of British Columbia, Vancouver, BC.

McKeever, D., and Adair, C. (1998). "Wood products used in non-residential building construction." Wood Products Promotion Council (Wood Products Council).

Mi, H., Ni, C., Chui, Y., and Karacabeyli, E. (2006). "Racking Performance of Tall Unblocked Shearwalls." *Journal of Structural Engineering*, ASCE, 132(1): 145-152.

NBCC (1995). *National Building Code of Canada.* Canadian Commission on Building and Fire Codes, National Research Council of Canada, Ottawa, ON.

NBCC (2005). *National Building Code of Canada.* Canadian Commission on Building and Fire Codes, National Research Council of Canada, Ottawa, ON.

NCMA (2003). National Concrete Association website, http://www.ncma.org.

Ni, C., Karacabeyli, E., and Ceccotti, A. (2000). "Lateral load capacities of horizontally sheathed unblocked shear walls." *CIB-W18 paper.*

Portland Cement Association. (1997). *Home builder report of 1997*, based on survey.

Rose, J. (1994). "Performance of wood structural panel shear walls under cyclic (reversed) loading." *Proceedings of Research Needs Workshop on Analysis, Design and Testing of Timber Structures Under Seismic Loads,* G.C. Foliente, ed., Forest Products Laboratory, University of California, Richmond, CA., 129-141.

Ruhnke, J., and Schexnayder, F. (2002). "Description of tilt-up practice." *Practice Periodical on Structural Design and Construction.* 7(3): 103-110.

Shenton, H., Dinehart, D., and Elliott, T. (1998). "Stiffness and energy degradation of wood frame shear walls." *Canadian Journal of Civil Engineering*, Vol. 25: 412-423.

Skaggs, T., and Rose, J. (1996). "Cyclic load testing of wood structural panel shear walls." *Proceedings of the 1996 International Wood Engineering Conference,* New Orleans, Vol. 2: 195-200.

Stewart, W. (1987). "The seismic design of plywood sheathed shear walls." Ph.D. thesis, University of Canterbury, Christchurch, New Zealand.

TCA (2006). Tilt-Up Concrete Association website, http://www.tilt-up.org.

Tissell, J. (1990). "Structural panel shear walls." *APA Research Report 154*, Tacoma, WA.

USBC 2000. (2000). United States Bureau of the Census.

White, M., and Dolan, J. (1995). "Non-linear shear-wall analysis." *Journal of Structural Enigneering,* ASCE, 121(11): 1629-1635.

Yasumura, M. (1992). "Mechanical properties of wood-framed shear walls subjected to reversed cyclic lateral loading." *Proceedings of 24th Meeting of International Council for Building Research Studies and Documentation*; Working Commission W18A-Timber Structures; Ahus, Sweden.

APPENDIX A: EXPERIMENTAL TEST PROGRAM RESULTS

Within Appendix A are the significant results of the experimental testing program including; the results of the tall wall tests, the stud-to-plate connection tests and the sheathing-to-framing connection tests. In addition, the loading protocols used for the cyclic testing portions of the tall wall tests and sheathing-to-framing connection tests are also provided.

A.1 Testing Information

Appendix A.1 gives the ISO standard loading protocol graphical representations for the cyclic tall wall tests as well as the sheathing-to-framing connection tests. The ISO 16670 standard with the A.2 (d) modification (ISO, 2003) was used to cyclically test both the 600 and 700 series tall walls. The ISO 16670 standard with no modification (ISO, 2003) was used for all cyclic sheathing-to-framing connection tests.

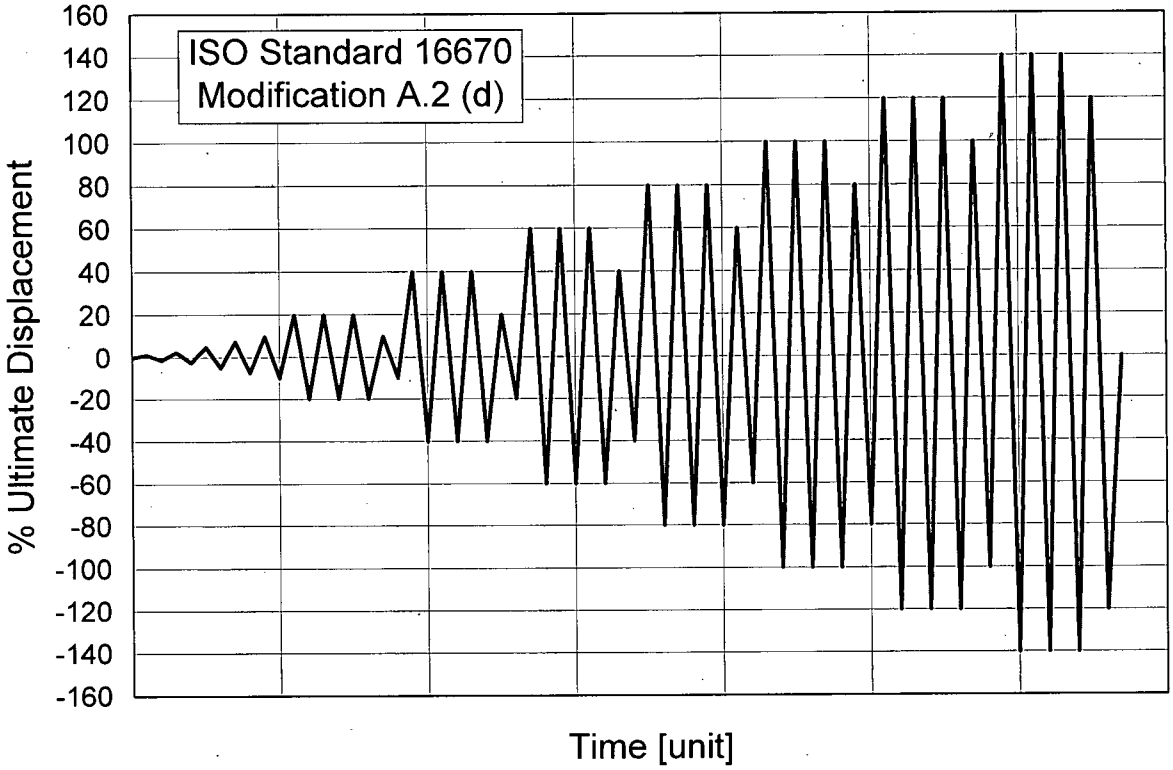
ISO Standard 16670
Modification A.2 (d)
% Ultimate Displacement
160
140
120
100
80
60
40
20
0
-20
-40
-60
-80
-100
-120
-140
-160
Time [unit]

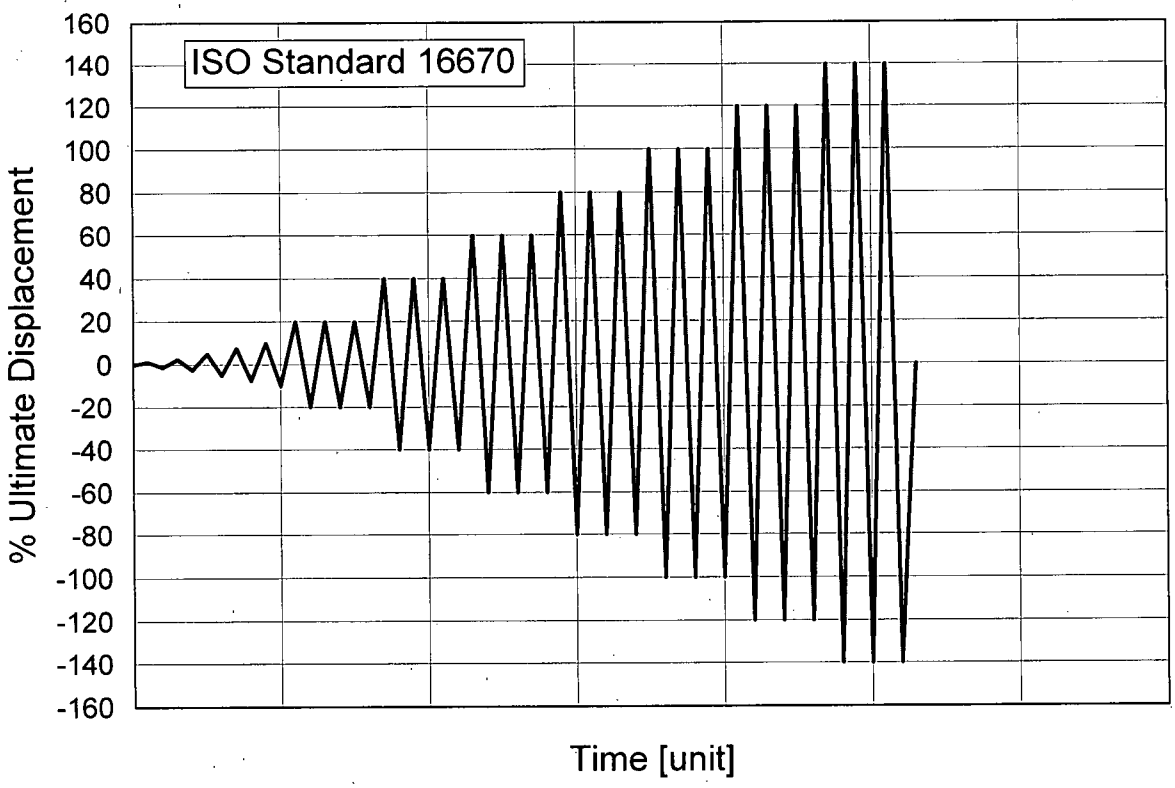
ISO Standard 16670
% Ultimate Displacement
160
140
120
100
80
60
40
20
0
-20
-40
-60
-80
-100
-120
-140
-160
Time [unit]

A.2 Tall Wall Test Results

The data presented in Section 4 as well as referred to through-out this thesis is shown in a more expanded form in this Appendix A.2. Load vs. displacement results as well as hysteretic energy dissipations of the tall wall tests are shown graphically and in numerical form. The geometric particulars to the wall specimens of concern are also shown. The parameters that are given are defined by the European CEN standard (CEN, 1995).

Description: **Tall-Walls 601 and 701**

Wall 601

Stud Type:	SPF No. 2 or better 38 mm x 234 mm
Stud Spacing:	610 mm c/c
Sheathing Type:	OSB 9.5 mm
Type of Nail:	Spiral, 2.5 mm diameter, 65 mm long
Nail Spacing: Perimeter	152 mm
Nail Spacing: Interior	305 mm
Blocking:	Present at every 1220 mm vertically
Stud-to-Plate Connection:	- One H6 tie on each of the studs on side opposite sheathing - One LU28L joist hanger on all studs - These properties apply to the top and bottom of the studs

Wall 701

Stud Type:	1.5E LSL 44 mm x 242 mm
Stud Spacing:	1220 mm c/c
Sheathing Type:	OSB 15.1 mm
Type of Nail:	Spiral, 2.5 mm diameter, 65 mm long
Nail Spacing: Perimeter	152 mm
Nail Spacing: Interior	305 mm
Blocking:	Present at every 1220 mm vertically
Stud-to-Plate Connection:	- Dual H6 ties on all studs - One HU9 joist hanger on all studs - These properties apply to the top and bottom of the studs

Load vs. Displacement Plot

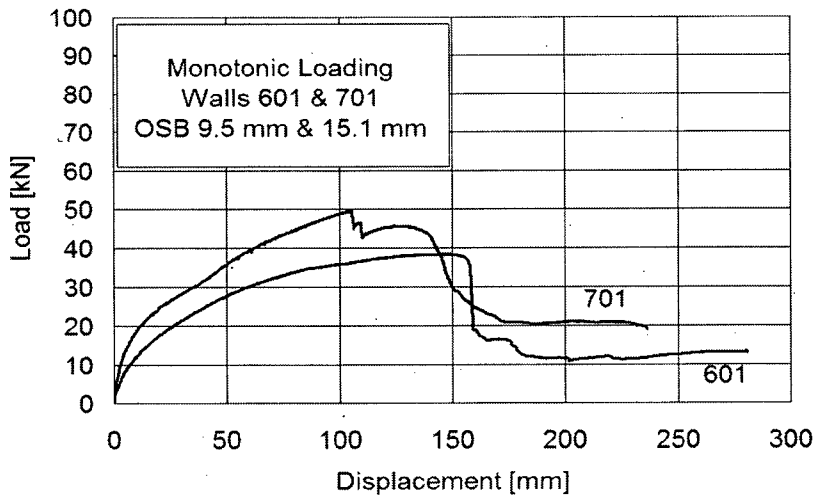

		Wall 601	Wall 701
Wall 601 / Wall 701*	Peak Load:	38.5 kN	49.5 kN
Monotonic	Displacement at Peak Load:	151.6 mm	110.4 mm

* Wall 701 failed prematurely due to poor anchorage

Description: **Tall-Wall 602**

Stud Type:	SPF No. 2 or better 38 mm x 234 mm
Stud Spacing:	610 mm c/c
Sheathing Type:	OSB 9.5 mm
Type of Nail:	Spiral, 2.5 mm diameter, 65 mm long
Nail Spacing: Perimeter	152 mm
Nail Spacing: Interior	305 mm
Blocking:	Present at every 1220 mm vertically

Stud-to-Plate Connection:

- Dual H6 ties on end-two-studs, both West and East
- One H6 tie on each of the remaining 5 studs on side opposite sheathing
- One LU28L joist hanger on all studs
- These properties apply to the top and bottom of the studs

Load vs. Displacement Plot

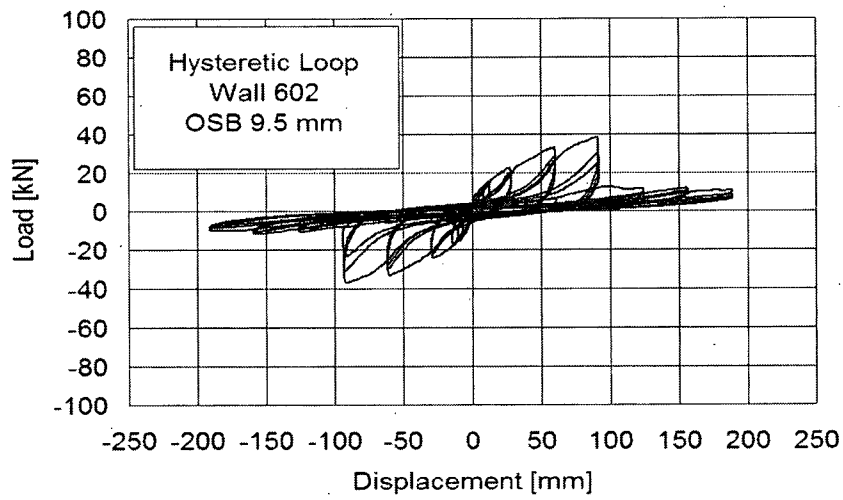

Quadrant 1 Results:	Peak Load:	38.2 kN
1st Envelope	Displacement at Peak Load:	94.4 mm
	Initial Stiffness:	0.987 kN/mm
	Ductility:	3.50
Quadrant 3 Results:	Peak Load:	36.9 kN
1st Envelope	Displacement at Peak Load:	93.7 mm
	Initial Stiffness:	1.426 kN/mm
	Ductility:	6.63
Overall:	Hysteretic Energy Dissipated:	25.0 kJ

Description: **Tall-Wall 603**

Stud Type:	SPF No. 2 or better 38 mm x 234 mm
Stud Spacing:	610 mm c/c
Sheathing Type:	OSB 15.1 mm
Type of Nail:	Spiral, 2.5 mm diameter, 65 mm long
Nail Spacing: Perimeter	152 mm
Nail Spacing: Interior	305 mm
Blocking:	Present at every 1220 mm vertically

Stud-to-Plate Connection:

- Dual H6 ties on end-two-studs, both West and East, and middle stud
- No H6 ties on the remaining 4 studs
- One LU28L joist hanger on all studs
- These properties apply to the top and bottom of the studs

Load vs. Displacement Plot

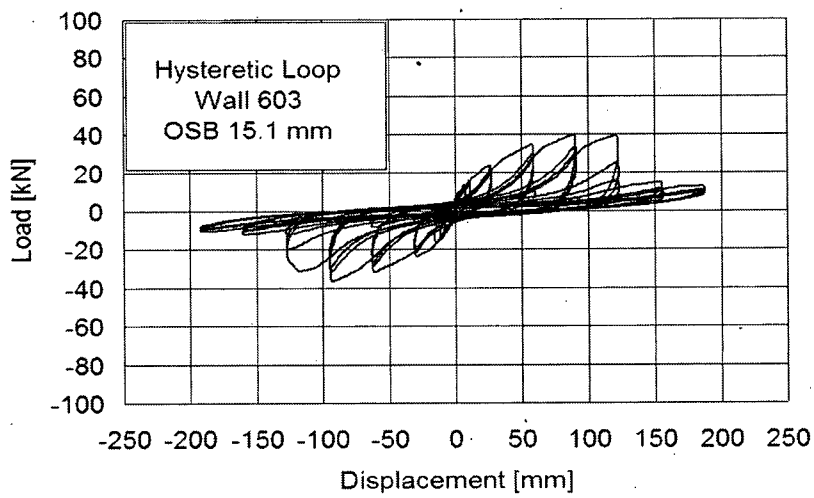

Quadrant 1 Results: 1st Envelope	Peak Load:	39.6 kN
	Displacement at Peak Load:	92.5 mm
	Initial Stiffness:	1.013 kN/mm
	Ductility:	4.78
Quadrant 3 Results: 1st Envelope	Peak Load:	36.6 kN
	Displacement at Peak Load:	93.9 mm
	Initial Stiffness:	1.300 kN/mm
	Ductility:	7.24
Overall:	Hysteretic Energy Dissipated:	32.3 kJ

Description: **Tall-Wall 604**

Stud Type:	SPF No. 2 or better 38 mm x 234 mm
Stud Spacing:	610 mm c/c
Sheathing Type:	OSB 15.1 mm
Type of Nail:	Spiral, 2.5 mm diameter, 65 mm long
Nail Spacing: Perimeter	152 mm
Nail Spacing: Interior	305 mm
Blocking:	Present at every 1220 mm vertically

Stud-to-Plate Connection:

- Dual H6 ties on end-two-studs, both West and East, and middle stud
- No H6 ties on the remaining 4 studs
- One LU28L joist hanger on all studs
- These properties apply to the top and bottom of the studs

Load vs. Displacement Plot

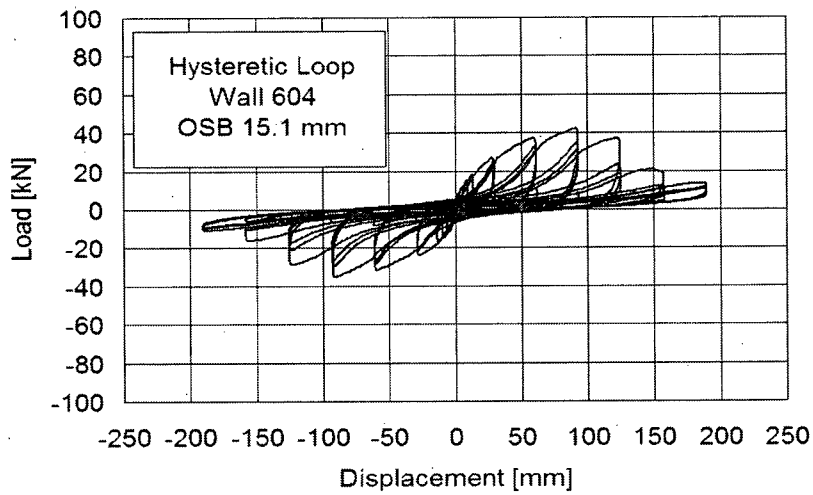

Quadrant 1 Results: 1st Envelope	Peak Load:	42.1 kN
	Displacement at Peak Load:	93.3 mm
	Initial Stiffness:	1.163 kN/mm
	Ductility:	5.01
Quadrant 3 Results: 1st Envelope	Peak Load:	35.3 kN
	Displacement at Peak Load:	93.9 mm
	Initial Stiffness:	1.361 kN/mm
	Ductility:	8.27
Overall:	Hysteretic Energy Dissipated:	34.9 kJ
Special Notes:	20 kN/m Vertical Load Applied	

Description: **Tall-Wall 605**

Stud Type:	SPF No. 2 or better 38 mm x 234 mm
Stud Spacing:	610 mm c/c
Sheathing Type:	OSB 15.1 mm
Type of Nail:	Spiral, 2.5 mm diameter, 65 mm long
Nail Spacing: Perimeter	102 mm
Nail Spacing: Interior	152 mm
Blocking:	Present at every 1220 mm vertically

Stud-to-Plate Connection:

- Dual H6 ties on end-two-studs, both West and East, and middle stud
- No H6 ties on the remaining 4 studs
- One LU28L joist hanger on all studs
- These properties apply to the top and bottom of the studs

Load vs. Displacement Plot

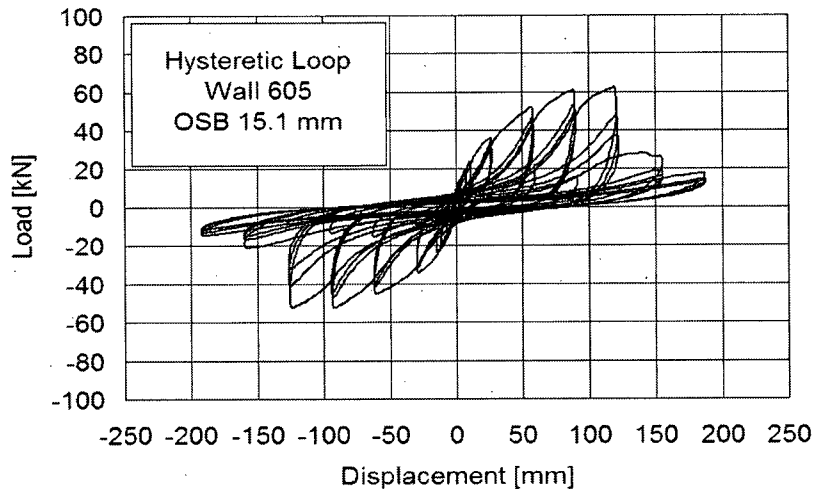

Quadrant 1 Results: 1st Envelope	Peak Load:	62.6 kN
	Displacement at Peak Load:	124.8 mm
	Initial Stiffness:	1.410 kN/mm
	Ductility:	3.92
Quadrant 3 Results: 1st Envelope	Peak Load:	52.5 kN
	Displacement at Peak Load:	93.5 mm
	Initial Stiffness:	1.727 kN/mm
	Ductility:	7.18
Overall:	Hysteretic Energy Dissipated:	51.6 kJ

Description: **Tall-Wall 702**

Stud Type:	1.5E LSL 44 mm x 242 mm
Stud Spacing:	1220 mm c/c
Sheathing Type:	OSB 15.1 mm
Type of Nail:	Spiral, 2.5 mm diameter, 65 mm long
Nail Spacing: Perimeter	152 mm
Nail Spacing: Interior	305 mm
Blocking:	Present at every 1220 mm vertically

Stud-to-Plate Connection:

- Dual H6 ties on all studs
- One HU9 joist hanger on all studs
- These properties apply to the top and bottom of the studs

Load vs. Displacement Plot

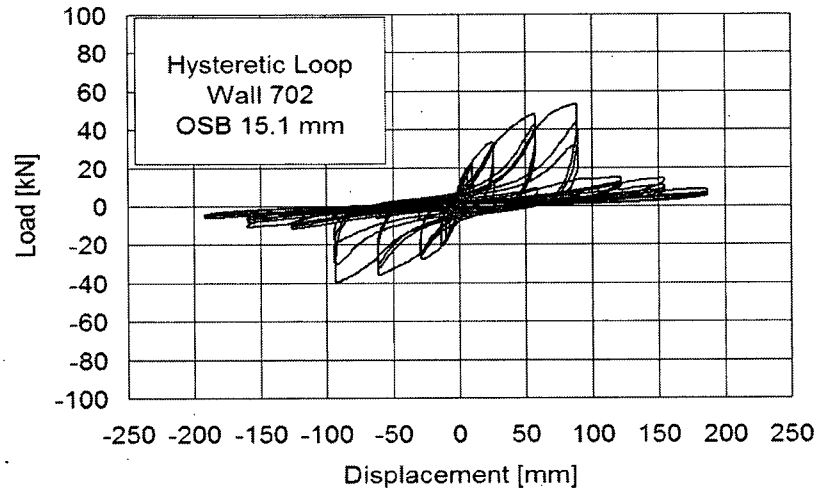

Quadrant 1 Results: 1st Envelope	Peak Load:	53.4 kN
	Displacement at Peak Load:	89.8 mm
	Initial Stiffness:	1.919 kN/mm
	Ductility:	5.38
Quadrant 3 Results: 1st Envelope	Peak Load:	39.4 kN
	Displacement at Peak Load:	92.9 mm
	Initial Stiffness:	1.906 kN/mm
	Ductility:	8.67
Overall:	Hysteretic Energy Dissipated:	29.6 kJ

Description: **Tall-Wall 703**

Stud Type:	1.5E LSL 44 mm x 242 mm
Stud Spacing:	1220 mm c/c
Sheathing Type:	OSB 15.1 mm
Type of Nail:	Spiral, 2.5 mm diameter, 65 mm long
Nail Spacing: Perimeter	152 mm
Nail Spacing: Interior	305 mm
Blocking:	Present at every 1220 mm vertically

Stud-to-Plate Connection:
- Dual H6 ties on all studs
- One HU9 joist hanger on all studs
- These properties apply to the top and bottom of the studs

Load vs. Displacement Plot

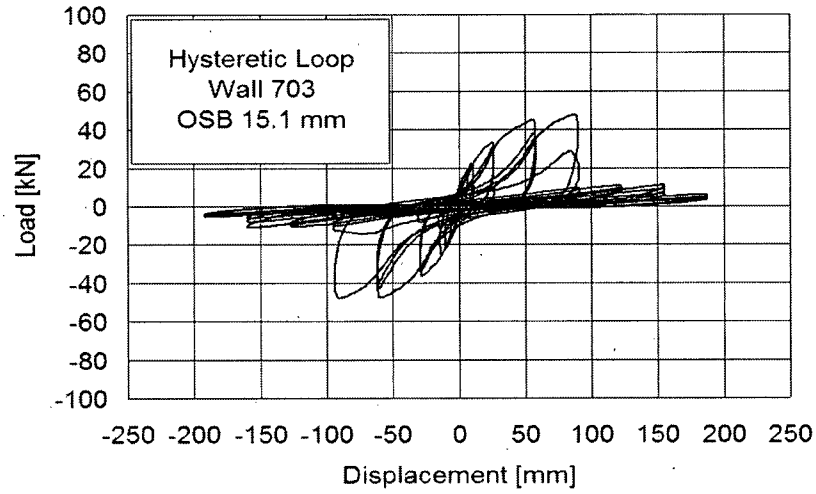

Quadrant 1 Results:	Peak Load:	48.1 kN
1st Envelope	Displacement at Peak Load:	90.1 mm
	Initial Stiffness:	2.058 kN/mm
	Ductility:	6.79
Quadrant 3 Results:	Peak Load:	48.0 kN
1st Envelope	Displacement at Peak Load:	91.9 mm
	Initial Stiffness:	2.069 kN/mm
	Ductility:	6.38
Overall:	Hysteretic Energy Dissipated:	29.0 kJ

Special Notes: 20 kN/m Vertical Load Applied

Description: **Tall-Wall 704**

Stud Type:	1.7E LSL 44 mm x 242 mm
Stud Spacing:	1220 mm c/c
Sheathing Type:	DFP 25.4 mm
Type of Nail:	Spiral, 3.0 mm diameter, 76 mm long
Nail Spacing: Perimeter	152 mm
Nail Spacing: Interior	305 mm
Blocking:	Present at every 1220 mm vertically

Stud-to-Plate Connection:

- Dual H6 ties on all studs
- One HU9 joist hanger on all studs
- These properties apply to the top and bottom of the studs

Load vs. Displacement Plot

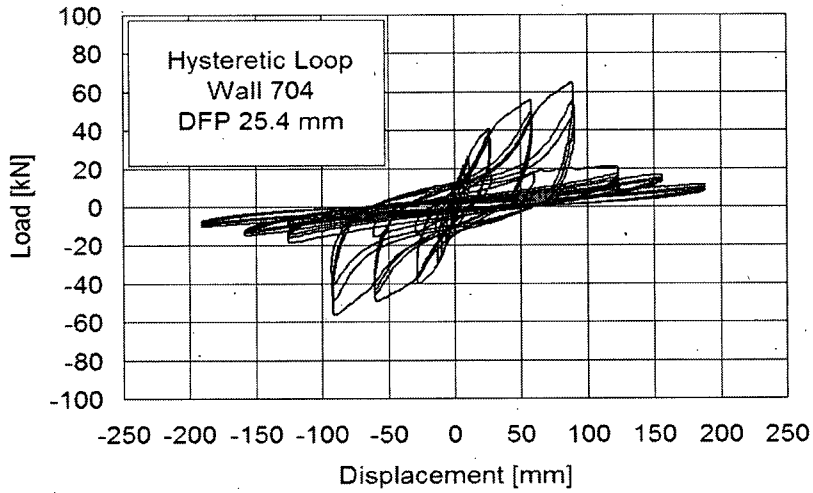

Quadrant 1 Results: 1st Envelope	Peak Load:	64.6 kN
	Displacement at Peak Load:	91.1 mm
	Initial Stiffness:	1.869 kN/mm
	Ductility:	4.23
Quadrant 3 Results: 1st Envelope	Peak Load:	56.5 kN
	Displacement at Peak Load:	92.8 mm
	Initial Stiffness:	2.307 kN/mm
	Ductility:	6.87
Overall:	Hysteretic Energy Dissipated:	45.8 kJ

Description: **Tall-Wall 705**

Stud Type:	1.7E LSL 44 mm x 242 mm
Stud Spacing:	1220 mm c/c
Sheathing Type:	DFP 25.4 mm
Type of Nail:	Common, 3.75 mm diameter, 76 mm long
Nail Spacing: Perimeter	152 mm
Nail Spacing: Interior	305 mm
Blocking:	Present at every 1220 mm vertically

Stud-to-Plate Connection:

- Dual H6 ties on all studs
- One HU9 joist hanger on all studs
- These properties apply to the top and bottom of the studs

Load vs. Displacement Plot

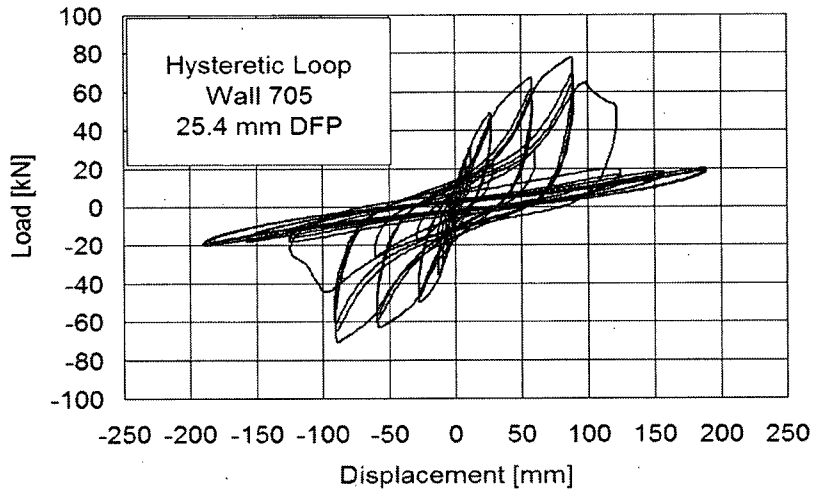

Quadrant 1 Results:	Peak Load:	77.8 kN
1st Envelope	Displacement at Peak Load:	90.5 mm
	Initial Stiffness:	2.095 kN/mm
	Ductility:	3.96
Quadrant 3 Results:	Peak Load:	70.8 kN
1st Envelope	Displacement at Peak Load:	89.7 mm
	Initial Stiffness:	2.907 kN/mm
	Ductility:	6.39
Overall:	Hysteretic Energy Dissipated:	58.4 kJ

Description: **Tall-Wall 706**

Stud Type:	1.7E LSL 44 mm x 242 mm
Stud Spacing:	2440 mm c/c
Sheathing Type:	DFP 25.4 mm
Type of Nail:	Spiral, 3.0 mm diameter, 76 mm long
Nail Spacing: Perimeter	102 mm
Nail Spacing: Interior	na
Blocking:	Present at every 1220 mm vertically
Stud-to-Plate Connection:	- Dual H6 ties on all studs - One HU9 joist hanger on all studs - These properties apply to the top and bottom of the studs

Load vs. Displacement Plot

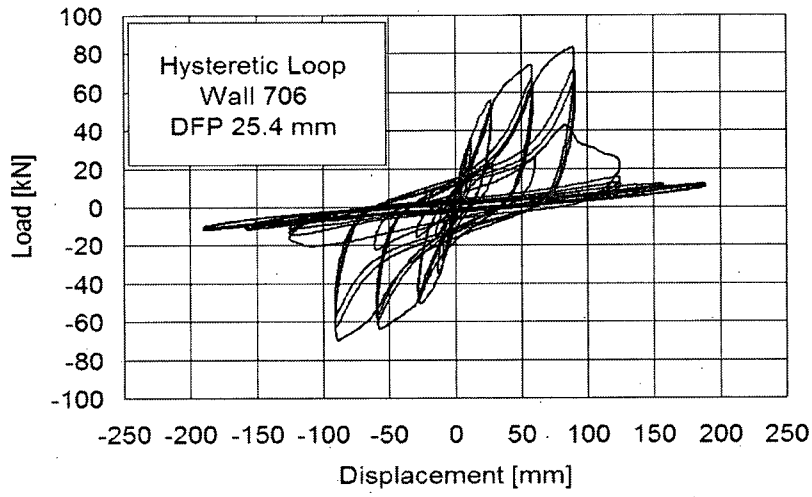

Quadrant 1 Results:	Peak Load:	83.2 kN
1st Envelope	Displacement at Peak Load:	91.3 mm
	Initial Stiffness:	2.562 kN/mm
	Ductility:	4.44
Quadrant 3 Results:	Peak Load:	70.7 kN
1st Envelope	Displacement at Peak Load:	89.4 mm
	Initial Stiffness:	3.065 kN/mm
	Ductility:	6.54
Overall:	Hysteretic Energy Dissipated:	51.6 kJ

Description: **Tall-Wall 707**

Stud Type:	1.7E LSL 44 mm x 242 mm
Stud Spacing:	1220 mm c/c
Sheathing Type:	DFP 25.4 mm
Type of Nail:	Spiral, 3.0 mm diameter, 76 mm long
Nail Spacing: Perimeter	152 mm
Nail Spacing: Interior	152 mm
Blocking:	None Present

Stud-to-Plate Connection:

- Dual H6 ties on all studs
- One HU9 joist hanger on all studs
- These properties apply to the top and bottom of the studs

Load vs. Displacement Plot

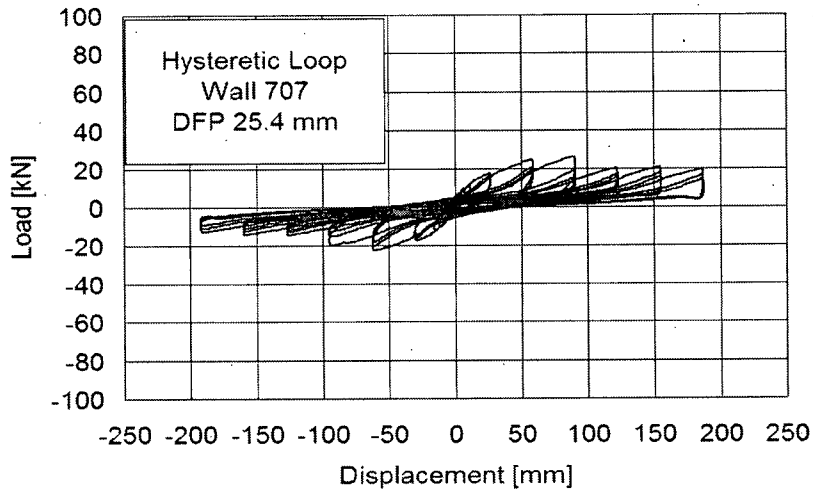

Quadrant 1 Results: 1st Envelope	Peak Load:	26.2 kN
	Displacement at Peak Load:	91.7 mm
	Initial Stiffness:	0.884 kN/mm
	Ductility:	5.63
Quadrant 3 Results: 1st Envelope	Peak Load:	22.4 kN
	Displacement at Peak Load:	61.9 mm
	Initial Stiffness:	0.932 kN/mm
	Ductility:	6.37
Overall:	Hysteretic Energy Dissipated:	23.0 kJ

Description: **Tall-Wall 708**

Stud Type:	1.5E LSL 44 mm x 242 mm
Stud Spacing:	1220 mm c/c
Sheathing Type:	OSB 15.1 mm and Type X Gypsum Wallboard 15.9 mm
Type of Nail/Screw:	Spiral, 2.5 mm diameter, 65 mm long & 41 mm long coarse-thread screws
Nail/Screw Spacing: Perimeter	152 mm (OSB) and 203 mm (Wallboard)
Nail/Screw Spacing: Interior	305 mm (OSB) and 203 mm (Wallboard)
Blocking:	Present at every 1220 mm vertically

Stud-to-Plate Connection:
- Dual H6 ties on all studs
- One HU9 joist hanger on all studs
- These properties apply to the top and bottom of the studs

Load vs. Displacement Plot

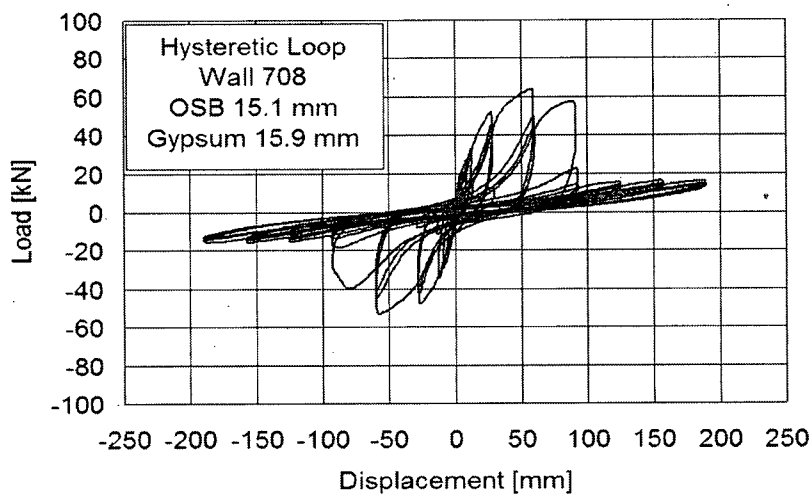

Quadrant 1 Results: 1st Envelope	Peak Load:	64.1 kN
	Displacement at Peak Load:	59.3 mm
	Initial Stiffness:	2.650 kN/mm
	Ductility:	5.35
Quadrant 3 Results: 1st Envelope	Peak Load:	53.4 kN
	Displacement at Peak Load:	59.0 mm
	Initial Stiffness:	3.699 kN/mm
	Ductility:	7.66
Overall:	Hysteretic Energy Dissipated:	32.5 kJ

Description: **Tall-Wall Energy Comparisons**

Hysteretic Energy Dissipation

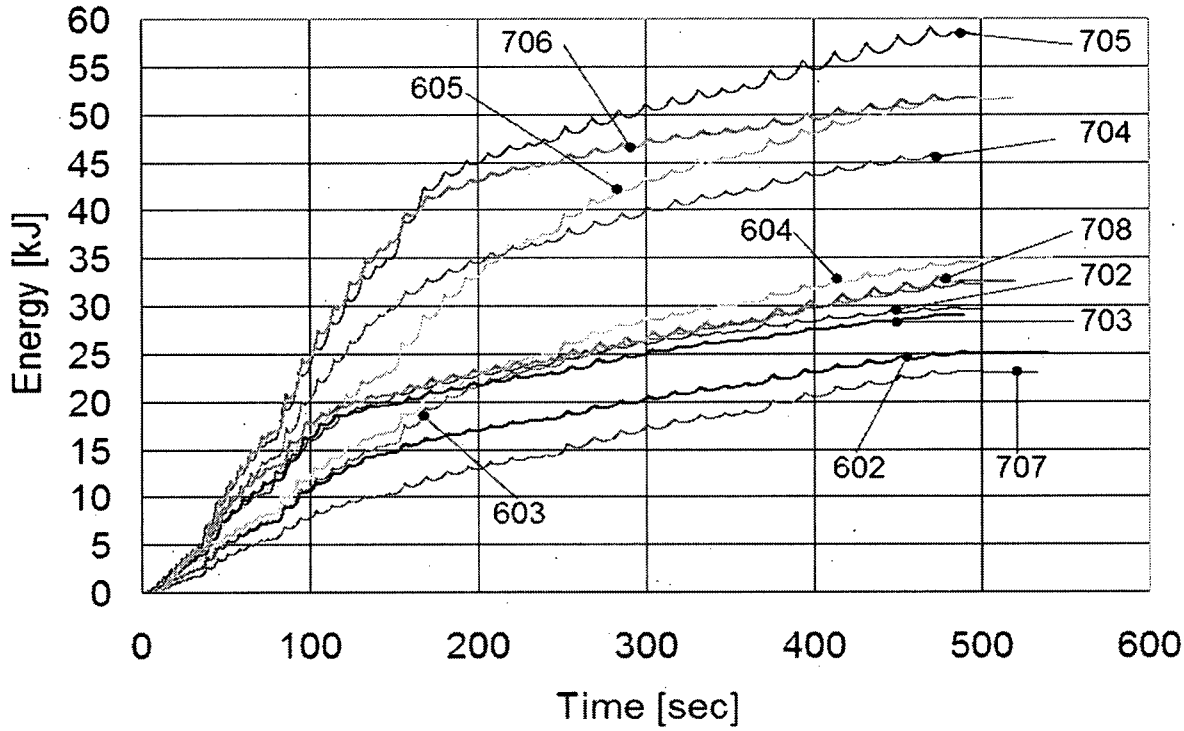

Hysteretic Energy Dissipation Results:

Tall-Wall Specimen	
602	25.0 kJ
603	32.3 kJ
604	34.9 kJ
605	51.6 kJ
702	29.6 kJ
703	29.0 kJ
704	45.8 kJ
705	58.4 kJ
706	51.6 kJ
707	23.0 kJ
708	32.5 kJ

A.3 Stud-to-Plate Connection Test Results

The data presented in Section 5 and referred to through-out this thesis is shown in a more expanded form in this Appendix A.3. Load vs. displacement results are shown graphically for the stud-to-plate connection tests and in numerical form. The geometric particulars to the connection specimens of concern are also shown. The parameters that are given are defined by the European CEN standard (CEN, 1995).

Description: **LSL Stud - to - LSL Plate Specimens**

LSL-to-LSL

Stud Type: 1.7E LSL Stud 44 mm x 242 mm
Plate Type: 1.7E LSL Plate 44 mm x 242 mm

Stud-to-Plate Connection:
- Dual H6 ties
- One HU9 joist hanger

Load vs. Displacement Plot

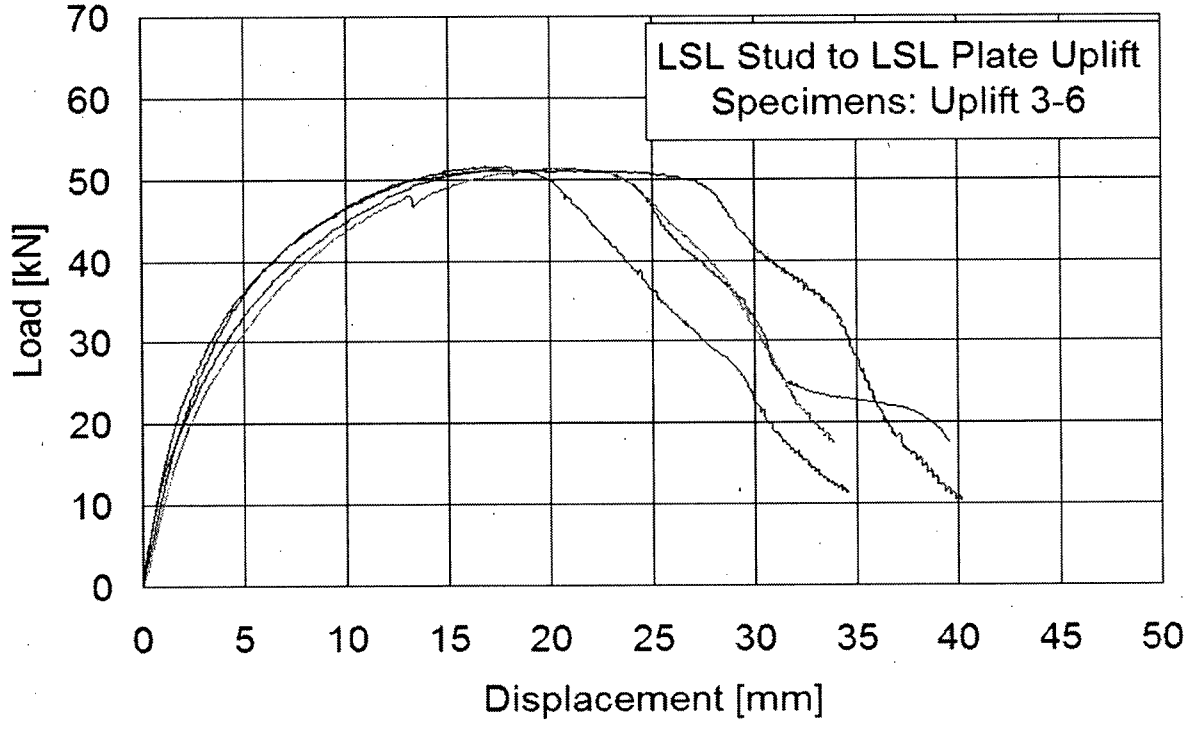

Results

Mean Peak Load:	51.3 kN
Mean Displacement at Peak Load:	17.8 mm
Mean 80% Load:	41.0 kN
Mean Displacement at 80% Load:	27.0 mm
Mean Yield Load:	35.9 kN
Mean Dispacement at Yield Load:	3.8 mm
Mean Initial Stiffness:	9.3 kN/mm
Mean Ductility:	7.4

Description: **SPF Stud - to - LSL Plate Specimens**

SPF-to-LSL

Stud Type:	SPF No. 2 or better 38 mm x 234 mm
Plate Type:	1.7E LSL Plate 44 mm x 242 mm
Stud-to-Plate Connection:	- Dual H6 ties - One LU28L joist hanger

Load vs. Displacement Plot

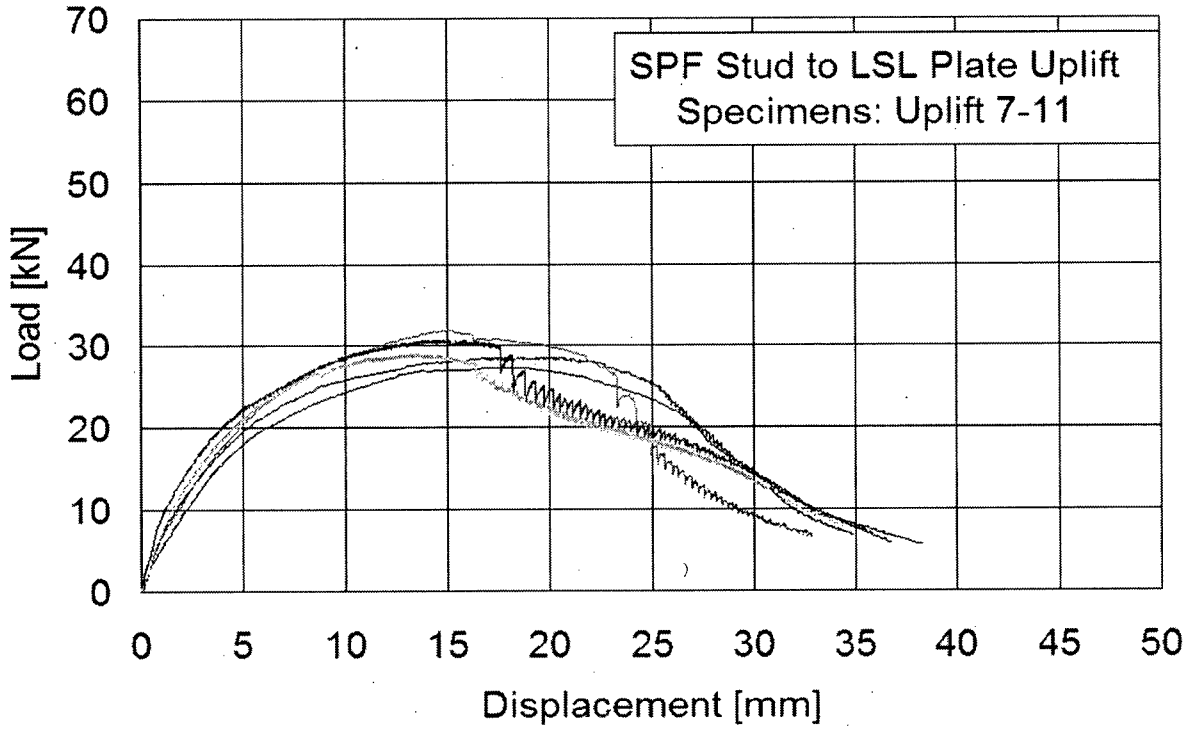

Results

Mean Peak Load:	29.5 kN
Mean Displacement at Peak Load:	16.0 mm
Mean 80% Load:	23.6 kN
Mean Displacement at 80% Load:	22.6 mm
Mean Yield Load:	22.2 kN
Mean Dispacement at Yield Load:	4.2 mm
Mean Initial Stiffness:	5.5 kN/mm
Mean Ductility:	5.2

A.4 Sheathing-to-Framing Connection Test Results

The data presented in Section 6 and referred to through-out this thesis is shown in a more expanded form in this Appendix A.4. Load vs. displacement results are shown graphically for the sheathing-to-framing connection tests and in numerical form. The geometric particulars to the connection specimens of concern are also shown. Both the longitudinal and perpendicular specimen results are given. The parameters that are given are defined by the European CEN standard (CEN, 1995).

Description: **Sheathing-to-Framing APARA Specimens**

Sample Size:	2 and 3
Loading Scenario:	Monotonic and Cyclic
Loading Direction:	Parallel as felt by stud
Stud Type:	1.7E LSL
Sheathing Type:	DFP 25.4 mm
Type of Nail:	Spiral, 3.0 mm diameter, 76 mm long

Load vs. Displacement Plot

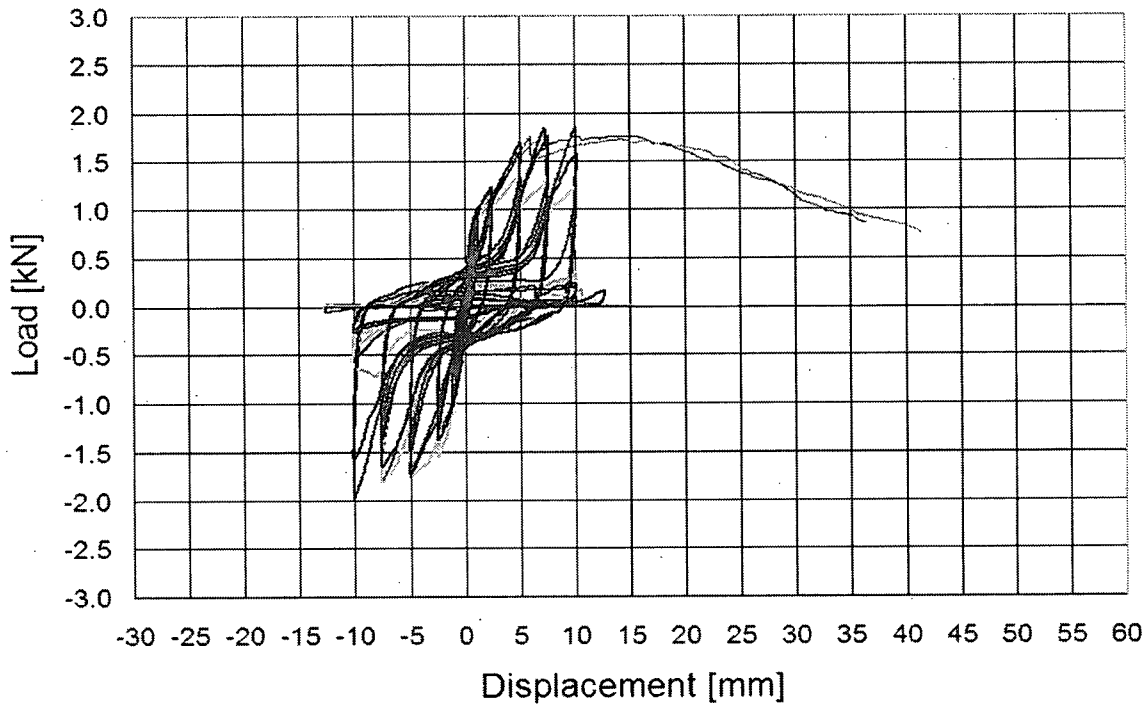

Average parameters		
Monotonic Results	Peak Load:	1.75 kN
	Displacement at Peak Load:	14.3 mm
Cyclic Quadrant 1 Results:	Peak Load:	1.70 kN
1st Envelope	Displacement at Peak Load:	7.6 mm
	Initial Stiffness:	1.180 kN/mm
	Ductility:	10.15
Cyclic Quadrant 3 Results:	Peak Load:	1.86 kN
1st Envelope	Displacement at Peak Load:	7.6 mm
	Initial Stiffness:	1.311 kN/mm
	Ductility:	11.89
Cyclic Overall Results:	Hysteretic Energy Dissipated:	96.7 J

Description: **Sheathing-to-Framing BPARA Specimens**

Sample Size:	2 and 3
Loading Scenario:	Monotonic and Cyclic
Loading Direction:	Parallel as felt by stud
Stud Type:	LVL
Sheathing Type:	DFP 25.4 mm
Type of Nail:	Spiral, 3.0 mm diameter, 76 mm long

Load vs. Displacement Plot

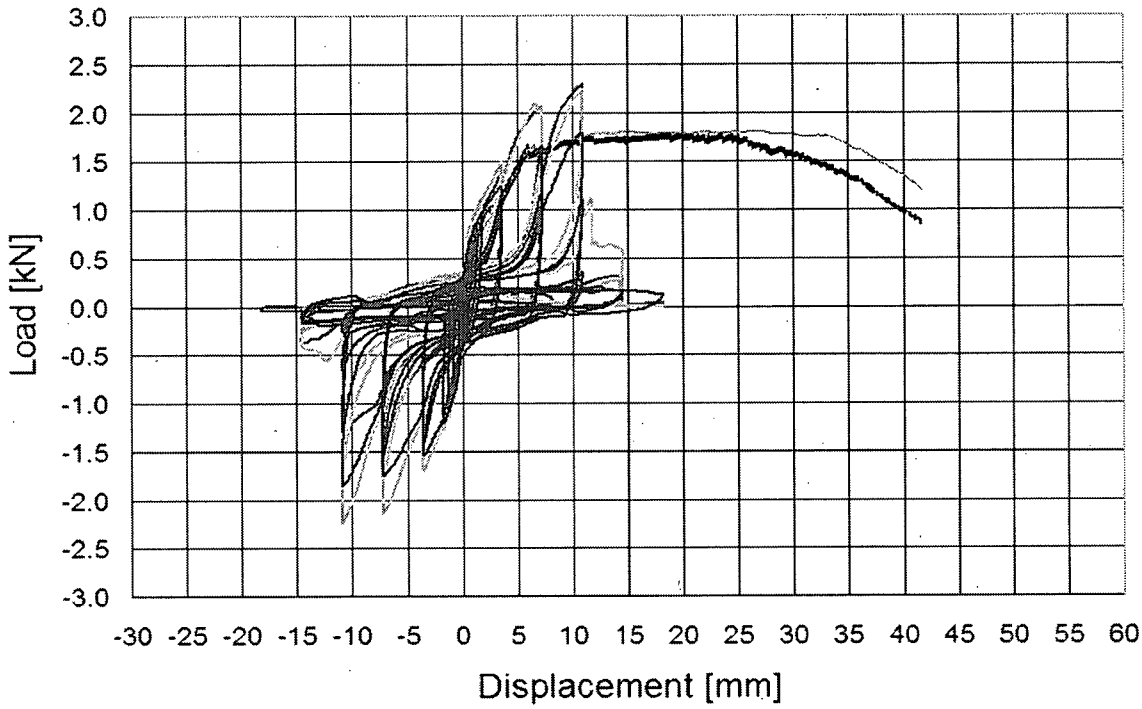

Average parameters

Monotonic Results	Peak Load:	1.79 kN
	Displacement at Peak Load:	24.0 mm
Cyclic Quadrant 1 Results: 1st Envelope	Peak Load:	2.11 kN
	Displacement at Peak Load:	10.9 mm
	Initial Stiffness:	0.735 kN/mm
	Ductility:	6.70
Cyclic Quadrant 3 Results: 1st Envelope	Peak Load:	1.92 kN
	Displacement at Peak Load:	10.9 mm
	Initial Stiffness:	1.272 kN/mm
	Ductility:	13.64
Cyclic Overall Results:	Hysteretic Energy Dissipated:	109.9 J

Description: **Sheathing-to-Framing CPARA Specimens**

Sample Size:	2 and 3
Loading Scenario:	Monotonic and Cyclic
Loading Direction:	Parallel as felt by stud
Stud Type:	1.7E LSL
Sheathing Type:	DFP 25.4 mm
Type of Nail:	Common, 3.75 mm diameter, 76 mm long

Load vs. Displacement Plot

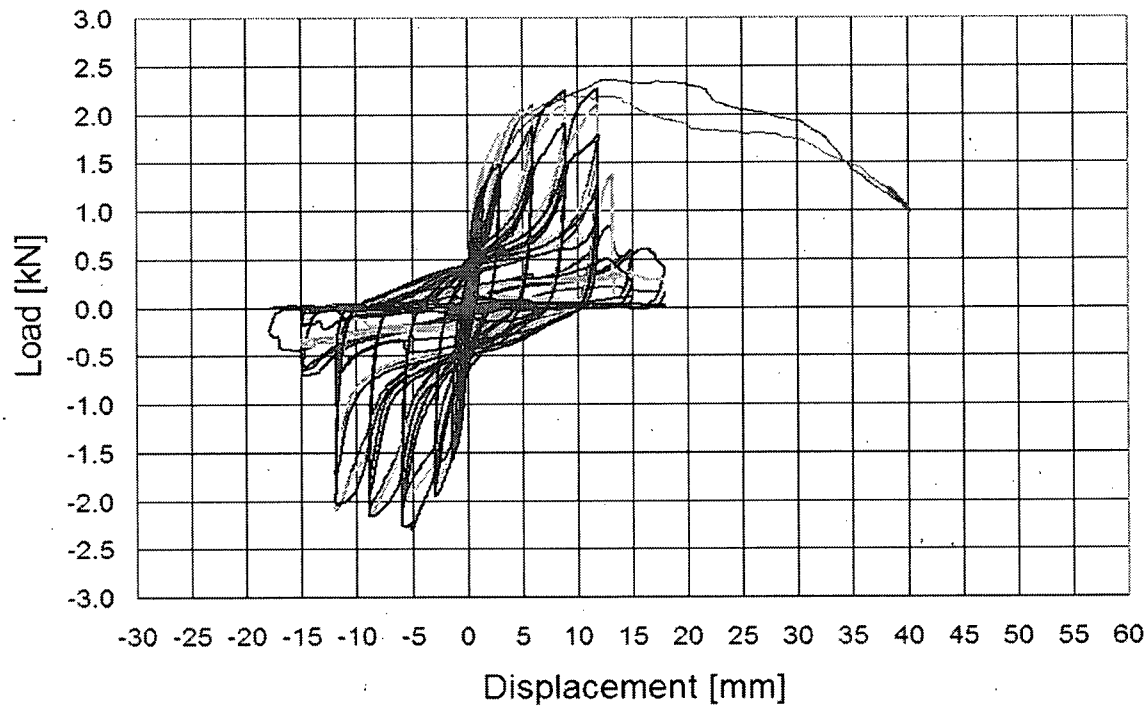

Average parameters

Monotonic Results	Peak Load:	2.28 kN
	Displacement at Peak Load:	10.9 mm
Cyclic Quadrant 1 Results: 1st Envelope	Peak Load:	2.10 kN
	Displacement at Peak Load:	11.0 mm
	Initial Stiffness:	1.513 kN/mm
	Ductility:	16.55
Cyclic Quadrant 3 Results: 1st Envelope	Peak Load:	2.18 kN
	Displacement at Peak Load:	8.6 mm
	Initial Stiffness:	2.772 kN/mm
	Ductility:	31.51
Cyclic Overall Results:	Hysteretic Energy Dissipated:	202.9 J

Description: **Sheathing-to-Framing EPARA Specimens**

Sample Size:	2 and 3
Loading Scenario:	Monotonic and Cyclic
Loading Direction:	Parallel as felt by stud
Stud Type:	1.7E LSL
Sheathing Type:	OSB 15.1 mm
Type of Nail:	Spiral, 2.5 mm diameter, 65 mm long

Load vs. Displacement Plot

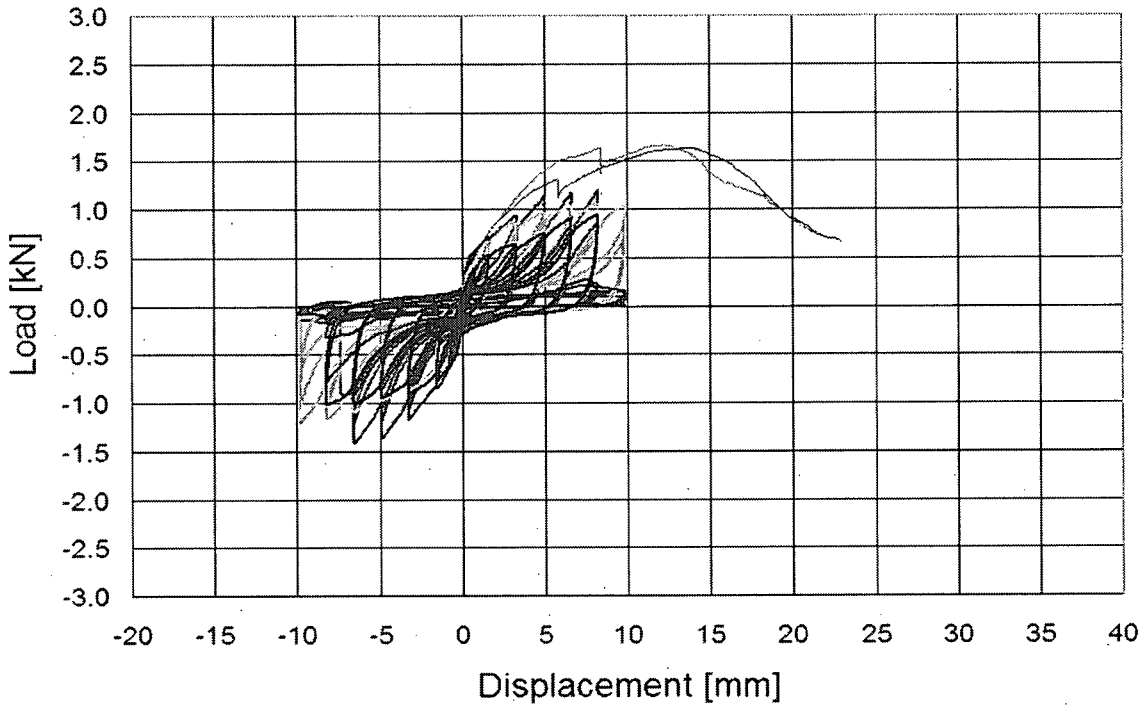

Average parameters		
Monotonic Results	Peak Load:	1.65 kN
	Displacement at Peak Load:	13.0 mm
Cyclic Quadrant 1 Results:	Peak Load:	1.07 kN
1st Envelope	Displacement at Peak Load:	8.3 mm
	Initial Stiffness:	0.660 kN/mm
	Ductility:	14.21
Cyclic Quadrant 3 Results:	Peak Load:	1.21 kN
1st Envelope	Displacement at Peak Load:	8.3 mm
	Initial Stiffness:	0.885 kN/mm
	Ductility:	7.29
Cyclic Overall Results:	Hysteretic Energy Dissipated:	65.3 J

Description: **Sheathing-to-Framing FPARA Specimens**

Sample Size:	2 and 3
Loading Scenario:	Monotonic and Cyclic
Loading Direction:	Parallel as felt by stud
Stud Type:	LVL
Sheathing Type:	OSB 15.1 mm
Type of Nail:	Spiral, 2.5 mm diameter, 65 mm long

Load vs. Displacement Plot

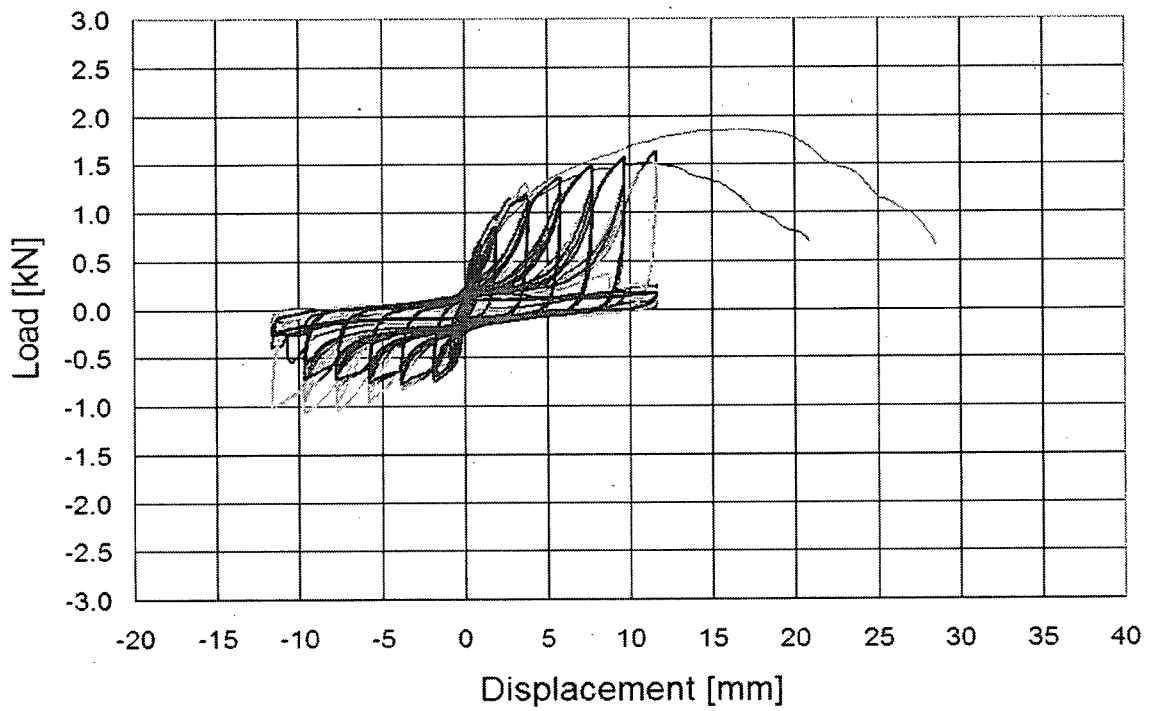

Average parameters		
Monotonic Results	Peak Load:	1.69 kN
	Displacement at Peak Load:	13.7 mm
Cyclic Quadrant 1 Results:	Peak Load:	1.58 kN
1st Envelope	Displacement at Peak Load:	10.5 mm
	Initial Stiffness:	0.588 kN/mm
	Ductility:	4.96
Cyclic Quadrant 3 Results:	Peak Load:	0.90 kN
1st Envelope	Displacement at Peak Load:	7.8 mm
	Initial Stiffness:	1.203 kN/mm
	Ductility:	34.10
Cyclic Overall Results:	Hysteretic Energy Dissipated:	82.7 J

Description: **Sheathing-to-Framing HPARA Specimens**

Sample Size:	2 and 3
Loading Scenario:	Monotonic and Cyclic
Loading Direction:	Parallel as felt by stud
Stud Type:	No. 2 SPF
Sheathing Type:	OSB 15.1 mm
Type of Nail:	Spiral, 2.5 mm diameter, 65 mm long

Load vs. Displacement Plot

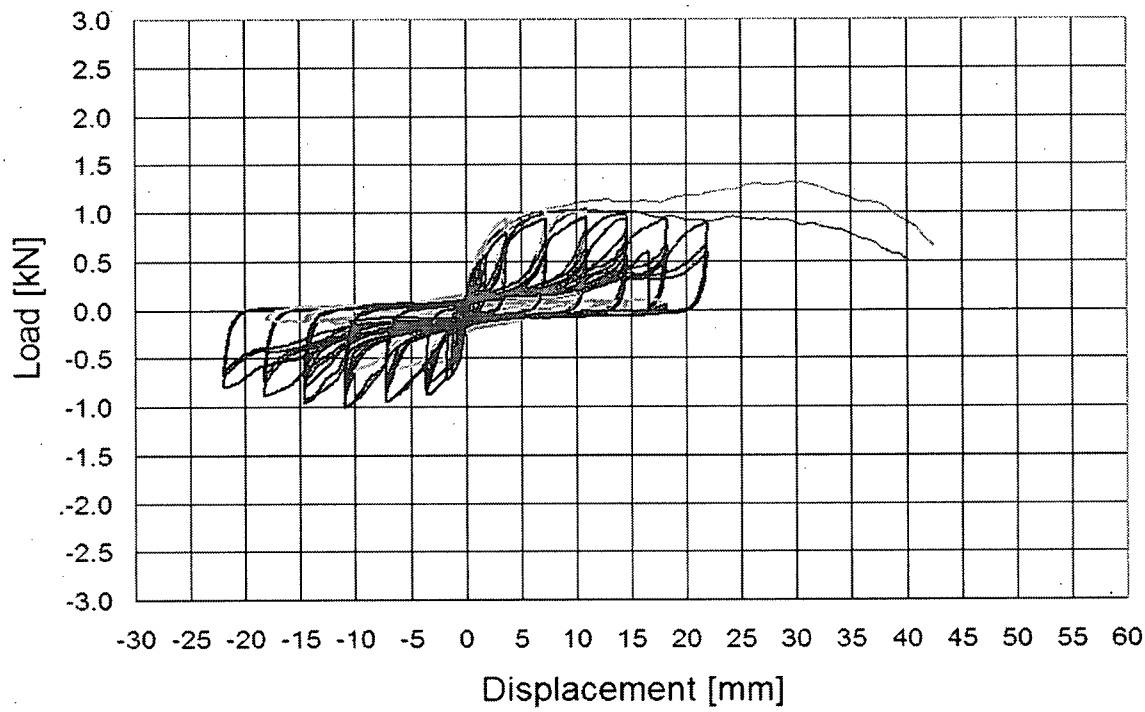

Average parameters

Monotonic Results	Peak Load:	1.18 kN
	Displacement at Peak Load:	19.0 mm
Cyclic Quadrant 1 Results: 1st Envelope	Peak Load:	1.01 kN
	Displacement at Peak Load:	9.8 mm
	Initial Stiffness:	0.544 kN/mm
	Ductility:	10.41
Cyclic Quadrant 3 Results: 1st Envelope	Peak Load:	0.89 kN
	Displacement at Peak Load:	9.7 mm
	Initial Stiffness:	0.745 kN/mm
	Ductility:	20.70
Cyclic Overall Results:	Hysteretic Energy Dissipated:	97.2 J

Description: **Sheathing-to-Framing IPARA Specimens**

Sample Size:	2 and 3
Loading Scenario:	Monotonic and Cyclic
Loading Direction:	Parallel as felt by stud
Stud Type:	No. 2 SPF
Sheathing Type:	OSB 9.5 mm
Type of Nail:	Spiral, 2.5 mm diameter, 65 mm long

Load vs. Displacement Plot

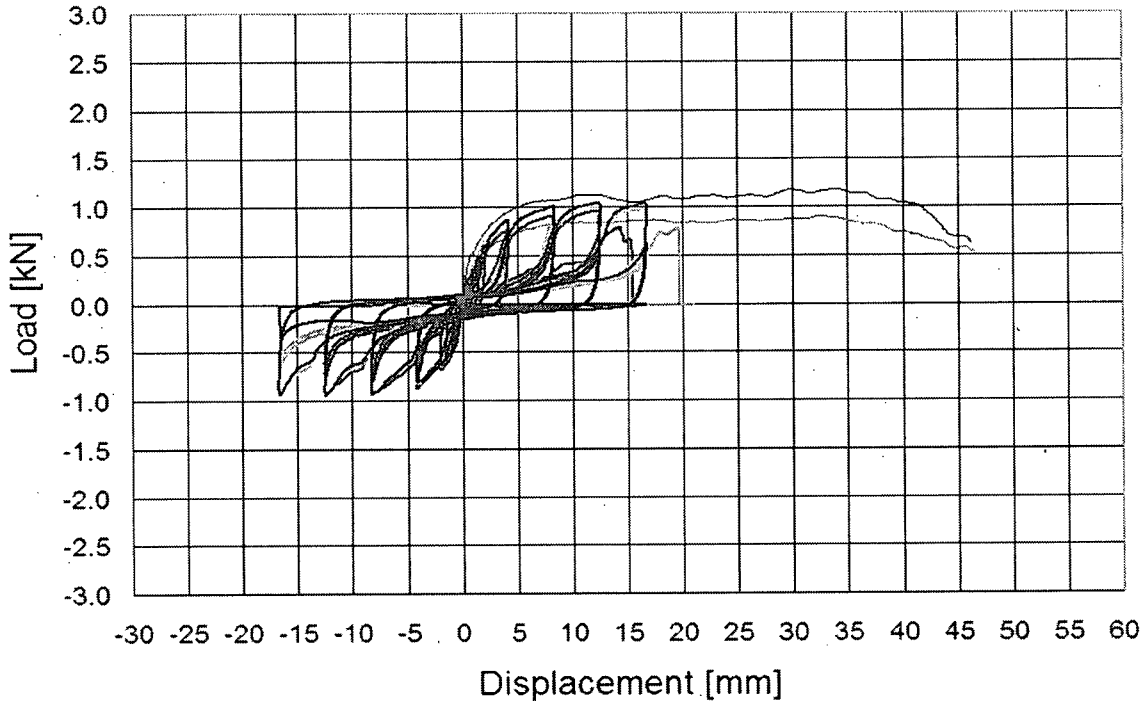

Average parameters

Monotonic Results	Peak Load:	1.04 kN
	Displacement at Peak Load:	33.1 mm
Cyclic Quadrant 1 Results: 1st Envelope	Peak Load:	1.00 kN
	Displacement at Peak Load:	14.0 mm
	Initial Stiffness:	0.314 kN/mm
	Ductility:	9.12
Cyclic Quadrant 3 Results: 1st Envelope	Peak Load:	0.95 kN
	Displacement at Peak Load:	11.2 mm
	Initial Stiffness:	0.549 kN/mm
	Ductility:	NA
Cyclic Overall Results:	Hysteretic Energy Dissipated:	70.5 J

Description: **Sheathing-to-Framing APERP Specimens**

Sample Size:	2 and 3
Loading Scenario:	Monotonic and Cyclic
Loading Direction:	Perpendicular as felt by stud
Stud Type:	1.7E LSL
Sheathing Type:	DFP 25.4 mm
Type of Nail:	Spiral, 3.0 mm diameter, 76 mm long

Load vs. Displacement Plot

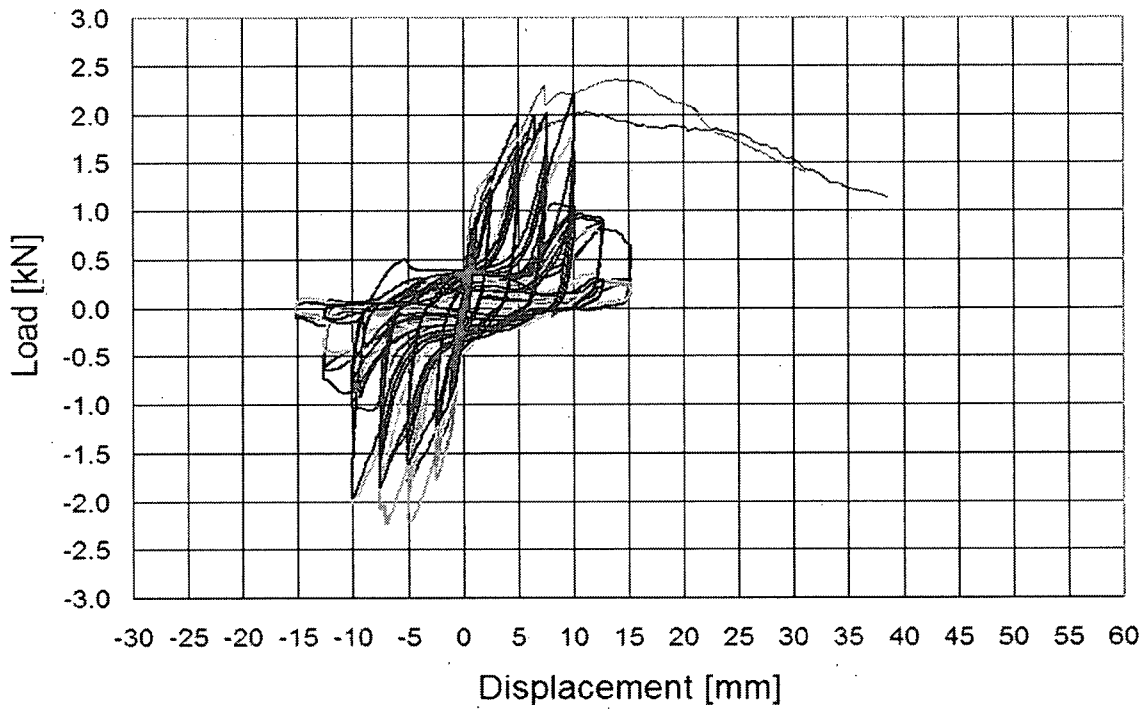

Average parameters

Monotonic Results	Peak Load:	2.20 kN
	Displacement at Peak Load:	12.5 mm
Cyclic Overall Results:	Hysteretic Energy Dissipated:	134.4 J

* Cyclic quardrant results are not shown numerically since graphical analysis determined that the connection responses of these perpendicular specimens do not represent how these connection types are to be subsequently modelled by CASHEW software.

Description: **Sheathing-to-Framing BPERP Specimens**

Sample Size:	2 and 3
Loading Scenario:	Monotonic and Cyclic
Loading Direction:	Perpendicular as felt by stud
Stud Type:	LVL
Sheathing Type:	DFP 25.4 mm
Type of Nail:	Spiral, 3.0 mm diameter, 76 mm long

Load vs. Displacement Plot

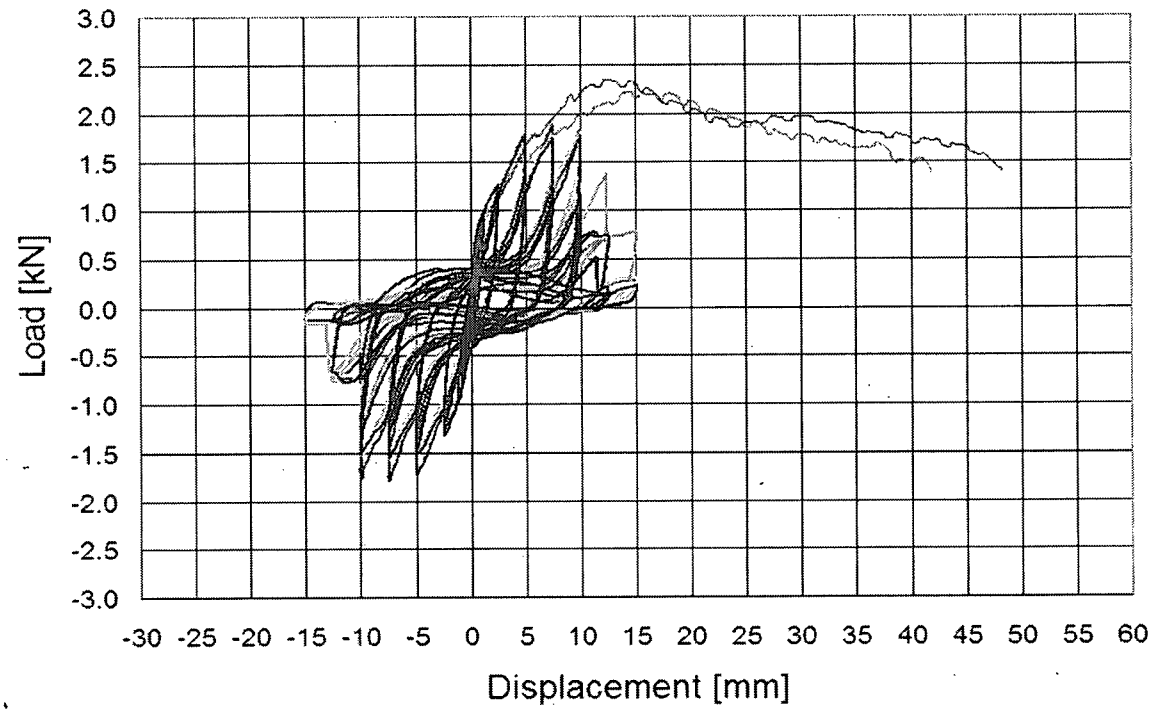

Average parameters

Monotonic Results	Peak Load:	2.29 kN
	Displacement at Peak Load:	13.4 mm
Cyclic Overall Results:	Hysteretic Energy Dissipated:	131.8 J

* Cyclic quardrant results are not shown numerically since graphical analysis determined that the connection responses of these perpendicular specimens do not represent how these connection types are to be subsequently modelled by CASHEW software.

Description: **Sheathing-to-Framing CPERP Specimens**

Sample Size:	2 and 3
Loading Scenario:	Monotonic and Cyclic
Loading Direction:	Perpendicular as felt by stud
Stud Type:	1.7E LSL
Sheathing Type:	DFP 25.4 mm
Type of Nail:	Common, 3.75 mm diameter, 76 mm long

Load vs. Displacement Plot

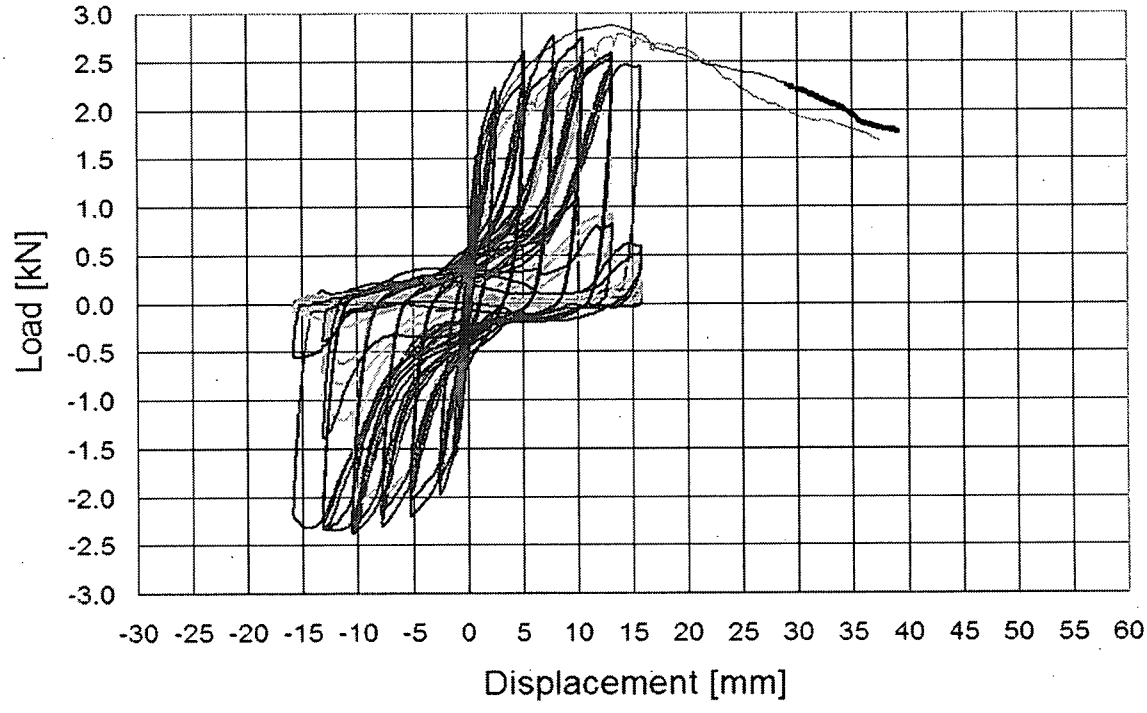

Average parameters

Monotonic Results	Peak Load:	2.84 kN
	Displacement at Peak Load:	13.5 mm
Cyclic Overall Results:	Hysteretic Energy Dissipated:	249.1 J

* Cyclic quardrant results are not shown numerically since graphical analysis determined that the connection responses of these perpendicular specimens do not represent how these connection types are to be subsequently modelled by CASHEW software.

Description: **Sheathing-to-Framing EPERP Specimens**

Sample Size:	2 and 3
Loading Scenario:	Monotonic and Cyclic
Loading Direction:	Perpendicular as felt by stud
Stud Type:	1.7E LSL
Sheathing Type:	OSB 15.1 mm
Type of Nail:	Spiral, 2.5 mm diameter, 65 mm long

Load vs. Displacement Plot

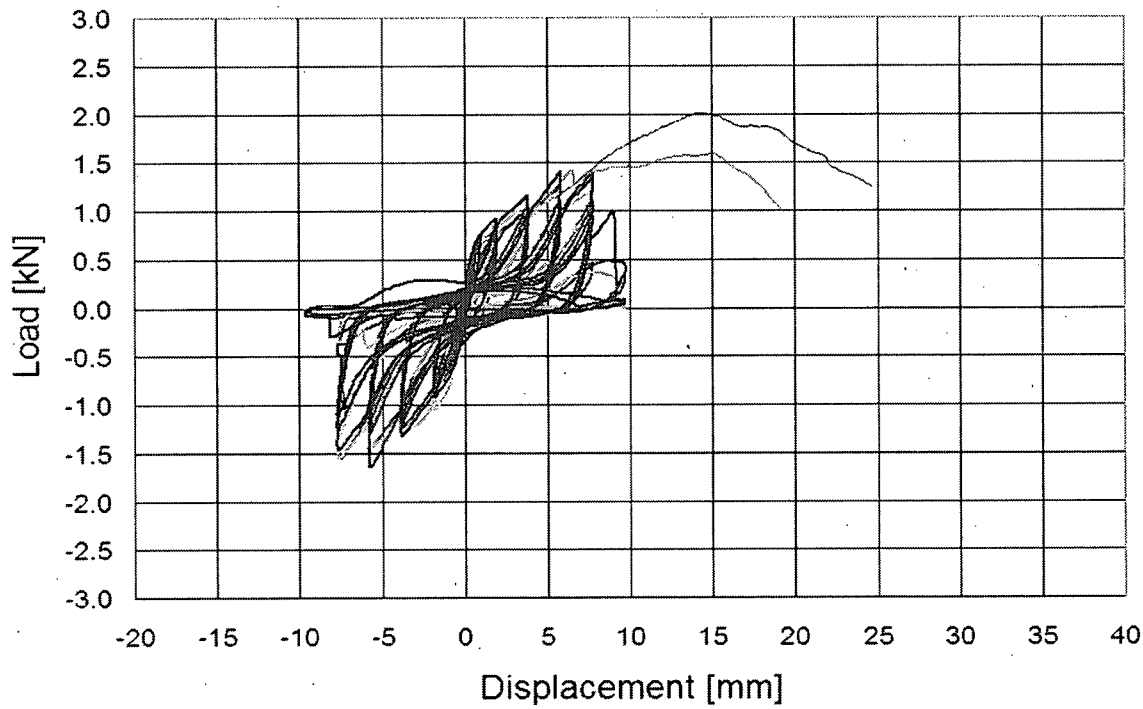

Average parameters

Monotonic Results	Peak Load:	1.8 kN
	Displacement at Peak Load:	14.6 mm
Cyclic Overall Results:	Hysteretic Energy Dissipated:	56.6 J

* Cyclic quardrant results are not shown numerically since graphical analysis determined that the connection responses of these perpendicular specimens do not represent how these connection types are to be subsequently modelled by CASHEW software.

Description: **Sheathing-to-Framing FPERP Specimens**

Sample Size:	2 and 3
Loading Scenario:	Monotonic and Cyclic
Loading Direction:	Perpendicular as felt by stud
Stud Type:	LVL
Sheathing Type:	OSB 15.1 mm
Type of Nail:	Spiral, 2.5 mm diameter, 65 mm long

Load vs. Displacement Plot

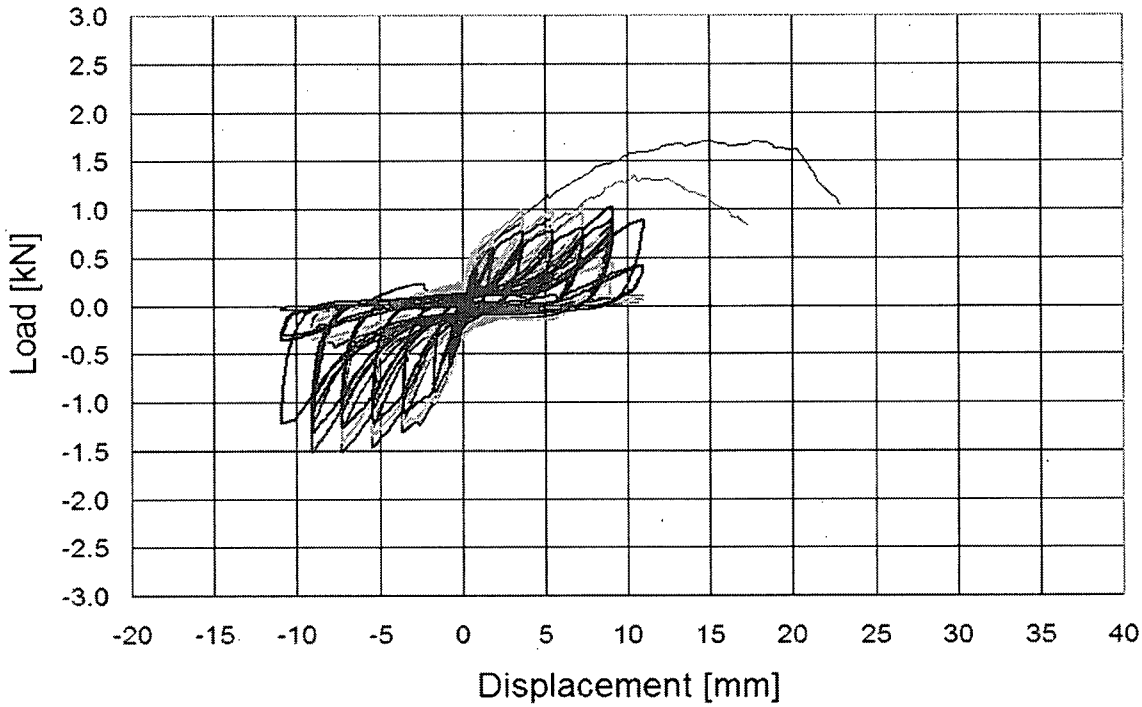

Average parameters

Monotonic Results	Peak Load:	1.53 kN
	Displacement at Peak Load:	12.6 mm
Cyclic Overall Results:	Hysteretic Energy Dissipated:	70.8 J

* Cyclic quardrant results are not shown numerically since graphical analysis determined that the connection responses of these perpendicular specimens do not represent how these connection types are to be subsequently modelled by CASHEW software.

Description: **Sheathing-to-Framing HPERP Specimens**

Sample Size:	2 and 3
Loading Scenario:	Monotonic and Cyclic
Loading Direction:	Perpendicular as felt by stud
Stud Type:	No. 2 SPF
Sheathing Type:	OSB 15.1 mm
Type of Nail:	Spiral, 2.5 mm diameter, 65 mm long

Load vs. Displacement Plot

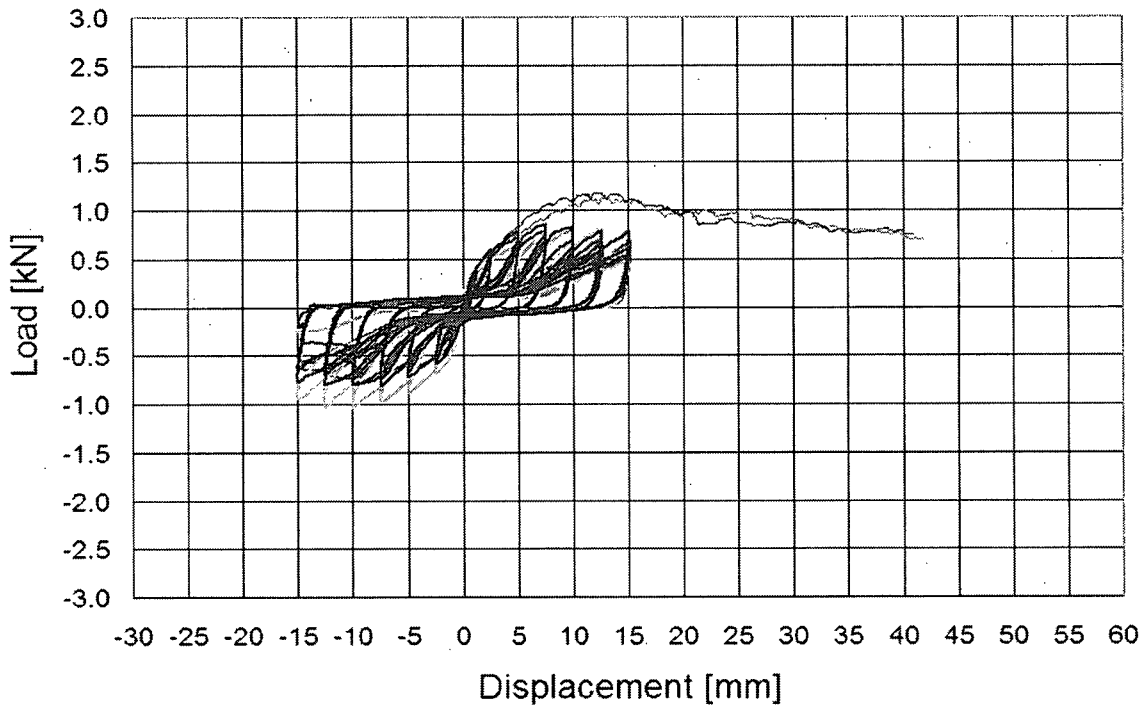

Average parameters

Monotonic Results	Peak Load:	1.16 kN
	Displacement at Peak Load:	12.4 mm
Cyclic Overall Results:	Hysteretic Energy Dissipated:	94.1 J

* Cyclic quardrant results are not shown numerically since graphical analysis determined that the connection responses of these perpendicular specimens do not represent how these connection types are to be subsequently modelled by CASHEW software.

Description: **Sheathing-to-Framing IPERP Specimens**

Sample Size:	2 and 3
Loading Scenario:	Monotonic and Cyclic
Loading Direction:	Perpendicular as felt by stud
Stud Type:	No. 2 SPF
Sheathing Type:	OSB 9.5 mm
Type of Nail:	Spiral, 2.5 mm diameter, 65 mm long

Load vs. Displacement Plot

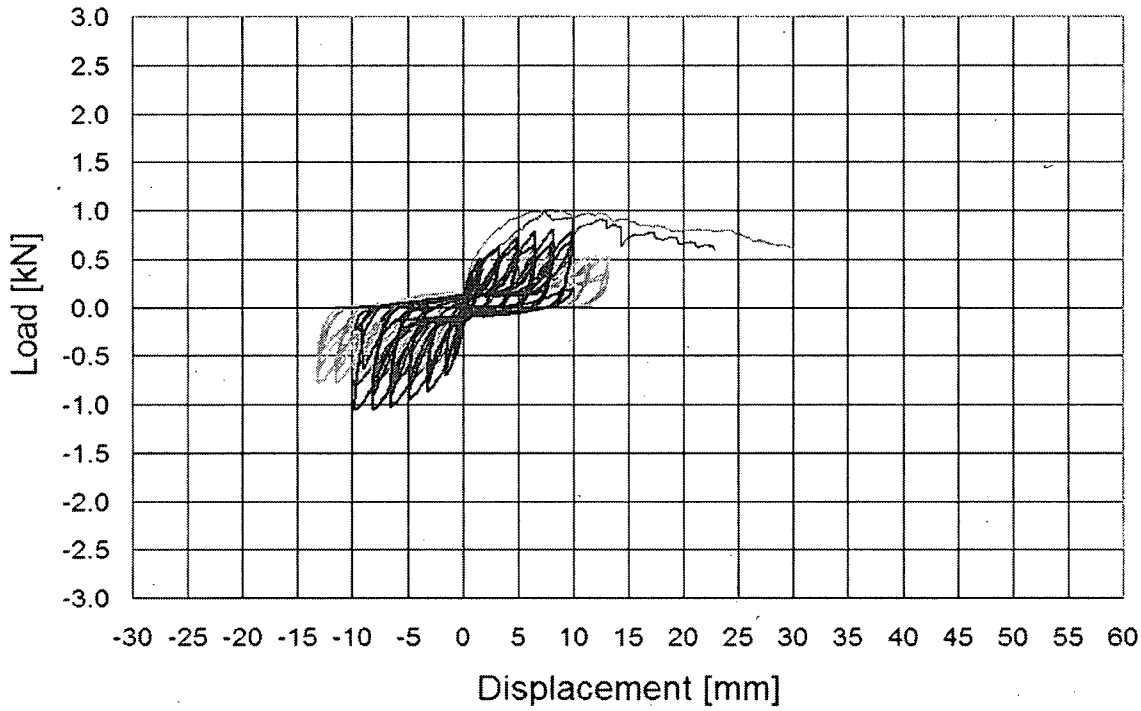

Average parameters

Monotonic Results	Peak Load:	1.01 kN
	Displacement at Peak Load:	7.3 mm
Cyclic Overall Results:	Hysteretic Energy Dissipated:	60.3 J

* Cyclic quardrant results are not shown numerically since graphical analysis determined that the connection responses of these perpendicular specimens do not represent how these connection types are to be subsequently modelled by CASHEW software.

APPENDIX B: ANALYTICAL CASHEW MODELLING RESULTS

The CASHEW modelling results that were discussed in Section 7 and referred to subsequently are presented more thoroughly in the following Appendices. Model input parameters and model results are given.

B.1 CASHEW Connection Inputs

The input parameters that are shown are based on the accompanying sheathing-to-framing connection test load vs. displacement plots. The parameters are as defined in Folz and Filiatrault (2000).

CASHEW connection input parameters

Connection Representation:	APARA	*Unaltered*
Modelled tested Wall:	704A, 706A, 707A	
Modelled untested Wall:		

Hysteretic Sheathing-to-Framing Response

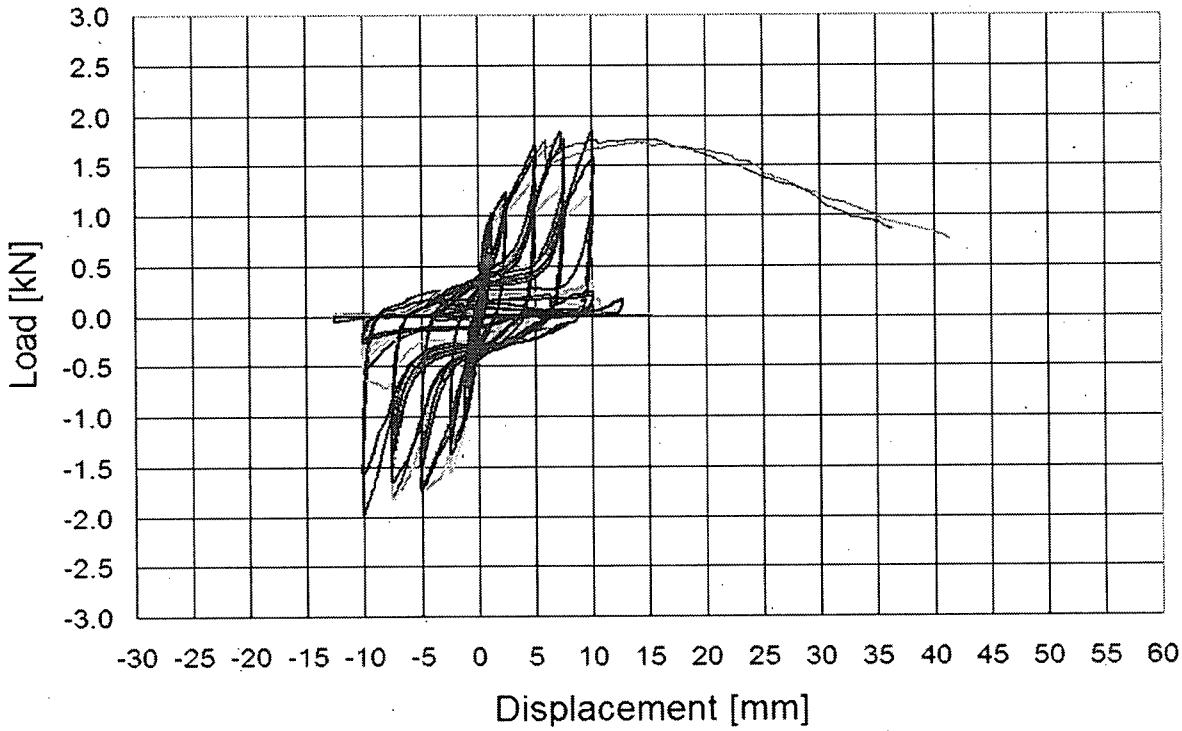

Parameters:	F0	1.20	kN
Based on Cyclic test results	F1	0.30	kN
	DU	9.00	mm
	K0	1.5000	kN/mm
	R1	0.0593	
	R2	-0.1113	
	R3	1.4667	
	R4	0.0427	
	ALPHA	0.5396	
	BETA	1.1000	
Sheathing Shear Modulus	*G*	0.5100	GPa
25.4 mm DFP			

CASHEW connection input parameters

Connection Representation:	APARA	*Altered*
Modelled tested Wall:	704B, 706B, 707B	
Modelled untested Wall:	710B, 711B	

Hysteretic Sheathing-to-Framing Response

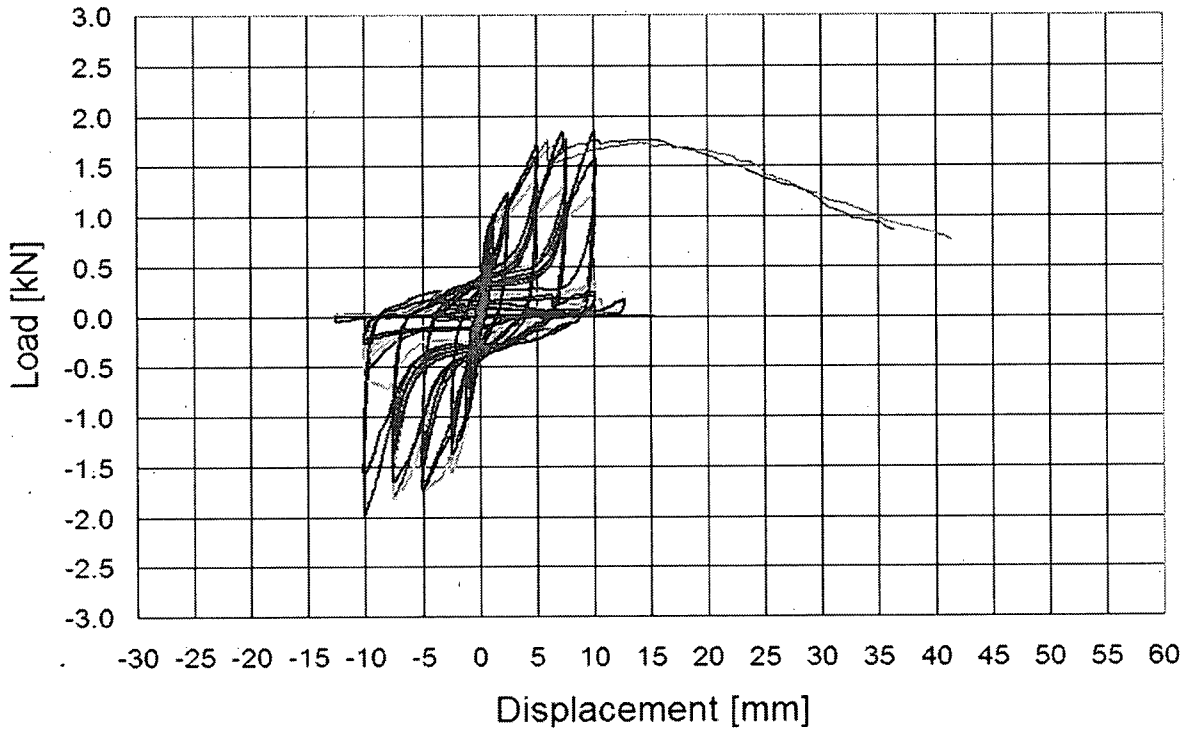

Parameters:	*F0*	*0.96*	*kN*
Based on Cyclic test results	F1	0.30	kN
	DU	9.00	mm
	K0	1.5000	kN/mm
	R1	0.0593	
	R2	-0.1113	
	R3	1.4667	
	R4	0.0427	
	ALPHA	*0.4836*	
	BETA	1.1000	
Sheathing Shear Modulus	*G*	0.5100	GPa
25.4 mm DFP			

* F0 was decreased by 20% from the original APARA determination, ALPHA changed accordingly

CASHEW connection input parameters

Connection Representation:	BPARA	*Unaltered*
Modelled tested Wall:		
Modelled untested Wall:	804, 805	

Hysteretic Sheathing-to-Framing Response

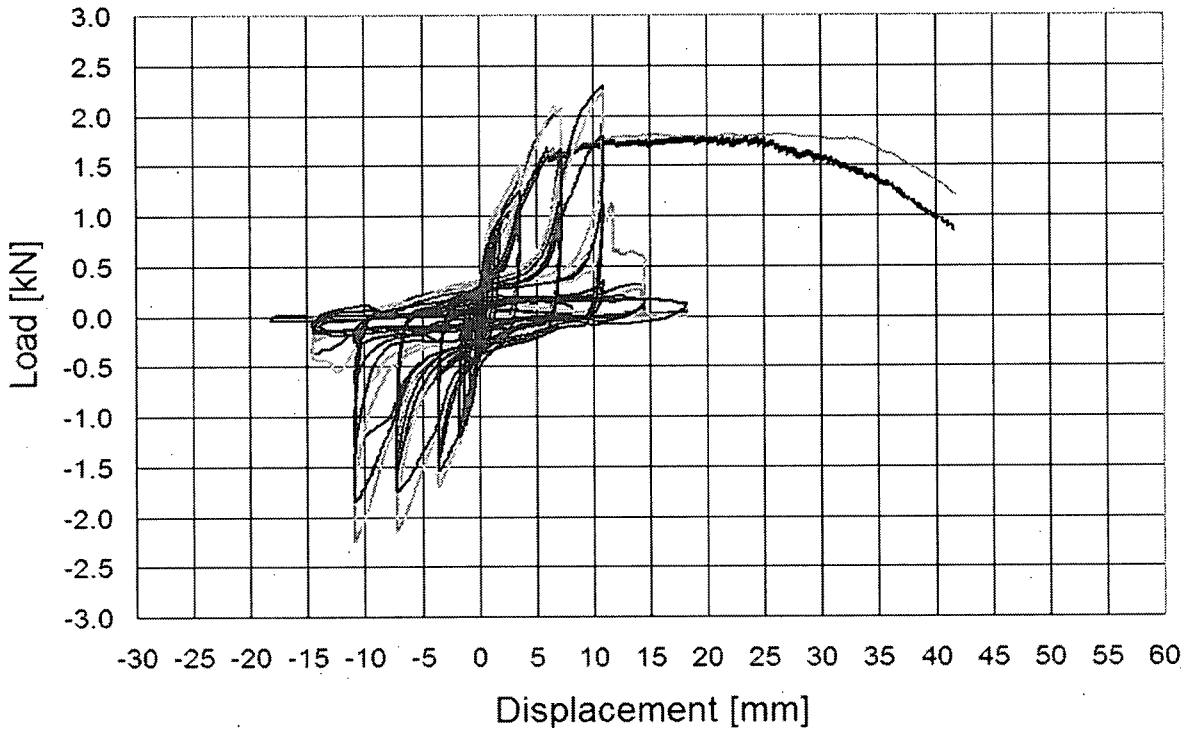

Parameters:	F0	1.25	kN
Based on Cyclic test results	F1	0.26	kN
	DU	11.00	mm
	K0	0.7500	kN/mm
	R1	0.1191	
	R2	-0.1333	
	R3	1.2222	
	R4	0.0251	
	ALPHA	0.5262	
	BETA	1.2570	
Sheathing Shear Modulus	*G*	0.5100	GPa
25.4 mm DFP			

CASHEW connection input parameters

Connection Representation:	FPARA	*Unaltered*
Modelled tested Wall:		
Modelled untested Wall:	801, 802	

Hysteretic Sheathing-to-Framing Response

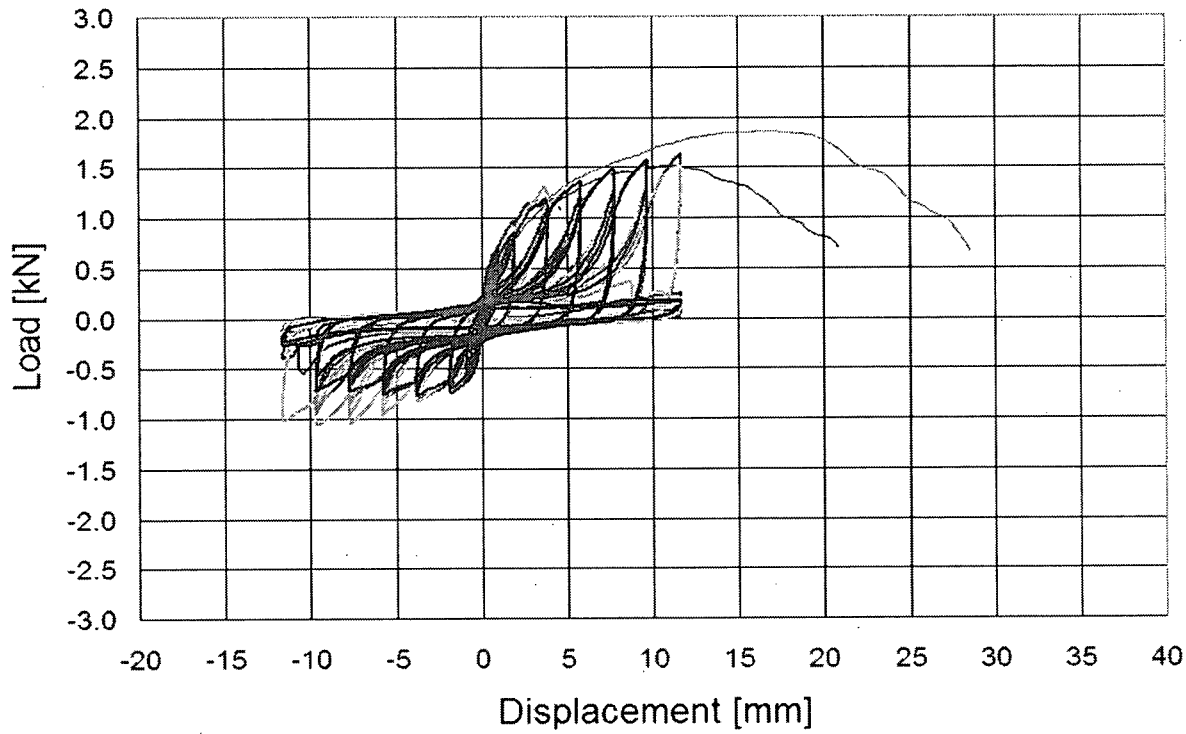

Parameters:	F0	1.00	kN
Based on Cyclic test results	F1	0.13	kN
	DU	9.60	mm
	K0	0.7500	kN/mm
	R1	0.0714	
	R2	-0.1000	
	R3	2.3333	
	R4	0.04167	
	ALPHA	0.4847	
	BETA	1.1184	
Sheathing Shear Modulus	*G*	0.7900	GPa
15.1 mm OSB			

CAŠHEW connection input parameters

Connection Representation:	CPARA	*Unaltered*
Modelled tested Wall:	705	
Modelled untested Wall:		

Hysteretic Sheathing-to-Framing Response

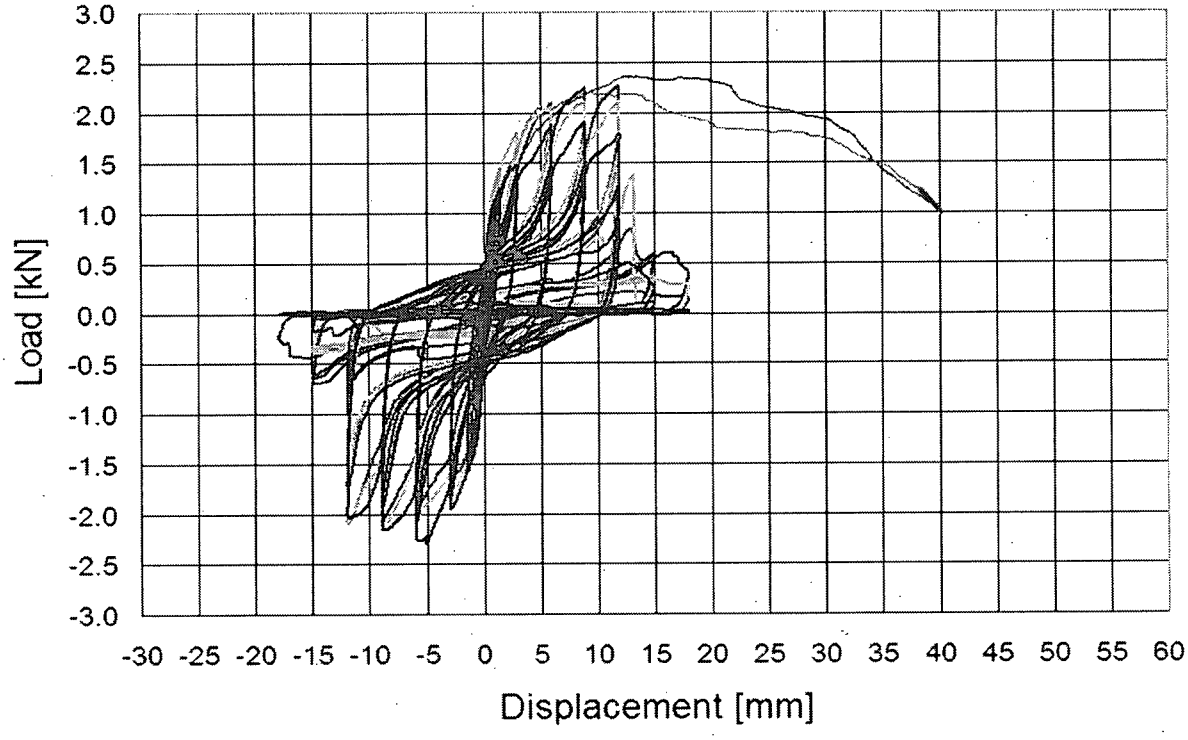

Parameters:	F0	1.40	kN
Based on Cyclic test results	F1	0.35	kN
	DU	10.00	mm
	K0	1.6000	kN/mm
	R1	0.0500	
	R2	-0.0375	
	R3	1.0000	
	R4	0.0402	
	ALPHA	0.7412	
	BETA	1.1333	
Sheathing Shear Modulus	*G*	0.5100	GPa
25.4 mm DFP			

CASHEW connection input parameters

Connection Representation:	IPARA	*Unaltered*
Modelled tested Wall:	602	
Modelled untested Wall:		

Hysteretic Sheathing-to-Framing Response

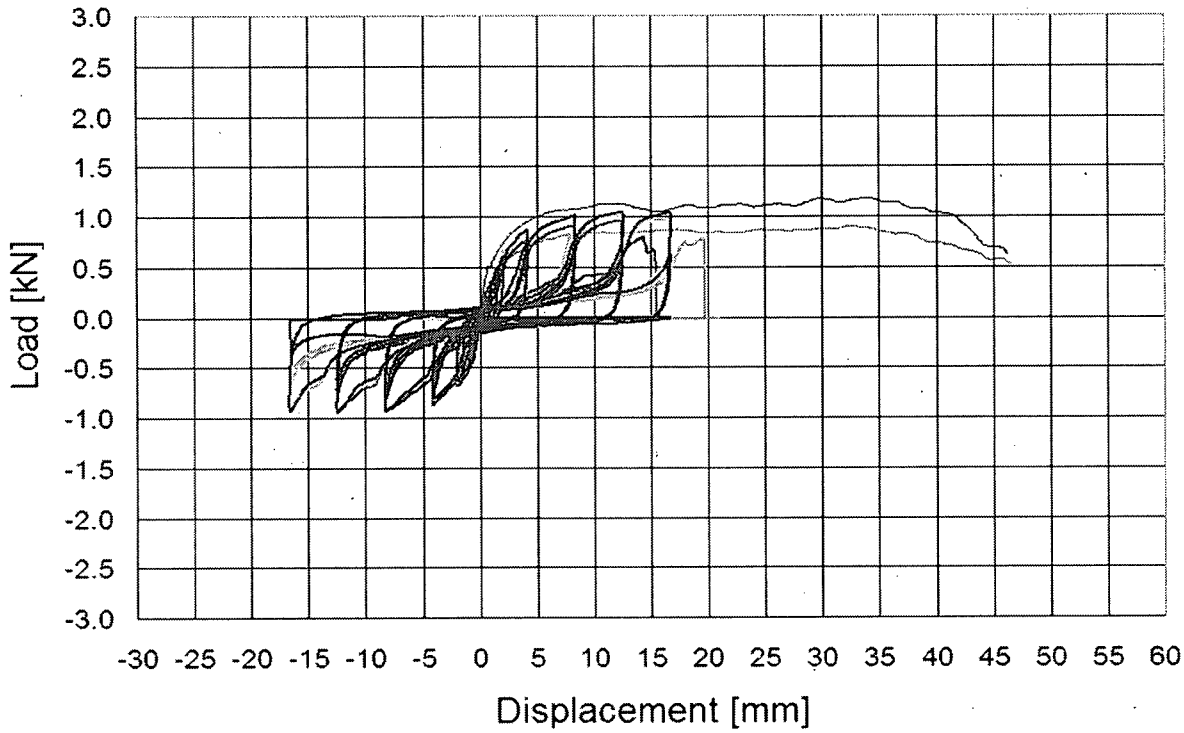

Parameters:	F0	0.80	kN
Based on Cyclic test results	F1	0.11	kN
	DU	12.50	mm
	K0	0.4500	kN/mm
	R1	0.0370	
	R2	-0.1624	
	R3	2.2778	
	R4	0.0242	
	ALPHA	0.2603	
	BETA	1.1325	
Sheathing Shear Modulus	*G*	1.0500	GPa
9.5 mm OSB			

CASHEW connection input parameters

Connection Representation:	HPARA	*Unaltered*
Modelled tested Wall:	603, 605	
Modelled untested Wall:	606, 608	

Hysteretic Sheathing-to-Framing Response

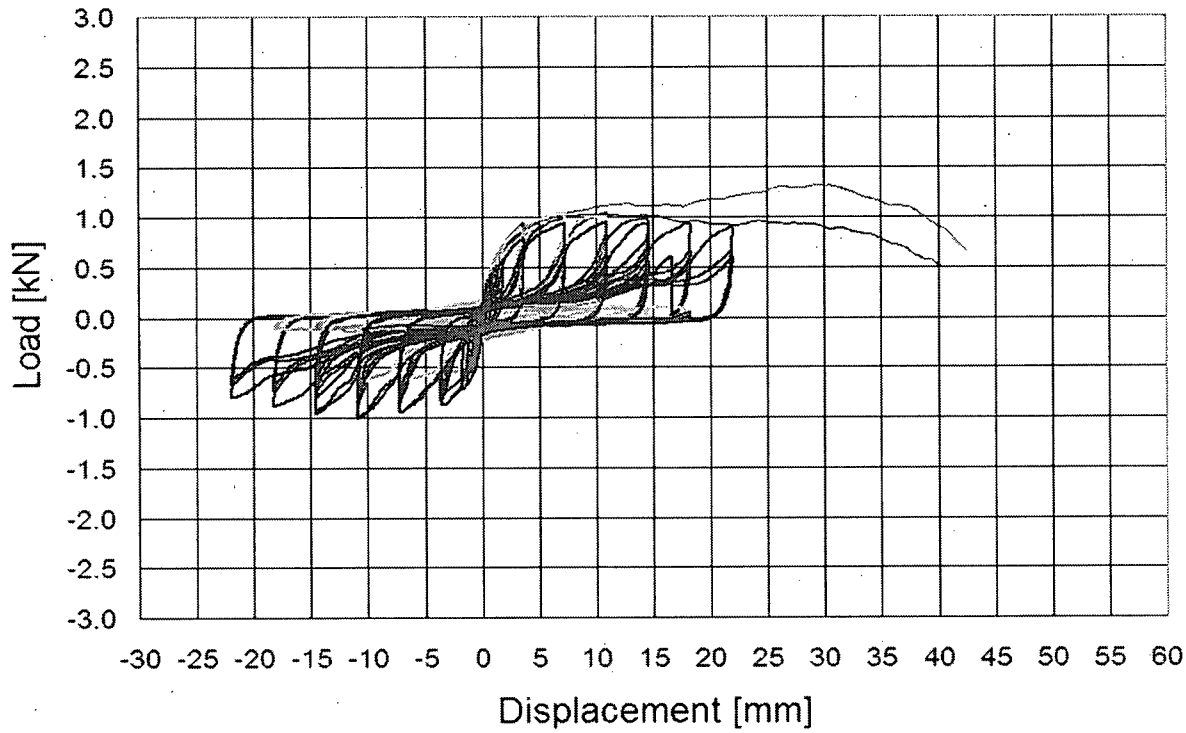

Parameters:	F0	0.75	kN
Based on Cyclic test results	F1	0.09	kN
	DU	11.00	mm
	K0	0.6500	kN/mm
	R1	0.0414	
	R2	-0.0846	
	R3	1.3846	
	R4	0.0186	
	ALPHA	0.4927	
	BETA	1.2055	
Sheathing Shear Modulus	*G*	0.7900	GPa
15.1 mm OSB			

CASHEW connection input parameters

Connection Representation:	EPARA	*Unaltered*
Modelled tested Wall:	702	
Modelled untested Wall:	709	

Hysteretic Sheathing-to-Framing Response

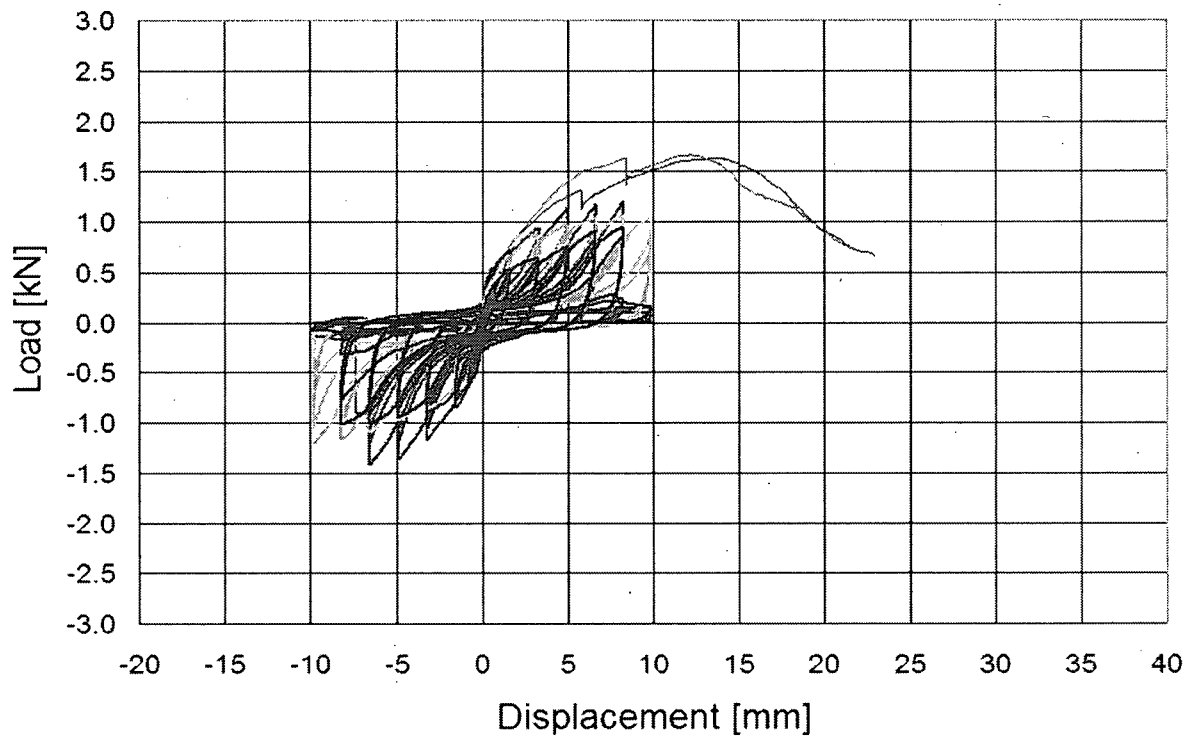

Parameters:	F0	0.75	kN
Based on Cyclic test results	F1	0.15	kN
	DU	8.20	mm
	K0	1.1000	kN/mm
	R1	0.0505	
	R2	-0.0818	
	R3	0.9091	
	R4	0.0270	
	ALPHA	0.7089	
	BETA	1.0938	
Sheathing Shear Modulus	*G*	0.7900	GPa
15.1 mm OSB			

B.2 CASHEW Modelling Results

The results from all the CASHEW modelling are presented herein. This includes the experimental tall wall test model verification attempts as well as the predicted untested tall wall configurations. Load vs. displacement results and hysteretic energy dissipation results are given.

Description: **CASHEW Tall-Wall 602**

Connection Input: IPARA

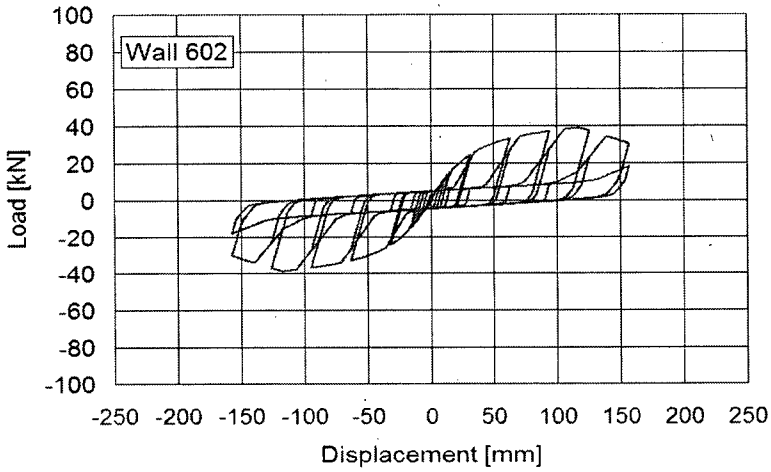

CASHEW
Load vs. Displacement Plot

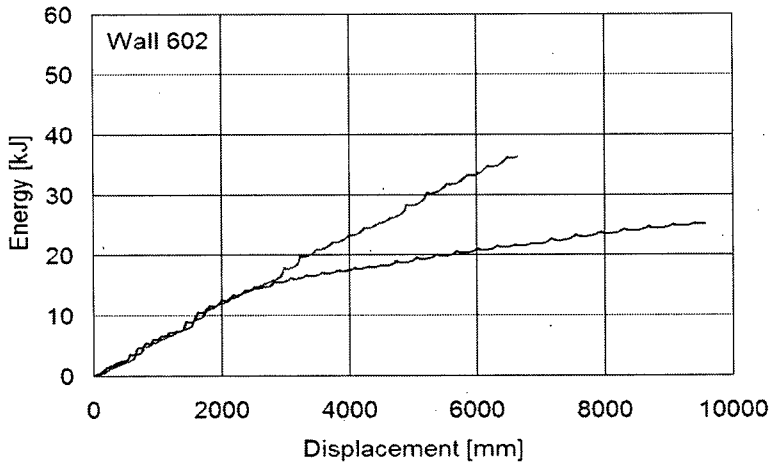

Hysteretic Energy Plot Comparison
CASHEW Wall in Red
Experimental Wall in Blue

Results:

CASHEW Peak Load:	37.1	kN
CASHEW Displacement at Peak Load:	94.3	mm
*CASHEW Hysteretic Energy Dissipated:	14.9	kJ
*Experimental Wall Hysteretic Energy Dissipated:	14.2	kJ

* Hysteretic energy dissipation determined at the end of the three cycle set corresponding with the experimental walls cycle set that corresponds with wall failure.

Description: **CASHEW Tall-Wall 603**

Connection Input: HPARA

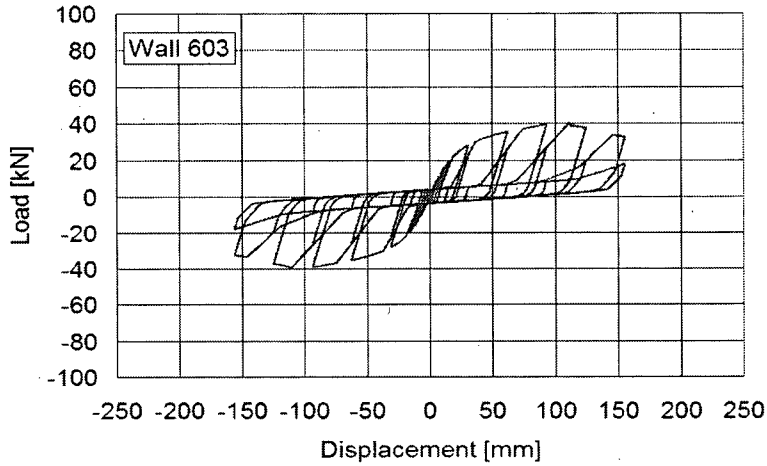

CASHEW
Load vs. Displacement Plot

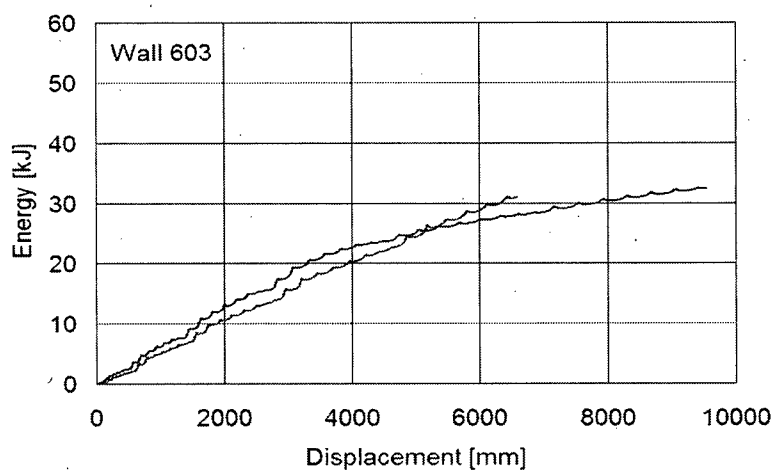

Hysteretic Energy Plot Comparison
CASHEW Wall in Red
Experimental Wall in Blue

Results:

CASHEW Peak Load:	39.3	kN
CASHEW Displacement at Peak Load:	93.5	mm
*CASHEW Hysteretic Energy Dissipated:	21.4	kJ
*Experimental Wall Hysteretic Energy Dissipated:	23.1	kJ

* Hysteretic energy dissipation determined at the end of the three cycle set corresponding with the experimental walls cycle set that corresponds with wall failure.

Description: **CASHEW Tall-Wall 605**

Connection Input: HPARA

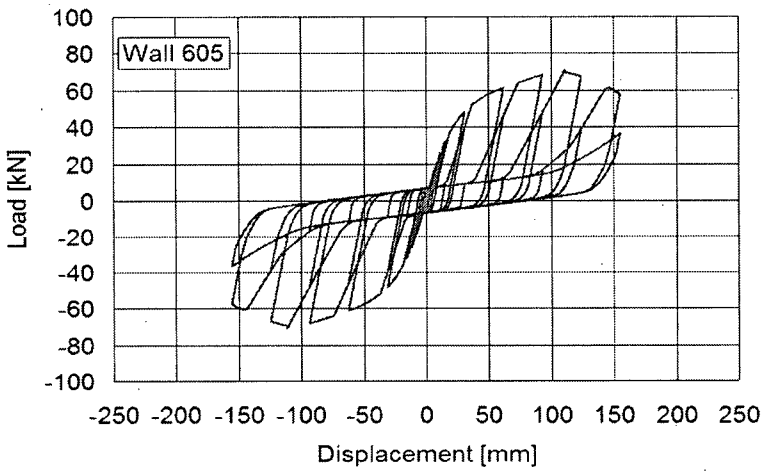

CASHEW
Load vs. Displacement Plot

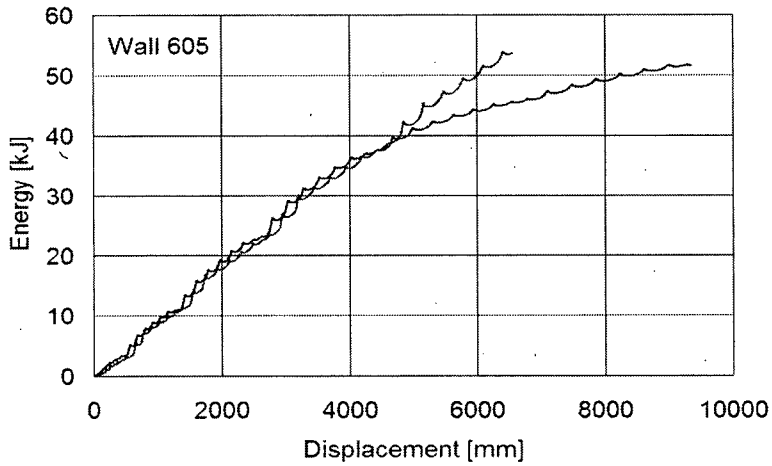

Hysteretic Energy Plot Comparison
CASHEW Wall in Red
Experimental Wall in Blue

Results:

CASHEW Peak Load:	70.8	kN
CASHEW Displacement at Peak Load:	111.1	mm
*CASHEW Hysteretic Energy Dissipated:	36.5	kJ
*Experimental Wall Hysteretic Energy Dissipated:	36.2	kJ

* Hysteretic energy dissipation determined at the end of the three cycle set corresponding with the experimental walls cycle set that corresponds with wall failure.

Description: **CASHEW Tall-Wall 606**

Connection Input: HPARA

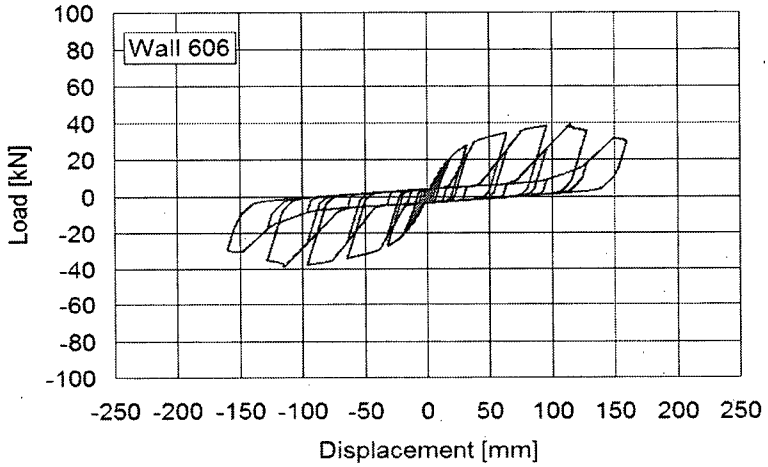

CASHEW
Load vs. Displacement Plot

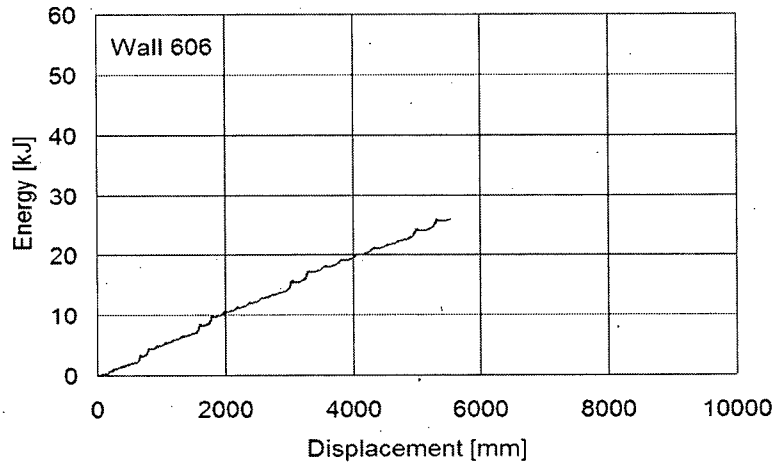

Hysteretic Energy Plot Comparison
CASHEW Wall in Red

Results:			
	CASHEW Peak Load:	39.0	kN
	CASHEW Displacement at Peak Load:	114.7	mm

Description: **CASHEW Tall-Wall 608**

Connection Input: HPARA

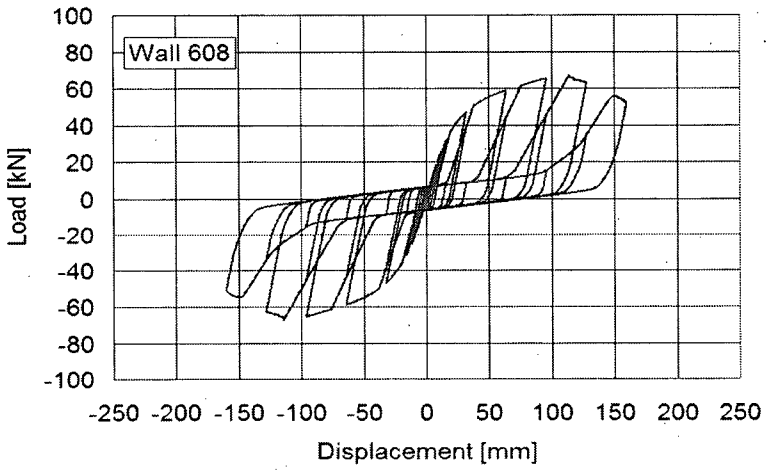

CASHEW
Load vs. Displacement Plot

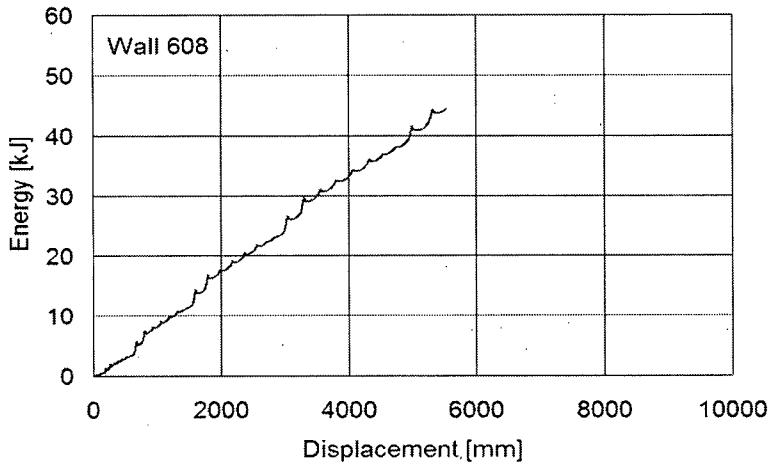

Hysteretic Energy Plot Comparison
CASHEW Wall in Red

Results:			
	CASHEW Peak Load:	67.6	kN
	CASHEW Displacement at Peak Load:	114.5	mm

Description: **CASHEW Tall-Wall 702**

Connection Input: EPARA

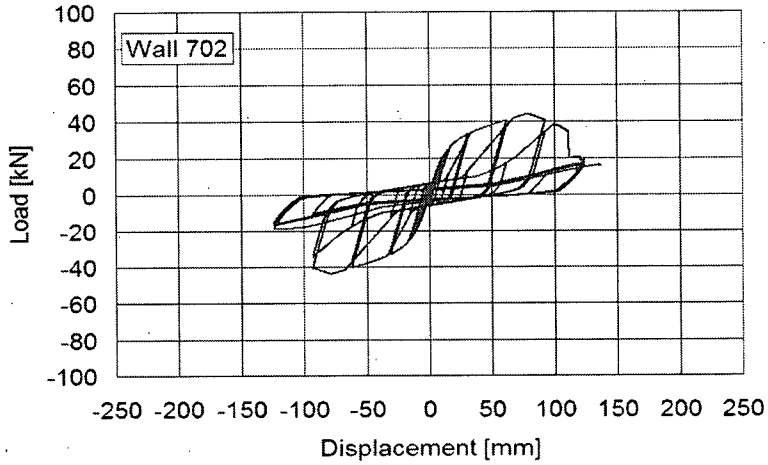

CASHEW
Load vs. Displacement Plot

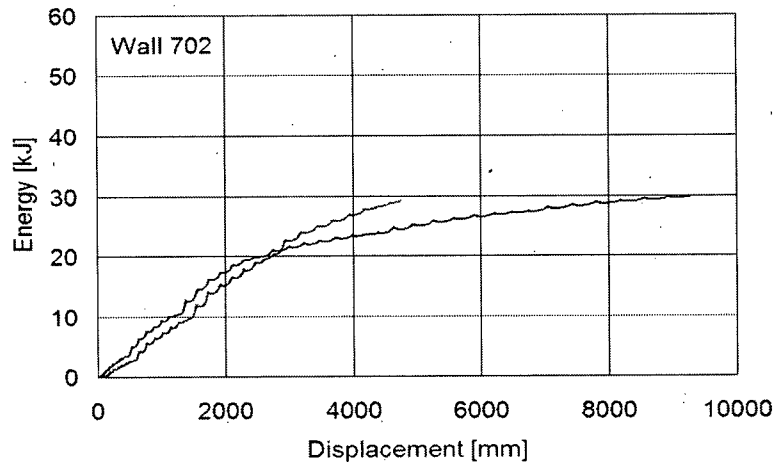

Hysteretic Energy Plot Comparison
CASHEW Wall in Red
Experimental Wall in Blue

Results:

CASHEW Peak Load:	44.0	kN
CASHEW Displacement at Peak Load:	78.4	mm
*CASHEW Hysteretic Energy Dissipated:	19.0	kJ
*Experimental Wall Hysteretic Energy Dissipated:	19.4	kJ

* Hysteretic energy dissipation determined at the end of the three cycle set corresponding with the experimental walls cycle set that corresponds with wall failure.

Description: **CASHEW Tall-Wall 704A**

Connection Input: APARA A (Unaltered)

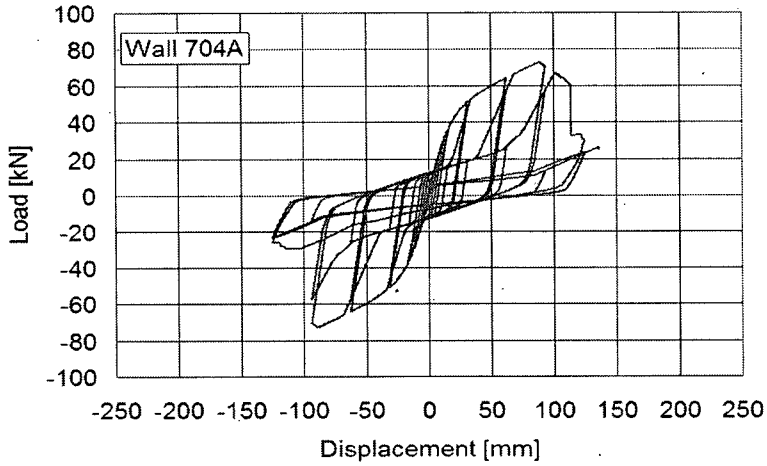

CASHEW
Load vs. Displacement Plot

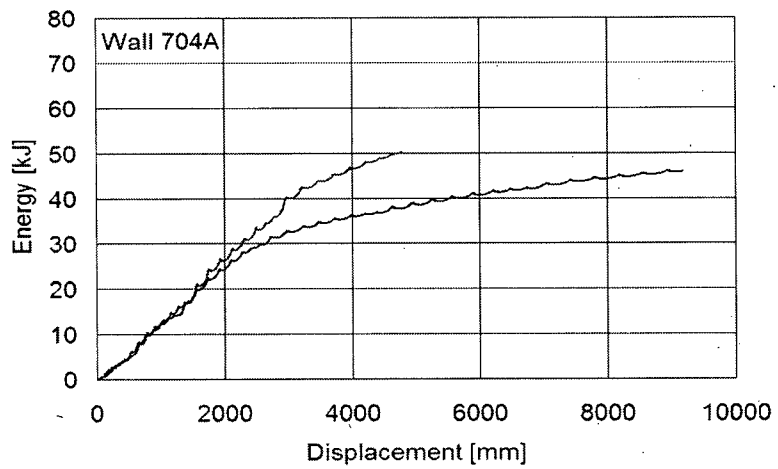

Hysteretic Energy Plot Comparison
CASHEW Wall in Red
Experimental Wall in Blue

Results:

CASHEW Peak Load:	72.8	kN
CASHEW Displacement at Peak Load:	88.7	mm
*CASHEW Hysteretic Energy Dissipated:	33.4	kJ
*Experimental Wall Hysteretic Energy Dissipated:	28.3	kJ

* Hysteretic energy dissipation determined at the end of the three cycle set corresponding with the experimental walls cycle set that corresponds with wall failure.

Description: **CASHEW Tall-Wall 704B**

Connection Input: APARA B (Altered)

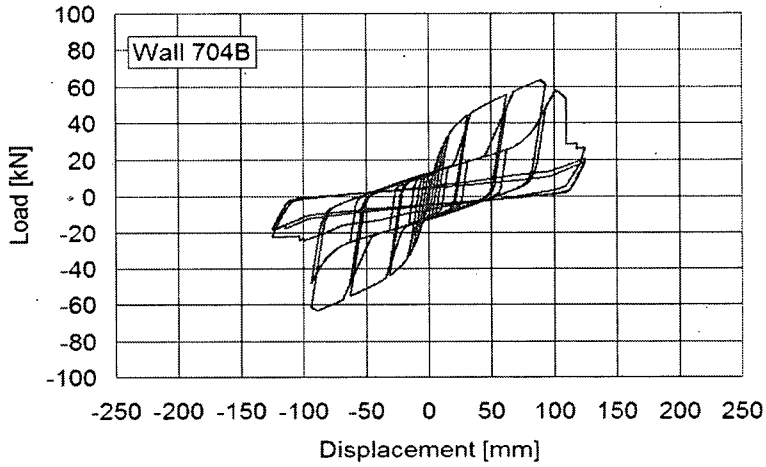

CASHEW
Load vs. Displacement Plot

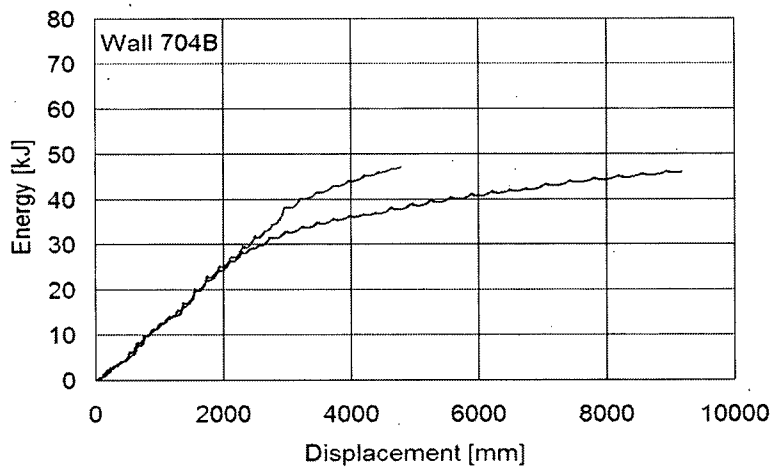

Hysteretic Energy Plot Comparison
CASHEW Wall in Red
Experimental Wall in Blue

Results:

CASHEW Peak Load:	63.5	kN
CASHEW Displacement at Peak Load:	88.9	mm
*CASHEW Hysteretic Energy Dissipated:	31.8	kJ
*Experimental Wall Hysteretic Energy Dissipated:	28.3	kJ

* Hysteretic energy dissipation determined at the end of the three cycle set corresponding with the experimental walls cycle set that corresponds with wall failure.

Description: **CASHEW Tall-Wall 705**

Connection Input: CPARA

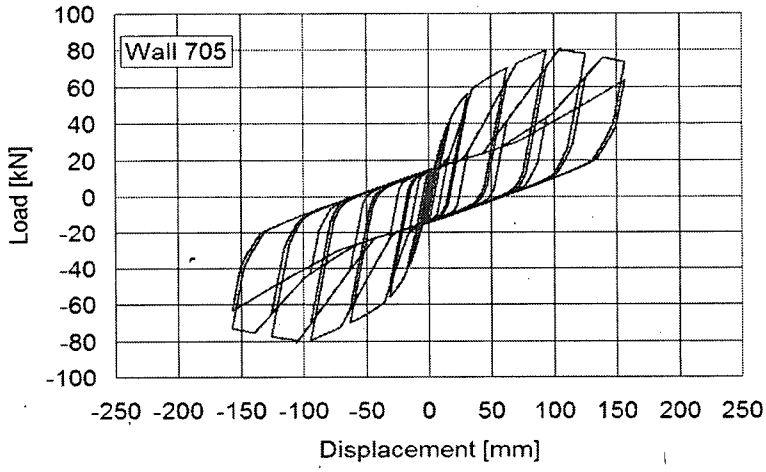

CASHEW
Load vs. Displacement Plot

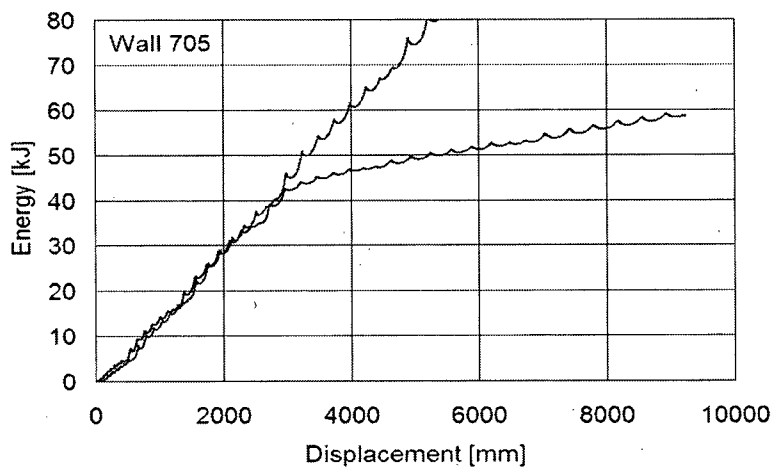

Hysteretic Energy Plot Comparison
CASHEW Wall in Red
Experimental Wall in Blue

Results:

CASHEW Peak Load:	81.0	kN
CASHEW Displacement at Peak Load:	105.6	mm
*CASHEW Hysteretic Energy Dissipated:	37.2	kJ
*Experimental Wall Hysteretic Energy Dissipated:	33.1	kJ

* Hysteretic energy dissipation determined at the end of the three cycle set corresponding with the experimental walls cycle set that corresponds with wall failure.

Description: **CASHEW Tall-Wall 706A**

Connection Input: APARA A (Unaltered)

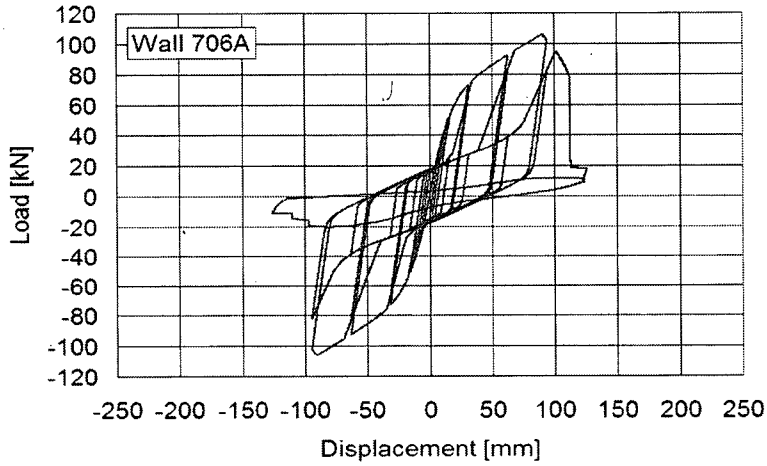

CASHEW
Load vs. Displacement Plot

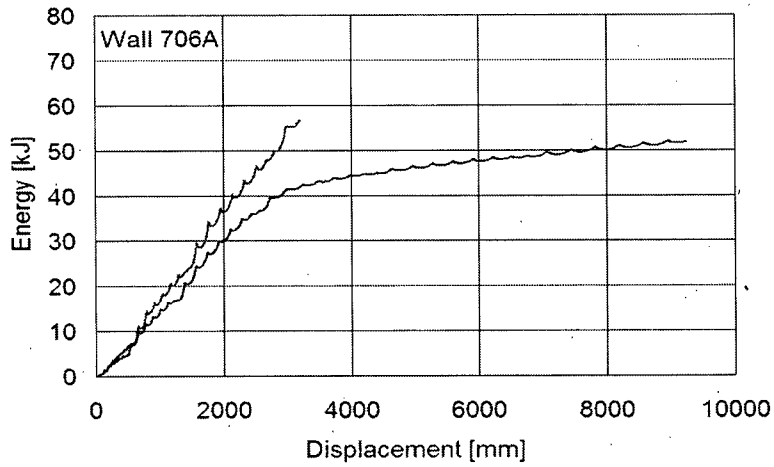

Hysteretic Energy Plot Comparison
CASHEW Wall in Red
Experimental Wall in Blue

Results:

CASHEW Peak Load:	106.1	kN
CASHEW Displacement at Peak Load:	90.7	mm
*CASHEW Hysteretic Energy Dissipated:	46.1	kJ
*Experimental Wall Hysteretic Energy Dissipated:	35.0	kJ

* Hysteretic energy dissipation determined at the end of the three cycle set corresponding with the experimental walls cycle set that corresponds with wall failure.

Description: **CASHEW Tall-Wall 706B**

Connection Input: APARA B (Altered)

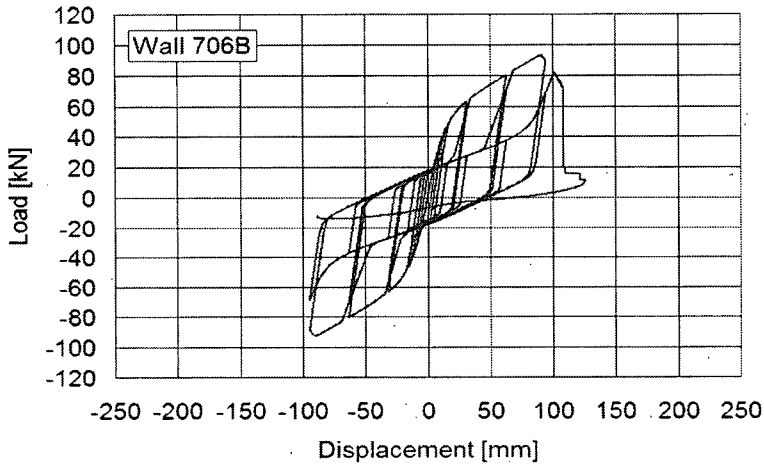

CASHEW
Load vs. Displacement Plot

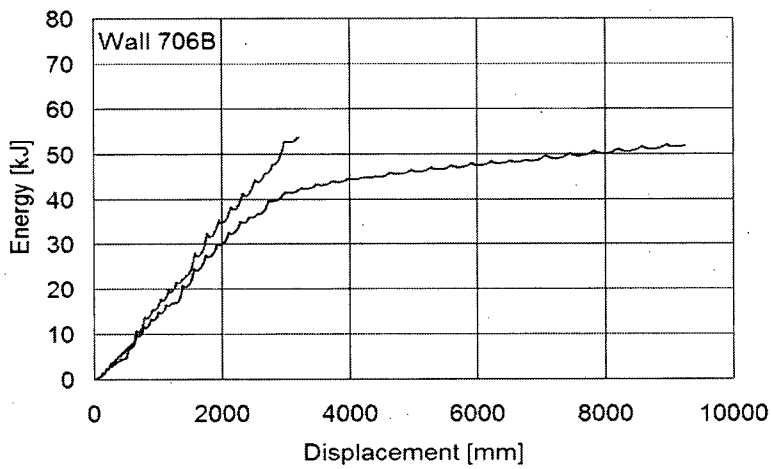

Hysteretic Energy Plot Comparison
CASHEW Wall in Red
Experimental Wall in Blue

Results:

CASHEW Peak Load:	93.1	kN
CASHEW Displacement at Peak Load:	90.5	mm
*CASHEW Hysteretic Energy Dissipated:	44.1	kJ
*Experimental Wall Hysteretic Energy Dissipated:	35.0	kJ

* Hysteretic energy dissipation determined at the end of the three cycle set corresponding with the experimental walls cycle set that corresponds with wall failure.

Description: **CASHEW Tall-Wall 707A**

Connection Input: APARA A (Unaltered)

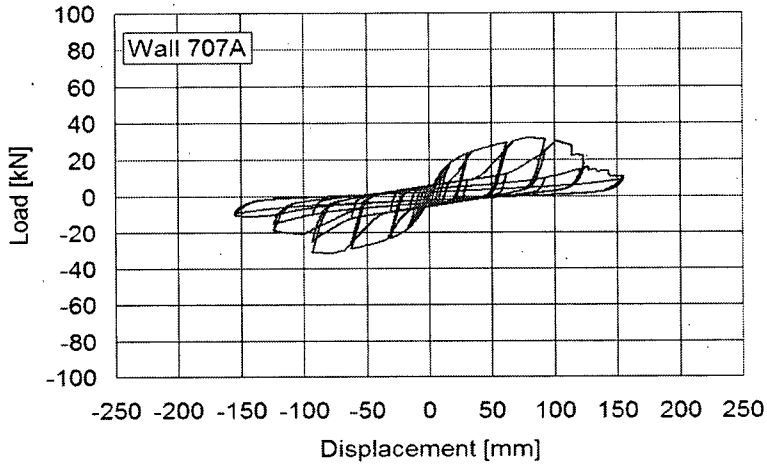

CASHEW
Load vs. Displacement Plot

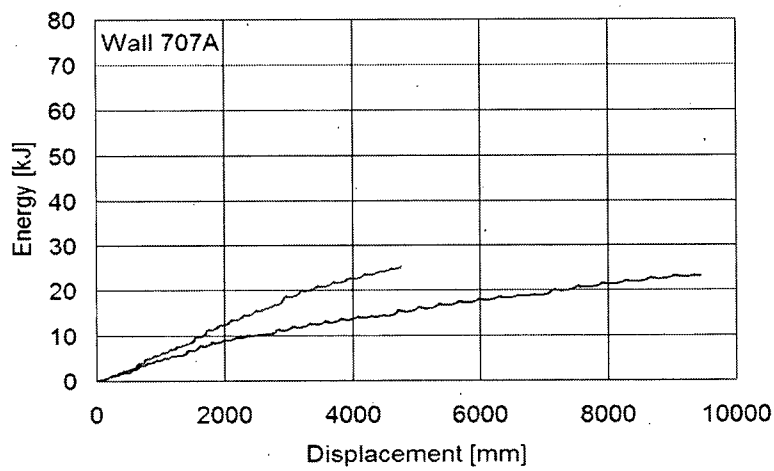

Hysteretic Energy Plot Comparison
CASHEW Wall in Red
Experimental Wall in Blue

Results:

CASHEW Peak Load:	31.7	kN
CASHEW Displacement at Peak Load:	78.0	mm
*CASHEW Hysteretic Energy Dissipated:	15.5	kJ
*Experimental Wall Hysteretic Energy Dissipated:	10.0	kJ

* Hysteretic energy dissipation determined at the end of the three cycle set corresponding with the experimental walls cycle set that corresponds with wall failure.

Description: **CASHEW Tall-Wall 707B**

Connection Input: APARA B (Altered)

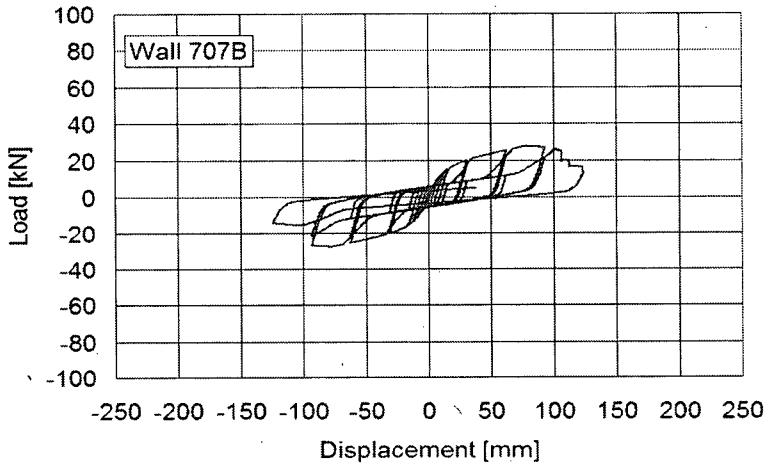

CASHEW
Load vs. Displacement Plot

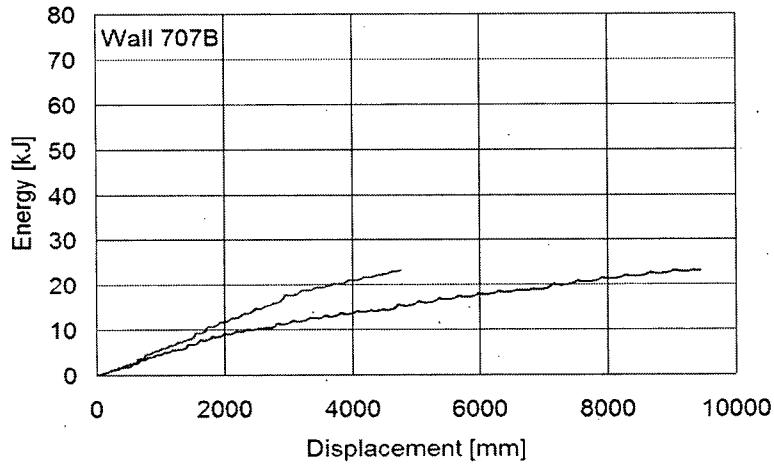

Hysteretic Energy Plot Comparison
CASHEW Wall in Red
Experimental Wall in Blue

Results:

CASHEW Peak Load:	27.6	kN
CASHEW Displacement at Peak Load:	77.4	mm
*CASHEW Hysteretic Energy Dissipated:	14.7	kJ
*Experimental Wall Hysteretic Energy Dissipated:	10.0	kJ

* Hysteretic energy dissipation determined at the end of the three cycle set corresponding with the experimental walls cycle set that corresponds with wall failure.

Description: **CASHEW Tall-Wall 709**

Connection Input: EPARA

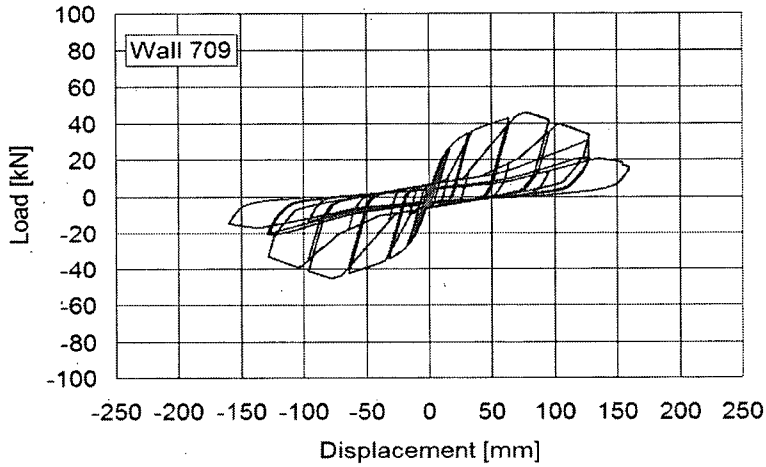

CASHEW
Load vs. Displacement Plot

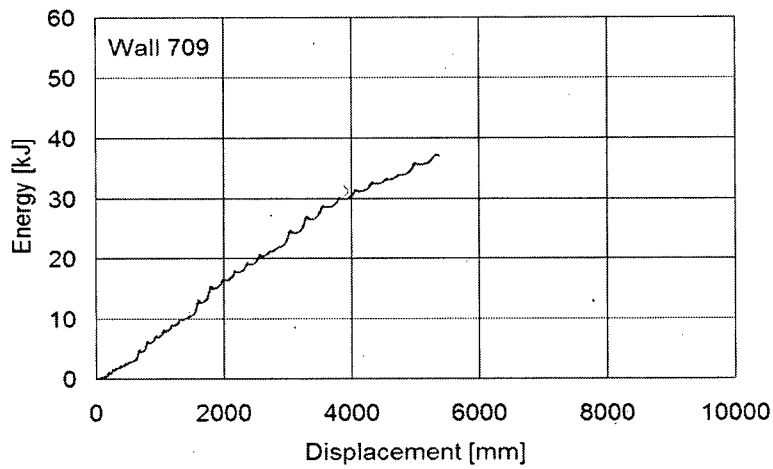

Hysteretic Energy Plot Comparison
CASHEW Wall in Red

Results:			
	CASHEW Peak Load:	45.7	kN
	CASHEW Displacement at Peak Load:	77.5	mm

Description: **CASHEW Tall-Wall 710B**

Connection Input: APARA B (Altered)

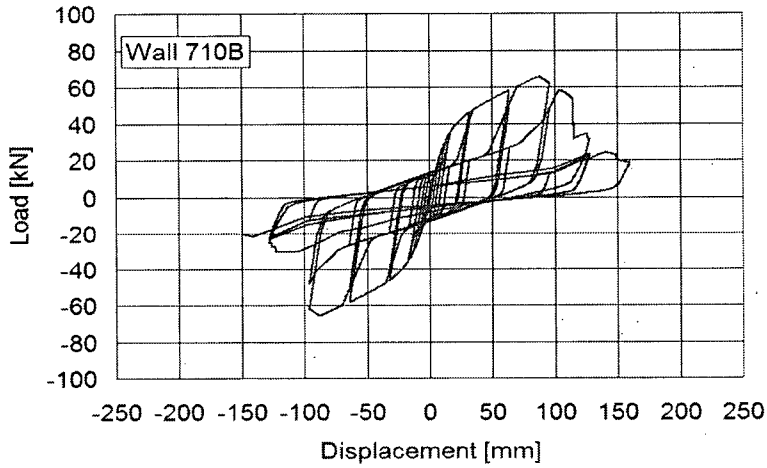

CASHEW
Load vs. Displacement Plot

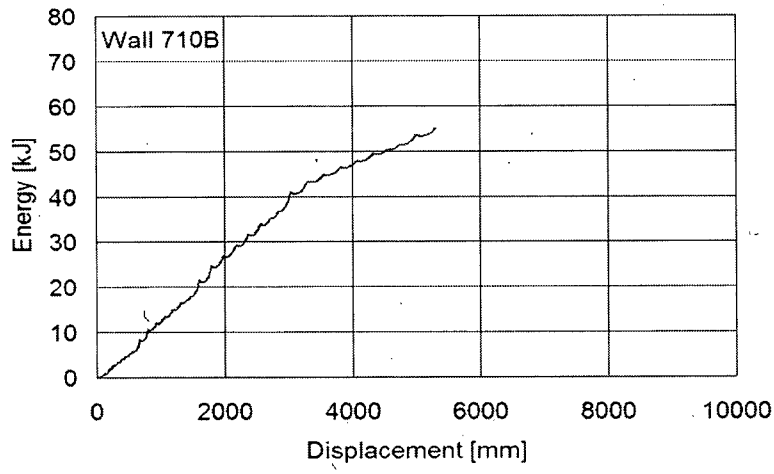

Hysteretic Energy Plot Comparison
CASHEW Wall in Red

Results:			
	CASHEW Peak Load:	65.8	kN
	CASHEW Displacement at Peak Load:	87.4	mm

Description: **CASHEW Tall-Wall 711B**

Connection Input: APARA B (Altered)

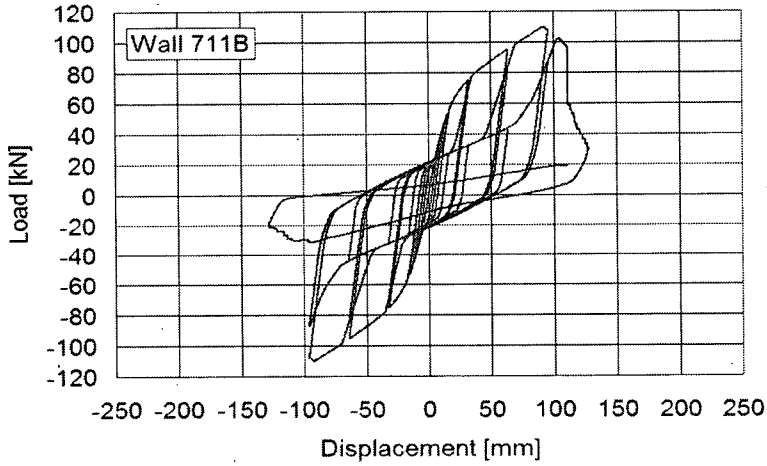

CASHEW
Load vs. Displacement Plot

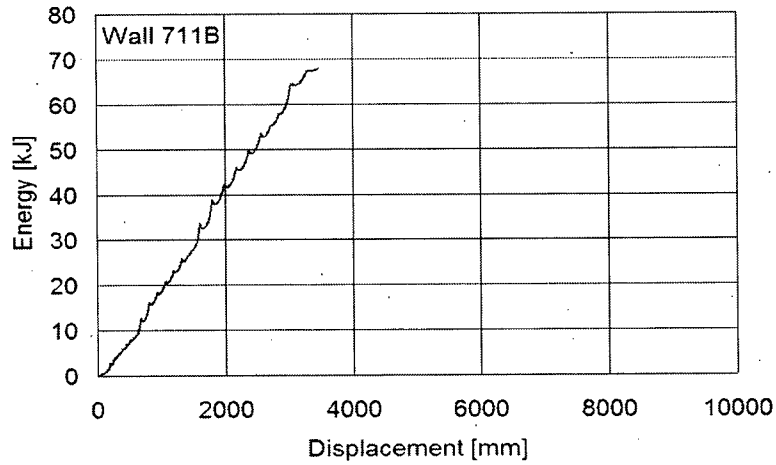

Hysteretic Energy Plot Comparison
CASHEW Wall in Red

Results:

CASHEW Peak Load:	109.8	kN
CASHEW Displacement at Peak Load:	92.0	mm

Description: **CASHEW Tall-Wall 801**

Connection Input: FPARA

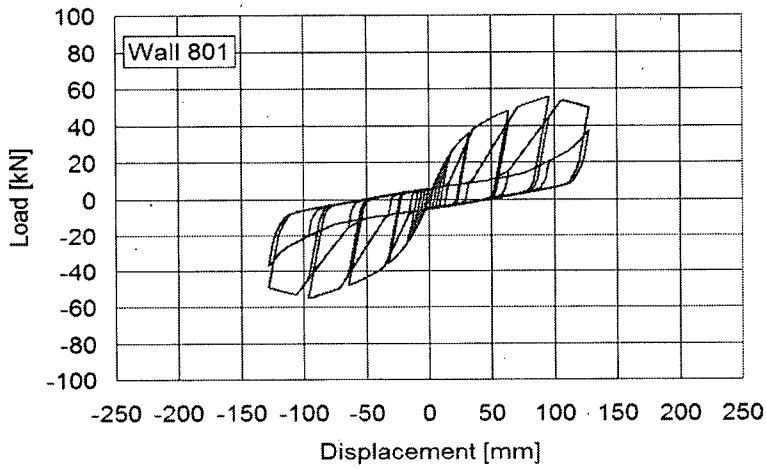

CASHEW
Load vs. Displacement Plot

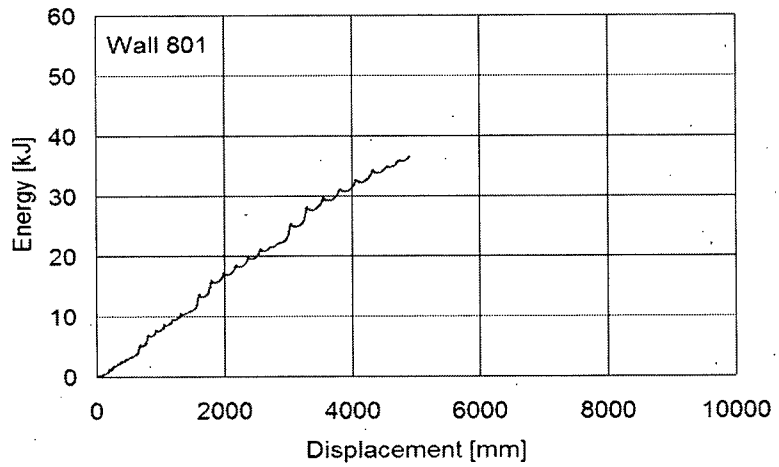

Hysteretic Energy Plot Comparison
CASHEW Wall in Red

Results:			
	CASHEW Peak Load:	55.2	kN
	CASHEW Displacement at Peak Load:	94.7	mm

Description: **CASHEW Tall-Wall 802**

Connection Input: FP/ARA

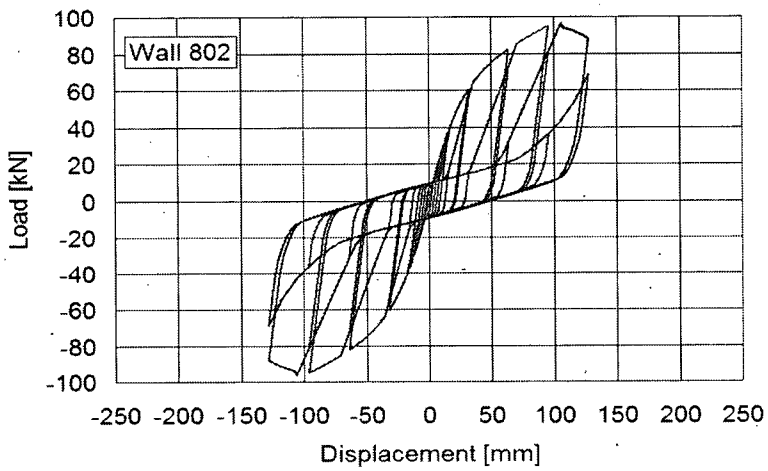

CASHEW
Load vs. Displacement Plot

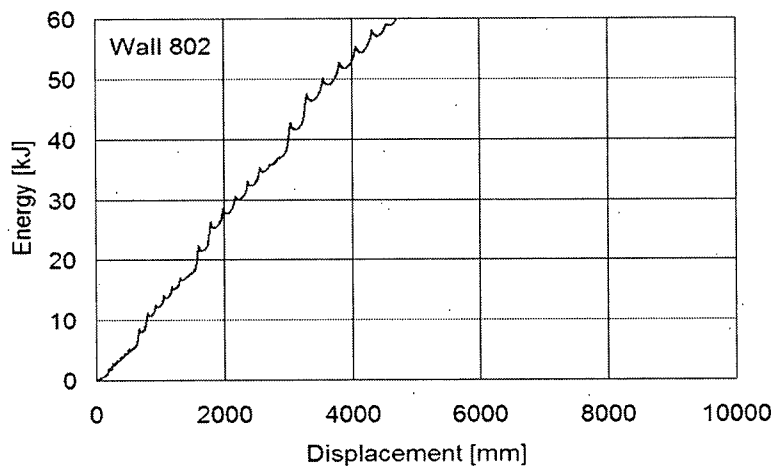

Hysteretic Energy Plot Comparison
CASHEW Wall in Red

Results:			
	CASHEW Peak Load:	96.6	kN
	CASHEW Displacement at Peak Load:	106.2	mm

Description: **CASHEW Tall-Wall 804**

Connection Input: BPARA

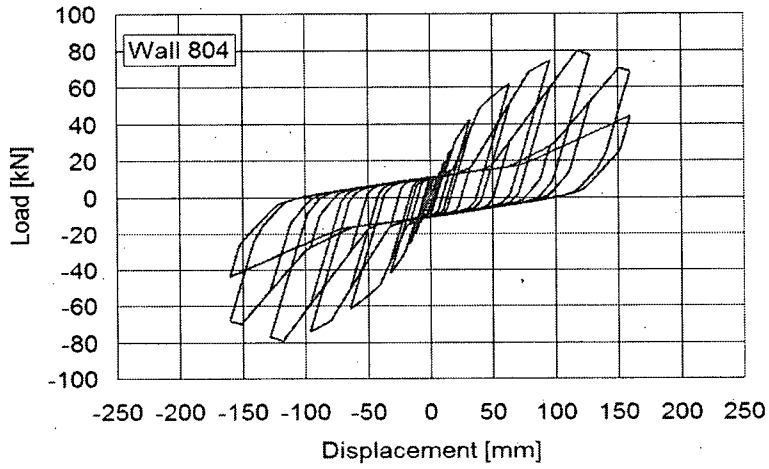

CASHEW
Load vs. Displacement Plot

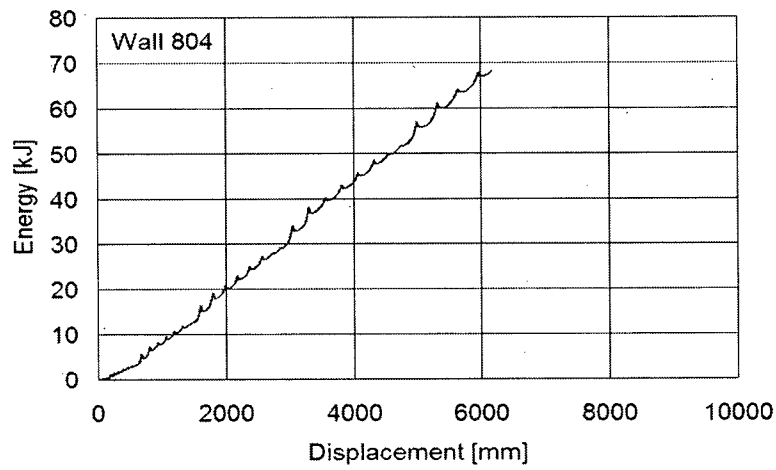

Hysteretic Energy Plot Comparison
CASHEW Wall in Red

Results:			
	CASHEW Peak Load:	80.3	kN
	CASHEW Displacement at Peak Load:	119.1	mm

Description: **CASHEW Tall-Wall 805**

Connection Input: BPARA

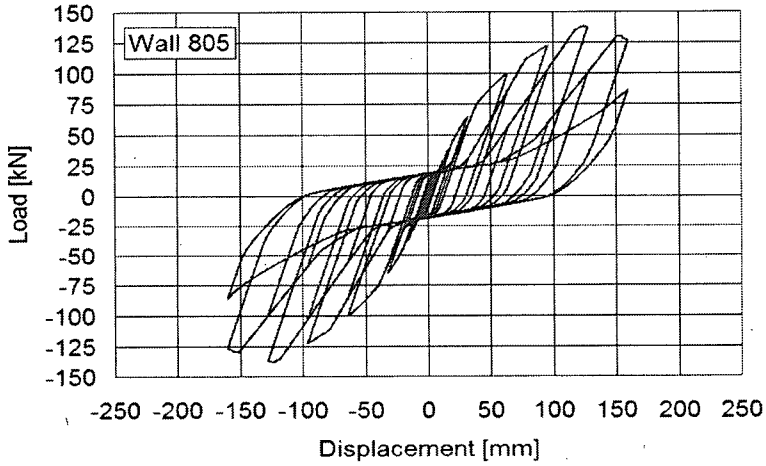

CASHEW
Load vs. Displacement Plot

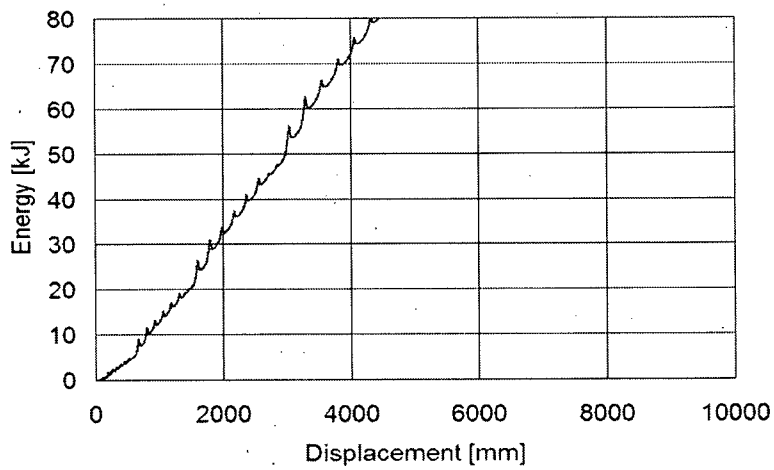

Hysteretic Energy Plot Comparison
CASHEW Wall in Red

Results:			
	CASHEW Peak Load:	106.1	kN
	CASHEW Displacement at Peak Load:	90.7	mm

B.3 Sample CASHEW Input File

The input file for the modelling of tall wall 602 is shown in a general form in this Appendix B.3. It includes the particulars on the geometry of the wall and the connection properties. Missing from the input file is the loading protocol displacement step values; the inclusion of these values is not necessary and would require over 350,000 added lines of text.

```
Tall Wall 602 , 4.88m x 4.88m 9.5 mm OSB Sheathed Tall Wall, Units are kN - mm
4,                                          ! Analysis Control Parameter
4880.,10                                    ! Height of Wall, Number of Panels
1,2440.,1220.,9.5,1220.,610.,2,5,1.05       ! Panel 1 Geometric Properties
2,2440.,1220.,9.5,3660.,610.,2,5,1.05       ! Panel 2
3,1220.,1220.,9.5,610.,1830.,2,3,1.05       ! Panel 3
4,2440.,1220.,9.5,2440.,1830.,2,5,1.05      ! Panel 4
5,1220.,1220.,9.5,4270.,1830.,2,3,1.05      ! Panel 5
6,2440.,1220.,9.5,1220.,3050.,2,5,1.05      ! Panel 6
7,2440.,1220.,9.5,3660.,3050.,2,5,1.05      ! Panel 7
8,1220.,1220.,9.5,610.,4270.,2,3,1.05       ! Panel 8
9,2440.,1220.,9.5,2440.,4270.,2,5,1.05      ! Panel 9
10,1220.,1220.,9.5,4270.,4270.,2,3,1.05     ! Panel 10
1,                                          ! Panel 1 Connector Properties
0.8,0.11,12.5,                              ! FO, F1, DU
0.45,0.037,-0.1624,2.2778,0.0242            ! KO, R1, R2, R3, R4
0.2603,1.1325                               ! ALPHA, BETA
2,                                          ! Panel 2 Connector Properties
0.8,0.11,12.5,
0.45,0.037,-0.1624,2.2778,0.0242
0.2603,1.1325
3,                                          ! Panel 3 Connector Properties
0.8,0.11,12.5,
0.45,0.037,-0.1624,2.2778,0.0242
0.2603,1.1325
4,                                          ! Panel 4 Connector Properties
0.8,0.11,12.5,
0.45,0.037,-0.1624,2.2778,0.0242
0.2603,1.1325
5,                                          ! Panel 5 Connector Properties
0.8,0.11,12.5,
0.45,0.037,-0.1624,2.2778,0.0242
0.2603,1.1325
6,                                          ! Panel 6 Connector Properties
0.8,0.11,12.5,
0.45,0.037,-0.1624,2.2778,0.0242
0.2603,1.1325
7,                                          ! Panel 7 Connector Properties
0.8,0.11,12.5,
0.45,0.037,-0.1624,2.2778,0.0242
0.2603,1.1325
8,                                          ! Panel 8 Connector Properties
0.8,0.11,12.5,
0.45,0.037,-0.1624,2.2778,0.0242
0.2603,1.1325
9,                                          ! Panel 9 Connector Properties
0.8,0.11,12.5,
0.45,0.037,-0.1624,2.2778,0.0242
0.2603,1.1325
10,                                         ! Panel 10 Connector Properties
0.8,0.11,12.5,
0.45,0.037,-0.1624,2.2778,0.0242
0.2603,1.1325
1,                                          ! Panel 1 Connector Placement
-610.,-1220.,1220.,152.5,                   ! Horizontal Nail Placement
610.,-1220.,1220.,152.5,
-1220.,-457.5,457.5,152.5,                  ! Vertical Nail Placement
-610.,-305.,305.,305,
0.,-305.,305.,305,
```

```
610.,-305.,305.,305,
1220.,-457.5,457.5,152.5,
2,                                  ! Panel 2 Connector Placement
-610.,-1220.,1220.,152.5,                ! Horizontal Nail Placement
610.,-1220.,1220.,152.5,
-1220.,-457.5,457.5,152.5,               ! Vertical Nail Placement
-610.,-305.,305.,305,
0.,-305.,305.,305,
610.,-305.,305.,305,
1220.,-457.5,457.5,152.5,
3,                                  ! Panel 3 Connector Placement
-610.,-610.,610.,152.5,                  ! Horizontal Nail Placement
610.,-610.,610.,152.5,
-610.,-457.5,457.5,152.5,                ! Vertical Nail Placement
0.,-305.,305.,305,
610.,-457.5,457.5,152.5,
4,                                  ! Panel 4 Connector Placement
-610.,-1220.,1220.,152.5,                ! Horizontal Nail Placement
610.,-1220.,1220.,152.5,
-1220.,-457.5,457.5,152.5,               ! Vertical Nail Placement
-610.,-305.,305.,305,
0.,-305.,305.,305,
610.,-305.,305.,305,
1220.,-457.5,457.5,152.5,
5,                                  ! Panel 5 Connector Placement
-610.,-610.,610.,152.5,                  ! Horizontal Nail Placement
610.,-610.,610.,152.5,
-610.,-457.5,457.5,152.5,                ! Vertical Nail Placement
0.,-305.,305.,305,
610.,-457.5,457.5,152.5,
6,                                  ! Panel 6 Connector Placement
-610.,-1220.,1220.,152.5,                ! Horizontal Nail Placement
610.,-1220.,1220.,152.5,
-1220.,-457.5,457.5,152.5,               ! Vertical Nail Placement
-610.,-305.,305.,305,
0.,-305.,305.,305,
610.,-305.,305.,305,
1220.,-457.5,457.5,152.5,
7,                                  ! Panel 7 Connector Placement
-610.,-1220.,1220.,152.5,                ! Horizontal Nail Placement
610.,-1220.,1220.,152.5,
-1220.,-457.5,457.5,152.5,               ! Vertical Nail Placement
-610.,-305.,305.,305,
0.,-305.,305.,305,
610.,-305.,305.,305,
1220.,-457.5,457.5,152.5,
8,                                  ! Panel 8 Connector Placement
-610.,-610.,610.,152.5,                  ! Horizontal Nail Placement
610.,-610.,610.,152.5,
-610.,-457.5,457.5,152.5,                ! Vertical Nail Placement
0.,-305.,305.,305,
610.,-457.5,457.5,152.5,
9,                                  ! Panel 9 Connector Placement
-610.,-1220.,1220.,152.5,                ! Horizontal Nail Placement
610.,-1220.,1220.,152.5,
-1220.,-457.5,457.5,152.5,               ! Vertical Nail Placement
-610.,-305.,305.,305,
0.,-305.,305.,305,
610.,-305.,305.,305,
```

```
1220.,-457.5,457.5,152.5,
10,                                  ! Panel 10 Connector Placement
-610.,-610.,610.,152.5,                ! Horizontal Nail Placement
610.,-610.,610.,152.5,
-610.,-457.5,457.5,152.5,              ! Vertical Nail Placement
0.,-305.,305.,305,
610.,-457.5,457.5,152.5,
382449,                                ! Number of loading protocol data input values

Loading protocol displacement steps follow
```